2014

# Proportioning and performance evaluation of self-consolidating concrete

Xuhao Wang
*Iowa State University*

**Proportioning and performance evaluation of self-consolidating concrete**

by

**Xuhao Wang**

A dissertation submitted to the graduate faculty

In partial fulfillment of the requirements for the degree of

DOCTOR OF PHILOSOPHY

Major: Civil Engineering (Civil Engineering Materials)

Program of Study Committee:

Kejin Wang, Co-Major Professor
Peter C. Taylor, Co-Major Professor
Halil Ceylan
Charles T. Jahren
Chris R. Rehmann
George Morcous

Iowa State University

Ames, Iowa

2014

# TABLE OF CONTENTS

## ACKNOWLEGEMENTS

A kid, who was born 27 years ago, may become a PhD in few weeks. Back then, he even got confused on what a doctor is for, helping the patients? Today, he finally understands that it is a degree and people who own this degree have responsibilities to contribute their knowledge to make this world go further. He sincerely appreciates his supervisors, Dr. Kejin Wang and Dr. Peter Taylor, because not even they have been teaching him how to deserve a PhD degree, but also leading him to be a good person and living a better life.

He is grateful to the committee members, Dr. Halil Ceylan, Dr. Charles Jahren, Dr. Chris Rehmann, and especially Dr. George Morcous from University of Nebraska at Lincoln for the research project support during the study. Also, Dr. Robert Stephenson from statistical analysis side gave him wholehearted help.

There was no way that he could successfully finish his work without collegeagues' help and support: Dr. Gilson Lomboy, Bob Steffes, Dr. Han Jianguo, Dr. Fatih Bektas, Bryan Zimmerman, and Jeremy Mclntyre.

He will never forget the place where he ever suffered from, stayed around, met his girlfriend (will be his wife this year), got drunk with his best friends, played with dirt, and learnt expert knowledge from.

He always feels so debt to his family and all real friends for their endless love, sacrifice, and encouragement: he did not make you feel disappointed.

Last but most, Xin Shi, you have been spending five beautiful years with him to let him win everything he deserved without hesitation. He must pay back his whole life to you.

By the way, that little kid named Xuhao Wang loves you all.

## ABSTRACT

A well-proportioned self-consolidating concrete (SCC) mixture can be achieved by controlling the aggregate system, paste quality, and paste quantity. The work presented in this dissertation involves an effort to study and improve particle packing of the concrete system and reduce the paste quantity while maintaining concrete quality and performance. This dissertation is composed of four papers resulting from the study: (1) Assessing Particle Packing Based Self-Consolidating Concrete Mix Design; (2) Using Paste-To-Voids Volume Ratio to Evaluate the Performance of Self-Consolidating Concrete Mixtures; (3) Image Analysis Applications on Assessing Static Stability and Flowability of Self-Consolidating Concrete, and (4) Using Ultrasonic Wave Propagation to Monitor Stiffening Process of Self-Consolidating Concrete. Tests were conducted on a large matrix of SCC mixtures that were designed for cast-in-place bridge construction. The mixtures were made with different aggregate types, sizes, and different cementitious materials.

In Paper 1, a modified particle-packing based mix design method, originally proposed by Brouwers (2005), was applied to the design of self-consolidating concrete (SCC) mixs. Using this method, a large matrix of SCC mixes was designed to have a particle distribution modulus (q) ranging from 0.23 to 0.29. Fresh properties (such as flowability, passing ability, segregation resistance, yield stress, viscosity, set time and formwork pressure) and hardened properties (such as compressive strength, surface resistance, shrinkage, and air structure) of these concrete mixes were experimentally evaluated.

In Paper 2, a concept that is based on paste-to-voids volume ratio (Vpaste/Vvoids) was employed to assess the performance of SCC mixtures. The relationship between excess paste

theory and Vpaste/Vvoids was investigated. The workability, flow properties, compressive strength, shrinkage, and surface resistivity of SCC mixtures were determined at various ages. Statistical analyses, response surface models and Tukey Honestly Significant Difference (HSD) tests, were conducted to relate the mix design parameters to the concrete performance.

The work discussed in Paper 3 was to apply a digital image processing (DIP) method associated with a MATLAB algorithm to evaluate cross sectional images of self-consolidating concrete (SCC). Parameters, such as inter-particle spacing between coarse aggregate particles and average mortar to aggregate ratio defined as average mortar thickness index (MTI), were derived from DIP method and applied to evaluate the static stability and develop statistical models to predict flowability of SCC mixtures.

The last paper investigated technologies available to monitor changing properties of a fresh mixture, particularly for use with self-consolidating concrete (SCC). A number of techniques were used to monitor setting time, stiffening and formwork pressure of SCC mixtures. These included longitudinal (P-wave) ultrasonic wave propagation, penetrometer based setting time, semi-adiabatic calorimetry, and formwork pressure.

The first study demonstrated that the concrete mixes designed using the modified Brouwers mix design algorithm and particle packing concept had a potential to reduce up to 20% SCMs content compared to existing SCC mix proportioning methods and still maintain good performance. The second paper concluded that slump flow of the SCC mixtures increased with Vpaste/Vvoids at a given viscosity of mortar. Compressive trength increases with increasing Vpaste/Vvoids up to a point (~150%), after which the strength becomes independent of Vpaste/Vvoids, even slightly decreases. Vpaste/Vvoids has little effect on the shrinkage mixtures, while SCC mixtures tend to have a higher shrinkage than CC for a given

Vpaste/Vvoids. Vpaste/Vvoids has little effects on surface resistivity of SCC mixtures. The paste quality tends to have a dominant effect. Statistical analysis is an efficient tool to identify the significance of influence factors on concrete performance.

In third paper, proposed DIP method and MATLAB algorithm can be successfully used to derive inter-particle spacing and MTI, and quantitatively evaluate the static stability in hardened SCC samples. These parameters can be applied to overcome the limitations and challenges of existing theoretical frames and construct statistical models associated with rheological parameters to predict flowability of SCC mixtures. The outcome of this study can be of practical value for providing an efficient and useful tool in designing mixture proportions of SCC. Last paper compared several concrete performance measurement techniques, the P-wave test and calorimetric measurements can be efficiently used to monitor the stiffening and setting of SCC mixtures.

# CHAPTER 1. INTRODUCTION

## BACKGROUND

The present thesis is developed from an on-going research project, *Self-Consolidating Concrete for Cast-in-Place Bridge Components*. This research is needed to address the factors that significantly influence the design, constructability, and performance of cast-in-place concrete bridge components using SCC, and to develop guidelines for its use in these applications, including recommended changes to the AASHTO LRFD Bridge Design and Construction Specifications. These guidelines will provide highway agencies with the information necessary for considering cast-in-place SCC to expedite construction and yield economic and other benefits.

To date, more than 17 proportion methods have been proposed worldwide for SCC. Even though there are an enormous number of publications on laboratory SCC mix design studies, there is no unique solution for any given application. Although the methods vary widely in overall approach and the level of complexity, most methods are proportioned to achieve desirable fresh concrete properties, such as passing ability, filling ability, segregation resistance, and etc. (Bui et al. 1999). It is generally agreed that controlling the aggregate system, paste quality, and paste quantity is essential for SCC mix design. Minimizing void content can permit more paste to cover aggregate surfaces in a given concrete system, thus improving workability. Achieving the designed aggregate distribution and proper excessive paste thickness is critical to control certain engineering properties and structural performance of concrete (Ozen and Guler, 2014). However, the concrete properties of interest are not limited to these properties, such as mechanical properties, shrinkage, and permeability, need

to be assessed as well. These are largely controlled by the paste quality, such as water to cementitious material ratio, supplementary cementitious material (SCMs) types and dosages, and use of chemical admixtures. In addition, in order to provide better quality control and predict construction activities, continuous monitoring on early age concrete behavior using field materials under field environment can result in benefits (Inaudi and Glisic 2006):

1. It helps to improve the knowledge concerning mixture behavior and improve calibration of numerical models.
2. It gives an early indication of malfunction so that precautions can be made in time.

This dissertation includes a selection of papers encompassing the development of an improved particle packing based mix proportion design method, the evaluation of SCC mixtures performance using paste-to-void volume ratio concept, the assessment of relationship on aggregate system and static stability and flowability using proposed digital image processing (DIP) method and programing algorithm, and the application of an efficient stiffening process monitoring method for quality control purposes. Another two supplementary papers are also involved to further investigate the rheological properties related behaviors, such as the change of viscosity, yield stress, thixotropy, and shear thickening. It is because the rheological properties of fresh concrete significantly affect the construction operations such as transportation, placement, consolidation and formwork pressure, which eventually influence the hardened properties and long term behavior of concrete.

## OBJECTIVE OF DISSERTATION

The main objective of this work is to investigate the relationship among the aggregate system, paste quality, and paste quantity to produce SCC mixtures with improved particle packing system and reduced paste quantity while maintaining concrete quality and performance. In order to accomplish this main purpose, the following objectives are included in this dissertation:

- Applying the improved particle packing based mix design method to SCC mix design and minimizing the paste quantity whilst maintaining concrete performance;
- Employing a concept that is based on a paste-to-voids volume ratio (Vpaste/Vvoids) to assess the performance of SCC mixtures;
- Introducing a digital image processing (DIP) method associated with a MATLAB algorithm to evaluate cross sectional images of SCC mixtures to achieve an appropriate aggregate distribution and paste quantity system;
- Understanding the rheological properties of three types of concrete mixtures, conventional concrete, SCC and slip-form SCC by evaluating the effects of set time, rheological properties (viscosity, yield stress, thixotropy) and hydration temperature on lateral pressure;
- Developing a model on the amount of aggregate particle collision in a flowing mortar to study the cementitious material shear thickening behavior;
- Evaluating reliable and accurate techniques for performance measurement and construction activities prediction of in-situ SCC mixtures.

## DISSERTATION ORGANIZATION

This dissertation is divided into eight chapters. Chapter 1 provides a background and objectives of this dissertation.

A brief literature review on particle packing theory development, particle packing based mix proportioning method, theoretical frames, and measurements from hardened concrete are included in Chapter 2.

The main findings and results are presented in Chapters 3 to 6. Each chapter comprises a paper that has been either published, submitted for publication, or ready for submission to peer reviewed journals. The papers are ordered in the thesis as follows:

- Chapter 3:

Wang X., Wang, K., Taylor P., and Morcous G. *Assessing Particle Packing Based Self-Consolidating Concrete Mix Design Method*.

Chapter 3 presents a study that applies a modified particle-packing based mix-design method to reduce the paste quantity in a mixture whilst still meeting project requirements. The essence of this method is to improve the solid ingredient system to achieve a better particle packing while maintaining a good performance. A modified mix designed method is proposed and assessed based on performance test.

- Chapter 4:

Wang X., Taylor P., Wang, K., and Morcous G. *Effect of Paste-to-Voids Volume Ratio on the Performance of Self-Consolidating Concrete Mixtures.*

Chapter 4 covers a study on applying a concept that is based on paste-to-voids volume ratio (Vpaste/Vvoids) to assess the performance of SCC mixtures. The relationship between excess paste theory and Vpaste/Vvoids is investigated. Statistical analyses, response surface models and Tukey Honestly Significant Difference (HSD) tests, are conducted to relate the mix design parameters to the concrete performance.

- Chapter 5:

Wang X., Wang, K., Han J., and Taylor P. *Image Analysis Applications on Assessing Static Stability and Flowability of Self-Consolidating Concrete*.

Chapter 5 provides an efficient method, digital image processing (DIP), associated with a MATLAB algorithm to evaluate cross sectional images of SCC samples. The results are used to assess the existing theoretical frames, such as Vpaste/Vvoids concept and excess paste/mortar theory, and overcome the limitations of both. The outcome of this study can be of practical value for providing an efficient and useful tool in designing mixture proportions of SCC.

- Chapter 6:

Wang X., Taylor P., Wang K., and Lim M. *Using Ultrasonic Wave Propagation Monitoring Stiffening Process of Self-Consolidating Concrete*. Submitted to American Concrete Institute James Instrument Award.

Chapter 6 introduces a study to investigate technologies available to monitor changing properties of a fresh mixture, particularly for use with SCC. A longitudinal ultrasonic wave propagation method is induced to monitor the setting and stiffening behavior of SCC. Comparisons are made among longitudinal ultrasonic wave propagation, penetrometer based setting time, semi-adiabatic calorimetry, and formwork pressure measurements.

Finally, Chapter 7 summarizes the major findings of this dissertation and Chapter 8 provides the recommendations for future research.

Appendix A includes the abstracts of papers written with other authors that are submitted to journals. The two papers were performed during the PhD study but not included as part of the main dissertation:

Lomboy G., Wang X., and Wang K. *Rheological Behavior and Formwork Pressure of NC, SCC and SFSCC Mixtures.* Accepted to be published in Journal of Cement and Concrete Composites SI: SCC 2013.

Lu G., Wang X., and Wang K. *Effect of Interparticle Action on Shear Thickening of Cementitious Suspensions*. Submitted to Journal of Rheology.

Appendix B contains a technical report from additional research during the PhD study.

Taylor P., and Wang X. *Comparison of Setting Time Measured Using Ultrasonic Wave Propagation With Saw-Cutting Times on Pavements in Iowa.* FHWA Pooled Fund Study TPF-5(205), Technical report, Institute of Transportation, Iowa State University, January 2014.

**REFERENCES**

Bui, V.; Montgomery, D., "Mixture Proportioning Method for Self-Compacting High Performance Concrete with Minimum Paste Volume," In: Proceedings of the First International RILEM Symposium on Self-Compacting Concrete, Stockholm, Sweden, RILEM Publications, Cachan, France, pp 373-396, Sep. 1999.

Ozen, M.; Guler, M., "Assessment of Optimum Threshold and Particle Shape Parameter for the Image Analysis of Aggregate Size Distribution of Concrete Sections," Optics and Lasers in Engineering, 53, pp. 122-132, 2014.

Inaudi, D., and Glisic, B., "Continuous Monitoring of Concrete Bridges During Construction and Service as A Tool for Data-Driven Bridge Health Monitoring," IABMAS'06 The Third Int'l Conference on Bridge Maintenance, Safety and Management, Porto, Portugal, July16-19, 2006.

# CHAPTER 2. LITERATURE REVIEW

## PARTICLE PACKING IN SCC

### Particle packing theory development

Self-consolidating concrete (SCC), as a type of high performance concrete, comprises materials that have an enormous size range, i.e., from powder in the nano-meter (nm) range, up to very coarse particles, which can be as large as 25 mm (Hunger 2010). The influence of the particle size distribution (PSD), governing both packing and internal specific surface area, has been reported (Feret 1892; Fuller et al. 1907; Furnas 1931).

There are a number of packing models available to describe both continuous and discrete packing. Five basic models were reviewed by Jones et al. (2002):

- Toufar, and modified Aim and Toufar model;
- Dewar model;
- Linear packing model (LPM);
- Further development of the solid suspension model (SSM);
- Compressible packing model (CPM). The LPM, the SSM and the CPM are so called third generation packing models.

Hunger (2010) stated that the amount of solids in coarse and fine sections should be optimized separately because the fine fractions primarily contribute to the porosity of a mixture. An integral approach based on the particle size distribution of all solids is not found very often.

Aggregate selection for optimal packing density may follow one of several suggested ideal particle size distributions, empirical tests on various blends of aggregates, or a mathematical model (Koehler 2007). In the majority of cases, continuously graded granular blends are described using the Fuller parabola, which represents the basic principle of most

standard aggregate grading curves (Hunger 2008). This power law size distribution is described by Equation 1:

$$P_t = (\frac{d}{d_{max}})^{\frac{1}{2}} \quad \text{Eq. 1}$$

where $P_t$ is a fraction of the total solids (aggregate and cementitious materials) being smaller than size d, and $d_{max}$ is the maximum particle size of the total grading. However, this equation has a deficiency in that it can never be fulfilled in practice because it assumes particles of infinite fineness, i.e., $d_{min}$ =0, which is not the real case. Moreover, in order to avoid the lean mixtures, researchers further stipulated that at least seven percent of the total solids should be finer than the No. 200 sieve (0.074 mm opening). Powers (1968) proposed another parabolic particle size distribution in which the power 0.5 is described as exponent q in Equation 2:

$$P_t = (\frac{d}{d_{max}})^{q} \quad \text{Eq. 2}$$

Andreasen and Andersen (1930) reported that the voids content only depends on the value of q, which is called the distribution modulus. However, when the q value approaches zero, the void content follows as well. Due to the inability of fine particles to pack in a similar manner as bigger but geometrically similar particles, Andreasen and Andersen limited the increase of packing to a range of q=0.33 to 0.50 (Hunger 2010). Asphalt concrete mixtures design has been using a distribution modulus of 0.45 as a theoretical maximum packing density (Kennedy et al. 1994). Stern (1932) extended the minimum $d_{min}$ down to 1 µm in order to include the particles. Hummel (1959) referred to a different q value of 0.4 for achieving maximum packing density with aggregate varying in shape. De Larrard (1999a) found that the values of the exponent for optimizing packing density varied with the packing

density of the individual size fractions and the degree of compaction. Therefore, it is not possible to establish an optimal particle size distribution for all cases.

Bolomey (1947) extended the parabolic grading by adding an empirical constant, f, to improve the relatively harsh mixture given by a Fuller parabola in Equation 3.

$$P_t = f + (1 - f)(\frac{d}{d_{max}})^{\frac{1}{2}} \quad \text{Eq. 3}$$

The empirical parameter f is selected based on the desired degree of workability, with higher values of "f" corresponding to higher degree of workability. The "f" value is typically between 0.10 and 0.14 depending upon the geometry of the particles.

Plum (1950) introduced a finite minimum size and measured minimum d = 0.291 μm that comes very close to the average size of cements used today. Including the minimum particle size, Plum (1950) derived the expression in Equation 4:

$$P_t = \frac{q^n - 1}{q^N - 1} \text{ for } q \neq 1 \quad \text{Eq. 4}$$

With q being the distribution modulus, and n and N being the sieve numbers of the respective and largest sieve. However, he was aware that this may not be a practical solution. In this respect, Plum remarked that the all fractions below 0.149 mm cannot be so easily derived. Also, he justified that the cement was practically the sole ingredient below that size and that cement had to be accepted in natural grading it was supplied (Hunger 2010). This mathematical expression was still in discussion and keep on changing during the last 60 years. Funk and Dinger (1994), who were interested in the packing of particles applied to ceramic manufacturing modified Andreasen and Andersen grading model (A&A model) in Equation 5:

$$P_t = \frac{d^q - d_{min}^q}{d_{max}^q - d_{min}^q} \quad \text{Eq. 5}$$

where, the exponent q is the distribution modulus that controls the character of the generated mix regarding its fineness of grain; d is the sieve size and $d_{max}$ and $d_{min}$ denote maximum sieve size (i.e., where 100% passing takes place) and minimum particle size, respectively. It is assumed that this distribution law delivers a feasible solution for a practical purpose. Higher values of q create coarser mixtures (q>0.5) whereas smaller values lead to fines-rich granular blends as shown in Figure 1.

**Particle packing based mix proportioning method**

To date, more than 17 proportion methods have been proposed worldwide. Even though there are an enormous number of publications on laboratory SCC mix design studies, there is no unique solution for any given application. Table 1 summarizes the possible ranges of the ingredient proportions recommended by a set of selected design methods. Table 2 lists the basic concepts, unique features, and limitations of each mix proportioning method.

Although the methods vary widely in overall approach, the level of complexity, the material ranges and performance characteristics, most methods are proportioned to achieve the fresh concrete properties, especially passing ability, filling ability, and segregation resistance (Bui et al. 1999). Daczko (2012) divided the design techniques into two groups:

1. "Those based on calculated values derived from testing and evaluation of the raw materials intended for use.
2. Those based on choosing aggregate, powder, and water amounts from a series of general tables."

A well-proportioned SCC mixture can be achieved by controlling the aggregate system, paste quality, and paste quantity. It is generally agreed that minimizing the concrete void content, especially the capillary pores, can increase the concrete performance in terms of workability, strength, and durability (Powers 1968).

Brouwers' (2005) proposed method includes overruling more conventional models and theories. SCC mixtures were defined as a mixture of solid (i.e., aggregate, powders, and solid material in admixtures), water, and air. Packing of the solid system depends on the shape of individual particles, surface potential of the solids, the amount of mixing water, and the applied of compaction energy. The solids could be both reactive and non-reactive in nature. However, their reactivity was considered to have no impact on packing in the fresh state. A water layer of constant thickness around every particle was considered to control flowing (Hunger 2010). The mix proportioning algorithm can be divided into following portions:

- Target grading: aims at minimizing the deviation of the actual from the desired grading by combining all the solid ingredients using the modified A&A grading model in Equation 5. A higher value of q may lead to a high segregation potential and blocking, while a lower value of q gives a fine-rich blends that may result in high apparent viscosity due to the high amount of fines and dense packing. A spreadsheet solver tool and Visual Basic can be used for target curve fitting based on minimizing sum of the squares of the residuals (RSS) expressed in Equation 6. The coefficient of determination, R2 in Equation 7, should be considered to evaluate the quality of the curve fit, which expresses the variation between the target line and the obtained values for the actual grading.

  $\text{RSS} = \sum_{i=1}^{n}(P_m(D_i) - P_t(D_i))^2$ => Minimum Eq. 6

  $R^2 = 1 - \frac{\sum_{i=1}^{n}(P_m(D_i) - P_t(D_i))}{\sum_{i=1}^{n}(P_m(D_i) - \overline{P}_m)}$ with $\overline{P_m} = \frac{1}{n}\sum_{i=1}^{n}(P_m(D_i))$ Eq. 7

  Where, $P_m(D_i)$ denotes the volume fraction of the solid ingredients in a mixture multiplied by percentage passing of those solids from each sieve. $P_t(D_i)$ denotes target percentage passing each corresponding sieve using modified A&A grading model multiplied by percentage passing each sieve.
- Adjustable values: One cubic meter of fresh concrete is composed of solids ($V_{solid}$), water ($V_w$), and voids ($V_{air}$) as shown in Equation 8:

  $V_{solid} = \sum_{k=1}^{m} V_{solid,k} = V_{total} - V_w - V_{air}$ Eq. 8

- Constraints: some physical and policy constraints and boundary conditions need to be applied to the algorithm.
  - Non-negativity constraint: the volumetric proportion of $V_{solid,k}$ of a selected material for k = 1, 2, …, m cannot be negative.
  - Volumetric constraint: the sum of volumetric proportion of raw materials must equal 100%.
  - Policy constraints:
    - Cement content: provide the range of minimum and maximum cement factor
    - Water content: ratio of w/cm ratio
    - Optimization target: set distribution modulus between 0.21 and 0.25.
    - Air content: desired air content.
- The mix proportion can be solved numerically based on selected solid materials, chemical admixtures, and physical properties of materials, such as specific gravity and absorption.

**Particle packing based theoretical frames**

*Excess paste theory*

The "excess paste theory" was originally developed by Kennedy (1940) and it was built on a two phase theory, i.e., a paste phase is used to fill up the voids between aggregates. Sufficient paste volume is needed to fill the voids and control friction between aggregates to provide desired workability. The "lubricating" layer of paste around aggregates needs to be thin enough to prevent coarse aggregates from sinking down and segregating, while it needs to be thick enough to achieve a good workability (Kosmatka et al. 2008; Koehler and Fowler 2007; Kennedy 1940). Hu and Wang (2007) extended this theory to "excess mortar theory", in which paste and fine aggregate were considered as a whole system to provide segregation resistance and lubrication effect of coarse aggregate for workability.

Ideally, the excess paste thickness can be approximated by using paste volume divided by the surface area of the aggregates. Heywood (1933) proposed a direct method to measure aggregates in terms of length, width, and thickness. However, what he proposed would only work for an individual grain size, and not for a continuous grading of aggregates. Oh and his coworkers (1999) modified the equations so that it would allow one to calculate the total surface area of aggregates. Meanwhile, they established the relationship between the relative thickness of excess paste and the relative Bingham parameters for a continuous grading of aggregates in Equation 9.

$$\tau = \frac{P_e}{\sum_i^n n_i s_i D_{pi}} \quad \text{Eq. (9)}$$

where, $P_e$ = the volume of excess paste; $n_i$ = the number of particles in size class i; $s_i$ = the surface area of particles in size class i, and $D_{pi}$ = the projected diameter of the particles in size class i.

This theory has been applied to design SCC mix proportions by Bui et al. (2002). The paste volume must be high enough to fill the voids between aggregate particles and create a layer enveloping the particles to achieve deformability and good segregation resistance. The average aggregate spacing is calculated by Equations 10 and 11 and defined as an average distance between surfaces of aggregate particles or as twice the thickness of paste layer around an aggregate particle as shown in Figure 2 (Bui et al. 2002).

$$D_{ss} = D_{av}\left(\sqrt[3]{1 + \frac{V_p - V_{void}}{V_c - V_p}} - 1\right) \quad \text{Eq. (10)}$$

where $D_{ss}$ = average spacing between aggregate particle surfaces (particles are assumed to be spherical); $V_p$ = paste volume; $V_{void}$ = volume of voids in densely compacted aggregate

determined in accordance with ASTM C29; $V_c$ = total concrete volume; and $D_{av}$ = the average aggregate diameter, which is given by

$$D_{av} = \frac{\sum d_i m_i}{\sum m_i} \quad \text{Eq. (11)}$$

where $d_i$ = average size of aggregate fraction i; and $m_i$ = percentage of aggregate mass retained between upper and lower sieve sizes in fraction i.

The relationships among paste rheology, average aggregate spacing, and average aggregate size were established and the general trends were found. Some satisfactory zones were defined for different average aggregate spacing, average aggregate diameter, cement contents, water-binder ratios as well as contents and types of fly ash (Bui et al. 2002).

A limitation to the excess paste approach is that it is based on the assumption that aggregate particles are spherical and that they are packed in a cubic lattice, neither of which is true (Yurdakul et al. 2013). The aggregate spacing can be considered as an average paste thickness because the average aggregate diameter is determined based on combined coarse and fine aggregate fractions.

*Paste-to-voids volume ratio*

An alternative concept, based on the paste-to-voids volume ratio (Vpaste/Vvoids), was applied to pavement concrete mixtures by Yurdakul et al. (2013). The Vpaste/Vvoids can be determined by calculating the paste volume of concrete mixtures and dividing that value by the volume of voids in the consolidated aggregate system determined in accordance with ASTM C29. The paste volume comprises the volume of water, the cementitious materials, and the measured air in the system. A figure of 100% means that all the space between the aggregates is just filled with paste with no excess.

The idea of relating performance of a mixture to paste volume for a given aggregate system was initially used to assess the SCC mixtures by Koehler and Fowler (2007). The Vpaste/Vvoids concept provides a quantitative means to consider the interaction between paste and aggregate system and achieve a quality concrete mixture with minimum impact whilst meeting specifications. The approach is believed to be more useful than parameters of "cementitious content" or "paste content" because it takes into account differences between aggregate systems (Yurdakul 2013). Like the excess paste approach, the aim is to:

- Coat the aggregate particles;
- Fill the voids between the combined aggregate system;
- Disperse the aggregate particles to provide the desired workability.

**Particle packing measurement from hardened concrete**

Digital Image Processing (DIP) methods have been popularly applied in characterizing portland cement concrete and asphalt concrete mixtures. It can offer powerful tools to distinguish among different features on a cross section of a hardened sample and to quantify a number of geometric and distribution variables that affect the properties of concrete (Ozen, 2007). The following advantages have been proposed according to Das (2006):

- It is a rapid method that can be applied in real-time for quality control in aggregate plants;
- A large number of aggregates can be evaluated at one time and the statistical reliability is enhanced;
- It is relatively free from subjectivity associated with human errors;
- Easy to characterize the aggregate features in a concrete sample which may be difficult to measure and analyze by physical means.

In general, the DIP methods comprise several steps: image acquisition, pre-processing, segmentation, representation and description, and recognition and interpretation (Ozen 2007).

The acquisition of image can be achieved by using an analog or digital camera. Recently, flatbed scanners have also been employed due to their ability to reach high resolution levels at reasonable cost (Ozen and Guler, 2014).

After converting the image scene into a digitized form and send to computer for recording, pre-processing is to improve the image so that further processing applications can be implemented, such as enhancement of the specific image features, noise removal, and elimination of the features that are not the area of interest (Gonzalez and Woods, 2001).

In a planar image, a segmentation operation can produce a binary image in which the object pixels are represented by one and the others by zero though a selected "thresholding" procedure. Pixels sharing similar brightness levels or color are clustered (Gonzalez and Woods, 2001). The discontinuities of the boundaries between parted regions can be recognized (Ozen 2007). This is a critical procedure for DIP because various factors may degrade the success of thresholding, such as poor contrast, non-uniform illumination, inherent noise from electronics, and noise from background. Literature has proposed three ways to tackle the challenge of selecting an optimum threshold to extract the object characteristics from the digital image: histogram shape, pixel clustering and entropy analysis (Sezgin and Sankur, 2004). Ozen and Guler (2014) pointed out the limitations of each way and proposed an algorithm for optimizing the threshold value to increase the accuracy of image analysis.

A set of row pixel data comprising the boundary information of the selected area of interest is developed for representation and description phase. "External representation" focuses on shape characteristics, such as corners and inflections, while "internal representation" focuses on color and texture. Both are required to identify the boundary of

the region of interest. Next step is the description of the data based on the chosen representation to highlight the objects of interest (Ozen, 2007; Gonzalez and Woods, 2001).

"Recognition" is the following step to assign a label to an object depending on the information provided by it descriptors. "Interpretation" is then used as a process to assign meaning to an ensemble of the recognized objects (Gonzalez and Woods, 2001).

With regard to the features of DIP methods, they have been widely used for the following applications:

- Development of a method of selecting an optimum threshold value and analyzing aggregate size distribution of concrete sections (Ozen and Guler, 2014);
- Analysis on crack length and fracture properties (Yao et al. 2011; Shah and Kishen, 2011);
- Evaluation of concrete brittleness using fractured aggregate area ratio method (Han and Yan, 2011);
- Measurement of particle tracking and pore size distribution (Yang et al. 2009; Aydilek et al. 2007; Guler et al. 1999);
- Investigation of the relationship between aggregate shape parameters and concrete strength (Ozen, 2007);
- Quantitative determination of the static segregation resistance of SCC mixtures (Shen et al. 2007);
- Determination of aggregate shape properties using X-ray tomographic methods and the effect of shape on concrete rheology (Erdogan, 2005);
- Determination of parameters of the air-void system in hardened concrete (ASTM C457 1998).

## SCC STIFFENING PROCESS MEASUREMENT APPROACHES

### Penetration resistance test

In ASTM C 403, penetration resistance is used to measure the setting and hardening behavior of a mixture. The initial and final setting times are defined as the times required for mortar extracted from the concrete to reach 500 [3.5 MPa] and 4000 psi [27.6 MPa], respectively, of resistance to penetration of a cylindrical probe. The test is labor intensive, especially for mixtures with a prolonged set time (Suraneni 2011).

### Calorimetry measurement

Calorimetry is the measurement of heat lost or gained during a chemical reaction such as cement hydration. The measurements can be used to assess hydration related properties, such as setting, stiffening, and maturity based on the obtained temperature-time curve. The test can also be used to assess the effect of mineral and chemical additives on the hydration kinetics and to check for incompatibility (Wang et al. 2006; Sandberg and Roberts 2005; Lerch 1987; Bensted 1946). It can be performed under isothermal conditions on paste in accordance with ASTM C1679, or under adiabatic or semi-adiabatic conditions on concrete or mortar.

Previous work reported in the literature has explored the use of semi-adiabatic calorimetry to define “thermal” setting times and to correlate them with setting times determined in accordance with ASTM C403 (Taylor et al. 2006). Figure 3 illustrates the method of a selected “fraction” of the main hydration response temperature rise (Sandberg and Liberman 2007). Because there may be variability in the magnitudes and shapes of the thermal profile of different mixtures, this method is suggested as the most efficient way to

evaluate thermal setting times for comparison. In the thermal profile obtained from semi-adiabatic calorimetry, 20% and 50% fraction thermal setting time are somewhat arbitrarily chosen as initial and final setting times, respectively.

**Ultrasonic pulse velocity (P-wave)**

There are two types of ultrasonic pulse velocity methods in use: wave transmission method and wave reflection method. The former method measures the velocity, relative energy and frequency of primary or compressional waves (P-waves) traveling through a material while the latter method monitors the reflection loss of transverse or shear waves (S-waves) at an interface between a steel plate and the cementitious material over time (Voigt et al. 2005). Both of the methods are based on Biot's theory (Biot 1956).

Based on Biot's theory, two compressional waves (fast and slow P-waves) and one shear wave propagate in a fluid saturated porous solid. The fast wave exists in all frequency ranges while the slow wave only exists in a high frequency range (Zhu et al. 2011). Studies have also shown that P-waves are less sensitive to difficulties with the sample-transducer contact than S-waves and allow a more accurate determination of the velocity through concrete due to their high signal-to-noise ratio (Robeyst et al. 2008). Both methods have been used to assess

- Setting behavior (Robeyst et al. 2008; Trinik et al. 2008; Grosse et al. 2006; Voigt et al. 2005; Subramaniam et al. 2005; Reinhardt and Grosse 2004; Ye et al. 2003; Chotard et al. 2001; Ozturk et al. 1999; Whitehurst 1951);
- Strength development (Pinto 2007; Erfurt 2002; Keating et al. 1989b; Byfors 1980; Elvery and Ibrahim 1976);
- Formwork pressure development (Suraneni 2011);
- Chemical shrinkage (Voigt et al. 2005).

Research has indicated that S- and P-wave velocities, relative energy as well as the frequency spectrum can indicate the setting and hardening behavior of concrete. Researchers have sought to correlate UPV data with the penetration resistance method using features of the ultrasonic velocity curves over time. These features include the point where P-wave velocity ($V_p$) starts to take off, the inflection point, or when $V_p$ reaches the velocity of water, i.e., 4700 ft/s [1430 m/s] (Zhu et al. 2011).

**Formwork pressure development**

The motivations for the industry to adopt SCC technology include a shortened casting time, reduced noise and labor, and production of esthetic surfaces with high quality. However, the fluid nature of SCC often leads to a high lateral pressure to the concrete formwork. For an element type, formwork pressure development is significantly influenced by casting rate and method, ambient environmental condition, rheological behavior, setting time, and binder type and content of the concrete (Khayat 2009; Gregori et al. 2008) .

The ACI guide to formwork (ACI 2004) recommends that the time to formwork removal should be based on maturity, rebound numbers, penetration resistance, or pullout tests to correlate the field concrete strength to elapsed time on removal of the formwork. There is limited data reported on the relationship between formwork pressure decay and form removals.

Each method discussed above has its own features and limitations and their application in assessing different properties of early age concrete is summarized in Table 3.

**REFERENCES**

ACI Committee 347. Guide to Formwork for Concrete (ACI 347-04), American Concrete Institute, Farmington Hills, MI., 2004.

Andreasen, A.; Andersen, J., "U¨ ber die Beziehung zwischen Kornabstufungund Zwischenraum in Produkten aus losen K¨ornern (mit einigen Experimenten)", Kolloid-Zeitschrift 50: 217 – 228 (in German), 1930.

ASTM C457. "Standard Test Method for Microscopical Determination of Parameters of the Air Void System in Hardened Concrete," American Society for Testing and Materials, Pennsylvania, 1998.

Aydilek, A.; D'Hondt, D.; Holtz, R., "Comparative Evaluation of Geotextile Pore Sizes Using Bubble Point Test and Image Analysis," Geotechnical Test Journal, 30 (3):173–81, 2007.

Bensted, J., "Some Applications of Conduction Calorimetry to Cement Hydration. Adv. Cement Res., Vol. 1, No. 1, 1946, pp 35-44.

Biot, M., "Theory of Propagation on Elastic Waves in A Fluid-Saturated Porous Solid. I. Low-Frequency Range," The Journal of the Acoustical Society of America, 28 (2, pp. 168-178), 1956.

Biot, M., "Theory of Propagation on Elastic Waves in A Fluid-Saturated Porous Solid. II. Higher-Frequency Range," The Journal of the Acoustical Society of America, 28 (2, pp. 179-191), 1956.

Bolomey, J., "The Grading of Aggregate and Its Influence on the Characteristics of Concrete," Revue Mater, Construction, Travaux Publiques, 1947.

Brouwers, H.; Radix, H., "Self-Compacting Concrete: Theoretical and Experimental Study," Cement and Concrete Research, 35, pp. 2116-2136, 2005.

Bui, V.; Akkaya, Y.; and Shah, S., "Rheological Model for Self-Consolidating Concrete," ACI Material Journal, V. 99, No. 6, 2002.

Bui, V.; Montgomery, D., "Mixture Proportioning Method for Self-Compacting High Performance Concrete with Minimum Paste Volume," In: Proceedings of the First International RILEM Symposium on Self-Compacting Concrete, Stockholm, Seweden, RILEM Publications, Cachan, France, pp 373-396, Sep. 1999.

Byfors, J., "Plain Concrete at Early Ages," CBI-Report 3:80, Swedish Cement and Concrete Research Institute, Stockholm, 1980.

Chotard, T.; Gimet-Breart, N.; Smith, A.; Fargeot, D.; Bonnet, J.; and Gault, C., "Application of Ultrasonic Testing to Describe The Hydration of calcium aluminate cement At The Early Age," Cement and Concrete Research, 31 (3, pp. 405–412), 2001.

Daczko, A., "Self-Consolidating Concrete: Appling What We Know," Abingdon: Spon Press, 2012.

Das, A., "A Revisit to Aggregate Shape Parameters", Workshop on Aggregates flakiness and elongation indices – *(WSOA)*, New Delhi, 2006.

De Larrard, F., "Concrete mixture proportioning: a scientific approach," London: E & FN Spon. 1999. durability)," PhD thesis, Bauhaus–University Weimar, Weimar, Germany, (in German), 2002.

Elvery, R., and Ibrahim, L., "Ultrasonic Assessment of concrete strength at Early Ages," Magazine of Concrete Research, vol. 28, no. 97, pp. 181–190, 1976.

Erdogan, S., "Determination of Aggregate Shape Properties Using X-ray Tomographic Methods and the Effect of Shape on Concrete Rheology," PhD dissertation, the University of Texas at Austin, 2005.

Erfurt, W., "Erfassung von Gef¨ugever¨anderungen in Beton durch Anwendung zerst¨orungsfreier Pr¨ufverfahren zur Einsch¨atzung der Dauerhaftigkeit (Determination of microstructural changes in concrete with nondestructive test methods to evaluate the concrete

Feret, R., "Sur la compacite des mortiers hydrauliques," Ann. Ponts Chaussee, memoires et documents, Serie 7, no. IV, p.5-164 (in French), 1892.

Fuller, W.; Thompson, S., "The Laws of Proportioning Concrete," Trans. Am. Soc. Civ. Eng., Vol. 33, pp. 222-298, 1907.

Funk, J.; Dinger, D., "Predictive Process Control of Crowded Particulate Suspensions – Applied to Ceramic Manufacturing," Kluwer Academic Publishers, Massachusetts, 1994.

Furnas, C., "Grading Aggregates I-Mathematical Relations for Beds of Broken Solids of Maximum Density," Ind. Eng. Chem., Vol. 23, pp. 1052-1058, 1931.

Gonzalez, R.; Woods R., "Digital Image Processing", Prentice Hall, USA, 2001.

Gregori, A.; Ferron, R.; Sun, Z.; and Shah, S., "Experimental simulation of Self-Consolidating Concrete Formwork Pressure," ACI Materials Journal, 105(1), pp. 97-104, 2008.

Grosse, C.; Reinhardt, H.; Krüger, M.; and Beutel, R., "Ultrasonic Through-Transmission Techniques for Quality Control of Concrete During Setting and Hardening, in: H.W. Reinhardt (Ed.)," Advanced Testing of Fresh Cementitious Materials, Stuttgart, pp. 83–93, 2006.

Guler, M.; Edil, T.; Bosscher, P., "Measurement of Particle Movement in Granular Soils Using Image Analysis," Journal of Computational Civil Engineering, 13(2):116–22, 1999.

Han, J.; Yan, P., "New Concrete Brittleness Evaluating Method—Fractured Aggregate Area Ratio Method," Concrete, Number 2, 2011.

Heywood H., Proceedings, Institute of Mechanical Engineers, Vol. 125, p.383, 1933.

Hu, J., and Wang, K., "Effects of Size and Uncompacted Voids of Aggregate on Mortar Flow Ability," Journal of Advanced Concrete Technology, 5, pp. 75-85, 2007.

Hummel, A., "Das Beton-ABC – Ein Lehrbuch der Technologie des Schwerbetons und des Leichtbetons", 11th edn, Wilhelm Ernst & Sohn, Berlin, 1959.

Hunger, M., "An Integral Design Concept for Ecological Self-Compacting Concrete," Ph.D thesis, Eindhoven University of Technology, The Netherlands, 2010.

Jones, M.; Zheng, L.; and Newlands, M., "Comparison of Particle Packing Models for Proportioning Concrete Constituents for Minimum Voids Ratio," Materials and Structures 35(249), pp. 301 – 309, 2002.

Keating, J.; Hannant, D.; and Hibbert, A., "Correlation between Cube Strength, Ultrasonic Pulse Velocity and Volume Change for Oil Well Cement Slurries," Cement and Concrete Research, vol. 19, no. 5, pp. 715–726, 1989b.

Kennedy, C., "The Design of Concrete Mixes," Journal of the American Concrete Institute, 36, pp. 373-400, 1940.

Kennedy, T.; Huber, G.; Harrigan, E.; Cominsky, R.; Hughes, C.; Quintus, H.; Moulthrop, J., "Superior Performing Asphalt Pavements (Superpave): The Product of SHRP Asphalt Research Program," National Research council, SI-IRP-A-410, 1994.

Khayat, K., "Self-consolidating Concrete Formwork Pressure," Final report, University of Sherbrooke, 2009.

Koehler, E., and Fowler, D., "Aggregates in Self-Consolidating Concrete," International Center for Aggregates Research (ICAR), Austin, TX, 2007.

Koehler, E.; Fowler, D., "Aggregates in Self-Consolidating Concrete. Final Report, ICAR Project 108: Aggregates in Self-Consolidating Concrete," International Center for Aggregates Research (ICAR), The University of Texas at Austin, March, 2007.

Kosmatka, S.; Kerkhoff, B.; and Panarese, W., "Design and Control of Concrete Mixtures," 14th ed., Portland Cement Association, Skokie, IL, USA, 2008.

Lerch, W., "The influence of gypsum on the hydration and properties of Portland Cement Pastes," Proceedings, Vol. 46, of the American Society for Testing Materials, 1987.

Oh, S.; Noguchi, T.; Tomosawa, F., "Toward Mix Design for Rheology of Self-Compacting Concrete," Proceedings of the First International RILEM Symposium on Self-Compacting Concrete, Stockholm, Sweden, pp. 361-372, 1999.

Ozen, M., "Investigation of Relationship between Aggregate Shape Parameters and Concrete Strength Using Imaging Techniques," Master thesis, Middle East Technical University, Turkey, 2007.

Ozen, M.; Guler, M., "Assessment of Optimum Threshold and Particle Shape Parameter for the Image Analysis of Aggregate Size Distribution of Concrete Sections," Optics and Lasers in Engineering, 53, pp. 122-132, 2014.

Ozturk, T.; Rapport, J.; Popovics, J.; and Shah, S., "Monitoring The Setting and Hardening of Cement-Based Materials with Ultrasound," Concrete Science and Engineering, Vol. 1, No.2, pp. 83-91, 1999.

Pinto, C., "Effect of Silica Fume and Superplasticizer Addition on setting behavior of High-Strength Mixtures," Journal of the Transportation Research Board, Vol.1574, pp. 56-65, 2007.

Plum, N., "The Predetermination of Water Requirement and Optimum Grading of Concrete: Under Various Conditions," Report 96, The Danish National Institute of Building Research - Statens Byggeforskningsinstitut, Copenhagen, 1950.

Powers, T., "The properties of fresh concrete," New York, 1968.

Reinhardt, H., and Grosse, C., "Continuous monitoring of setting and hardening of Mortar and Concrete," Construction and Building Materials, 18 (3), pp. 145–154, 2004.

Robeyst, N.; Gruyaert, E.; Grosse, C.; and Belie, N., "Monitoring the setting of Concrete Containing Blast-Furnace Slag by Measuring the Ultrasonic P-Wave Velocity," Cement and Concrete Research, 38, pp. 1169-1176, 2008.

Sandberg, J., and Liberman, S., "Monitoring and Evaluation of cement hydration by Semi-Adiabatic Field Calormetry, Journal of American Concrete Institute, Volume 241, pp. 13-24, 2007.

Sandberg, P., and Roberts, L., "Cement-Admixture Interactions Related to Aluminate Control," J. of ASTM Int., Vol. 2, No. 6, 2005.

Sezgin, M.; Sankur, B., "Survey Over Image Thresholding Techniques and Quantitative Performance Evaluation," Journal of Electron Imaging, 13(1):146–65, 2004.

Shah, S.; Kishen, J., "Fracture Properties of Concrete-Concrete Interfaces Using Digital Image Correlation," Experimental Mechanics, 51(3), 303–13, 2011.

Shen, L.; Struble, L.; Lange, D., "New Method for Measuring Static Segregation of Self-Consolidating Concrete," Journal of ASTM International, Volume 35, Issue 3, 2007.

Stern, O., "Vorschlag f¨ur eine Norm: Kornpotenz (Feinheitsmodul) loser Haufwerke, Sparwirtschaft 4: (in German), 1932.

Subramaniam, K.; Lee, J.; and Christensen, B., "Monitoring The Setting Behavior of Cementitious Materials Using One-Sided Ultrasonic Measurements," Cement and Concrete Research, Vol. 35, pp. 850-857, 2005.

Suraneni, P., "Ultrasonic Wave Reflection Measurements on Self-Compacting Pastes And Concretes," Master thesis in University of Illinois at Urbana-Champaign, 2011.

Taylor, P.; Johansen, V.; Graf, L.; Kozikowski, R.; Zemajtis, J.; and Ferraris, C., "Identifying Incompatible Combinations of Concrete Materials: Volume I-Final Report," FHWA-HRT-06-079 report, August, 2006.

Trinik, G.; Turk, G.; Kavcic, F.; and Bosiljkov, V., "Possibility of Using the Ultrasonic Wave Transmission Method to Estimate Initial Setting Time of Cement Paste," Cement and Concrete Research, 38, pp. 1336-1342, 2008.

Voigt, T.; Grosse, C.; Sun, Z.; Shah, S.; and Reinhardt, H., "Comparison of Ultrasonic Wave Transmission and Reflection Measurements with P- and S-Waves on Early Age Mortar and Concrete," Materials and Structures 38, pp. 729-738, 2005.

Wang, H.; Qi, C.; Farzam, H.; and Turici, J., "Interactions of Materials Used in Concrete," Concrete International, Vol. 28, no. 4, pp. 47-52, 2006.

Whitehurst, E., "Use of The Soniscope for Measuring Setting Time of Concrete," ASTM Proceedings, vol. 51, pp. 1166–1183, 1951.

Winden van der, N., and Brant, A., "Ultrasonic Testing for Fresh Mixes," Concrete, vol. 11, no. 12, pp. 25–28, 1977.

Yang, Z.; Peng, X.; Lee, D.; Chen, M., "An Image-Based Method for Obtaining Pore-Size Distribution of Porous Media," Environmental Science Technology, 43 (9):3248–53, 2009.

Yao, X.; Yao, M.; Xu, B., "Automated Measurements of Road Cracks Using Line-Scan Imaging", Journal of Test Evaluation, 39(4):1–9, 2011.

Ye, G.; Van Breugel, K.; and Fraaij, A., "Experimental Study and Numerical Simulation on The Formation of Microstructure in Cementitious Materials at Early Age," Cement and Concrete Research, 33 (2, pp. 233–239), 2003.

Yurdakul, E., "Proportioning for Performance-Based Concrete Pavement Mixtures," Doctor of Philosophy Dissertation, Iowa State University, 2013.

Yurdakul, E.; Taylor, P.; Ceylan, H.; and Bektas, F., "Effects of Paste-to-Voids Volume Ratio on the Performance of Concrete Mixtures," Journal of Materials in Civil Engineering (ASCE), Volume 25, Issue 12, pp. 1840-1851, 2013.

Zhu, J.; Kee, S.; Han, D.; and Tsai, Y., "Effects of Air Voids on Ultrasonic Wave Propagation in Early Age Cement Pastes," Cement and Concrete Research. 41, pp. 872-881, 2011.

## LIST OF TABLES



## LIST OF FIGURES

**Table 1: Existing methods for proportioning SCC**

| Method | Cement, kg/m³ | Filler, kg/m³ | Water, kg/m³ | Fine Agg., kg/m³ | Coarse Agg. , kg/m³ | w/c | w/cm |
|---|---|---|---|---|---|---|---|
| Rational Mix Design by Okamura and Ozawa (1995) | Rest of mixture volume | | - | 40 to 50% of mortar volume | 50 to 60% of solid volume | - | 0.9 to 1.0 by volume |
| Sedran et al. (1996) | Combination of binders is fixed based on previous knowledge to satisfy compressive strength and material availability. | | - | Saturation level is determined and 50% of this amount is used | - | With previous knowledge of material properties to determine the water demand of the binder combination with HRWRA | |
| Excess paste theory (1999) | Not specified, based on the applications | | | Not specified, based on the applications | | Optimum between 0.8-0.9 | |
| CBI and extension (1999) | If the determined paste volume for both blocking and liquid criteria is higher than 420 l/m3, smaller size aggregate need to be considered. | | | Make sure the average particle diameter is smaller than 6.5 mm. | | - | |
| LCPC (2000) | 430 | 50 | 170 | 847 | 825 | - | |
| Particle-Matrix model (2001) | Flow resistance ratio between 0.6-0.8 | | | - | | - | |
| Su et al. (2001) | >270 | - | - | Sand to total aggregates ranges from 50% to 57%, total aggregate ranges from 59% to 68%. | | - | |
| Statistical design | 250-600 kg/m3 | | - | Varied to achieve volume | Hold constant | 0.37-0.50 | 0.38 - 0.72 |
| ACBM (2002) | Similar to extension of CBI method | | | Similar to extension of CBI method | | - | |
| EFNARC (2005) | 400 to 600 kg/m3 | | Maximum 200 kg/m3 | Rest of mixture | 28 to 35% by volume | Use slump cone and v-funnel test to determine | |
| Concrete Manager Software | Not specified, based on the applications | | | | | | |
| DMDA (2005) | Fly ash is considered as part of the aggregate. | | Minimum 160 kg/m3 | - | | Minimum 0.42 to prevent autogenous shrinkage | |
| Brouwers et al. (2005) | Based on prior knowledge to provide the range. | | - | Combined aggregate gradation with the preferred range of distribution modulus q between 0.21 and 0.25. | | Depend on application and provide the ranges. | |
| ACI 237R (2007) | 386 to 475 kg/m3; Paste fraction: 34 to 40% | | | 0.32 to 0.44 | 28 to 32% | - | 0.32 to 0.45 |
| ICAR (2007) | Paste volume: 28 - 40% | | - | 16 mm for most applications; 9.5 mm for challenging passing ability, uniform grading with high packing density preferred, S/A = 0.40 -0.50, equidimensional, rounded aggregates preferred | | - | 0.30-0.45, higher with VMA |
| UCL (2009) | - | | - | 45% of mortar volume | 30% to 40% | - | 0.28-0.36 |
| Strength based method (2010) | Based on predetermined water content and w/cm | | Based on air content and aggregate size | - | 44% to 56% | wide range | wide range |

**Table 2: Basic concepts, unique features, and limitations of each SCC proportioning method**

| Method | Basic Concepts | Unique Features | Limitations |
|---|---|---|---|
| Rational Mix Design | Coarse aggregate content in the mixture is set to 50% to 60% of concrete bulk density. The fine aggregate content is set to 40-50% of the mortar volume. The w/p ratio and WR dosage are determined by mini-slump flow and mini v-funnel measurements of paste to reach prescribed target values. | A unique method of selecting optimum paste rheology with mini-slump flow and mini v-funnel | The method is rather restrictive in the way it sets the CA and FA contents and establishes the target paste flow. The proportions may not be optimal in concrete. No inclusion of a concrete strength requirement in the mix design. |
| Sedran et al. (1996) | Based on solid suspension model. The main principle is that partial water is used to fill up the voids in between the binder and coarse aggregate, while the rest of water is used to control the workability of concrete. Minimizing the void space can be achieved by optimizing the packing densities of solid materials. | Solid suspension model is used to optimize binder and aggregate. Water content is minimized and arbitrary viscosity is chosen. | The use of the model requires proprietary software. The calculations of rheology parameters are empirical with the BTRHEOM rheometer which typically gives higher numbers than other rheometers. |
| LCPC (2000) | Similar to Sedran method using solid suspension model and compressible packing model. The intent of the model is to reduce the high paste volumes sometimes associated with SCC. | By using a computer software SCCMix to simulate mix proportion based on selecting of a set of requirements. | Similar to Sedran method but it is difficult for others to adopt their method without purchasing the software. |
| Particle-Matrix model | The model takes advantages of de Larrard (1992) two-phase model. The aggregates are characterized with the air voids modulus. Paste rheology is characterized with the flow resistance ratio which can be measured with the FlowCyl device. Workability is measured at various paste volumes for each ratio and modulus. The derived equations are used to predict the changes of mix design and help to select the mix proportions. | Using flow resistance ratio and air voids modulus to characterize the paste rheology and aggregate characteristics, respectively. | Both flow resistance ratio and air voids modulus may not be the best parameters to characterize the paste rheology and aggregate features. More work is needed to optimize the paste rheology. The workability is only characterized by the use of a BML viscometer. |
| Excess paste theory | By calculating the relative excess paste thickness to predict the yield stress and plastic viscosity of the concrete related to the paste. | Accurate model to predict Bingham parameters based on aggregate properties, paste volume, and paste rheology parameters. | The Bingham parameters for paste and concrete need to be tested by a consistent manner so that they can be predicted accurately. The calculation process is intensive. |
| Su et al. (2001) | The fine and coarse aggregates are chosen based on loosely packed densities and packing factors. Cementitious materials, such as fly ash and slag, are added to fill up the voids between aggregates. Flow table test is used to determine the water demands. | A packing factor is used to select the contents of aggregate and a flow table test is used to determine the water content. | Little or no guidelines are provided to choose the slag, fly ash, and packing factor. Strength determination is very empirical. |
| CBI and extension | Concrete is considered as a solid aggregate phase in a liquid paste phase formed by the powder, water and admixtures. Aggregate properties are used to support the minimum required paste volume selection. Aggregates are treated spherically. | Mixes can be designed for a specific bar spacing and for achieving sufficient lubrication between the aggregate particles. | Criteria for the selection of micro-mortar rheology and the amount of micro-mortar are not well defined. |
| Statistical design | Central composite response surface is most commonly used technique. Ranges of binder content, HRWRA dosage range, w/p ratio range, and coarse aggregate range are given to develop a testing matrix in order to reduce the intensive labor work and trial mixes. | Statistical design of experiment is introduced. Regression models are used to evaluate data and optimize the proportions. | The regression models are specific to the materials and range of proportions considered. Statistical mix design background is needed to develop the test plan. |

**Table 2: Basic concepts, unique features, and limitations of each SCC proportioning method (cont.)**

| Method | Basic Concepts | Unique Features | Limitations |
|---|---|---|---|
| ACBM | Similar to the extension of CBI method: select the minimum paste volume based on blocking, segregation, flowability, and surface finishability criteria. Self-flow zone is introduced with paste rheology model. Proper yield stress and apparent viscosity must be obtained experimentally to ensure a good flowability and segregation resistance. | Specific equations are provided to calculate the paste volume. Rheology model is established in order to reduce the extensive lab work and materials use. | Some assumption must be made, such as spherical aggregate particle size and averaged spacing between aggregates. Limited guidance is provided for selecting the average aggregate particle distance. A particular rheometer is necessary to fulfill the self-flow zone. |
| EFNARC | Similar to Rational Mix Design Method | Similar to Rational Mix Design Method | Similar to Rational Mix Design Method |
| Concrete Manager Software | A theoretical packing model and Mooney's equation are used to predict the relative viscosity which can be related to concrete workability. Compare the software developed mix proportion and rheology results to the trial batch results, and then adjust the mix proportions. | By using a computer software and a unique capillary rheometer to generate mix proportion and evaluate trial concrete batches base on selecting of a set of requirements. | It is difficult for others to adopt their method without purchasing the software. Hardened concrete properties are not taken into considerations of mix design. The calculations are complex. |
| DMDA | To select the optimum blend of aggregate and fly ash that result in minimum voids. A factor is set as the volume of voids between aggregates and fly ash. Hardened concrete requirements decide the paste compositions. | Fly ash is treated as a part of aggregates rather than that of the paste. | The combination of aggregate and fly ash may not give a desired workability for a particular application. |
| Brouwers et al. (2005) | Mix design algorithm is built on Su et al. (2001) method, solid suspension model (de Larrard et al. 1994), packing density model, and two phase model. A curve fitting problem regarding modified A&A grading is addressed by least square method. Based on the provided ranges for each of the volumetric portions and predefined constraints, Solver Tool and Visual Basic can be used to design the mix. | All the solid ingredients are taken into considerations of packing. A modified A&A packing model is introduced. | The mix design algorithm is complex and some of the materials ranges of the direct inputs for the algorithm are not established clearly. |
| ACI Committee 237R-07 | Similar to ACI mix design method of conventional concrete. Take considerations of real structure features and limit the volume of coarse aggregate, paste and mortar fractions, typical w/p ratio and powder content. | Structure type is considered from precast industry and concrete strength requirements are specified. | It is an empirical method and may not be able to identify the effects of SCMs on mixtures. |
| ICAR | Aggregates, paste volume, and paste composition are selected based on the application and typical ranges are given to help on selection. | Aggregate characteristics and packing density theory are used to minimize paste content in SCC mixtures. | Lab work intensive. |
| UCL | Performance based design method. Mortar flow (mini slump and mini v-funnel) is used to determine the w/cm ratio. | Design criteria are specified and practical. | This method is more suitable for powder type SCC with coarse aggregate of 20 mm or 16 mm maximum size, crushed or uncrushed. It is a highly empirical method using plots generated from limited materials. |
| Compressive strength based | Based on the required strength to determine the w/cm ratio and water content. | Especially emphasize the mix design based on concrete strength, as is the case in the design of conventional concrete mixtures. The effect of grading and fineness of fine and coarse aggregate is considered. | Lack of considerations on SCMs effects. More mechanical and durability tests are needed to evaluate this mix design method. |

**Table 3 - The relationship between test methods and the properties that they measure**

| Test method | Early age concrete performance | | | | limitations |
|---|---|---|---|---|---|
| | Stiffening | Setting | Hardening | Strength | |
| Penetration resistance [1] | Not useful | Standard test to measure setting times | Up to final set | Penetration resistance of sieved mortar mixture, but not useful to predict concrete strength | The definitions of initial and final setting based on penetration resistance seem to be arbitrary. It is a time consuming method with large error of single operator and multi-laboratory. |
| Calorimetry [9-13] | Not useful | Potential to predict setting time based on temperature rise | Not useful | Maturity is used very often by field engineers to predict early age strength of concrete. | Need more guidelines to interpolate hydration temperature with concrete performance. |
| Wave propagation method [15-34] | Not useful | Features on UPV development have a potential to predict initial setting time. | Not useful | Can be used to predict elastic modulus and Poisson's ratio associated with Rayleigh wave | Contradictory conclusions may be drawn from previous researchers. |
| Formwork pressure [2, 35] | Highly related to thixotropy of a mixture before setting | Autogenous shrinkage caused volume change occurs around initial setting time. | Not useful | Not useful | Laboratory test apparatus may not be able to rigorously simulate the in-situ formwork pressure beyond initial set. |

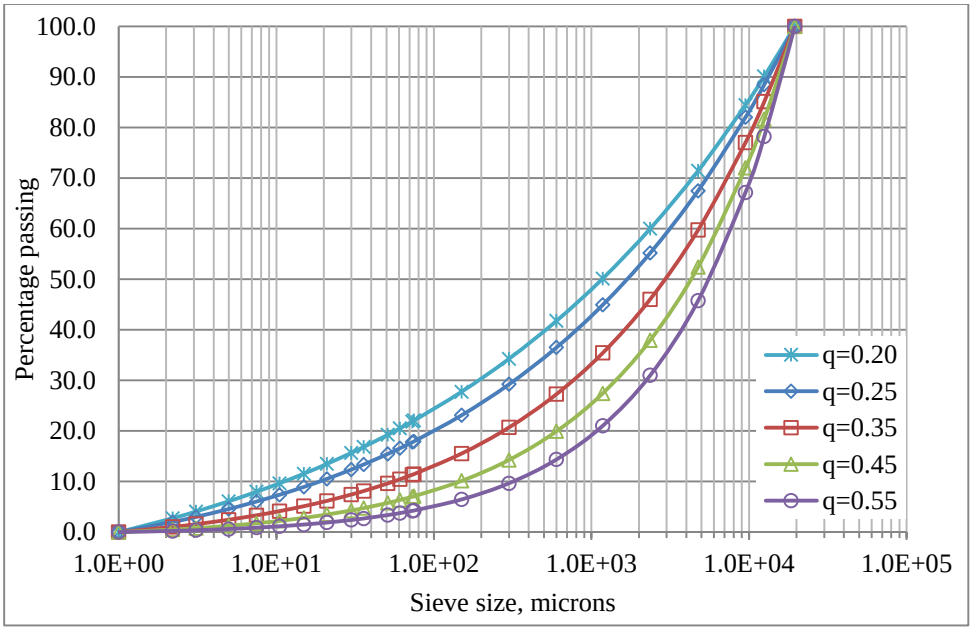


**Figure 1. Modified A&A model with various q values.**

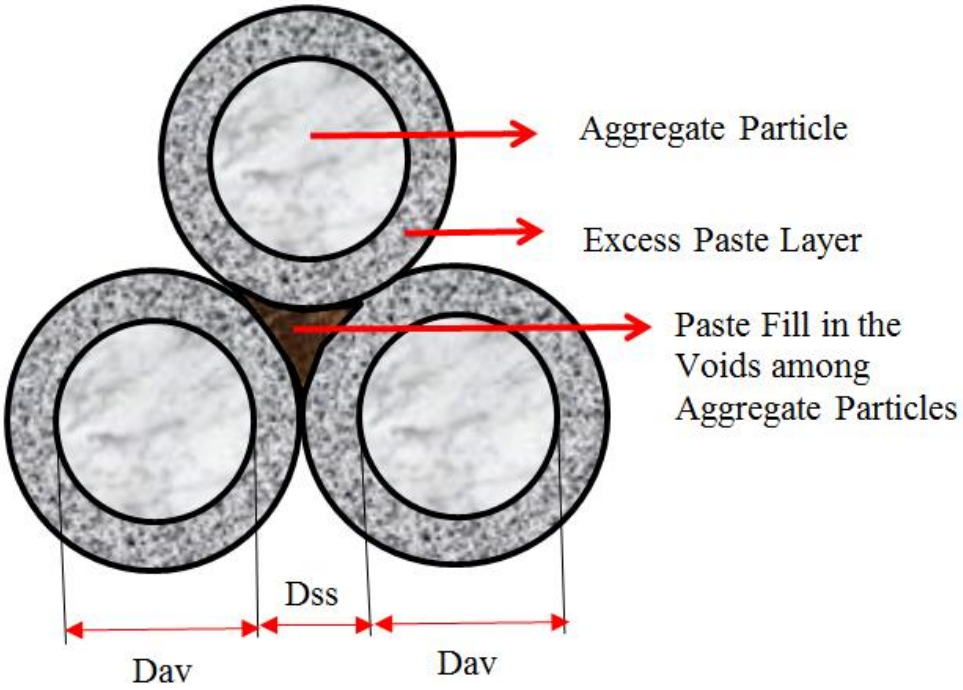


**Figure 2. Spherical aggregate particles, aggregate spacing $D_{ss}$, and average aggregate diameter $D_{av}$ (Bui et al. 2002).**

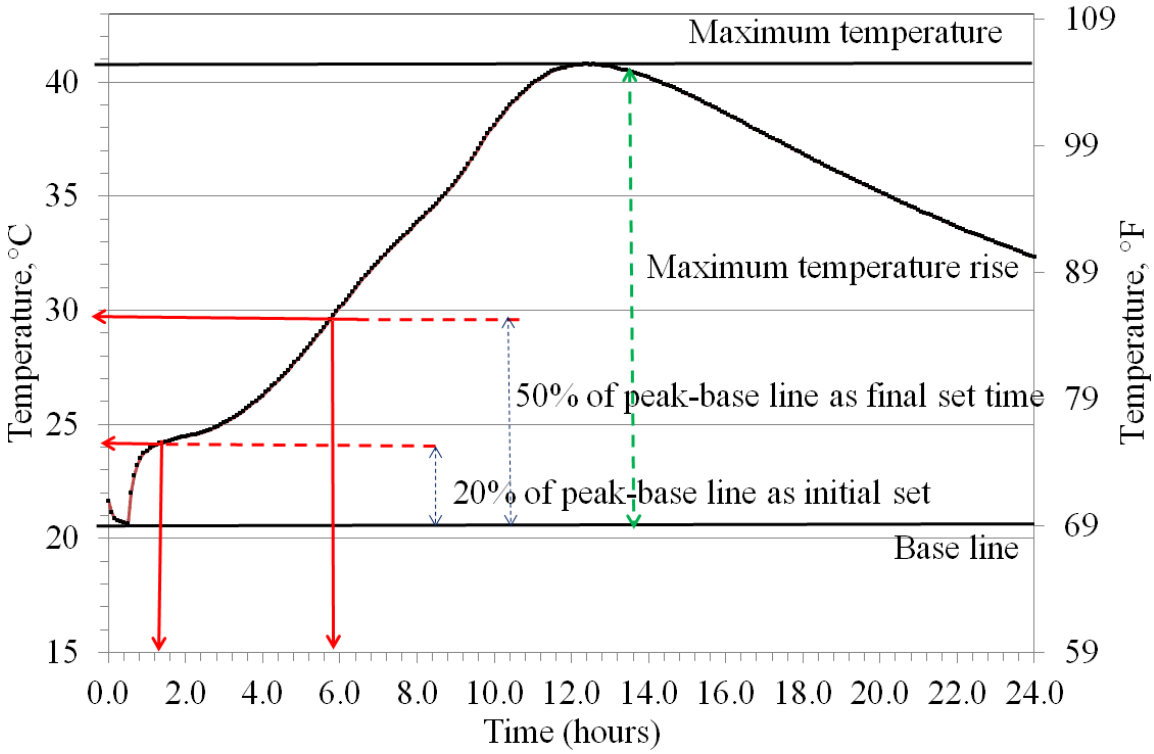


**Figure 3. Calculation of setting times determined by "fraction" method of a typical thermal profile.**

# CHAPTER 3. ASSESSING PARTICLE PACKING BASED SELF-CONSOLIDATING CONCRETE MIX DESIGN

A paper submitted to Journal of Construction and Building Materials

*Xuhao Wang[1], Kejin Wang[2], Peter Taylor[3], George Morcous[4]*

## ABSTRACT

A particle-packing based mix design method, originally proposed by Brouwers, is modified and applied to the design of self-consolidating concrete (SCC) mix proportions. The essence of this method is to improve particle packing of the concrete system and reduce the paste quantity while maintaining concrete quality and performance. Using this method, a large matrix of SCC mixes, made of different aggregate types, sizes, and supplementary cementitious material (SCMs) types, was designed to have a particle distribution modulus (q) ranging from 0.23 to 0.29. Fresh properties (such as flowability, passing ability, segregation resistance, yield stress, viscosity, set time and formwork pressure) and hardened properties (such as compressive strength, surface resistance, shrinkage, and air structure) of these concrete mixes were experimentally evaluated. The concrete mixes designed using the

[1] Research Assistant, Department of Civil, Construction and Environmental Engineering, Iowa State University, 136 Town Engineering, Ames, Iowa 50011, Tel: 515-294-2252, Email: wangxh@iastate.edu

[2] Professor, Department of Civil, Construction and Environmental Engineering, Iowa State University, 492 Town Engineering, Ames, Iowa 50011, Tel: 515-294-2152, Email: kejinw@iastate.edu

[3] Associate Director, National Concrete Pavement Technology Center, Iowa State University, Ames, Iowa 50011, Tel: 515-294-9333, Email: ptaylor@iastate.edu

[4] Associate Professor, The Durham School of Architectural Engineering and Construction, University of Nebraska-Lincoln, Peter Kiewit Institute 105B, Omaha, NE 68182, Tel: 402-554-2544, Email: gmorcous2@unl.edu

modified Brouwers mix design algorithm and particle packing concept had a potential to reduce up to 20% SCMs content compared to existing SCC mix proportioning methods and still maintain good performance.

**Keywords:** Self-consolidating concrete, mix design, particle packing, performance test, rheology

## INTRODUCTION

Self-consolidating concrete (SCC), as an innovation in concrete technology, has passed from the research stage to field application in the precast and cast-in-place (CIP) industries. To date, more than 17 proportion methods have been proposed worldwide. Even though there are an enormous number of publications on laboratory SCC mix design studies, there is no unique solution for any given application. Table 1 summarizes the possible ranges of the ingredient proportions recommended by a set of selected design methods.

Although the methods vary widely in overall approach and the level of complexity, most methods are proportioned to achieve desirable fresh concrete properties, such as passing ability, filling ability, segregation resistance, etc. (Bui et al. 1999). It is generally agreed that controlling the aggregate system, paste quality, and paste quantity is essential for SCC mix design. Minimizing void content can permit more paste to cover aggregate surfaces in a given concrete system, thus improving workability. Reducing capillary pores, can further enhance concrete strength and durability (Powers 1968). Previous studies have evaluated the performance of SCC mixtures using the paste-to-voids volume ratio concept that emphasized assessing the effect of paste quantity and voids of mix in a given aggregate system (Wang et al. 2014).

This study aims to apply the improved particle packing based mix design method to SCC mix design and to minimize the paste quantity whilst maintaining concrete performance.

## BACKGROUND

SCC, as a type of high performance concrete, comprises materials that have an enormous size range, i.e., from powder in the nano-meter (nm) range, up to very coarse particles, which can be as large as 25 mm (Hunger 2010). The influence of the particle size distribution (PSD), governing both packing and internal specific surface area, has been reported (Feret 1892; Fuller et al. 1907; Furnas 1931). Brouwers and Radix (2005) proposed a particle packing based mix design method that considered the grading of all solids in a SCC mixture.

### Particle packing theory development

There is a number of packing models available to describe both continuous and discrete packing. Five basic models were reviewed by Jones et al. (2002): (1) Toufar, and modified Aim and Toufar model; (2) Dewar model; (3) Linear packing model (LPM); (4) Further development of the solid suspension model (SSM); (5) Compressible packing model (CPM). The LPM, the SSM and the CPM are so called third generation packing models.

Hunger (2010) stated that the amount of solids in coarse and fine sections should be optimized separately because the fine fractions primarily contribute to the porosity of a mixture. An integral approach based on the particle size distribution of all solids is not found very often.

Aggregate selection for optimal packing density may follow one of several suggested ideal particle size distributions, empirical tests on various blends of aggregates, or a mathematical model (Koehler 2007). In the majority of cases, continuously graded granular

blends are described using the Fuller parabola, which represents the basic principle of most standard aggregate grading curves (Hunger 2010). This power law size distribution is described in Equation 1:

$$P_t = (\frac{d}{d_{max}})^{\frac{1}{2}} \quad \text{Eq. 1}$$

where $P_t$ is a fraction of the total solids (aggregate and SCMs) being smaller than size d, and $d_{max}$ is the maximum particle size of the total grading. However, this equation has a deficiency in that it can never be fulfilled in practice because it assumes particles of infinite fineness, i.e., $d_{min}$ =0, which is not the real case. Moreover, in order to avoid the lean mixtures, researchers further stipulated that at least seven percent of the total solids should be finer than the No. 200 sieve (0.074 mm opening). Powers (1968) proposed another parabolic particle size distribution in which the power 0.5 is described as exponent q in Equation 2:

$$P_t = (\frac{d}{d_{max}})^{q} \quad \text{Eq. 2}$$

Andreasen and Andersen (1930) reported that the voids content only depends on the value of q, which is called the distribution modulus. However, when the q value approaches zero, the void content follows as well. Due to the inability of fine particles to pack in a similar manner as bigger but geometrically similar particles, Andreasen and Andersen limited the increase of packing to a range of q=0.33 to 0.50 (Hunger 2010). Asphalt concrete mixtures design has been using a distribution modulus of 0.45 as a theoretical maximum packing density (Kennedy et al. 1994). Stern (1932) extended the minimum $d_{min}$ down to 1 µm in order to include the particles. Hummel (1959) referred to a different q value of 0.4 for achieving maximum packing density with aggregate varying in shape. De Larrard (1999) found that the values of the exponent for optimizing packing density varied with the packing

density of the individual size fractions and the degree of compaction. Therefore, it is not possible to establish an optimal particle size distribution for all cases.

Plum (1950) introduced a finite minimum size and measured minimum d = 0.291 µm that comes very close to the average size of cements used today. Including the minimum particle size, Plum (1950) derived the expression in Equation 3:

$$P_t = \frac{q^n - 1}{q^N - 1} \text{ for } q \neq 1 \qquad \text{Eq. 3}$$

With q being the distribution modulus, and n and N being the sieve numbers of the respective and largest sieve. However, he was aware that this may not be a practical solution. In this respect, Plum remarked that the all fractions below 0.149 mm cannot be so easily derived. Also, he justified that the cement was practically the sole ingredient below that size and that cement had to be accepted in natural grading it was supplied (Hunger 2010). Funk and Dinger (1994), who were interested in the packing of particles applied to ceramic manufacturing modified Andreasen and Andersen grading model (A&A model) in Equation 4:

$$P_t = \frac{d^q - d_{min}^q}{d_{max}^q - d_{min}^q} \qquad \text{Eq. 4}$$

where, the exponent q controls the character of the generated mix regarding its fineness of grain; $d_{max}$ and $d_{min}$ denote maximum sieve size (i.e., where 100% passing takes place) and minimum particle size, respectively. It is assumed that this distribution law delivers a feasible solution for a practical purpose.

**Brouwers' mix design method**

Brouwers (2005) proposed method includes overruling more conventional models and theories. SCC mixtures were defined as a mixture of solid (i.e., aggregate, powders, and solid

material in admixtures), water, and air. Packing of the solid system depends on the shape of individual particles, surface potential of the solids, the amount of mixing water, and the applied of compaction energy. The solids could be both reactive and non-reactive in nature. However, their reactivity was considered to have no impact on packing in the fresh state. A water layer of constant thickness around every particle was considered to control flowing (Hunger 2010). The mix proportioning algorithm can be divided into following portions:

- Step 1: Fit target grading curve. It aims at minimizing the deviation of the actual from the desired grading by combining all the solid ingredients using the modified A&A grading model in Equation 5. A spreadsheet solver tool and Visual Basic can be used for target curve fitting based on minimizing sum of the squares of the residuals (RSS) expressed in Equation 5. The coefficient of determination, $R^2$ in Equation 6, should be considered to evaluate the quality of the curve fit, which expresses the variation between the target line and the obtained values for the actual grading.

  $$\text{RSS} = \sum_{i=1}^{n}(P_m(D_i) - P_t(D_i))^2 \Rightarrow \text{Minimum} \quad \text{Eq. 5}$$

  $$R^2 = 1 - \frac{\sum_{i=1}^{n}(P_m(D_i) - P_t(D_i))}{\sum_{i=1}^{n}(P_m(D_i) - \overline{P_m})} \text{ with } \overline{P_m} = \frac{1}{n}\sum_{i=1}^{n}(P_m(D_i)) \quad \text{Eq. 6}$$

  where, $P_m(D_i)$ denotes the volume fraction of the solid ingredients in a mixture multiplied by percentage passing of those solids from each sieve. $P_t(D_i)$ denotes target percentage passing each corresponding sieve using modified A&A grading model multiplied by percentage passing each sieve.
- Step 2: Adjust volumetric fractions. One cubic meter of fresh concrete is composed of solids ($V_{solid}$), water ($V_w$), and voids ($V_{air}$) as shown in Equation 7:

  $$V_{solid} = \sum_{k=1}^{m} V_{solid,k} = V_{total} - V_w - V_{air} \quad \text{Eq. 7}$$
- Step 3: Provide boundary conditions and constraints. Some physical and policy constraints and boundary conditions need to be applied to the algorithm.
  - Non-negativity constraint: the volumetric proportion of $V_{solid,k}$ of a selected material for k = 1, 2, …, m cannot be negative.
  - Volumetric constraint: the sum of volumetric proportion of raw materials must equal 100%.

- Policy constraints:
  - Cement content: provide the range of minimum and maximum cement factor
  - Water content: ratio of w/cm ratio
  - Optimization target: set distribution modulus between 0.21 and 0.25.
  - Air content: desired air content.

The mix proportion can be solved numerically based on selected solid materials, chemical admixtures, and physical properties of materials, such as specific gravity and absorption.

However, several limitations exist in Brouwers' method:

- Lack of diversified materials, such as different aggregate types, gradations, sizes, and SCMs types and dosages, were used to evaluate the recommended range of distribution modulus, i.e., 0.21 to 0.25.
- Constraints were not clearly defined, such as coarse aggregate volume content, w/cm ratio, sand to aggregate ratio, and paste volume, e.g., a w/cm ratio of 0.55 can be yield from the design method, but it may result in unexpected free shrinkage.
- The definitions of maximum and minimum particle diameter were not clearly defined. This may dramatically change the mix proportion of given materials with specified q value.
- The economical comparison was not made to the other existing SCC design method for a given mixture.

**PROPOSED MIX DESIGN METHOD**

The proposed SCC mix design method has similar algorithm as Brouwers' method but it was modified to overcome the limitations. The summary of input parameters and constraints of both methods is shown in Table 2.

With the help of the modified algorithm, an example of a mix (dashed line) is presented in comparison to the target function (solid line) given in Figure 1 as along with PSDs of all

solids in the mixture. The distribution modulus amounts was 0.25. Output is the volume of selected materials. Selected chemical admixtures, such as air entraining agent (AEA) and high range water reducer (HRWR) admixtures, are calculated based on recommended dosage and SCMs contents.

The key to apply the modified A&A model to design SCC mixtures is the distribution modulus, q. Brouwers (2006) stated that the q value in the range from 0.25 to 0.35 was found to be reasonable based on dry packing tests. He also mathematically proved that a q of 0.28 resulted in optimum packing in terms of minimized voids ratio. Hunger (2010) recommended using distribution moduli in a range between 0.21 and 0.25 for SCC mix proportions because higher values lead to mixtures ($q>0.25$) which are too coarse and prone to segregation and blocking. However, lower values mixtures ($q<0.21$) deliver fines-rich granular blends which suffer from high cohesion due to the dense packing and high amount of fines. In this study, the range between 0.23 and 0.29 for q was selected to cover both the above extremes.

Table 3 gives the mix proportion of a typical SCC mix with varied q values within the range between 0.23 and 0.29. The mix proportions seem to be sensitive to the selected q values (0.23 and 0.29): at a given w/cm and fine aggregate/total aggregate ratio, the binder content and paste volume may have up to 70 kg/m$^3$ and 5% difference, respectively. An increment of q value tends to reduce the cementitious material content and paste volume, resulting in a more economical mixture.

Table 4 summarizes the mix proportions for a typical SCC mixture following different mix design methods. All of the mix proportions were designed for a CIP application, and the materials were chosen from following section. Up to 20% reduction of cementitious material content can be observed from proposed method resulting in a cost-efficient mix proportion.

In this study, the modified Brouwers' method is applied to the design of various self-consolidating concrete (SCC) mix proportions. To ensure such designed mixes to meet required performance, fresh and hardened concrete properties of the SCC mixes were experimentally evaluated. The experimental work is presented in the following.

## EXPERIMENTAL WORK

### Materials

Materials for the SCC mixtures prepared include:

- Coarse aggregate types: crushed limestone (LS) and river gravel (G);
- Coarse aggregate sizes: 19 mm (a), 12.5 mm (b), and 9.5 mm (c);
- SCMs: Class C and F fly ashes (C and F) with 25% replacement level, slag cement (S) 30% replacement level;
- Limestone dust (LD) amounts: 0 and 15% cement replacement.

Six conventional concrete (CC) mixtures with 25% class F fly ash were used as controls.

The physical properties of aggregate used in this research are shown in Table 5. The PSDs of all the solids used in this study are given in Figure 2. Table 6 lists the chemical properties of SCMs.

The chemical admixtures used were Air-Entraining Agent (AEA), polycarboxylate based High Range Water Reducer (HRWR), and Viscosity-Modifying Admixture (VMA).

### Mix proportions

The mixture proportions listed in Table 7 are designed based on modified Brouwers' method.

**Test equipment and procedures**

*Workability*

Slump flow, segregation resistance, and blocking assessment were determined in accordance with ASTM C1611, C1611, and C1621, respectively. The flow time for SCC mixtures reaching diameter of 500 mm, $t_{50}$, and flow time until concrete stopped flowing, $t_{final}$, were recorded.

The workability retention was determined by the difference between slump flow after mixing and 30 minutes after mixing.

*Air content*

Air contents of all the mixtures were determined in accordance with ASTM C231.

*Rheology of mortar mixtures*

The Bingham model parameters, yield stress and viscosity, were used to characterize the mortar rheology using a Brookfield rheometer. Mortar samples were sieved from the concrete mixtures using a 4.75 mm size sieve. The sample was placed in a 50 mm diameter by 100 mm tall cylindrical vessel and sheared by a 15×30 mm vane spindle. The employed loading history is shown in Figure 3(a) based on Wang et al. (2013) and a typical flow curve for a SCC mixture used in this study is shown in Figure 3(b). The intersection to the y-axis and the slope of the linear fit model represent the yield stress and viscosity, respectively.

*Rheology of concrete mixtures*

Immediately after workability test, the concrete was poured into an IBB rheometer sample bowl for testing using an H-shaped impeller. The loading history is showed in Figure 4(a) (Hu and Wang 2010). In order to obtain a uniform sample, the concrete sample was

- Pre-sheared at 0.2 rev./s for 25 s
- Stopped for 25 s

- 100 s of increasing impeller speed from 0 to 1 rev./s
- 100 s of decreasing impeller speed to 0.

Similar to rheology testing of mortar mixtures, the yield torque (G) and slope (H) were obtained from the unloading part of the flow curve (Figure 4(b)). Thixotropy was assessed by determining the difference between the up curve and down curve.

*Formwork pressure*

The lateral pressure of both CC and SCC mixtures was measured using the test setup shown in Figure 5 (Lomboy et al. 2013). The test apparatus comprised a 0.9 m long by 0.2 m diameter PVC water pipe with removable steel caps on both ends. Three flush diaphragm pressure sensors were installed through the side of the pipe 0.3 m apart to measure the pressure distribution over the height of the column. An air pressure gauge and an air valve were installed at the top cap to simulate high concrete pressures by increasing the air pressure at the top portion of the concrete column.

Concrete was poured in the pipe at a constant rate of 0.15 m/min to simulate reasonable field concrete practice starting approximately 40 minutes after mixing. No mechanical consolidation was used for SCC mixtures, while an internal vibrator was used to consolidate the CC mixtures in 0.3 m lifts. Air was pumped into the pipe at the same loading rate up to 0.2 MPa to simulate 9.1 m of concrete head after the concrete was filled up to 0.3 m above the top sensor. The pressure at each sensor was continuously recorded every minute until the lateral pressure reached a constant value.

*Setting time*

Setting times of selected mixtures were determined in accordance with ASTM C 403.

*Compressive strength and shrinkage*

Compressive strength and free shrinkage of the concrete mixtures were measured in accordance with ASTM C39 and C157, respectively. The compressive strengths were taken at 56 days and free shrinkage was measured up to 56 days. The concrete prisms for free shrinkage test were moist cured for 7 days and then transferred to the drying room and maintained at 50% ± 4% relative humidity and a temperature of 23 ± 2˚C.

Two concrete rings were cast to assess the potential for shrinkage induced cracking in accordance with modified ASTM C1581. The geometry of the restrained ring was similar to Wang (2012) as shown in Figure 6. Paraffin wax was used to seal the top surface of the ring to only allow the moisture loss from the side. The changes of steel strain attributed by concrete shrinking were measured by two strain gages mounted on the inner face of the ring. Data were recorded every one minute up to 28 days or until the concrete cracked.

*Surface resistivity*

The surface resistivity test is a promising alternative to the rapid chloride penetrability test (RCPT) to indirectly assess the permeability of concrete mixtures (Rupnow and Icenogle 2012; AASHTO TP 95 2011; Kessler et al. 2008). Surface resistivity results were determined in accordance with the instructions for a commercial device (Proceq 2011). Three concrete cylindrical specimens for each mixture were prepared. The specimens were stored in a moisture room at 23 ˚C after casting. Tests were conducted at 28 days and recorded as an average value of three specimens.

*Rapid air test*

The air content, spacing factor, and specific surface of hardened concrete specimen at 28 days for each mix were determined using a linear traverse method in accordance with ASTM C457.

## RESULTS AND DISCUSSION

Criteria used to evaluate the performance of the designed SCC mixes were determined based on the recommendations from literature and the States Department of Transportation Specifications as listed in Table 8. The measured fresh and hardened concrete properties are tabulated in Table 9. Test results falling within the acceptable and bad ranges of criteria are highlighted in yellow and red cells, respectively. The results falling into the good ranges of criteria are not highlighted.

### Fresh properties

*Workability*

The slump flow, measured after approximately 15 minutes of mixing, ranged from 597 to 762 mm. Only one SCC mix has less than one second $T_{50}$ value, which provides an indication of the relative low viscosity and the segregation resistance (Khayat et al. 2004). The passing ability assessed by J-ring test indicates that all SCC mixtures fall within no visible blocking or minimal to noticeable blocking categories in accordance with ASTM C1621. Few SCC mixtures with larger size coarse aggregate (19.0 and 12.5 mm) and low slump flow (550 – 650 mm) tend to have a noticeable blocking potential.

Most mixtures have Visual Stability Index (VSI) less than 1 that indicates good static segregation resistance in accordance with ASTM C1611. Mixtures designed by the modified method tend to have a higher segregation potential when slump flows are greater than 700 mm. This observation is apparent for those mixtures made by 19.0 and 12.5 mm coarse aggregate because larger aggregate with higher self-weight may require a more viscous paste to resist the segregation. Even though the VSI test may be subjective depending on the

operator and it cannot reflect the dynamic stability during the transporting and pumping for CIP structure, it still provides a valuable quality control prospective.

Workability retention was quantified by measuring the difference in slump flow after mixing and 30 minutes after mixing. From Table 9, the differences of very few mixtures are less than 62 mm which was recommended by Khayat and Mitchell (2009) for precast and prestressed concrete bridge elements. However, they also stated that the required consistency retention will depend on the application and precast concrete is likely to require a shorter retention time than cast-in-place concrete.

*Rheology and formwork pressure*

Previous researchers have studied the interaction between the slump flow spread, flow time ($T_{50}$), yield stress, viscosity and thixotropy for SCC mixtures (Grunewald and Walraven 2003; Jin and Domone 2002; Domone and Jin 1999). It is generally agreed that the slump flow spread is not a unique function of yield stress, but rather a complex function of both yield stress and viscosity. Due to differing mortar and concrete rheometer and shear histories used worldwide, it is difficult to provide a unique range for charactering the SCC mixtures by simply using Bingham parameters, i.e., yield stress and viscosity.

The correlation between slump flow values and rheological parameters is shown in Figure 7 which is different from previously established manner (ACM Centre 2005; Nielsen and Wallevik 2003). Generally, slump flow increases with decreased yield torque and slope. SCC mixtures made by gravel have higher yield torque but lower slope than limestone SCC mixtures regardless of size. Limestone particles of more angularity cause more particle-to-particle interlock than gravel particles resulting in higher viscosity, while the characteristics of limestone particles may lead to an increased packing density that improves the flow and

reduces the yield torque (Erdogan and Fowler 2005). Lu and Wang (2008) stated that the shear resistance of granular materials is directly correlated to inter-particle fraction or friction coefficient, and independent of the size and gradation of granular materials. This explains difference rheological behavior of limestone and gravel mixtures.

A relationship between the yield stress derived from mortar rheology measurements and the yield torque from concrete flow curve is given in Figure 8. Linear relationships are found for both gravel and limestone SCC mixtures. This is in agreement with reports that the effect of coarse aggregate particles on rheological properties is not significantly influenced by the properties of the suspending medium (Erdogan and Fowler 2005).

Currently, formwork pressure for SCC is based on the assumption that the pressure exerted to the form is equal to the hydrostatic pressure exerted by a fluid having the same density of concrete (Gregori et al. 2008). The high pressure requires robust formwork construction and joint sealing that adversely affects the profitability. Researchers have been working on finding out the factors that affect formwork pressure and have concluded that formwork pressures less than hydrostatic are achievable (Gregori et al. 2008; Assaad 2004; Fedroff and Frosch 2004; Brameshuber and Uebachs 2003). Results have indicated that mix composition affects the kinetics of a structure buildup and thixotropy which are the key factors that influence the formwork pressure.

In this study, selected CC and SCC mixtures have been investigated to see the correlations between maximum exerted-pressure to hydrostatic-pressure ratio ($P_{maximum}/P_{hydrostatic}$) and thixotropy and yield torque of concrete mixtures. Results are shown in Figures 9 (a) and (b), respectively. All tested SCC mixtures exhibit high initial lateral pressures, greater than 93% of hydrostatic pressure, which is higher than CC mixtures with

external vibration during casting. Gravel mixtures seem to have a lower ratio of $P_{maximum}/P_{hydrostatic}$ compared to limestone mixtures which is most likely attributed to their higher yield torque and faster structural buildup. $P_{maximum}/P_{hydrostatic}$ exhibits a linear relationship with thixotropy and yield torque of concrete mixtures which is in agreement with literature (Assaad et al. 2003).

**Hardened properties**

*Surface resistivity and compressive strength*

The criteria for surface resistivity were set in accordance with the classifications proposed by Louisiana Department of Transportation and Development (LADOTD) (2011). The qualitative relationship between the charge passing using ASTM C1202 and the surface resistivity for 100 × 200 mm cylindrical specimens was established in Table 10 and a dimensionless correction factor was applied to account for the geometry and size of the specimen.

The test results shown in Table 9 indicate that the surface resistivity values of only three SCC mixtures correspond to moderate permeability, while others fall within the low and very low ranges. Generally, higher paste volume tends to have higher permeability despite the reduction in the amount of the more porous interfacial transition zone (Scrivener and Nemati 1996). This is because paste is more permeable than aggregate (Kosmatka 2011). The mixtures containing slag cement seem to have much higher resistivity than the others.

The compressive strengths of all tested mixtures at 56 days are higher than 27.6 MPa. The w/cm, aggregate type and sizes, and paste compositions effects on the strength have been discussed elsewhere (Wang et al. 2014).

*Air structure*

Established thresholds for air void structure, >6±1 percent air, specific surface ≥ 24 $mm^{-1}$, and spacing factor ≤ 0.20 mm are expected to give good concrete freeze-thaw resistance (FHWA 2007). However, Ley and his coworkers (2012) extended minimum air content to 3.5% for yielding a durable concrete in accordance with ASTM C666, despite using a synthetic, wood rosin, and Vinsol resin air entraining agent.

The air void parameters listed in Table 9 indicate all the tested mixtures have spacing factors less than 0.20 mm. Only SCC 19 has a specific surface value slightly smaller than 24 $mm^{-1}$, while others satisfy the 24 $mm^{-1}$ threshold. Four mixtures with air content measured in accordance with ASTM C457 were lower than 3.5%, while only one mix had fresh air content lower than 3.5%. The relationship between air content measured by linear traverse and pressure methods is shown in Figure 10. A linear trend line passing origin with R square value of 61% indicates a good correlation between air content measured by those two methods.

*Shrinkage*

The 28-day free shrinkage was evaluated and listed in Table 9 in order to compare with the restrained shrinkage strain. The free shrinkage strain of SCC mixtures varied between 310 and 640 microstrain while that of the control mixtures varied from 360 to 520 microstrain. The ranges of shrinkage for both SCC and CC mixtures are higher than the mixtures evaluated by Schindler and his coworkers (2007) for prestressed members, i.e., 280 to 437 and 330 to 353 for SCC and CC mixtures, respectively. It is noted that only a single size and type of coarse aggregate and lower w/cm were used in their study. In addition, a shortened curing period, 7 days, was applied in this research to simulate the field condition. These factors likely increase the measured free shrinkage.

The shrinkage prediction equation in AASHTO LRFD only accounts for the humidity, curing method, age of the specimen, and volume-to-surface ratio, and only provides a single drying shrinkage strain at each age. A shrinkage value of 400 microstrain can be estimated in accordance with AASHTO LRFD (Section 5.4.2.3.3) yielding a range between 320 and 480 microstrain with 20% error. Therefore, 500 microstrain at 28 days was set as an empirical threshold value. The shrinkage of 75% of SCC mixtures is lower than this threshold as shown in Table 9.

Restrained shrinkage test was performed in order to assess the cracking behavior of SCC mixtures. Average cracking time of each mixture was recorded in Table 9. Average stress rates caused by shrinkage were estimated for both restrained and free shrinkage in the same manner based upon the method proposed by ASTM C1581, i.e., the slope of a linear fit on the shrinkage strain versus square root of age. Both parameters can be used to evaluate the cracking risk under a certain degree of restraint. 14 out of 40 mixtures were identified to have high cracking potential in accordance with ASTM C1581.

## CONCLUSIONS

The results of this study support the following conclusions:

The modified Brouwers' mix design algorithm using particle packing concept can be appropriately applied to produce SCC mix proportions for CIP applications, especially with the distribution modulus between 0.23 and 0.29. Relatively economical SCC mixtures can be developed with this modified algorithm that meets the proposed criteria and thresholds of CIP applications in fresh and hardened states:

1. The modified Brouwers mix design algorithm using particle packing concept can be appropriately applied to produce SCC mix proportions. The distribution modulus generally ranges from 0.23 to 0.29.
2. The mixes designed using the modified Brouwers' method contain relatively low paste quantity and therefore, they are relatively economical.
3. Almost all mixes designed using the modified Brouwers method exhibit good performance based on the criteria obtained from literature.
    - Workability: in general, the flowability, passing ability, stability, and workability retention of the SCC designed were satisfied with recommended dosage of HRWR admixture. Few mixtures may exhibit static stability violation and longer workability retention time, which can be improved by adjusting the HRWR dosage depending on the applications.
    - Surface resistivity and strength: most SCC mixtures fell within low and very low permeability class and have an estimated 28 days compressive strength higher than 27.6 Mpa.
    - Air structure: most tested SCC mixtures satisfied the well-established threshold on spacing factor, specific surface, and air content.
    - Shrinkage: 75% of tested mixtures satisfied the threshold of free shrinkage strain calculated based on AASHTO LRFD specifications, while 65% fell within moderate-high or moderate cracking potential classes in accordance with ASTM C1581.
4. The following relationships between the test results are found:
    - There is a relationship between slump and Bingham rheological parameters, a linear correlation between yield stress of mortar and yield torque of corresponding concrete mixtures measured from IBB and Brookfield rheometers, respectively.
    - The maximum exerted formwork pressure to hydrostatic pressure ratio was shown to linearly relate to thixotropy and yield torque of concrete mixtures. CC mixtures generally have much lower $P_{maximum}/P_{hydrostatic}$ compared to SCC mixtures which were mostly higher than 96%.

- A linear relationship was found between fresh air content and hardened air content measured by pressure and linear traverse methods, respectively.

## ACKNOWLEDGEMENTS

The authors acknowledge the research sponsorship and the cooperation from Northwestern University (NU) and the University of Nebraska – Lincoln (UNL). The opinions, findings, and conclusions presented in this paper are those of the authors and do not reflect those of the research sponsors.

## REFERENCES

AASHTO TP 95, "Standard Method of Test for Surface Resistivity of Concrete's Ability to Resist Chloride Ion Penetration," American Association of State Highway and Transportation Officials, Washington, DC., 2011.

ACM Centre; University of Paisley, "Measurement of Properties of Fresh Self- Compacting Concrete," European Union Growth Contract Final Report, Sep. 2005.

American Association of Highway and Transportation Officials (AASHTO), AASHTO LRFD Bridge Design Specifications, 6th Edition, Washington, DC., 2012.

American Concrete Institute (ACI) Committee 237, "Self-Consolidating Concrete," ACI 237R-07, Farmington Hills, MI: ACI.2007.

Andreasen, A.; Andersen, J., "U¨ ber die Beziehung zwischen Kornabstufungund Zwischenraum in Produkten aus losen K¨ornern (mit einigen Experimenten)", Kolloid-Zeitschrift 50: 217 – 228 (in German), 1930.

Assaad, J., "Formwork Pressure of Self-Consolidating Concrete—Influence of Thixotropy," Department de Genie Civil, Université de Sherbrooke, Sherbrooke, QC, Canada, pp. 445, 2004.

Assaad, J.; Khayat, K.; Mesbah, H., "Variation of Formwork Pressure with Thixotropy of Self-Consolidating Concrete," ACI Material Journal, V. 100, No.1, 2003.

Brameshuber, W.; and Uebachs, S., "Investigations on Formwork Pressure Using Self-Compacting Concrete," 3rd International Symposium on Self-Compacting Concrete, Reykjavik, Iceland, RILEM Publications, S.A.R.L., pp. 281-287, 2003.

Brouwers, H.; Radix, H., "Self-Compacting Concrete: Theoretical and Experimental Study," Cement and Concrete Research, 35, pp. 2116-2136, 2005.

Brouwers, H., "The Role of Nanotechnology for The Development of Sustainable Concrete," Proceedings of ACI Session on "Nanotechnology of Concrete: Recent Developments and Future Perspectives", Denver, USA, November 7, 2006.

Bui, V.; Montgomery, D., "Mixture Proportioning Method for Self-Compacting High Performance Concrete with Minimum Paste Volume," In: Proceedings of the First International RILEM Symposium on Self-Compacting Concrete, Stockholm, Sweden, RILEM Publications, Cachan, France, pp 373-396, Sep. 1999.

Daczko, A., "Self-Consolidating Concrete: Appling What We Know," Abingdon: Spon Press, 2012.

De Larrard, F., "Concrete mixture proportioning: a scientific approach," London: E & FN Spon. 1999.

Domone, P.; and Jin, J., "Properties of Mortar for Self-Compacting Concrete," RILEM symposium on SCC, pp. 109-120, Stockholm, 1999.

Domone, P., "Self-Compacting Concrete: An Analysis of 11 Years of Case Studies," Cement and Concrete Composites, 28, pp. 197-208, 2006.

Domone, P., "Proportioning of Self-Compacting Concrete – the UCL Method," University College London, November, 2009.

EFNARC European Project Group, "The European Guidelines for Self-Compacting Concrete: Specification, Production and Use," http://www. Efnarc.org/pdf/SCCGuidelinesMay2005.pdf. May, 2005.

Erdogan, S.; Fowler, D., "Determination of Aggregate Shape Properties Using X-Ray Tomographic Methods and the Effect of Shape on Concrete Rheology," ICAR report 106-1, the University of Texas at Austin, August, 2005.

Federal Highway Administration, "Freeze-Thaw Resistance of Concrete with Marginal Air Content," FHWA-HRT-06-118 TechBrief, 2007.

Fedroff, D.; Frosch, R., "Formwork for Self-Consolidating Concrete," *Concrete International*, V. 26, No. 10, pp. 32-37, Oct. 2004.

Feret, R., "Sur la compacite des mortiers hydrauliques," Ann. Ponts Chaussee, memoires et documents, Serie 7, no. IV, p.5-164 (in French), 1892.

Fuller, W.; Thompson, S., "The Laws of Proportioning Concrete," Trans. Am. Soc. Civ. Eng., Vol. 33, pp. 222-298, 1907.

Funk, J.; Dinger, D., "Predictive Process Control of Crowded Particulate Suspensions – Applied to Ceramic Manufacturing," Kluwer Academic Publishers, Massachusetts, 1994.

Furnas, C., "Grading Aggregates I-Mathematical Relations for Beds of Broken Solids of Maximum Density," Ind. Eng. Chem., Vol. 23, pp. 1052-1058, 1931.

Ghezal, A.; Khayat, K., "Optimization of Cost-Effective Self-Consolidating Concrete," Proceedings of the Second International Symposium on Self-Compacting Concrete, Tokyo, Japan, pp. 329-338, 2001.

Ghezal, A.; Khayat, K., "Optimizing Self-Consolidating Concrete with Limestone Filler by Using Statistical Factorial Design Methods," ACI Materials Journal, 99(3), pp. 264-272, 2002.

Gregori, A.; Ferron, R.; Sun, Z.; and Shah, S., "Experimental simulation of SCC Formwork Pressure," ACI Materials Journal, 105(1): pp. 97-104, 2008.

Grünewald, S.; Walraven J., "Rheological Measurements on Self-Compacting Fiber Reinforced Concrete", RILEM Symposium on SCC, PRO 33, Reykjavik, pp. 49-58, 2003.

Hu, J.; Wang, K., "Effect of Coarse Aggregate Characteristics on Concrete Rheology," Construction and Building Materials, 25, pp. 1196-1204, 2011.

Hummel, A., "Das Beton-ABC – Ein Lehrbuch der Technologie des Schwerbetons und des Leichtbetons", 11th edn, Wilhelm Ernst & Sohn, Berlin, 1959.

Hunger, M., "An Integral Design Concept for Ecological Self-Compacting Concrete," Ph.D thesis, Eindhoven University of Technology, The Netherlands, 2010.

Hwang, C.; Hung, M., "Durability Design and Performance of Self-Consolidating Lightweight Concrete," Construction and Building Materials,19, pp. 619-626, 2005.

Jin, J.; Domone, P., "Relationships between the Fresh Properties of SCC and Its Mortar Component," North American Conference on the Design and Use of Self-Consolidating Concrete, Chicago, pp. 33-38, 2002.

Jones, M.; Zheng, L.; and Newlands, M., "Comparison of Particle Packing Models for Proportioning Concrete Constituents for Minimum Voids Ratio," Materials and Structures 35(249), pp. 301 – 309, 2002.

Kennedy, T.; Huber, G.; Harrigan, E.; Cominsky, R.; Hughes, C.; Quintus, H.; Moulthrop, J., "Superior Performing Asphalt Pavements (Superpave): The Product of SHRP Asphalt Research Program," National Research council, SI-IRP-A-410, 1994.

Kessler, R.; Powers, R.; Vivas, E.; Paredes, M.; and Virmani, Y., "Surface Resistivity as an Indicator of Concrete Chloride Penetration Resistance," Presented at the 2008 Concrete Bridge Conference, St. Louis, MO, 2008.

Khayat, K.; Assaad, J.; Daczko, J. "Comparison of Field-Oriented Test Methods to Assess Dynamic Stability of Self-Consolidating Concrete, ACI Material Journal, V. 101, No. 2, Mar.-Apr., pp. 168-172, 2004.

Khayat, K.; Ghezal, A.; Hadriche, M., "Utility of Statistical Models in Proportioning Self-Consolidating Concrete," Proceedings of First International RILEM Symposium on Self Compacting Concrete, Stockholm, Sweden, pp. 345-359. 1999.

Khayat, K.; Mitchell, D., "Self-Consolidating Concrete for Precast, Prestressed Concrete Bridge Elements," National Cooperative Highway Research Program Report 628, Washinton, D.C., 2009.

Koehler, E.; Fowler, D., "Aggregates in Self-Consolidating Concrete. Final Report, ICAR Project 108: Aggregates in Self-Consolidating Concrete," International Center for Aggregates Research (ICAR), The University of Texas at Austin, March, 2007.

Kosmatka, H.; Wilson, L., "Design and Control of Concrete Mixtures", 15th edition, Portland Cement Association, Skokie, Illinois, USA, 460 pages, 2011.

Kheder, G.; Jadiri, R., "New Method for Proportioning Self-Consolidating Concrete Based on Compressive Strength Requirements," ACI Materials Journal, V. 107, No. 5, September-October 2010.

Ley, T.; Felice, R.; Freeman, J., "Concrete Pavement Mixture Design and Analysis (MDA): Assessment of Air Void System Requirements for Durable Concrete," Federal Highway Administration (DTFH61-06-H-00011 (Work Plan 25)) Technical Report, 2012.

Lomboy, G.; Wang, X.; Wang. K., "Rheological Behavior and Formwork Pressure of SCC, SFSCC, and NC Mixtures," Proceedings of 5th North American Conference on the Design and Use of Self-Consolidating Concrete, Chicago, 2013.

Lu, G., "Rheological Studies on the Flow Behavior of Two-Phase Solid-Liquid Materials," Doctor of Philosophy Dissertation, Iowa State University, 2008.

Nielsen, I.; Wallevik, O., "Rheological Evaluation of Some Empirical Test Methods – Preliminary Result," Proceedings of the RILEM symposium on Self-Compacting Concrete, Reykjavik, pp. 55-68, 2003.

Okamura, H.; Ozawa, K., "Mix Design Method for Self-Compacting Concrete," Concrete Library of Japan Society of Civil Engineers, No25, pp107-120, June, 1995.

Oh, S.; Noguchi, T.; Tomosawa, F., "Toward Mix Design for Rheology of Self-Compacting Concrete," Proceedings of the First International RILEM Symposium on Self-Compacting Concrete, Stockholm, Sweden, pp. 361-372, 1999.

Partner, S., "Mix Design Methods," Final Report of Task 5, Brite EuRam, LCPC, France, 81 pp. 2000.

Patel, R.; Hossain, K.; Shehata, M.; Bouzoubaa, N.; Lachemi, M., "Development of Statistical Models for Mixture Design of High-Volume Fly Ash Self- Consolidating Concrete," ACI Materials Journal, 101(4), pp. 294-302, 2004.

Plum, N., "The Predetermination of Water Requirement and Optimum Grading of Concrete: Under Various Conditions," Report 96, The Danish National Institute of Building Research - Statens Byggeforskningsinstitut, Copenhagen, 1950.

Powers, T., "The properties of fresh concrete," New York, 1968.

Proceq SA, "Resipod Operating Instructions." Schewerzenbach, Switzerland, 2011.

Roshavelov, T., "Concrete Mixture Proportioning Based on Rheological Approach," First North American Conference on the Design and Use of Self-Consolidating Concrete, Chicago, IL:ACBM, pp. 113-119, 2002.

Roshavelov, T., "Concrete Mixture Proportioning Based on Bingham Model," Bulgarian Academy of Science, Tome 57, No. 5, 2004.

Rupnow, T.; Icenogle, P., "Evaluation of Surface Resistivity Measurements as an Alternative to the Rapid Chloride Permeability Test for Quality Assurance and Acceptance," TRB 91st Annual Meeting, Transportation Research Board, Washington, DC., 2012.

Schindler, A.; Barnes, R.; Roberts, J.; and Rodrigues, S., "Properties of Self-Consolidating Concrete for Prestressed Members," ACI Material Journal, V. 104, No. 1, 2007.

Scrivener, K.; Nemati, K., "The Percolation of Pore Space in the Cement Paste/Aggregate Zone of Concrete, Cement Concrete Research, 26(1), pp. 35-40, 1996.

Sedran, T.; De Larrard, F.; Hours, F.; Contamines, C. "Mix Design of Self-Compacting Concrete," RILEM International Conference on Production Methods and Workability of Concrete, Glasgow, Scotland, June 3-5, pp. 439-451, 1996.

Smeplass, S.; Mortsell, E., "The Particle Matrix Model Applied on SCC," Proceedings

of the Second International Symposium on Self-Compacting Concrete, Tokyo, Japan, pp. 267-276, 2001.

Sonebi, M.; Bahadori-Jahromi, A.; Bartos, P., "Development and Optimization of Medium Strength Self-Compacting Concrete by Using Pulverized Fly Ash," 3rd International Symposium on Self-Compacting Concrete, Reykjavik, Iceland, pp. 514-524. 2003.

Sonebi, M., "Applications of Statistical Models in Proportioning Medium Strength Self-Consolidating Concrete," ACI Materials Journal, 101(5), pp. 339-346. 2004a.

Sonebi, M., "Medium Strength Self-Compacting Concrete Containing Fly Ash: Modeling Using Statistical Factorial Plans," Cement and Concrete Research, 34, pp. 1199-1208, 2004b.

Stern, O., "Vorschlag f¨ur eine Norm: Kornpotenz (Feinheitsmodul) loser Haufwerke, Sparwirtschaft 4: (in German), 1932.

Su, N.; Hsu K.; Chai, H., "A Simple Mix Design Method for Self-Compacting Concrete," Cement and Concrete Research, 31, pp. 1799-1807, 2001.

Wang, X.; Wang, K.; Bektas, F.; and Taylor, P., "Drying Shrinkage of Ternary Blend Concrete in Transportation Structures," Journal of Sustainable Cement-Based Materials, 1:1-2, pp. 56-66, 2012.

Wang, X.; Taylor, P.; Wang, K.; and Morcous, G., "Using Paste-To-Voids Volume Ratio Evaluating the Performance of Self-Consolidating Concrete Mixtures," Submitted to Journal of Construction and Building Materials, 2014.

**LIST OF TABLES**

**LIST OF FIGURES**

**Table 1: Existing methods for proportioning SCC**

| Method | Cement, kg/m³ | Filler, kg/m³ | Water, kg/m³ | Fine Agg., kg/m³ | Coarse Agg. , kg/m³ | w/c | w/cm |
|---|---|---|---|---|---|---|---|
| Rational Mix Design by Okamura and Ozawa (1995) | Rest of mixture volume | | - | 40 to 50% of mortar volume | 50 to 60% of solid volume | - | 0.9 to 1.0 by volume |
| Sedran et al. (1996) | Combination of binders is fixed based on previous knowledge to satisfy compressive strength and material availability. | | - | Saturation level is determined and 50% of this amount is used | - | With previous knowledge of material properties to determine the water demand of the binder combination with HRWRA | |
| Excess paste theory (1999) | Not specified, based on the applications | | | Not specified, based on the applications | | Optimum between 0.8-0.9 | |
| CBI and extension (1999) | If the determined paste volume for both blocking and liquid criteria is higher than 420 l/m3, smaller size aggregate need to be considered. | | | Make sure the average particle diameter is smaller than 6.5 mm. | | - | |
| LCPC (2000) | 430 | 50 | 170 | 847 | 825 | - | |
| Particle-Matrix model (2001) | Flow resistance ratio between 0.6-0.8 | | | - | | - | |
| Su et al. (2001) | >270 | - | - | Sand to total aggregates ranges from 50% to 57%, total aggregate ranges from 59% to 68%. | | - | |
| Statistical design | 250-600 kg/m3 | | - | Varied to achieve volume | Hold constant | 0.37-0.50 | 0.38 - 0.72 |
| ACBM (2002) | Similar to extension of CBI method | | | Similar to extension of CBI method | | - | |
| EFNARC (2005) | 400 to 600 kg/m3 | | Maximum 200 kg/m3 | Rest of mixture | 28 to 35% by volume | Use slump cone and v-funnel test to determine | |
| Concrete Manager Software | Not specified, based on the applications | | | | | | |
| DMDA (2005) | Fly ash is considered as part of the aggregate. | | Minimum 160 kg/m3 | - | | Minimum 0.42 to prevent autogenous shrinkage | |
| Brouwers et al. (2005) | Based on prior knowledge to provide the range. | | - | Combined aggregate gradation with the preferred range of distribution modulus q between 0.21 and 0.25. | | Depend on application and provide the ranges. | |
| ACI 237R (2007) | 386 to 475 kg/m3; Paste fraction: 34 to 40% | | | 0.32 to 0.44 | 28 to 32% | - | 0.32 to 0.45 |
| ICAR (2007) | Paste volume: 28 - 40% | | - | 16 mm for most applications; 9.5 mm for challenging passing ability, uniform grading with high packing density preferred, S/A = 0.40 -0.50, equidimensional, rounded aggregates preferred | | - | 0.30-0.45, higher with VMA |
| UCL (2009) | - | | - | 45% of mortar volume | 30% to 40% | - | 0.28-0.36 |
| Strength based method (2010) | Based on predetermined water content and w/cm | | Based on air content and aggregate size | - | 44% to 56% | wide range | wide range |

**Table 2: Summary of input parameters and constraints required by Brouwers' (2005) method and proposed method in this study**

| Input Parameter | Brouwers' method | Proposed method | Reference |
|---|---|---|---|
| ***Direct input*** | | | |
| Distribution modulus, q | Preferred range for SCC is $0.21 < q < 0.25$ | $0.23 \leq q \leq 0.29$ | Hunger (2010); Brouwers (2006) |
| Mineral admixture dosage | Not defined | Depending upon applications | |
| All solid PSDs | Based on material selection | Based on material selection | |
| Air content | % of entrapped/entrained air | Based on applications, i.e., requirement for freeze-thaw durability, normally 5-8% | |
| Defined maximum and minimum particle diameter | Not defined | Maximum particle diameter: the smallest sieve size that 95-100% of aggregate passes through. Minimum particle diameter: the smallest sieve size that PSD test can be analyzed | |
| ***Constraints*** | | | |
| Coarse aggregate volume content | Not defined | 28 to 32% for >12 mm NMAS, but the range can be 28 to 38% for NMAS > 9.5 mm | ACI 237 (2007) |
| Water to cementitious material ratio (w/cm) | Not defined | 0.32-0.45 | ACI 237 (2007) |
| Sand to aggregate ratio | Not defined | 0.4-0.5 | |
| Paste volume | Not defined | 0.34-0.40 | ACI 237 (2007) |

**Table 3: Comparison of SCC mix proportions using proposed design method with varied q values**

| Ingredient | Type | q value | | |
|---|---|---|---|---|
| | | 0.23 | 0.25 | 0.29 |
| CA, kg/m$^3$ | Limestone | 892 | 927 | 965 |
| FA, kg/m$^3$ | River sand | 735 | 764 | 796 |
| C I,II, kg/m$^3$ | | 336 | 311 | 285 |
| SCM, kg/m$^3$ | Class C | 112 | 104 | 95 |
| Water, kg/m$^3$ | | 177 | 164 | 150 |
| Air, % | | 5 | 5 | 5 |
| Total weight, kg/m$^3$ | | 2251 | 2270 | 2290 |
| Cementitious material content, kg/m$^3$ | | 448 | 415 | 380 |
| w/cm | | 0.40 | 0.40 | 0.40 |
| FA/Total Aggregate | | 0.45 | 0.45 | 0.45 |
| Paste volume, % | | 39.0 | 36.6 | 34.0 |

**Table 4: Comparisons of different mix design methods on a typical SCC mixture**

| Ingredient | Type | Mix design method | | | | | |
|---|---|---|---|---|---|---|---|
| | | Rational | ACI | ICAR | UCL | Strength-based | Proposed |
| CA, kg/m3 | Limestone | 779 | 783 | 923 | 858 | 848 | 927 |
| FA, kg/m3 | River sand | 844 | 869 | 755 | 809 | 752 | 764 |
| C I,II, kg/m3 | | 393 | 355 | 328 | 332 | 382 | 311 |
| SCM, kg/m3 | Class C | 131 | 118 | 109 | 111 | 137 | 104 |
| Water, kg/m3 | | 167 | 194 | 175 | 177 | 172 | 164 |
| Air, % | | 5 | 5 | 5 | 5 | 5 | 5 |
| Total weight, kg/m3 | | 2314 | 2319 | 2291 | 2287 | 2291 | 2270 |
| Cementitious material content, kg/m3 | | 524 | 473 | 438 | 443 | 519 | 415 |
| w/cm | | 0.32 | 0.40 | 0.40 | 0.40 | 0.33 | 0.39 |
| FA/Total Aggregate | | 0.52 | 0.53 | 0.45 | 0.49 | 0.47 | 0.45 |
| Paste volume, % | | 39.6 | 40.6 | 37.5 | 37.9 | 40.1 | 37.0 |
| Reference | | Okamura and Ozawa, 1995 | ACI 237R 2007 | Koehler and Fowler, 2007 | Domone 2009 | Kheder and Jadiri, 2010 | Brouwers and Radix, 2005 |

**Table 5: The physical properties of aggregates**

| Aggregates used in the research | | Type | Nominal Maximum Size, mm | Absorption, % | Fineness Modulus | Specific Gravity |
|---|---|---|---|---|---|---|
| Coarse Aggregate | a(LS) | Limestone | 19.0 | 1.3 | - | 2.66 |
| | b(LS) | Limestone | 12.5 | 1.3 | - | 2.66 |
| | c(LS) | Limestone | 9.5 | 1.3 | - | 2.66 |
| | a(G) | gravel | 19.0 | 1.1 | - | 2.74 |
| | b(G) | gravel | 12.5 | 1.4 | - | 2.68 |
| | c(G) | gravel | 9.5 | 1.4 | - | 2.69 |
| Fine Aggregate | | River sand | - | 0.5 | 2.62 | 2.68 |

Note: "-" indicates that the data are not available. "a(LS)" indicates limestone coarse aggregate with 19.0 mm maximum size.

**Table 6: Chemical compositions of cementitious materials**

| Chemical Composition | Type I/II Cement | Class F fly ash | Class C fly ash | Slag cement |
|---|---|---|---|---|
| $SiO_2$ | 20.10 | 50.87 | 42.46 | 37.00 |
| $Al_2O_3$ | 4.44 | 20.17 | 19.46 | 9.00 |
| $Fe_2O_3$ | 3.09 | 5.27 | 5.51 | 0.68 |
| $SO_3$ | 3.18 | 0.61 | 1.20 | - |
| CaO | 62.94 | 15.78 | 21.54 | 36.86 |
| MgO | 2.88 | 3.19 | 4.67 | 10.40 |
| $Na_2O$ | 0.10 | 0.69 | 1.42 | 0.30 |
| $K_2O$ | 0.61 | 1.09 | 0.68 | 0.38 |
| $P_2O_5$ | 0.06 | 0.44 | 0.84 | 0.01 |
| $TiO_2$ | 0.24 | 1.29 | 1.48 | 0.44 |
| SrO | 0.09 | 0.35 | 0.32 | 0.04 |
| BaO | - | 0.35 | 0.67 | - |
| LOI | 2.22 | 0.07 | 0.19 | - |
| Total | 99.95 | 100.17 | 100.44 | 95.11 |

Note: "-" indicates that the data are not available.

**Table 7: Mix proportions based on modified design concept**

| ID | ID in the following paper | C I,II | SCM | Filler | CA | FA | Water | HRWRA | VMA | AEA | w/cm | Distribution modulus, q | Paste content |
|---|---|---|---|---|---|---|---|---|---|---|---|---|---|
| | | kg/m3 | kg/m3 | kg/m3 | kg/m3 | kg/m3 | kg/m3 | ml/100kg SCMs | ml/100kg SCMs | ml/100kg SCMs | | | % |
| CC Control-a(LS) | CC1 | 295 | 98 | 0 | 993 | 698 | 169 | 0.0 | 0 | 36.5 | 0.43 | - | 36.4 |
| CC Control-b(LS) | CC2 | 351 | 117 | 0 | 881 | 696 | 187 | 0.0 | 0 | 52.2 | 0.40 | - | 40.7 |
| CC Control-c(LS) | CC3 | 339 | 113 | 0 | 801 | 804 | 181 | 0.0 | 0 | 97.8 | 0.40 | - | 39.6 |
| CC Control-a(G) | CC4 | 272 | 91 | 0 | 993 | 758 | 154 | 0.0 | 0 | 97.8 | 0.42 | - | 33.9 |
| CC Control-b(G) | CC5 | 306 | 102 | 0 | 881 | 806 | 163 | 0.0 | 0 | 97.8 | 0.40 | - | 36.3 |
| CC Control-c(G) | CC6 | 317 | 106 | 0 | 801 | 863 | 169 | 0.0 | 0 | 97.8 | 0.40 | - | 37.4 |
| SCC-L-a(LS)-C | SCC1 | 315 | 105 | 0 | 915 | 749 | 166 | 652.0 | 0 | 97.8 | 0.40 | 0.25 | 36.5 |
| SCC-L-a(LS)-F | SCC2 | 315 | 105 | 0 | 915 | 749 | 166 | 489.0 | 0 | 97.8 | 0.40 | 0.25 | 37.0 |
| SCC-L-a(LS)-S | SCC3 | 309 | 132 | 0 | 915 | 749 | 166 | 652.0 | 0 | 97.8 | 0.38 | 0.24 | 37.0 |
| SCC-L-a(LS)-FLD | SCC4 | 271 | 83 | 62 | 915 | 749 | 166 | 586.8 | 0 | 97.8 | 0.40 | 0.25 | 37.0 |
| SCC-H-a(LS)-C | SCC5 | 337 | 112 | 0 | 901 | 737 | 166 | 521.6 | 0 | 52.2 | 0.37 | 0.24 | 37.5 |
| SCC-H-a(LS)-F | SCC6 | 337 | 112 | 0 | 901 | 737 | 166 | 521.6 | 130 | 52.2 | 0.37 | 0.24 | 38.0 |
| SCC-H-a(LS)-S | SCC7 | 320 | 137 | 0 | 908 | 743 | 166 | 521.6 | 130 | 52.2 | 0.36 | 0.23 | 37.5 |
| SCC-H-a(LS)-FLD | SCC8 | 290 | 89 | 63 | 901 | 737 | 166 | 782.4 | 0 | 97.8 | 0.37 | 0.24 | 37.8 |
| SCC-L-b(LS)-C | SCC9 | 317 | 106 | 0 | 867 | 769 | 175 | 521.6 | 0 | 65.2 | 0.41 | 0.27 | 37.5 |
| SCC-L-b(LS)-F | SCC10 | 317 | 106 | 0 | 867 | 769 | 175 | 391.2 | 130 | 97.8 | 0.41 | 0.28 | 38.0 |
| SCC-L-b(LS)-S | SCC11 | 311 | 129 | 0 | 874 | 775 | 175 | 521.6 | 0 | 97.8 | 0.39 | 0.27 | 37.8 |
| SCC-L-b(LS)-FLD | SCC12 | 273 | 84 | 63 | 867 | 769 | 175 | 391.2 | 0 | 97.8 | 0.41 | 0.28 | 38.0 |
| SCC-H-b(LS)-C | SCC13 | 339 | 113 | 0 | 854 | 757 | 175 | 586.8 | 196 | 52.2 | 0.39 | 0.26 | 38.5 |
| SCC-H-b(LS)-F | SCC14 | 339 | 113 | 0 | 854 | 757 | 175 | 521.6 | 196 | 65.2 | 0.39 | 0.25 | 39.0 |
| SCC-H-b(LS)-S | SCC15 | 322 | 138 | 0 | 860 | 763 | 175 | 619.4 | 196 | 65.2 | 0.38 | 0.26 | 38.5 |
| SCC-H-b(LS)-FLD | SCC16 | 291 | 90 | 67 | 854 | 757 | 175 | 456.4 | 196 | 65.2 | 0.39 | 0.25 | 39.0 |
| SCC-H-c(LS)-C | SCC17 | 348 | 116 | 0 | 791 | 791 | 181 | 717.2 | 0 | 81.5 | 0.39 | 0.27 | 39.5 |

**Table 7: Mix proportions based on modified design concept (cont.)**

| ID | ID in the following paper | C I,II | SCM | Filler | CA | FA | Water | HRWRA | VMA | AEA | w/cm | Distribution modulus, q | Paste content |
|---|---|---|---|---|---|---|---|---|---|---|---|---|---|
| | | kg/m3 | kg/m3 | kg/m3 | kg/m3 | kg/m3 | kg/m3 | ml/100kg SCMs | ml/100kg SCMs | ml/100kg SCMs | | | % |
| SCC-H-c(LS)-F | SCC18 | 348 | 116 | 0 | 791 | 791 | 181 | 684.6 | 196 | 97.8 | 0.39 | 0.28 | 40.0 |
| SCC-H-c(LS)-S | SCC19 | 331 | 142 | 0 | 798 | 798 | 181 | 782.4 | 0 | 97.8 | 0.38 | 0.27 | 39.5 |
| SCC-H-c(LS)-FLD | SCC20 | 299 | 92 | 69 | 791 | 791 | 181 | 717.2 | 0 | 97.8 | 0.39 | 0.29 | 40.0 |
| SCC-L-a(G)-C | SCC21 | 315 | 105 | 0 | 911 | 746 | 166 | 456.4 | 0 | 97.8 | 0.40 | 0.25 | 36.5 |
| SCC-L-a(G)-F | SCC22 | 315 | 105 | 0 | 911 | 746 | 166 | 391.2 | 0 | 97.8 | 0.40 | 0.25 | 37.0 |
| SCC-L-a(G)-S | SCC23 | 309 | 132 | 0 | 911 | 746 | 166 | 521.6 | 0 | 97.8 | 0.38 | 0.24 | 37.0 |
| SCC-L-a(G)-FLD | SCC24 | 271 | 83 | 62 | 911 | 746 | 166 | 391.2 | 0 | 97.8 | 0.40 | 0.25 | 37.0 |
| SCC-H-a(G)-C | SCC25 | 337 | 112 | 0 | 897 | 734 | 166 | 652.0 | 196 | 97.8 | 0.37 | 0.24 | 37.5 |
| SCC-H-a(G)-F | SCC26 | 337 | 112 | 0 | 897 | 734 | 166 | 652.0 | 196 | 97.8 | 0.37 | 0.24 | 38.0 |
| SCC-H-a(G)-S | SCC27 | 320 | 137 | 0 | 904 | 740 | 166 | 652.0 | 196 | 97.8 | 0.36 | 0.23 | 37.5 |
| SCC-H-a(G)-FLD | SCC28 | 290 | 89 | 67 | 897 | 734 | 166 | 847.6 | 196 | 97.8 | 0.37 | 0.24 | 38.0 |
| SCC-L-b(G)-C | SCC29 | 317 | 106 | 0 | 864 | 766 | 175 | 456.4 | 0 | 97.8 | 0.41 | 0.27 | 37.5 |
| SCC-L-b(G)-F | SCC30 | 317 | 106 | 0 | 864 | 766 | 175 | 293.4 | 0 | 97.8 | 0.41 | 0.28 | 38.0 |
| SCC-L-b(G)-S | SCC31 | 311 | 133 | 0 | 864 | 766 | 175 | 391.2 | 0 | 97.8 | 0.39 | 0.27 | 38.0 |
| SCC-L-b(G)-FLD | SCC32 | 273 | 84 | 63 | 864 | 766 | 175 | 391.2 | 0 | 97.8 | 0.41 | 0.28 | 38.0 |
| SCC-H-b(G)-C | SCC33 | 339 | 113 | 0 | 850 | 754 | 175 | 717.2 | 196 | 97.8 | 0.39 | 0.26 | 38.5 |
| SCC-H-b(G)-F | SCC34 | 339 | 113 | 0 | 850 | 754 | 175 | 652.0 | 391 | 97.8 | 0.39 | 0.25 | 39.0 |
| SCC-H-b(G)-S | SCC35 | 322 | 138 | 0 | 857 | 760 | 175 | 782.4 | 326 | 97.8 | 0.38 | 0.26 | 38.5 |
| SCC-H-b(G)-FLD | SCC36 | 291 | 90 | 67 | 850 | 754 | 175 | 652.0 | 196 | 97.8 | 0.39 | 0.25 | 39.0 |
| SCC-H-c(G)-C | SCC37 | 348 | 116 | 0 | 788 | 788 | 181 | 652.0 | 0 | 97.8 | 0.39 | 0.27 | 39.5 |
| SCC-H-c(G)-F | SCC38 | 348 | 116 | 0 | 788 | 788 | 181 | 586.8 | 0 | 97.8 | 0.39 | 0.28 | 40.0 |
| SCC-H-c(G)-S | SCC39 | 331 | 142 | 0 | 795 | 795 | 181 | 782.4 | 228 | 97.8 | 0.38 | 0.27 | 39.5 |
| SCC-H-c(G)-FLD | SCC40 | 291 | 92 | 69 | 788 | 788 | 181 | 619.4 | 0 | 97.8 | 0.39 | 0.29 | 39.7 |

Note: C = Class C fly ash; F = Class F fly ash; S = slag cement; FLD = F fly ash and limestone dust; a = 19.0 mm NMSA; b = 12.5 mm NMSA; c = 9.5 mm NMSA; H = high slump flow range (i.e., 650 - 750 mm); L = low slump flow range (i.e., 550 – 650 mm); C I,II = Type I/II portland cement; LD = limestone dust; CA = coarse aggregate; FA = fine aggregate; LS = crushed limestone; G = river gravel.

**Table 8: Criteria used to evaluate the performance test results**

| Fresh property | Test method | Criteria | | | Reference |
|---|---|---|---|---|---|
| | | Good | Acceptable | Bad | |
| Flow ability | Slump flow and T50 | 550-750 mm, 1.0-2.7 s | - | <550 or >750 mm, | ASTM C1611; Daczko (2012) |
| Passing ability | J-ring | ΔD: 0-25 mm or ΔH <13 mm | ΔD: 25-50 mm | ΔD >50 mm or ΔH>13 mm | ASTM C1621 |
| Static stability | Visual stability index (VSI) | 0-1 | - | >1 | ASTM C1611 |
| Workability retention | Slump flow retention | SF/30 mins<25 mm | 25 mm<SF/30 mins<62 mm | SF/30 mins>62 mm | Khayat and Mitchell (2009) |
| | Time of setting | - | - | - | ASTM C403 |
| Formwork pressure | ISU formwork | P≤Phydrostatic | - | - | Gregori et al. (2008) |
| Heat of hydration | Adiabatic calorimetry | - | - | - | Sandberg and Liberman (2007) |
| Rheology | Rheometer | - | - | - | ASTM C1749 |
| Air content | Pressure method | 5-8% | 4-9% | <4% or >9 % | ASTM C231 |
| Hardened property | | Good | Acceptable | Bad | |
| Surface resistivity | Resistivity meter | >21 kΩ-cm | 12-21 kΩ-cm | <12 kΩ-cm | LADOTD (2011) |
| Compressive strength | Cylinder specimens | >27.6 or >41.4 Mpa depend on applications | - | <27.6 Mpa | ASTM C39; Domone (2006); AASHTO LRFD (2012) |
| Air void system | Linear-traverse method | Air content between 5 and 7%; Specific surface ≥ 24 mm-1, spacing factor ≤ 0.20 mm | Air content: 3.5-5.0% or 7.0-8.0% | Air content out of 5 to 7%; Specific surface < 24 mm-1, spacing factor > 0.20 mm | ASTM C457; FHWA 2007; Ley et al. 2012 |
| Shrinkage | Free length change | <500 με | - | - | ASTM C157, AASHTO LRFD |
| | Restrained ring method | Ave. stress rate≤0.17 Mpa/day, no cracking | 0.34 Mpa/day>Ave. stress rate>0.17 Mpa/day or 7 day<cracking time<14 day | Ave. stress rate>0.34 Mpa/day or cracking time<7 day | ASTM C1581 |

**Table 9: Results of fresh and hardened properties**

| ID | Workability | | | | | | | Mortar rheology | | Concrete rheology | | | | | | Free and restrained shrinkage | | | Air void system | | |
|---|---|---|---|---|---|---|---|---|---|---|---|---|---|---|---|---|---|---|---|---|---|
| | Slump/Slump Flow after mixing | | | Workability retention | J-ring test | | Total air | Dynamic yield stress | Plastic viscosity | Thixotropy | Yield torque | Slope | Setting time | Compressive strength @ 56 days | Surface resistivity @ 28 days | Free shrinkage @ 28 days | Cracking time | Average stress rate | Air content | Spacing factor | Specific surface |
| | $T_{50}$(s) | D (mm) | VSI | Δflow (mm) | ΔD (mm) | ΔH (mm) | % | Pa | Pa-s | J-rev/s | N-m | N-m-s | mins | MPa | kΩcm | μ-strain | days | MPa/day | % | mm | $mm^{-1}$ |
| CC1 | - | 165 | - | - | - | - | 5.0 | 142.05 | 1.56 | 0.58 | 2.84 | 4.91 | 298 | 44.9 | 32.0 | -360 | no | 0.20 | 4.9 | 0.096 | 52.22 |
| CC2 | - | 178 | - | - | - | - | 4.5 | 150.40 | 1.31 | 0.57 | 2.93 | 1.15 | 286 | 48.8 | 30.2 | -425 | 11.81 | 0.38 | 4.4 | 0.140 | 36.44 |
| CC3 | - | 165 | - | - | - | - | 5.5 | 144.89 | 1.50 | 0.53 | 4.60 | 3.12 | 268 | 44.2 | 28.3 | -520 | 6.02 | 0.47 | 4.7 | 0.103 | 46.21 |
| CC4 | - | 152 | - | - | - | - | 5.3 | 147.56 | 1.80 | 1.20 | 6.15 | 6.08 | 351 | 39.7 | 30.8 | -475 | no | 0.12 | 5.1 | 0.112 | 40.55 |
| CC5 | - | 203 | - | - | - | - | 6.5 | 115.50 | 1.38 | 0.60 | 3.60 | 3.47 | 296 | 35.2 | 25.7 | -480 | no | 0.28 | 6.5 | 0.109 | 37.81 |
| CC6 | - | 178 | - | - | - | - | 7.8 | 119.61 | 1.49 | 0.45 | 3.88 | 4.28 | 277 | 36.0 | 31.0 | -470 | no | 0.12 | 7.7 | 0.099 | 36.28 |
| SCC1 | 1.9 | 610 | 0 | 95 | 32 | 13 | 6.2 | 78.70 | 1.07 | 0.21 | 1.11 | 2.95 | - | 45.1 | 25.7 | -495 | 10.4 | 0.43 | 5.5 | 0.132 | 37.78 |
| SCC2 | 1.2 | 660 | 0 | 102 | 50 | 11 | 6.0 | 61.95 | 0.93 | 0.06 | 1.01 | 2.94 | - | 45.1 | 34.5 | -410 | 12.84 | 0.32 | 5.4 | 0.121 | 42.66 |
| SCC3 | 1.7 | 641 | 0 | 89 | 38 | 14 | 8.0 | 53.54 | 1.17 | 0.00 | 1.14 | 3.34 | - | 45.3 | 47.6 | -460 | 11.16 | 0.43 | 6.8 | 0.147 | 34.46 |
| SCC4 | 1.9 | 597 | 0 | 70 | 25 | 14 | 5.5 | 49.87 | 0.83 | 0.08 | 1.02 | 2.87 | - | 46.8 | 27.3 | -450 | no | 0.12 | 5.0 | 0.141 | 33.46 |
| SCC5 | ≤2 | 705 | 1 | 13 | 16 | 13 | 5.2 | 37.87 | 1.73 | 0.21 | 0.78 | 3.89 | 578 | 53.9 | 31.2 | -445 | 8.590 | 0.30 | 3.2 | 0.162 | 35.73 |
| SCC6 | ≤2 | 730 | 1 | 13 | 25 | 11 | 3.5 | 26.80 | 0.87 | 0.06 | 0.61 | 3.32 | 490 | 51.6 | 36.7 | -430 | no | 0.22 | 3.7 | 0.147 | 36.68 |
| SCC7 | 2 | 740 | 1 | 38 | 3 | 10 | 6.5 | 10.73 | 1.95 | 0.07 | 0.54 | 4.78 | 473 | 53.7 | 53.6 | -310 | no | 0.15 | 5.2 | 0.140 | 34.36 |
| SCC8 | 1.3 | 699 | 1 | 70 | 44 | 11 | 6.0 | 53.11 | 1.08 | 0.11 | 0.88 | 3.83 | 568 | 41.1 | 31.4 | -425 | 14.9 | 0.27 | 5.7 | 0.130 | 32.14 |
| SCC9 | ≤2 | 616 | 0 | 83 | 22 | 8 | 4.0 | 45.44 | 0.97 | 0.08 | 1.03 | 3.29 | 466 | 55.3 | 23.6 | -510 | 9.92 | 0.37 | 3.0 | 0.145 | 40.73 |
| SCC10 | ≤2 | 616 | 0 | 38 | 25 | 6 | 5.0 | 51.56 | 1.07 | 0.02 | 0.84 | 3.13 | 398 | 45.4 | 32.9 | -385 | 13.5 | 0.31 | 4.6 | 0.138 | 38.41 |
| SCC11 | ≤2 | 597 | 0 | 51 | 25 | 17 | 6.8 | 47.08 | 1.39 | 0.00 | 1.00 | 3.96 | 344 | 43.5 | 48.0 | -470 | 5.79 | 0.55 | 6.2 | 0.110 | 42.31 |
| SCC12 | ≤2 | 629 | 0 | 57 | 6 | 6 | 5.0 | 40.73 | 0.89 | 0.08 | 0.84 | 2.48 | 388 | 39.1 | 30.6 | -380 | no | 0.16 | 4.8 | 0.106 | 44.69 |
| SCC13 | 2 | 711 | 1 | 89 | 29 | 13 | 3.0 | 29.29 | 0.71 | 0.31 | 0.65 | 2.03 | - | 56.5 | 27.1 | -455 | 12.25 | 0.35 | 3.4 | 0.128 | 43.86 |
| SCC14 | ≤2 | 711 | 1 | 64 | 13 | 16 | 6.5 | 39.50 | 1.03 | 0.00 | 0.80 | 3.08 | - | 49.2 | 34.5 | -400 | no | 0.23 | 3.3 | 0.121 | 46.64 |
| SCC15 | ≤2 | 730 | 1 | 83 | 19 | 8 | 7.5 | 14.77 | 1.08 | 0.05 | 0.68 | 3.30 | - | 55.0 | 44.2 | -335 | no | 0.26 | 6.6 | 0.112 | 34.00 |
| SCC16 | ≤2 | 667 | 0 | 57 | 19 | 11 | 4.5 | 30.88 | 0.82 | 0.04 | 0.86 | 3.11 | - | 45.4 | 30.2 | -360 | no | 0.24 | 4.2 | 0.103 | 48.59 |
| SCC17 | ≤2 | 737 | 0 | 57 | 25 | 6 | 5.0 | 24.61 | 1.00 | 0.00 | 0.87 | 3.35 | 490 | 54.3 | 29.6 | -640 | 11.16 | 0.35 | 3.9 | 0.134 | 38.70 |

**Table 9: Results of fresh and hardened properties (cont.)**

| ID | Slump/Slump Flow after mixing | | | Workability retention | J-ring test | | Total air | Dynamic yield stress | Plastic viscosity | Thixotropy | Yield torque | Slope | Setting time | Compressive strength @ 56 days | Surface resistivity @ 28 days | Free shrinkage @ 28 days | Cracking time | Average stress rate | Air content | Spacing factor | Specific surface |
|---|---|---|---|---|---|---|---|---|---|---|---|---|---|---|---|---|---|---|---|---|---|
| | $T_{50}$(s) | D (mm) | VSI | Δflow (mm) | ΔD (mm) | ΔH (mm) | % | Pa | Pa-s | J-rev/s | N-m | N-m-s | mins | MPa | kΩcm | μ-strain | days | MPa/day | % | mm | $mm^{-1}$ |
| SCC18 | <2 | 699 | 0 | 70 | 19 | 8 | 6.5 | 27.60 | 0.88 | 0.01 | 0.87 | 2.47 | 455 | 48.4 | 33.9 | -490 | 11.16 | 0.37 | 5.9 | 0.109 | 38.75 |
| SCC19 | 2.7 | 686 | 0 | 51 | 13 | 6 | 7.0 | 20.29 | 1.73 | 0.03 | 0.78 | 4.69 | 480 | 52.7 | 49.3 | -470 | 5.8 | 0.53 | 6.7 | 0.195 | 20.39 |
| SCC20 | 1.7 | 692 | 0 | 51 | 19 | 13 | 6.5 | 33.30 | 1.09 | 0.02 | 0.70 | 2.64 | 485 | 42.9 | 26.7 | -410 | 14.35 | 0.28 | 4.9 | 0.140 | 33.98 |
| SCC21 | 1.6 | 616 | 0 | 89 | 13 | 14 | 8.0 | 87.63 | 1.89 | 0.12 | 3.79 | 1.28 | - | 39.1 | 20.3 | -445 | 8.44 | 0.44 | 7.0 | 0.120 | 34.89 |
| SCC22 | 1.2 | 622 | 0 | 64 | 32 | 14 | 7.4 | 50.72 | 0.79 | 0.10 | 2.71 | 1.04 | - | 35.9 | 28.7 | -440 | no | 0.14 | 7.1 | 0.111 | 32.62 |
| SCC23 | 1.87 | 660 | 0 | 83 | 32 | 17 | 7.8 | 45.16 | 1.42 | 0.01 | 3.24 | 1.50 | - | 36.5 | 47.0 | -470 | 13.76 | 0.33 | 7.3 | 0.093 | 33.14 |
| SCC24 | 1.44 | 597 | 0 | 70 | 19 | 13 | 6.6 | 43.50 | 0.64 | 0.09 | 2.51 | 1.17 | - | 33.3 | 38.2 | -420 | no | 0.24 | 7.3 | 0.099 | 32.57 |
| SCC25 | 1.29 | 711 | 1 | 57 | 50 | 6 | 5.7 | 38.63 | 1.23 | 0.48 | 3.01 | 0.98 | 658 | 39.9 | 25.5 | -510 | 12.05 | 0.31 | 6.0 | 0.107 | 35.49 |
| SCC26 | 1.2 | 762 | 1 | 57 | 25 | 3 | 5.5 | 18.58 | 0.82 | 0.11 | 2.63 | 0.76 | 635 | 32.1 | 37.4 | -465 | no | 0.32 | 5.6 | 0.118 | 38.66 |
| SCC27 | 2.3 | 718 | 1 | 48 | 25 | 6 | 5.7 | 13.50 | 1.98 | 0.24 | 2.15 | 1.19 | 483 | 36.6 | 52.1 | -430 | 10.61 | 0.24 | 5.9 | 0.112 | 36.79 |
| SCC28 | 1.6 | 718 | 1 | 76 | 32 | 6 | 4.6 | 12.83 | 0.57 | 0.07 | 2.11 | 0.65 | 566 | 39.9 | 36.5 | -555 | no | 0.14 | 5.1 | 0.061 | 43.24 |
| SCC29 | 1.04 | 622 | 0 | 76 | 13 | 6 | 5.6 | 55.20 | 0.77 | 0.13 | 2.68 | 1.18 | 486 | 32.1 | 18.1 | -625 | 9.19 | 0.51 | 6.8 | 0.070 | 39.90 |
| SCC30 | 1.4 | 629 | 0 | 51 | 6 | 6 | 6.0 | 44.47 | 0.62 | 0.11 | 2.32 | 0.99 | 455 | 30.1 | 26.3 | -395 | no | 0.16 | 6.4 | 0.104 | 39.35 |
| SCC31 | 1.8 | 603 | 0 | 57 | 6 | 13 | 6.5 | 31.10 | 1.15 | 0.17 | 2.72 | 1.06 | 484 | 33.8 | 41.9 | -425 | no | 0.24 | 8.2 | 0.078 | 36.25 |
| SCC32 | 1.03 | 641 | 0 | 70 | 6 | 6 | 5.6 | 25.92 | 0.59 | 0.11 | 1.91 | 0.72 | 448 | 33.4 | 29.6 | -425 | no | 0.19 | 6.0 | 0.127 | 32.90 |
| SCC33 | 1.5 | 730 | 1 | 108 | 13 | 8 | 6.0 | 25.98 | 0.52 | 0.05 | 2.17 | 0.84 | - | 39.8 | 16.4 | -510 | 10.50 | 0.41 | 6.7 | 0.092 | 42.00 |
| SCC34 | 1.1 | 737 | 2 | 76 | 6 | 6 | 6.0 | 8.36 | 0.40 | 0.09 | 1.49 | 0.79 | - | 40.6 | 23.6 | -325 | no | 0.15 | 5.6 | 0.171 | 28.44 |
| SCC35 | 2.3 | 762 | 2 | 83 | 6 | 6 | 7.8 | 1.39 | 0.68 | 0.52 | 1.38 | 0.58 | - | 45.7 | 39.4 | -405 | no | 0.24 | 8.0 | 0.077 | 41.63 |
| SCC36 | 0.9 | 762 | 2 | 76 | 13 | 5 | 7.6 | 15.77 | 0.46 | 0.08 | 1.56 | 0.87 | - | 40.1 | 29.8 | -455 | no | 0.29 | 6.6 | 0.122 | 35.00 |
| SCC37 | 1.39 | 743 | 0 | 64 | 6 | 6 | 6.6 | 18.93 | 0.88 | 0.05 | 2.61 | 0.56 | 472 | 43.3 | 24.8 | -640 | 6.90 | 0.54 | 6.8 | 0.108 | 35.30 |
| SCC38 | 1.28 | 737 | 0 | 89 | 6 | 6 | 6.0 | 9.75 | 0.74 | 0.14 | 1.44 | 0.68 | 419 | 39.3 | 40.6 | -590 | no | 0.32 | 6.1 | 0.108 | 34.85 |
| SCC39 | 1.8 | 762 | 2 | 70 | 6 | 6 | 5.4 | 0.00 | 0.53 | 0.03 | 1.49 | 0.53 | 553 | 38.3 | 40.4 | -580 | 7.20 | 0.47 | 5.1 | 0.151 | 32.98 |
| SCC40 | 1.13 | 737 | 0 | 76 | 19 | 6 | 6.2 | 11.36 | 0.69 | 0.00 | 2.03 | 0.45 | 489 | 32.0 | 33.7 | -626 | 9.69 | 0.40 | 6.7 | 0.120 | 37.78 |

Note: red=bad; yellow=acceptable refer to Table 9; $T_{50}$ = the time it takes for the outer edge of the concrete mass to reach a diameter of 500 mm from the time the mold is first raised; D = slump flow diameter; ΔD = slump flow diameter - J-ring flow diameter; ΔH = the difference between the height of concrete inside the ring and outside the ring at four locations around the ring; Δ Flow = the difference of slump flow between after mixing and 30 minutes after mixing; "-" indicates the data are not available.

**Table 10 – LADOTD surface resistivity and permeability classes (LADOTD 2011)**

| Permeability class | 56-Day rapid chloride permeability charge passed (Coulombs) | 28-Day surface resistivity (kΩ-cm) |
|---|---|---|
| High | > 4,000 | < 12 |
| Moderate | 2,000 - 4,000 | 12 - 21 |
| Low | 1,000 - 2,000 | 21 - 37 |
| Very Low | 100 - 1,000 | 37- 254 |
| Negligible | <100 | > 254 |

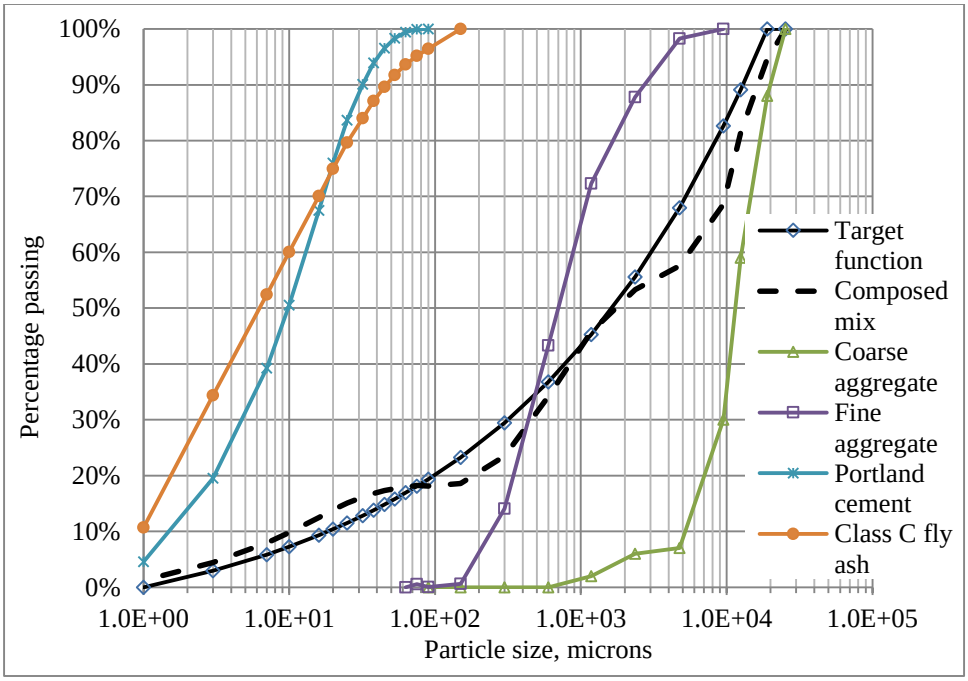


**Figure 1 – PSD of a mix (dash line) composed with the help of the modified design concept**

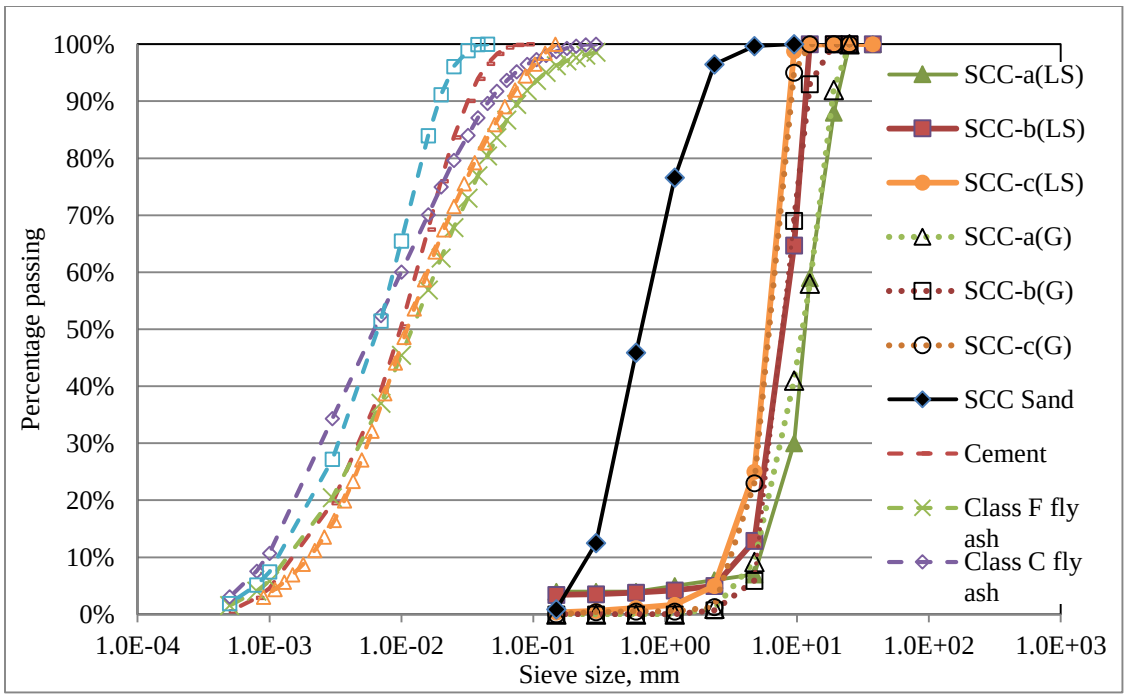


**Figure 2 – PSDs of the solid ingredients used in this study**

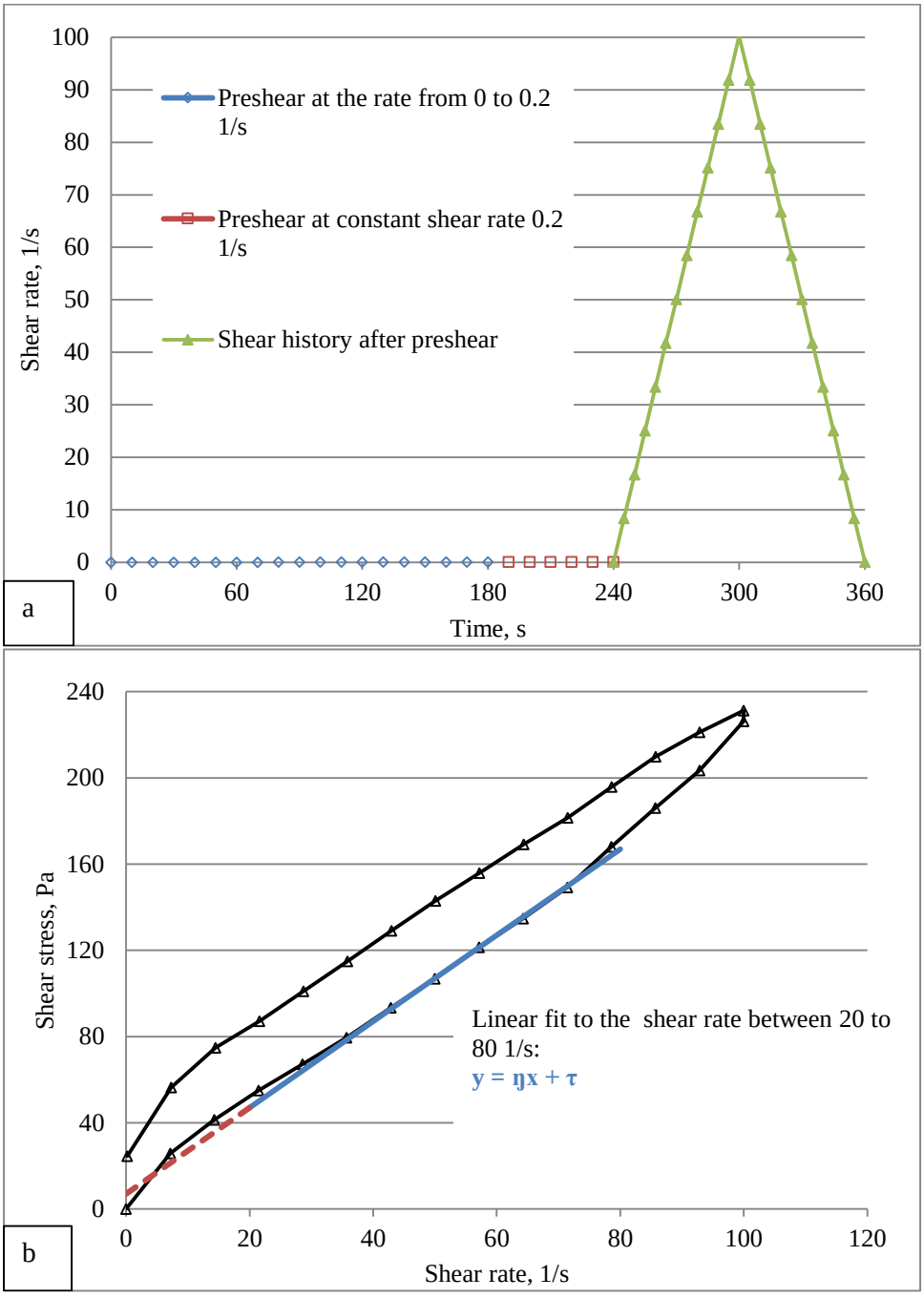


**Figure 3 – Rheology for mortar mixtures (a) loading history with preshear; (b) flow curve of a typical SCC mortar mixture used in this study**

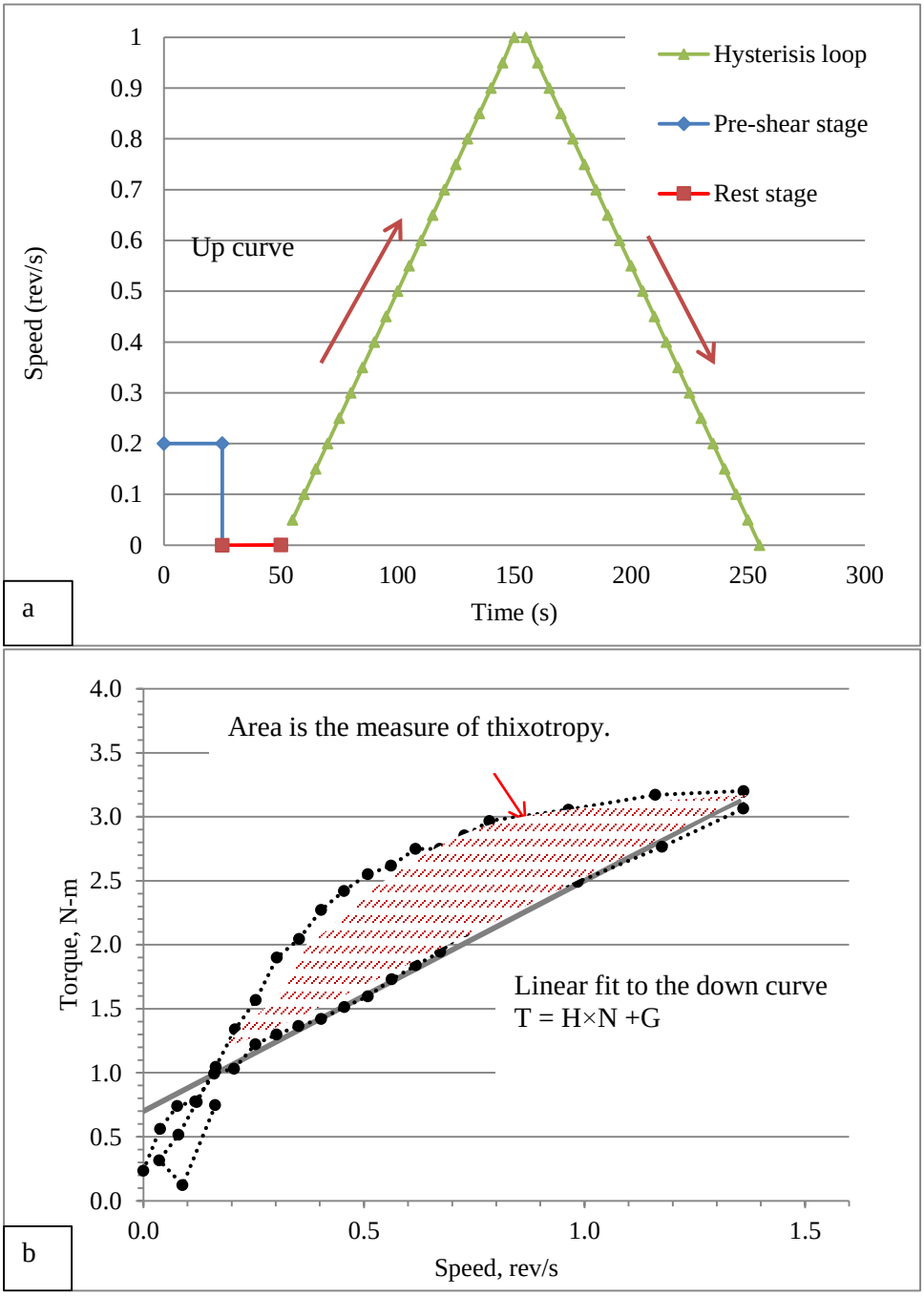


**Figure 4 – Rheology for concrete mixtures (a) loading history with preshear; (b) flow curve of a typical SCC mixture used in this study**

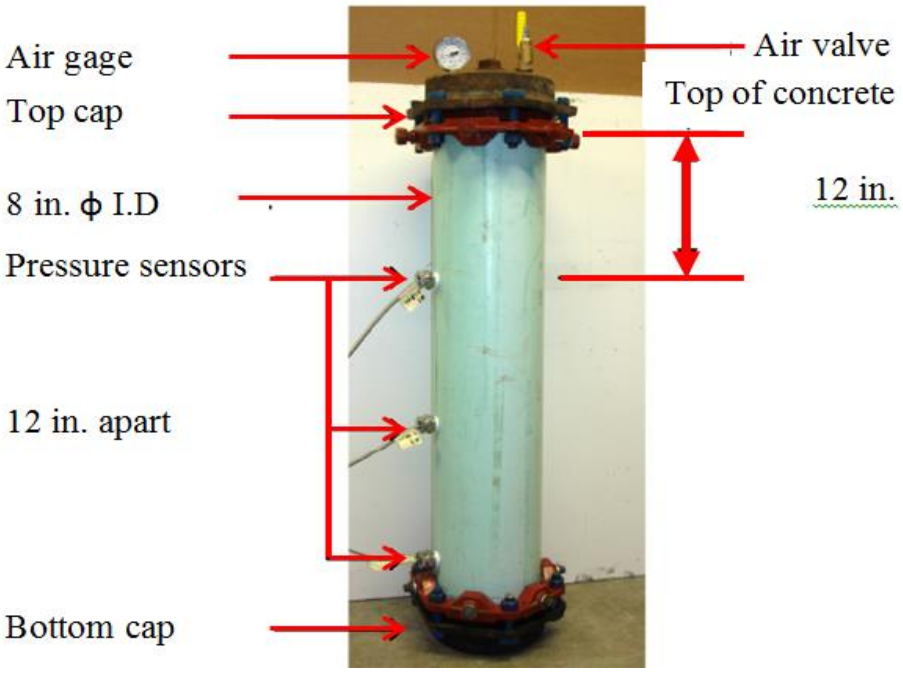


**Figure 5: Form pressure device setup (Lomboy et al. 2013)**

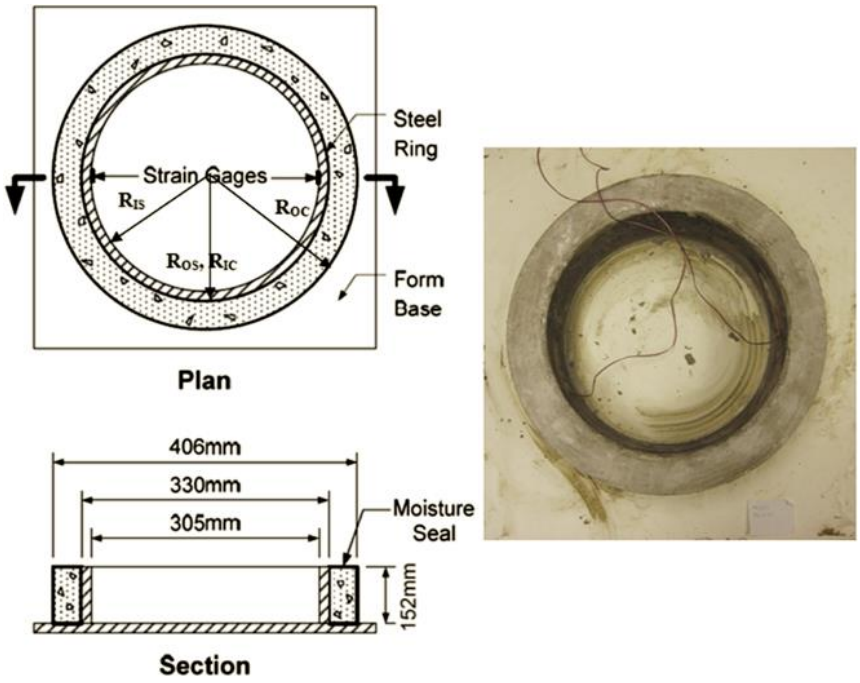


**Figure 6: Configuration of restrained concrete ring samples (Wang et al. 2012)**

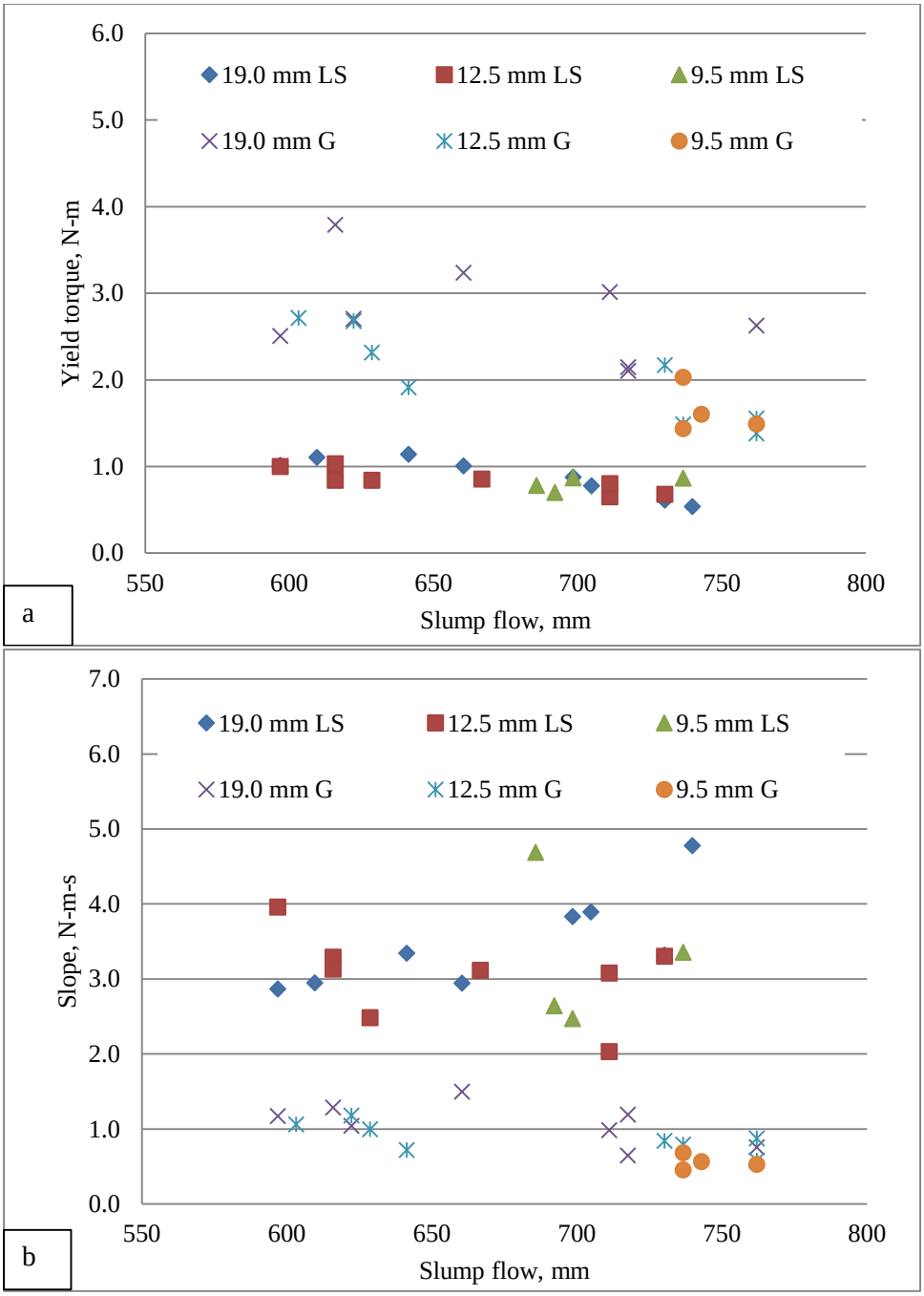


**Figure 7: Correlation between the measurements of slump flow values and concrete rheological parameters (a) yield torque; (b) slope**

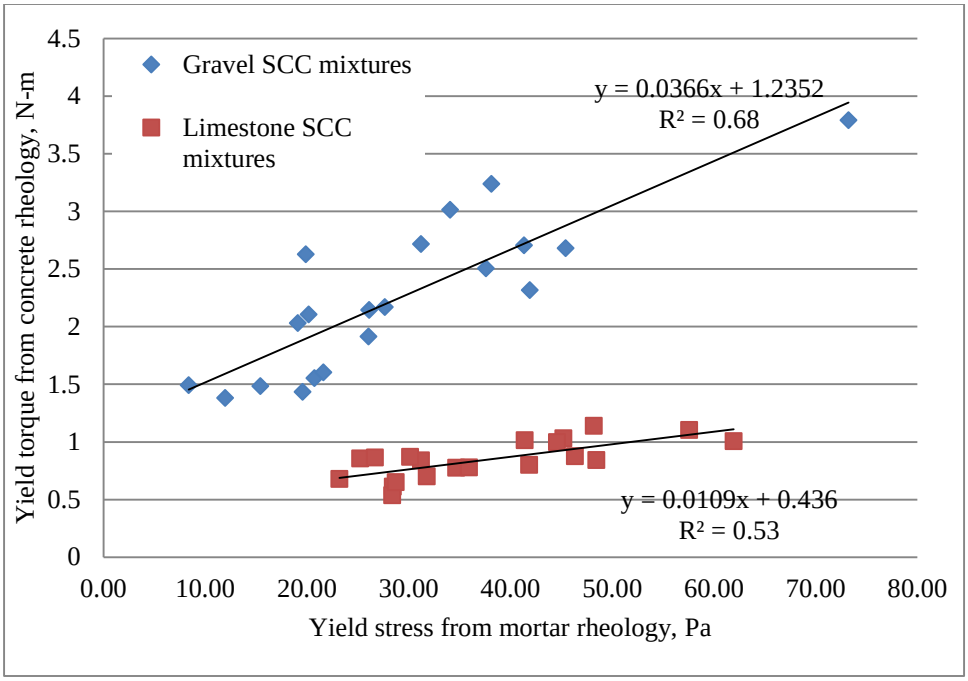


**Figure 8: Correlations between yield stress from mortar and yield torque from concrete mixtures**

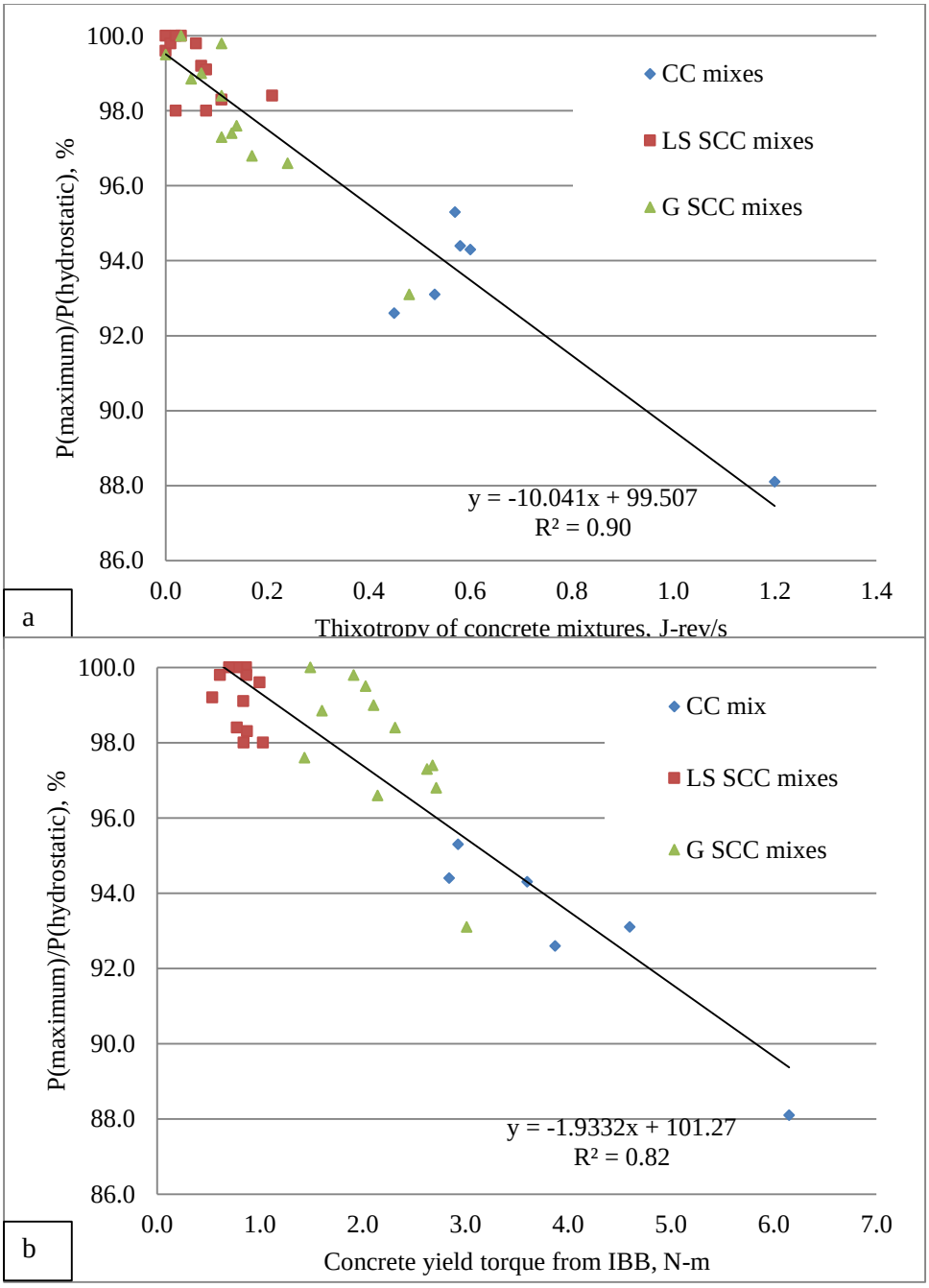


**Figure 9: Correlations between P(maximum)/P(hydrostatic) of formwork pressure and (a) thixotropy of concrete mixtures (b) concrete yield torque**

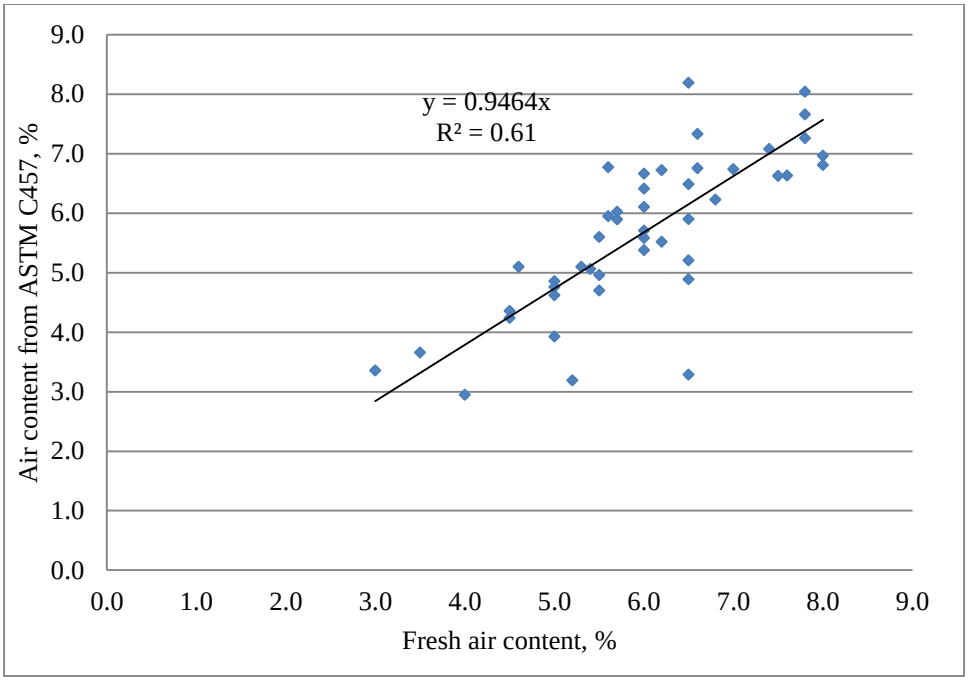


**Figure 10: Correlation of air content measured from linear traverse and pressure methods**

# CHAPTER 4. EFFECTS OF PASTE-TO-VOIDS VOLUME RATIO ON THE PERFORMANCE OF SELF-CONSOLIDATING CONCRETE MIXTURES

A paper submitted to Journal of Materials in Civil Engineering

*Xuhao Wang[1], Peter Taylor[2], Kejin Wang[3], George Morcous[4]*

## ABSTRACT

A well-proportioned self-consolidating concrete (SCC) mixture can be achieved by controlling the aggregate system, paste quality, and paste quantity. This study aims at applying a concept that is based on paste-to-voids volume ratio (Vpaste/Vvoids) to assess the performance of SCC mixtures. The relationship between excess paste theory and Vpaste/Vvoids was investigated. Tests were conducted on a large matrix of SCC mixtures that were designed for bridge construction applications. The mixtures were made with different aggregate types, sizes, and different cementitious materials. The workability, flow properties, compressive strength, shrinkage, and surface resistivity of SCC mixtures were determined at various ages. Statistical analyses, response surface models and Tukey Honestly Significant Difference (HSD) tests, were conducted to relate the mix design parameters to the

[1] Research Assistant, Department of Civil, Construction and Environmental Engineering, Iowa State University, 136 Town Engineering, Ames, Iowa 50011, Tel: 515-294-2252, Email: wangxh@iastate.edu

[2] Associate Director, National Concrete Pavement Technology Center, Iowa State University, Ames, Iowa 50011, Tel: 515-294-9333, Email: ptaylor@iastate.edu

[3] Professor, Department of Civil, Construction and Environmental Engineering, Iowa State University, 492 Town Engineering, Ames, Iowa 50011, Tel: 515-294-2152, Email: kejinw@iastate.edu

[4] Associate Professor, The Durham School of Architectural Engineering and Construction, University of Nebraska-Lincoln, Peter Kiewit Institute 105B, Omaha, NE 68182, Tel: 402-554-2544, Email: gmorcous2@unl.edu

concrete performance. Slump flow of the SCC mixtures increased with Vpaste/Vvoids at a given viscosity of mortar. Strength increases with an increases Vpaste/Vvoids up to a point (~150%), after which the strength becomes independent of Vpaste/Vvoids, even slightly decreases. Vpaste/Vvoids has little effect on the shrinkage mixtures, while SCC mixtures tend to have a higher shrinkage than CC for a given Vpaste/Vvoids. Vpaste/Vvoids has little effect on surface resistivity of SCC mixtures. The paste quality tends to have a dominant effect. Statistical analysis is an efficient tool to identify the significance of influence factors on concrete performance.

**Keywords:** Self-consolidating concrete; Paste-to-voids volume ratio; performance tests; rheology; statistical models and analysis

## INTRODUCTION

The overall performance of self-consolidating concrete (SCC) "combines concrete's existing ability to produce a wide range of engineering properties with an increased potential for constructability that exceeds anything possible with conventional concrete (CC)" (Daczko 2012). Nowadays, how to achieve a quality SCC with minimum impact whilst meeting application requirements have become a key issue in designing mix proportions. A critical aim of research dedicated to mix proportioning is to ensure that SCC mixtures have better performance and sustainability.

A well-proportioned SCC mixture can be achieved by controlling the aggregate system, paste quality, and paste quantity. The unique features of SCC mixtures are the fresh properties: flow ability, passing ability, filling ability, and stability. This can be obtained by properly selecting the aggregate system and paste quantity. However, the concrete properties

of interest are not limited to these properties, such as mechanical properties, shrinkage, and permeability, need to be assessed as well. These are largely controlled by the paste quality, such as water to cementitious material ratio, supplementary cementitious material (SCMs) types and dosages, and use of chemical admixtures.

This study aims at applying a concept that is based on a paste-to-voids volume ratio (Vpaste/Vvoids) to assess the performance of SCC mixtures. Aggregate system, and paste quality are varied in order to comprehensively understand the Vpaste/Vvoids influences in a given paste system.

## BACKGROUND

### Excess paste theory and applications on SCC

The "excess paste theory" was originally developed by Kennedy (1940) and it was built on a two phase theory, i.e., a paste phase is used to fill up the voids between aggregates. Sufficient paste volume is needed to fill the voids and control friction between aggregates to provide desired workability. The "lubricating" layer of paste around aggregates needs to be thin enough to prevent coarse aggregates from sinking down and segregating, while it needs to be thick enough to achieve a good workability (Kosmatka et al. 2008; Koehler and Fowler 2007; Hu and Wang 2007; Kennedy 1940).

Ideally, the excess paste thickness can be approximated by using paste volume divided by the surface area of the aggregates. Heywood (1933) proposed a direct method to measure aggregates in terms of length, width, and thickness. However, what he proposed would only work for an individual grain size, and not for a continuous grading of aggregates. Oh et al. (1999) modified the equations so that it would allow one to calculate the total surface area of

aggregates. Meanwhile, they established the relationship between the relative thickness of excess paste and the relative Bingham parameters for a continuous grading of aggregates by

$$\tau = \frac{P_e}{\sum_i^n n_i s_i D_{pi}} \quad \text{Eq. (1)}$$

where, $P_e$ = the volume of excess paste; $n_i$ = the number of particles in size class i; $s_i$ = the surface area of particles in size class i, and $D_{pi}$ = the projected diameter of the particles in size class i.

This theory has been applied to design SCC mix proportions by Bui et al. (2002). The paste volume must be high enough to fill the voids between aggregate particles and create a layer enveloping the particles to achieve deformability and good segregation resistance. The average aggregate spacing is calculated by Equations 2 and 3 and defined as an average distance between surfaces of aggregate particles or as twice the thickness of paste layer around an aggregate particle as shown in Figure 1 (Bui et al. 2002).

$$D_{ss} = D_{av}\left(\sqrt[3]{1 + \frac{V_p - V_{void}}{V_c - V_p}} - 1\right) \quad \text{Eq. (2)}$$

where $D_{ss}$ = average spacing between aggregate particle surfaces (particles are assumed to be spherical); $V_p$ = paste volume; $V_{void}$ = volume of voids in densely compacted aggregate determined in accordance with ASTM C29; $V_c$ = total concrete volume; and $D_{av}$ = the average aggregate diameter, which is given by

$$D_{av} = \frac{\sum d_i m_i}{\sum m_i} \quad \text{Eq. (3)}$$

where $d_i$ = average size of aggregate fraction i; and $m_i$ = percentage of aggregate mass retained between upper and lower sieve sizes in fraction i.

The relationships among paste rheology, average aggregate spacing, and average aggregate size were established and the general trends were found. Some satisfactory zones

were defined for different average aggregate spacing, average aggregate diameter, cement contents, water-binder ratios as well as contents and types of fly ash (Bui et al. 2002).

**Paste-to-void volume ratio**

An alternative concept, based on the paste-to-voids volume ratio (Vpaste/Vvoids), was applied to pavement concrete mixtures by Yurdakul et al. (2013). The Vpaste/Vvoids can be determined by calculating the paste volume of concrete mixtures and dividing that value by the volume of voids in the consolidated aggregate system determined in accordance with ASTM C29. The paste volume comprises the volume of water, the cementitious materials, and the measured air in the system. A figure of 100% means that all the space between the aggregates is just filled with paste with no excess.

The idea of relating performance of a mixture to paste volume for a given aggregate system was initially used to assess the SCC mixtures by Koehler and Fowler (2007). The Vpaste/Vvoids concept provides a quantitative means to consider the interaction between paste and aggregate system and achieve a quality concrete mixture with minimum impact whilst meeting specifications. The approach is believed to be more useful than parameters of "cementitious content" or "paste content" because it takes into account differences between aggregate systems (Yurdakul 2013). Like the excess paste approach, the aim is to:

- Coat the aggregate particles;
- Fill the voids between the combined aggregate system;
- Disperse the aggregate particles to provide the desired workability.

**Relationship between parameters from excess paste theory and Vpaste/Vvoids**

A limitation to the excess paste approach is that it is based on the assumption that aggregate particles are spherical and that they are packed in a cubic lattice, neither of which

is true (Yurdakul et al. 2013). The aggregate spacing can be considered as an average paste thickness because the average aggregate diameter is determined based on combined coarse and fine aggregate fractions. The reason for choosing Vpaste/Vvoids to assess SCC mixture performance is that the process includes the effects of aggregate characteristics, such as size, shape, and gradation.

For comparison, the aggregate spacing, $D_{ss}$, and average aggregate diameter, $D_{av}$, of all the mixtures discussed in this paper were calculated using equations 2 and 3, respectively. The data are listed in Table 3. The relationship between average aggregate spacing and Vpaste/Vvoids is shown in Figure 2. A linear relationship is found for a given aggregate system, but varies for different coarse/fine combinations.

As shown in Figure 3, the gradations of both limestone and gravel coarse aggregates were similar. Gravel aggregate with particles more spherical in nature tends to have higher Vpaste/Vvoids at a given binder content, size and sand-to-aggregate ratio system compared to limestone aggregate with more angular particles.

This is because the angular aggregate particles tend to decrease packing density, resulting in higher void content in the combined aggregate system (Quiroga and Fowler, 2003). However, there is an increased effect on packing density with decreased size of aggregate, which is in agreement with Compressible Packing Model proposed by de Larrard (1999).

## MIX PROPORTION AND MATERIALS

Forty SCC mixes, designed for bridge construction applications, were developed with the following targeted parameters:

- Low slump flow range between 550 and 650 mm or high flow range between 650 and 750 mm

- Visual stability index, (VSI)≤1
- J-ring ≤ 75 mm

The SCC mixes were made with limestone and river gravel coarse aggregates. Each coarse aggregate was used in three different nominal maximum sizes, 19.0 mm, 12.5 mm, and 9.5 mm. The physical properties of the aggregates are shown in Table 1 and the aggregate gradations are given in Figure 3.

Cementitious blends containing, 25% Class C fly ash, 25% Class F fly ash, 30% slag cement, or 15% limestone dust with 20% Class F fly ash, were used. Table 2 provides the chemical properties of cementitious materials.

The chemical admixtures used were Air-Entraining Agent (AEA), polycarboxylate based High Range Water Reducer (HRWR), and Viscosity-Modifying Admixture (VMA).

The mix proportions of all the mixtures are shown in Table 3.

## TEST EQUIPMENT AND PROCEDURES

### Workability

Slump flow, segregation resistance, and blocking assessment were determined in accordance with ASTM C1611 and C1621. The flow time for SCC mixtures reaching diameter of 500 mm, $t_{50}$, and flow time until concrete stopped flowing, $t_{final}$, were recorded.

The workability retention was determined by the difference between slump flow soon after mixing and 30 minutes after mixing.

### Air content

Air contents of all the mixtures were determined in accordance with ASTM C231.

**Mortar rheology**

Mortar was sieved from the concrete mixtures using a 4.75 mm size sieve. The dynamic yield stress and plastic viscosity were determined using a Brookfield rheometer. The sample was placed in a 50 mm diameter by 100 mm tall cylindrical vessel and sheared with a 15 by 30 mm vane spindle. The loading history employed based on Lomboy et al. (2013) initially ramps the spindle rotation from 0 to 0.2 $s^{-1}$ in 180 s, and then is sustained at 0.2 $s^{-1}$ for 60 s. The spindle rotation was subsequently increased from 0.2 to 100 $s^{-1}$ in the following 60 s and decreased to 0 $s^{-1}$ during the last 60 s as shown in Figure 4(a). The dynamic yield stress, $\tau$, and plastic viscosity, $\eta$, can be captured based on a Bingham model from the downward curve of the plot shown in Figure 4(b). The intersection with the y-axis and the slope of the linear fit Bingham model represent the yield stress and viscosity, respectively.

**Surface resistivity**

Research studies have shown that the surface resistivity test is a promising alternative to the rapid chloride penetrability test (RCPT) as a means of indirectly assessing the permeability of concrete mixtures (Rupnow and Icenogle 2012; Chini et al. 2003; Kessler et al. 2008; AASHTO TP 95 2011). Surface resistivity results were determined in accordance with the instructions of the device supplier (Proceq 2011).

The device comprises four electrodes that are linearly-aligned and uniformly-spaced (3.8 cm in this study). A potential is applied across the outside probes and the resistivity is measured on the inside probes.

Three concrete cylindrical specimens for each tested material were prepared so that averaged responses can be measured. The specimens were stored in the fog room at 23 ˚C after casting and tests were conducted at 1, 3, 7, and 28 days.

Four indelible marks were made oriented 90 degrees apart on the outer edge of one of the end faces to help place the device evenly about the circumference of the cylinder. Eight readings were taken on each cylinder. A dimensionless correction factor is needed to account for the geometry and size of the specimen.

The qualitative relationship between the charge passed using ASTM C1202 and the surface resistivity for 100 × 200 mm cylindrical specimens was proposed by Louisiana Department of Transportation and Development (LADOTD) (2011) in Table 4.

**Compressive strength and free shrinkage**

Compressive strength and free shrinkage of the concrete mixtures were measured following ASTM C39 and C157, respectively. The compressive strengths were taken at 56 days and free shrinkage was measured at 3, 7, 28, and 56 days. The concrete prisms for free shrinkage tests were moist cured for 7 days and then transferred to the drying room and maintained at 50% ± 4% relative humidity and a temperature of 23 ± 2˚C. Initial readings were taken right after demolding at the first day.

**RESULTS AND DISCUSSION**

**Workability**

The measured fresh properties are summarized in Table 5. The slump flows for all the mixtures fell within the targeted ranges, i.e., low flow range between 550 and 650 mm and high flow range between 650 and 750 mm. The $t_{50}$ times of most mixtures were less than 2s and the $t_{final}$ times ranged from 5.5 to 10.0s. The lower values of $t_{50}$ and $t_{final}$ correspond to a low viscosity.

In terms of blocking assessment in accordance with ASTM C1621, all the mixtures fell within “no visible blocking” and “minimal to noticeable blocking” categories.

For passing ability, the difference between the height of concrete inside the J-ring and outside the J-ring should be less than 13 mm, for acceptable passing ability for most applications (Koehler and Fowler, 2007). Only three mixtures made with 19 mm coarse aggregate and targeted for low flow range exceeded this limit. However, these mixtures should still acceptable for some applications requiring lower passing ability, such as bridge foundation.

The slump flow of SCC mixtures is considered to be dominated by the quantity of paste and the yield stress and viscosity of the mortar. A commercially available statistical analysis software (JMP 2005) was used to develop a quadratic response surface model for the mixtures in Figure 5 (a) and (b). The contour lines developed from the response surfaces are shown on the top surface in 2-Dimension. The discrete gradients provide visualized ranges for slump flow diameters and the legends indicate the slump flow ranges for each gradient. The prediction model of Eq. (4) is valid for the materials and ranges tested in this study.

Figure 5 gives the response surfaces fitted to the data of all SCC mixtures with prediction equation whose $R^2$ value was 70%.

$$SF = 1080.46 - 1.31 \times Vpaste/Vvoids + 16.60 \times \tau - (Vpaste/Vvoids - 251.18) \times (\eta - 0.99) - 105 \times (\eta - 0.99)^2 \quad \text{Eq. (4)}$$

where, SF stands for slump flow in mm; $\tau$ is the dynamic yield stress; $\eta$ is the plastic viscosity. The general trends can be observed from Figure 5 are:

- Slump flow increases with increased Vpaste/Vvoids at a given viscosity of mortar;

- At a given Vpaste/Vvoids, it is not surprising that higher viscosity of the mortar gives a lower flow diameter because more viscous paste can result in a higher resistivity of flow;
- At a given Vpaste/Vvoids, slump flow tends to decrease with increased yield stress.

Figure 6 shows the relationship between measured and model predicted slump flow. It implies a good slump flow prediction by the models because the data are closely scattered around the line of equality.

**Compressive strength**

In Figure 7, the correlation between Vpaste/Vvoids and 28-day compressive strength is graphically depicted, combined with the data for conventional and SCC mixtures reported by Taylor and his coworkers (Taylor et al. 2012a & 2012b), Cook and his coworkers (Cook et al. 2013), National Ready Mixed Concrete Association (NRMCA), and the present study. It is noted that an empirical factor, 1.15, was applied to estimate 28-day strength of the SCC mixtures from measured 56-day test results.

The strength increases with an increased Vpaste/Vvoids up to a point (~150%), above which the strength becomes independent of Vpaste/Vvoids, or even slightly decrease as shown by the envelope in Figure 7. Also, the data from the SCC mixtures falls within the same trend as the conventional mixtures, although the paste contents are relatively high.

The trend of reducing strength with increasing paste content may be attributed to crack tortuosity because increased paste content will lead to a shorter path that a crack needs to follow to go from one side of a sample to another. The greater the amount of aggregate, and so greater tortuosity, will mean higher energy required to propagate the crack, and so higher strength (Kolias and Georgiou 2005).

However, compressive strength will also be affected by other factors, such as SCM type, SCM dosage, and w/cm. In particular, a lower w/cm ratio will yield a higher compressive strength in a given mixture and it is considered as one of the most important influence factors on the strength development (Mehta and Monteiro 2006).

**Free shrinkage**

Figure 8 shows that the 56-day shrinkage strain versus Vpaste/Vvoids, using data from SCC mixtures in this study and that reported by Taylor and his coworkers (2012a) and NRMCA. Across the range of Vpaste/Vvoids, shrinkage is not significantly affected (Figure 8). However, the SCC mixtures are observed to shrink more than the conventional mixtures. The size and volume of capillary voids which can be determined by w/cm and degree of hydration drive the mechanism of drying shrinkage behavior. The paste composition also modifies the microstructure of a paste system (Wang et al. 2012 and Malhotra and Mehta 1996). Shrinkage can be affected by HRWR as well: the higher dosage of HRWR used to achieve a higher workability may result in an increased shrinkage for the SCC mixtures with similar mix proportions (Wang 2011; Kosmatka et al. 2008; Alsayed 1998). Therefore, Vpaste/Vvoids is not the only significant factor on shrinkage behavior and SCC mixtures made with similar compositions but higher HRWR dosages compared to CC mixtures tend to have higher shrinkage as shown in Figure 8.

**Surface resistivity measurements**

The surface resistivity results shown in Figure 9 indicate that the majority of SCC mixtures fall within the “low” and “very low” permeability classes in Table 4. The data

presented in Figure 9 show that the effect of Vpaste/Vvoids on surface resistivity categorized by SCMs types at 28 days.

The mixtures containing slag cement have significantly higher resistivity than the others, while the mixtures with class F fly ash have similar resistivity to those with both limestone dust and class F fly ash. Slag cement is comparatively quite reactive and may significantly improve the pore structure, thus increase the resistivity of concrete (Shi 2004). This is likely because the low replacement level of limestone dust has marginal effect on surface resistivity at 28 days. Class C fly ash mixtures have an unexpected low resistivity compared to the other SCMs at 28 days. It is most likely due to its low reactivity that can be demonstrated from X-ray diffractogram shown in Figure 10. The relatively low $C_3A$ and free lime intensity indicate the class C fly ash used in this study is likely slowly reactive.

**Full factorial statistical analysis**

Compressive strength, shrinkage, and surface resistivity are affected by factors other than paste content, including w/cm and system chemistry. Statistically full factorial analyses and Tukey Honestly Significant Difference (HSD) tests are therefore appropriate tools to integrate and analyze the 40 mixtures in this study. These tests provide a quantitative method to identify the differences of material on SCC performances from a statistical perspective and these differences may not be easily shown in figures. A commercially available statistical analysis software was employed (JMP 2005).

As shown in Table 6, input numerical categorical variables, aggregate types, sizes, and SCMs types, and numerical variables, Vpaste/Vvoids and w/cm, were applied to perform multiple comparisons on compressive strength, shrinkage, and surface resistivity results. Only statistically significant factors influencing the properties are listed in the table.

The analysis outputs give an indication on the variables that are statistically significant for 56-day strength, free shrinkage, and surface resistivity, respectively. The partition of sums of squares value (i.e., sum of squares/degree of freedom) is a concept that scales for the number of degree of freedom and estimates the variance or spread of the observation about their mean value. In this study, a higher value illustrates that the corresponding variable has a stronger effect on a particular property.

For instance, the partition of sums of squares value of 285.6 for aggregate types is higher than the other variables that are statistically significant on 56-day compressive strength. It indicates that they play the most important role on influencing 56-day compressive strength, followed by SCMs types and Vpaste/Vvoids. The effect of the aggregate types is likely because the angular and rough-textured limestone aggregate tends to improve the quality of the interfacial transition zone and exhibit improved bond to the cement paste compared to gravel aggregate with round and smooth surface. Moreover, the use of calcareous limestone aggregates may result in increased strength relative to siliceous gravel aggregate (Mehta and Monteiro 2006).

For 56-day shrinkage, aggregate sizes have the strongest effect because of the higher value of 46000, followed by Vpaste/Vvoids and SCMs types. SCMs types are likely to play dominant roles on surface resistivity of mixtures in this study as indicated by the higher value of 483.7 compared to the other variables.

A single-step multiple comparison procedure, HSD test, is employed in conjunction with least square mean to find out the means that are significantly different from each other. The least square mean and Tukey HSD analysis results for aggregate types (limestone and

gravel), aggregate sizes (19.0, 12.5 and 9.5 mm), and SCMs types (class C and F fly ashes, slag cement, and class F fly ash plus limestone dust) are shown in Table 7.

The levels that are not connected by the same letters are significantly different, i.e., A, B and C. For instance, the 56-day compressive strengths of SCC mixtures with 9.5 mm NMSA are significantly different from that of 19.0 mm NMSA mixtures. Generally, concrete mixtures containing larger aggregate particles require less mixing water when the paste composition is similar to those containing smaller size aggregate. This will result in a lower effective w/cm, yielding a higher strength. On the contrary, larger aggregates containing more microcracks tend to form weaker interfacial transition zone, therefore decrease compressive strength (Mehta and Monteiro 2006). Therefore, the HSD test provides a quantitative manner to identify the net effect of aggregate sizes.

The 56-day shrinkage strains of 19.0 mm mixtures are significantly lower than that of 12.5 and 9.5 mm NMSA mixtures. It is likely attributed to the larger size of coarse aggregate yields a lower paste content in a mixture which is one of the dominant factors on reducing shrinkage.

Class F fly ash and class F fly ash plus limestone mixtures have no significant differences on surface resistivity, while slag cement mixtures are significantly higher and class C fly ash mixtures are significantly lower. It is also in agreement with the observations from Figure 11.

## CONCLUSIONS

The following conclusions are derived from the present study:

1. The Vpaste/Vvoids concept can be used in SCC mixtures to assess
    - Workability: Based on response surface model, slump flow increases with increased Vpaste/Vvoids at a given viscosity of mortar. At a given

Vpaste/Vvoids, it is not surprising that higher viscosity of the mortar gives a lower flow diameter because more viscous paste can result in a higher resistivity of flow. At a given Vpaste/Vvoids, slump flow tends to decrease with increased yield stress.

- Strength: it increases with an increased Vpaste/Vvoids up to a point, after which the strength becomes independent of Vpaste/Vvoids, even slightly decreases based upon the analysis of CC and SCC mixtures.
- Surface resistivity: Vpaste/Vvoids has little effect on surface resistivity of SCC mixtures. The paste quality tends to have a dominant effect.

2. Drying shrinkage: Vpaste/Vvoids has little effect on SCC shrinkage, while SCC mixtures tend to have a higher shrinkage than CC for a given Vpaste/Vvoids. HRWR dosage used in SCC mixtures may severely increase the shrinkage.
3. Statistical analysis, such as response surface models and HSD tests, provides a systematic and quantitative means to predict and assess performance of SCC mixtures. It is also an efficient tool to identify the significance of influence factors on concrete performance. Aggregate types, sizes, and SCMs types are statistically evidenced to have most effects on 56-day compressive strength, shrinkage, and surface resistivity, respectively. Further research is needed to valid the models.

## ACKNOWLEDGEMENTS

The authors acknowledge the research sponsorship and the collaboration among Iowa State University (ISU), the University of Nebraska – Lincoln (UNL), and Northwestern University (NU). The authors would like to thank Dr. Robert Stephenson for his guidance, suggestions, and contributions of statistical analysis to this paper. The opinions, findings, and conclusions presented in this paper are those of the authors and do not reflect those of the research sponsors.

**REFERENCES**

AASHTO TP 95, "Standard Method of Test for Surface Resistivity of Concrete's Ability to Resist Chloride Ion Penetration," American Association of State Highway and Transportation Officials, Washington, DC., 2011.

ASTM C29. "Standard Test Method for Bulk Density ("Unit Weight") and Voids in Aggregate," American Society for Testing and Materials, Pennsylvania, 1999.

ASTM C1611. "Standard Test Method for Slump Flow of Self-Consolidating Concrete," American Society for Testing and Materials, Pennsylvania, 2005.

ASTM C1621. "Standard Test Method for Passing Ability of Self-Consolidating Concrete by J-Ring," American Society for Testing and Materials, Pennsylvania, 2009.

Bagheri, A.; Zanganeh, H., "Comparison of Rapid Tests for Evaluation of Chloride Resistance of Concretes with Supplementary Cementitious Materials." Journal of Material in Civil Engineering (ASCE), 24(9), pp: 1175–1182, 2012.

Bui, V.; Akkaya, Y.; and Shah, S., "Rheological Model for Self-Consolidating Concrete," ACI Material Journal, V. 99, No. 6, 2002.

Chini, A.; Muszynski, L.; and Hicks, J., "Determination of Acceptance Permeability Characteristics for Performance-Related Specifications for Portland Cement Concrete," Report No. BC 354-41, Florida Department of Transportation,Tallahassee, FL, 2003.

Cook, D.; Ghaeezadeh, A.; Ley, T.; and Russell, B., "Investigation of Optimized Graded Concrete for Oklahoma – Phase I," Final report, ODOT SP&R Item Number 2160, 2013.

Daczko, J., "Self-Consolidating Concrete: Applying What We Know," Spon Press, Milton Park, Abingdon, OX, published in 2012.

De Larrard, F., "Concrete Mixture Proportioning: A Scientific Approach," London, 1999.

DOTD TR 233 "Test Method for Surface Resistivity Indication of Concrete's Ability to 35 Resist Chloride Ion Penetration." LADOTD, Baton Rouge, LA, 2011. Electronically 36 accessible at:
http://www.dotd.la.gov/highways/construction/lab/testproc/tr_233_final.pdf.

Heywood H., Proceedings, Institute of Mechanical Engineers, Vol. 125, p.383, 1933.

Hu, J., and Wang, K., "Effects of Size and Uncompacted Voids of Aggregate on Mortar Flow Ability," Journal of Advanced Concrete Technology, 5, pp. 75-85, 2007.

JMP 8.0.0. Statistical Discovery. SAS Institute Inc., 2005.

Kennedy, C., "The Design of Concrete Mixes." Journal of the American Concrete Institute, 36, pp. 373-400, 1940.

Kessler, R.; Powers, R.; Vivas, E.; Paredes, M.; and Virmani, Y., "Surface Resistivity as an Indicator of Concrete Chloride Penetration Resistance," Presented at the 2008 Concrete Bridge Conference, St. Louis, MO, 2008.

Koehler, E., and Fowler, D., "Aggregates in Self-Consolidating Concrete," International Center for Aggregates Research (ICAR), Austin, TX, 2007.

Kolias, S.; Georgiou, C., "The Effect of Paste Volume and of Water Content on The Strength and Water Absorption of Concrete," Cement and Concrete Composites, 27, pp. 211-216, 2005.

Kosmatka, S.; Kerkhoff, B.; and Panarese, W., "Design and Control of Concrete Mixtures," 14th ed., Portland Cement Association, Skokie, IL, USA, 2008.

Lomboy, G.; Wang, X.; and Wang. K., "Rheological Behavior and Formwork Pressure of SCC, SFSCC, and NC Mixtures," Proceedings of 5th North American Conference on the Design and Use of Self-Consolidating Concrete, Chicago, 2013.

Malhotra, V.; Metha, P., "Advances in Concrete Technology, Volume 1: Pozzolanic and Cementitious Materials," Gordon and Breach Publishers, Amsterdam, Netherlands, 1996.

Mehta, P.; Monteiro, P., "Concrete: Structure, Properties and Materials," Englewood Cliffs, NJ; Prentice Hall, 548 pp, 2006.

Oh, S.; Noguchi, T.; Tomosawa, F., "Toward Mix Design for Rheology of Self-Compacting Concrete," Proceedings of the First International RILEM Symposium on Self-Compacting Concrete, Stockholm, Sweden, pp. 361-372, 1999.

Proceq SA, "Resipod Operating Instructions." Schewerzenbach, Switzerland, 2011.

Quiroga, P.; Fowler, D., "The Effects of Aggregates Characteristics on the Performance of Portland and Cement Concrete," Project report ICAR 104-1F, the University of Texas at Austin, 2003.

Rupnow, T.; Icenogle, P., "Evaluation of Surface Resistivity Measurements as an Alternative to the Rapid Chloride Permeability Test for Quality Assurance and Acceptance," TRB 91st Annual Meeting, Transportation Research Board, Washington, DC., 2012.

Shi, C., "Effect of Mixing Proportions of Concrete on Its Electrical Conductivity and the Rapid Chloride Permeability Test (ASTM C1202 or ASSHTO T277) Results," Cement and Concrete Research, 34, pp. 537-545, 2003.

Taylor, P., "Performance-Based Specifications for Concrete," Concrete International, 26(8), pp. 91–93, 2004.

Taylor, P.; Bektas, F.; Yurdakul, E.; and Ceylan, H., "Optimizing Cementitious Content in Concrete Mixtures for Required Performance," Final report, Federal Highway Administration (DTFH61-06-H-00011), 2012a.

Taylor, P.; Yurdakul, E.; Ceylan, H.; and Bektas, F., "Development of Performance Properties of Ternary Mixtures and Concrete Pavement Mixture Design and Analysis (MDA): Effect of Paste Quality on Fresh and Hardened Properties of Ternary Mixtures," Technical Report, Federal Highway Administration (DTFH61-06-H-00011), 2012b.

Yurdakul, E.; Taylor, P.; Ceylan, H.; and Bektas, F., "Effects of Paste-to-Voids Volume Ratio on the Performance of Concrete Mixtures," Journal of Materials in Civil Engineering (ASCE), Volume 25, Issue 12, pp. 1840-1851, 2013.

Yurdakul, E., "Proportioning for Performance-Based Concrete Pavement Mixtures," Doctor of Philosophy Dissertation, Iowa State University, 2013.

Wang, X.; Wang, K; Bektas, F.; and Taylor, P., "Drying Shrinkage of Ternary Blend Concrete in Transportation Structures," Journal of Sustainable Cement-Based Materials. 1:1-2, pp. 56-66, 2012.

Wang, X., "Drying Shrinkage of Ternary Blends in Mortar and Concrete," Master Thesis, Iowa State University, 2011.

**LIST OF TABLES**

**LIST OF FIGURES**

**Table 1. The physical properties of aggregates**

| Aggregates used in the research | | Type | Nominal Maximum Size, mm | Absorption, % | Fineness Modulus | Specific Gravity |
|---|---|---|---|---|---|---|
| Coarse Aggregate | a(LS) | Limestone | 19.0 | 1.3 | - | 2.66 |
| | b(LS) | Limestone | 12.5 | 1.3 | - | 2.66 |
| | c(LS) | Limestone | 9.5 | 1.3 | - | 2.66 |
| | a(G) | gravel | 19.0 | 1.1 | - | 2.74 |
| | b(G) | gravel | 12.5 | 1.4 | - | 2.68 |
| | c(G) | gravel | 9.5 | 1.4 | - | 2.69 |
| Fine Aggregate | | River sand | - | 0.5 | 2.62 | 2.68 |

Note: "-" indicates that the data are not available.

**Table 2. Chemical compositions of cementitious materials**

| Chemical Composition, % | Type I/II Cement | Class F fly ash | Class C fly ash | Slag cement |
|---|---|---|---|---|
| $SiO_2$ | 20.10 | 50.87 | 42.46 | 37.00 |
| $Al_2O_3$ | 4.44 | 20.17 | 19.46 | 9.00 |
| $Fe_2O_3$ | 3.09 | 5.27 | 5.51 | 0.68 |
| $SO_3$ | 3.18 | 0.61 | 1.20 | - |
| CaO | 62.94 | 15.78 | 21.54 | 36.86 |
| MgO | 2.88 | 3.19 | 4.67 | 10.40 |
| $Na_2O$ | 0.10 | 0.69 | 1.42 | 0.30 |
| $K_2O$ | 0.61 | 1.09 | 0.68 | 0.38 |
| $P_2O_5$ | 0.06 | 0.44 | 0.84 | 0.01 |
| $TiO_2$ | 0.24 | 1.29 | 1.48 | 0.44 |
| SrO | 0.09 | 0.35 | 0.32 | 0.04 |
| BaO | - | 0.35 | 0.67 | - |
| LOI | 2.22 | 0.07 | 0.19 | - |
| Total | 99.95 | 100.17 | 100.44 | 95.11 |

Note: "-" indicates that the data are not available.

**Table 3. Mix proportions**

| ID | C I,II | SCM | Filler | CA | FA | Water | HRWRA | VMA | AEA | Paste Volume | Vpaste/V voids | Dav | Dss |
|---|---|---|---|---|---|---|---|---|---|---|---|---|---|
| | kg/m3 | kg/m3 | kg/m3 | kg/m3 | kg/m3 | kg/m3 | ml/100kg SCMs | ml/100kg SCMs | ml/100kg SCMs | % | % | mm | mm |
| SCC-L-a(LS)-C | 315 | 105 | 0 | 915 | 749 | 166 | 652.0 | 0 | 97.8 | 36.5 | 230.5 | 7.110 | 0.408 |
| SCC-L-a(LS)-F | 315 | 105 | 0 | 915 | 749 | 166 | 489.0 | 0 | 97.8 | 37.0 | 235.4 | 7.110 | 0.427 |
| SCC-L-a(LS)-S | 309 | 132 | 0 | 915 | 749 | 166 | 652.0 | 0 | 97.8 | 37.0 | 235.4 | 7.110 | 0.427 |
| SCC-L-a(LS)-FLD | 271 | 83 | 62 | 915 | 749 | 166 | 586.8 | 0 | 97.8 | 37.0 | 235.1 | 7.110 | 0.426 |
| SCC-H-a(LS)-C | 337 | 112 | 0 | 901 | 737 | 166 | 521.6 | 0 | 52.2 | 37.5 | 240.2 | 7.110 | 0.446 |
| SCC-H-a(LS)-F | 337 | 112 | 0 | 901 | 737 | 166 | 521.6 | 130 | 52.2 | 38.0 | 245.6 | 7.110 | 0.467 |
| SCC-H-a(LS)-S | 320 | 137 | 0 | 908 | 743 | 166 | 521.6 | 130 | 52.2 | 37.5 | 240.5 | 7.110 | 0.447 |
| SCC-H-a(LS)-FLD | 290 | 89 | 63 | 901 | 737 | 166 | 782.4 | 0 | 97.8 | 37.8 | 244.0 | 7.110 | 0.461 |
| SCC-L-b(LS)-C | 317 | 106 | 0 | 867 | 769 | 175 | 521.6 | 0 | 65.2 | 37.5 | 245.7 | 4.543 | 0.297 |
| SCC-L-b(LS)-F | 317 | 106 | 0 | 867 | 769 | 175 | 391.2 | 130 | 97.8 | 38.0 | 250.9 | 4.543 | 0.310 |
| SCC-L-b(LS)-S | 311 | 129 | 0 | 874 | 775 | 175 | 521.6 | 0 | 97.8 | 37.8 | 249.3 | 4.543 | 0.306 |
| SCC-L-b(LS)-FLD | 273 | 84 | 63 | 867 | 769 | 175 | 391.2 | 0 | 97.8 | 38.0 | 250.8 | 4.543 | 0.310 |
| SCC-H-b(LS)-C | 339 | 113 | 0 | 854 | 757 | 175 | 586.8 | 196 | 52.2 | 38.5 | 256.2 | 4.543 | 0.323 |
| SCC-H-b(LS)-F | 339 | 113 | 0 | 854 | 757 | 175 | 521.6 | 196 | 65.2 | 39.0 | 261.9 | 4.543 | 0.337 |
| SCC-H-b(LS)-S | 322 | 138 | 0 | 860 | 763 | 175 | 619.4 | 196 | 65.2 | 38.5 | 256.5 | 4.543 | 0.323 |
| SCC-H-b(LS)-FLD | 291 | 90 | 67 | 854 | 757 | 175 | 456.4 | 196 | 65.2 | 39.0 | 261.5 | 4.543 | 0.336 |
| SCC-H-c(LS)-C | 348 | 116 | 0 | 791 | 791 | 181 | 717.2 | 0 | 81.5 | 39.5 | 240.4 | 3.534 | 0.226 |
| SCC-H-c(LS)-F | 348 | 116 | 0 | 791 | 791 | 181 | 684.6 | 196 | 97.8 | 40.0 | 245.8 | 3.534 | 0.237 |
| SCC-H-c(LS)-S | 331 | 142 | 0 | 798 | 798 | 181 | 782.4 | 0 | 97.8 | 39.5 | 240.7 | 3.534 | 0.226 |
| SCC-H-c(LS)-FLD | 299 | 92 | 69 | 791 | 791 | 181 | 717.2 | 0 | 97.8 | 40.0 | 245.5 | 3.534 | 0.236 |
| SCC-L-a(G)-C | 315 | 105 | 0 | 911 | 746 | 166 | 456.4 | 0 | 97.8 | 36.5 | 235.8 | 6.593 | 0.396 |
| SCC-L-a(G)-F | 315 | 105 | 0 | 911 | 746 | 166 | 391.2 | 0 | 97.8 | 37.0 | 240.8 | 6.593 | 0.413 |
| SCC-L-a(G)-S | 309 | 132 | 0 | 911 | 746 | 166 | 521.6 | 0 | 97.8 | 37.0 | 240.8 | 6.593 | 0.413 |
| SCC-L-a(G)-FLD | 271 | 83 | 62 | 911 | 746 | 166 | 391.2 | 0 | 97.8 | 37.0 | 240.5 | 6.593 | 0.412 |
| SCC-H-a(G)-C | 337 | 112 | 0 | 897 | 734 | 166 | 652.0 | 196 | 97.8 | 37.5 | 245.8 | 6.593 | 0.431 |
| SCC-H-a(G)-F | 337 | 112 | 0 | 897 | 734 | 166 | 652.0 | 196 | 97.8 | 38.0 | 251.2 | 6.593 | 0.451 |
| SCC-H-a(G)-S | 320 | 137 | 0 | 904 | 740 | 166 | 652.0 | 196 | 97.8 | 37.5 | 246.0 | 6.593 | 0.432 |
| SCC-H-a(G)-FLD | 290 | 89 | 67 | 897 | 734 | 166 | 847.6 | 196 | 97.8 | 38.0 | 251.3 | 6.593 | 0.451 |

**Table 3. Mix proportions (cont.)**

| ID | C I,II | SCM | Filler | CA | FA | Water | HRWRA | VMA | AEA | Paste Volume | Vpaste/Vvoids | Dav | Dss |
|---|---|---|---|---|---|---|---|---|---|---|---|---|---|
| | kg/m3 | kg/m3 | kg/m3 | kg/m3 | kg/m3 | kg/m3 | ml/100kg SCMs | ml/100kg SCMs | ml/100kg SCMs | % | % | mm | mm |
| SCC-L-b(G)-C | 317 | 106 | 0 | 864 | 766 | 175 | 456.4 | 0 | 97.8 | 37.5 | 257.1 | 4.829 | 0.340 |
| SCC-L-b(G)-F | 317 | 106 | 0 | 864 | 766 | 175 | 293.4 | 0 | 97.8 | 38.0 | 262.5 | 4.829 | 0.354 |
| SCC-L-b(G)-S | 311 | 133 | 0 | 864 | 766 | 175 | 391.2 | 0 | 97.8 | 38.0 | 262.7 | 4.829 | 0.354 |
| SCC-L-b(G)-FLD | 273 | 84 | 63 | 864 | 766 | 175 | 391.2 | 0 | 97.8 | 38.0 | 262.4 | 4.829 | 0.354 |
| SCC-H-b(G)-C | 339 | 113 | 0 | 850 | 754 | 175 | 717.2 | 196 | 97.8 | 38.5 | 268.1 | 4.829 | 0.368 |
| SCC-H-b(G)-F | 339 | 113 | 0 | 850 | 754 | 175 | 652.0 | 391 | 97.8 | 39.0 | 274.1 | 4.829 | 0.383 |
| SCC-H-b(G)-S | 322 | 138 | 0 | 857 | 760 | 175 | 782.4 | 326 | 97.8 | 38.5 | 268.3 | 4.829 | 0.368 |
| SCC-H-b(G)-FLD | 291 | 90 | 67 | 850 | 754 | 175 | 652.0 | 196 | 97.8 | 39.0 | 273.6 | 4.829 | 0.381 |
| SCC-H-c(G)-C | 348 | 116 | 0 | 788 | 788 | 181 | 652.0 | 0 | 97.8 | 39.5 | 261.2 | 3.660 | 0.272 |
| SCC-H-c(G)-F | 348 | 116 | 0 | 788 | 788 | 181 | 586.8 | 0 | 97.8 | 40.0 | 267.1 | 3.660 | 0.283 |
| SCC-H-c(G)-S | 331 | 142 | 0 | 795 | 795 | 181 | 782.4 | 228 | 97.8 | 39.5 | 261.6 | 3.660 | 0.272 |
| SCC-H-c(G)-FLD | 291 | 92 | 69 | 788 | 788 | 181 | 619.4 | 0 | 97.8 | 39.7 | 264.0 | 3.660 | 0.277 |

Note: C = Class C fly ash; F = Class F fly ash; S = slag cement; FLD = F fly ash and limestone dust; a = 19.0 mm NMSA; b = 12.5 mm NMSA; c = 9.5 mm NMSA; H = high slump flow range (i.e., 650 - 750 mm); L = low slump flow range (i.e., 550 – 650 mm); C I,II = Type I/II portland cement; LD = limestone dust; CA = coarse aggregate; FA = fine aggregate; LS = crushed limestone; G = river gravel; SCMs = supplementary cementitious materials.

**Table 4. LADOTD surface resistivity and permeability classes (LADOTD 2011)**

| Permeability class | 56-Day rapid chloride permeability charge passed (Coulombs) | 28-Day surface resistivity (kΩ-cm) |
|---|---|---|
| High | > 4,000 | < 12 |
| Moderate | 2,000 - 4,000 | 12 - 21 |
| Low | 1,000 - 2,000 | 21 - 37 |
| Very Low | 100 - 1,000 | 37- 254 |
| Negligible | <100 | > 254 |

**Table 5. Fresh properties of mixtures**

| ID | Slump/Slump Flow after mixing | | | | J-ring test | | Total air | Unit Weight | Slump flow after 30 mins of mixing | | Dynamic yield stress | Plastic viscosity |
|---|---|---|---|---|---|---|---|---|---|---|---|---|
| | T50(s) | Tfinal (s) | D (mm) | VSI | ΔD (mm) | ΔH (mm) | % | kg/m3 | D (mm) | Δ Flow (mm) | Pa | Pa-s |
| SCC-L-a(LS)-C | 1.9 | 7.9 | 610 | 0 | 32 | 13 | 6.2 | 2297 | 514 | 95 | 78.7 | 1.07 |
| SCC-L-a(LS)-F | 1.2 | 6.8 | 660 | 0 | 51 | 11 | 6.0 | 2262 | 559 | 102 | 62.0 | 0.93 |
| SCC-L-a(LS)-S | 1.7 | 6.5 | 641 | 0 | 38 | 13 | 8.0 | 2223 | 552 | 89 | 53.5 | 1.17 |
| SCC-L-a(LS)-FLD | 1.9 | 7.9 | 597 | 0 | 25 | 13 | 5.5 | 2291 | 527 | 70 | 49.9 | 0.83 |
| SCC-H-a(LS)-C | <2 | 6.8 | 705 | 1 | 16 | 13 | 5.2 | 2310 | 692 | 13 | 37.9 | 1.73 |
| SCC-H-a(LS)-F | <2 | 7.8 | 730 | 1 | 25 | 11 | 3.5 | 2342 | 718 | 13 | 26.8 | 0.87 |
| SCC-H-a(LS)-S | 2 | 6.2 | 740 | 1 | 3 | 10 | 6.5 | 2262 | 702 | 38 | 10.7 | 1.95 |
| SCC-H-a(LS)-FLD | 1.3 | 7.0 | 699 | 1 | 44 | 11 | 6.0 | 2278 | 629 | 70 | 53.1 | 1.08 |
| SCC-L-b(LS)-C | <2 | 6.8 | 616 | 0 | 22 | 8 | 4.0 | 2339 | 533 | 83 | 45.4 | 0.97 |
| SCC-L-b(LS)-F | <2 | 7.1 | 616 | 0 | 25 | 6 | 5.0 | 2287 | 578 | 38 | 51.6 | 1.07 |
| SCC-L-b(LS)-S | <2 | 6.8 | 597 | 0 | 25 | 17 | 6.8 | 2255 | 546 | 51 | 47.1 | 1.39 |
| SCC-L-b(LS)-FLD | <2 | 8.3 | 629 | 0 | 6 | 6 | 5.0 | 2268 | 572 | 57 | 40.7 | 0.89 |
| SCC-H-b(LS)-C | 2 | 9.8 | 711 | 1 | 29 | 13 | 3.0 | 2342 | 622 | 89 | 29.3 | 0.71 |
| SCC-H-b(LS)-F | <2 | 6.9 | 711 | 1 | 13 | 16 | 6.5 | 2326 | 648 | 64 | 39.5 | 1.03 |
| SCC-H-b(LS)-S | <2 | 6.7 | 730 | 1 | 19 | 8 | 7.5 | 2281 | 648 | 83 | 14.8 | 1.08 |
| SCC-H-b(LS)-FLD | <2 | 6.5 | 667 | 0 | 19 | 11 | 4.5 | 2310 | 610 | 57 | 30.9 | 0.82 |
| SCC-H-c(LS)-C | <2 | 6.8 | 737 | 0 | 25 | 6 | 5.0 | 2291 | 679 | 57 | 24.6 | 1.00 |
| SCC-H-c(LS)-F | <2 | 7.6 | 699 | 0 | 19 | 8 | 6.5 | 2291 | 629 | 70 | 27.6 | 0.88 |
| SCC-H-c(LS)-S | 2.7 | 6.5 | 686 | 0 | 13 | 6 | 7.0 | 2249 | 635 | 51 | 20.3 | 1.73 |
| SCC-H-c(LS)-FLD | 1.7 | 8.9 | 692 | 0 | 19 | 13 | 6.5 | 2239 | 641 | 51 | 33.3 | 1.09 |
| SCC-L-a(G)-C | 1.6 | 6.4 | 616 | 0 | 13 | 13 | 8.0 | 2236 | 527 | 89 | 87.6 | 1.89 |
| SCC-L-a(G)-F | 1.2 | 6.8 | 622 | 0 | 32 | 13 | 7.4 | 2287 | 559 | 64 | 50.7 | 0.79 |
| SCC-L-a(G)-S | 1.9 | 6.5 | 660 | 0 | 32 | 17 | 7.8 | 2178 | 578 | 83 | 45.2 | 1.42 |
| SCC-L-a(G)-FLD | 1.4 | 7.7 | 597 | 0 | 19 | 13 | 6.6 | 2265 | 527 | 70 | 43.5 | 0.64 |
| SCC-H-a(G)-C | 1.3 | 7.3 | 711 | 1 | 51 | 6 | 5.7 | 2265 | 654 | 57 | 38.6 | 1.23 |
| SCC-H-a(G)-F | 1.2 | 7.8 | 762 | 1 | 25 | 3 | 5.5 | 2300 | 705 | 57 | 18.6 | 0.82 |
| SCC-H-a(G)-S | 2.3 | 8.7 | 718 | 1 | 25 | 6 | 5.7 | 2166 | 670 | 48 | 13.5 | 1.98 |
| SCC-H-a(G)-FLD | 1.6 | 7.3 | 718 | 1 | 32 | 6 | 4.6 | 2287 | 641 | 76 | 12.8 | 0.57 |

**Table 5. Fresh properties of mixtures (cont.)**

| ID | Slump/Slump Flow after mixing | | | | J-ring test | | Total air | Unit Weight | Slump flow after 30 mins of mixing | | Dynamic yield stress | Plastic viscosity |
|---|---|---|---|---|---|---|---|---|---|---|---|---|
| | T50 (s) | Tfinal (s) | D (mm) | VSI | ΔD (mm) | ΔH (mm) | % | kg/m3 | D (mm) | Δ Flow (mm) | Pa | Pa-s |
| SCC-L-b(G)-C | 1.0 | 6.0 | 622 | 0 | 13 | 6 | 5.6 | 2252 | 546 | 76 | 55.2 | 0.77 |
| SCC-L-b(G)-F | 1.4 | 5.5 | 629 | 0 | 6 | 6 | 6.0 | 2281 | 578 | 51 | 44.5 | 0.62 |
| SCC-L-b(G)-S | 1.8 | 10.0 | 603 | 0 | 6 | 13 | 6.5 | 2185 | 546 | 57 | 31.1 | 1.15 |
| SCC-L-b(G)-FLD | 1.0 | 5.9 | 641 | 0 | 6 | 6 | 5.6 | 2265 | 572 | 70 | 25.9 | 0.59 |
| SCC-H-b(G)-C | 1.5 | 7.9 | 730 | 1 | 13 | 8 | 6.0 | 2265 | 622 | 108 | 26.0 | 0.52 |
| SCC-H-b(G)-F | 1.1 | 7.4 | 737 | 2 | 6 | 6 | 6.0 | 2284 | 660 | 76 | 8.4 | 0.40 |
| SCC-H-b(G)-S | 2.3 | 9.7 | 762 | 2 | 6 | 6 | 7.8 | 2182 | 679 | 83 | 1.4 | 0.68 |
| SCC-H-b(G)-FLD | 0.9 | 6.2 | 762 | 2 | 13 | 5 | 7.6 | 2233 | 686 | 76 | 15.8 | 0.46 |
| SCC-H-c(G)-C | 1.4 | 7.2 | 743 | 0 | 6 | 6 | 6.6 | 2259 | 679 | 64 | 18.9 | 0.88 |
| SCC-H-c(G)-F | 1.3 | 9.5 | 737 | 0 | 6 | 6 | 6.0 | 2255 | 648 | 89 | 9.8 | 0.74 |
| SCC-H-c(G)-S | 1.8 | 7.6 | 762 | 2 | 6 | 6 | 5.4 | 2220 | 692 | 70 | 0.00 | 0.53 |
| SCC-H-c(G)-FLD | 1.1 | 5.8 | 737 | 0 | 19 | 6 | 6.2 | 2233 | 660 | 76 | 11.4 | 0.69 |

Note: T50 = the time it takes for the outer edge of the concrete mass to reach a diameter of 500 mm from the time the mold is first raised; Tfinal = flow time until flow stopping; D = slump flow diameter; ΔD = slump flow diameter - J-ring flow diameter; ΔH = the difference between the height of concrete inside the ring and outside the ring at four locations around the ring; Δ Flow = the difference of slump flow between after mixing and 30 minutes after mixing.

**Table 6. Input and output parameters for full factorial statistical analysis on strength, shrinkage, and surface resistivity**

| Input numerical and categorical variables | | | | |
|---|---|---|---|---|
| Aggregate types | Aggregate sizes | SCMs types | Vpaste/Vvoids | w/cm |
| Limestone (LS)<br>Gravel (G) | 19.0 mm<br>12.5 mm<br>9.5 mm | C<br>F<br>S<br>FLD | Range from 230 to 275% | Range from 0.36 to 0.41 |
| **Output parameters** | | | | |
| | Variables that are statistically significant | Sum of squares/Degree of freedom | Coefficient of correlation, $R^2$ | |
| 56-day compressive strength | Aggregate types<br>SCMs types<br>Vpaste/Vvoids | 285.6<br>165.2<br>122.4 | 86.1% | |
| 56-day shrinkage | Aggregate sizes<br>Vpaste/Vvoids<br>SCMs types | 4.6E+04<br>2.1E+04<br>1.8E+04 | 86.0% | |
| 56-day surface resistivity | SCMs types<br>Aggregate sizes<br>Agg. types*Agg. sizes<br>Agg. types*SCMs type<br>w/cm | 483.7<br>66.3<br>65.2<br>59.6<br>33.4 | 97.8% | |

**Table 7. Statistical LSMeans Differences Tukey HSD tests results**

| 56-day compressive strength | | | | | | | |
|---|---|---|---|---|---|---|---|
| Aggregate types | Least Square Mean, Mpa | Aggregate sizes, mm | Least Square Mean, Mpa | LSMeans Differences Tukey HSD | SCMs types | Least Square Mean, Mpa | LSMeans Differences Tukey HSD |
| G | 33.3 | 19 | 49.5 | A | C | 49.5 | A |
| LS | 53.0 | 12.5 | 42.4 | AB | S | 45.5 | AB |
| | | 9.5 | 37.6 | B | F | 40.6 | BC |
| | | | | | FLD | 37.0 | C |
| 56-day shrinkage | | | | | | | |
| Aggregate types | Least Square Mean, µ-strain | Aggregate sizes, mm | Least Square Mean, µ-strain | LSMeans Differences Tukey HSD | SCMs types | Least Square Mean, µ-strain | LSMeans Differences Tukey HSD |
| G | -647 | 19 | -456 | A | S | -532 | A |
| LS | -489 | 12.5 | -592 | B | F | -543 | A |
| | | 9.5 | -655 | B | FLD | -559 | AB |
| | | | | | C | -637 | B |
| 28-day surface resistivity | | | | | | | |
| Aggregate types | Least Square Mean, kΩcm | Aggregate sizes, mm | Least Square Mean, kΩcm | LSMeans Differences Tukey HSD | SCMs types | Least Square Mean, kΩcm | LSMeans Differences Tukey HSD |
| G | 31.5 | 19 | 38.2 | A | S | 47.4 | A |
| LS | 36.8 | 9.5 | 34.5 | A | F | 33.0 | B |
| | | 12.5 | 29.7 | B | FLD | 30.7 | B |
| | | | | | C | 25.3 | C |

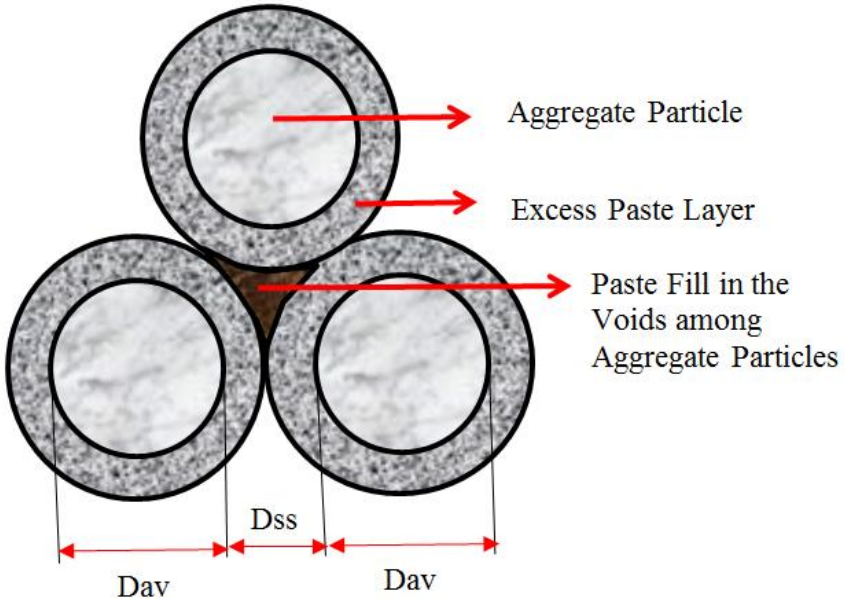


**Figure 1. Spherical aggregate particles, aggregate spacing $D_{ss}$, and average aggregate diameter $D_{av}$ (Bui et al. 2002).**

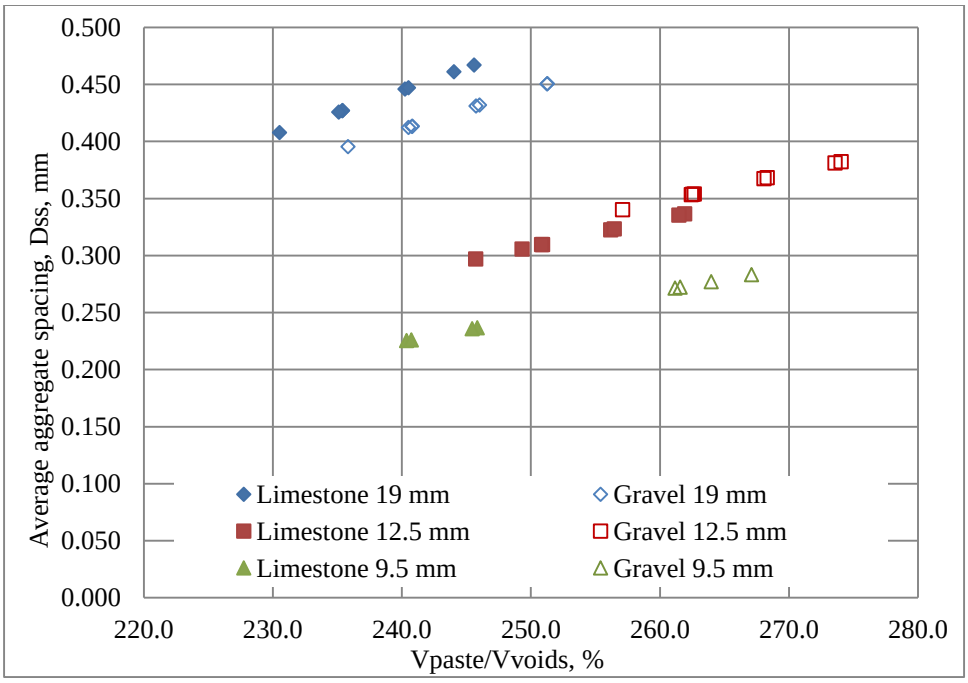


**Figure 2. Relationship between average aggregate spacing and Vpaste/Vvoids of the SCC mixtures investigated in the present study.**

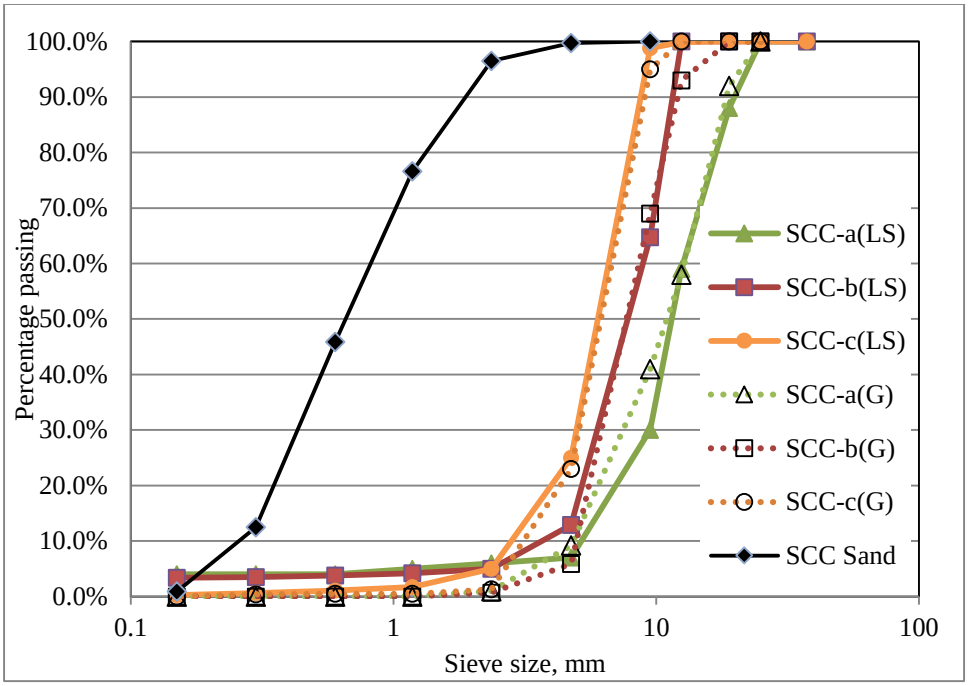


**Figure 3. Aggregate gradations.**

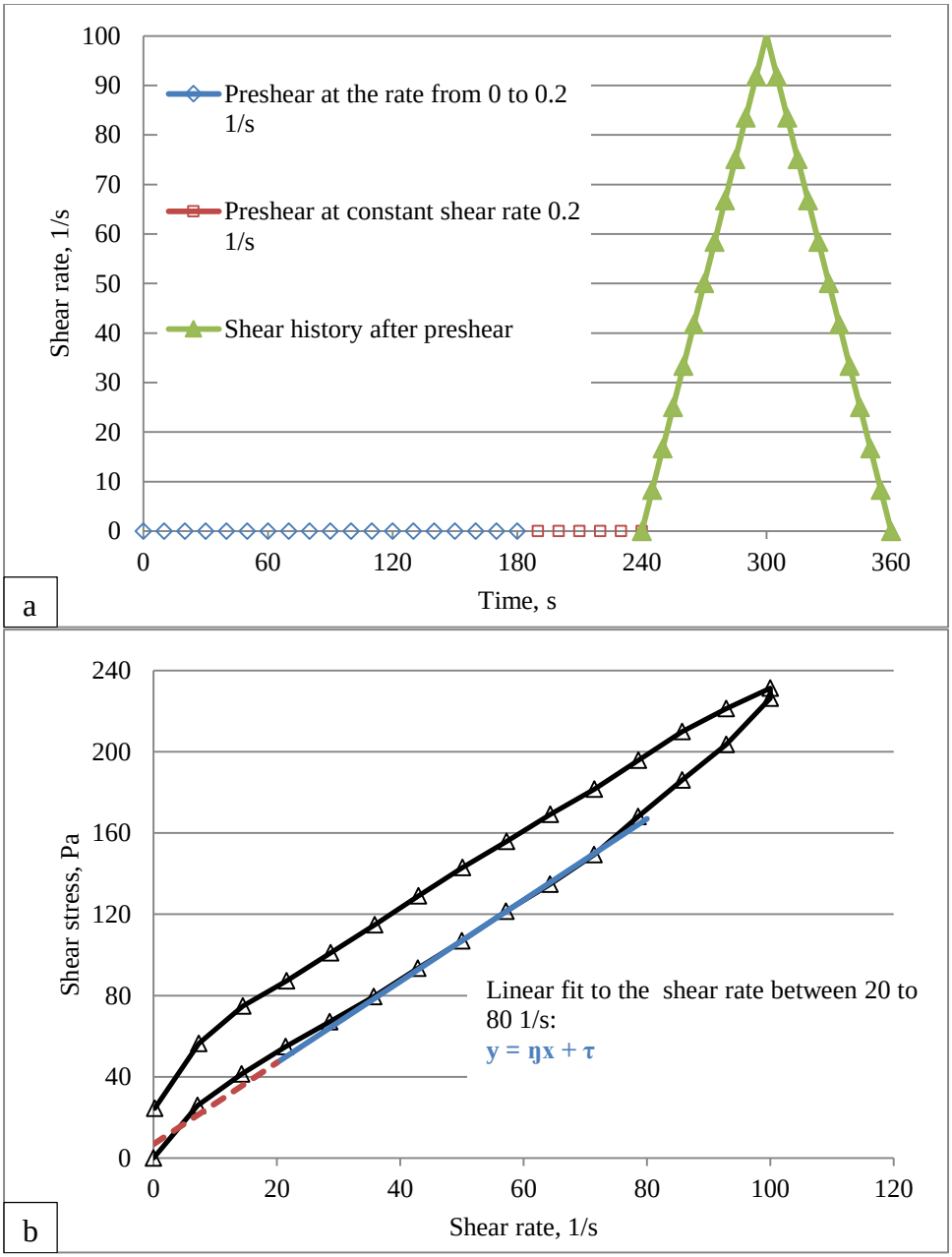


**Figure 4. (a) Loading history with preshear; (b) flow curve of a typical SCC mixture used in this study (Lomboy et al. 2013).**

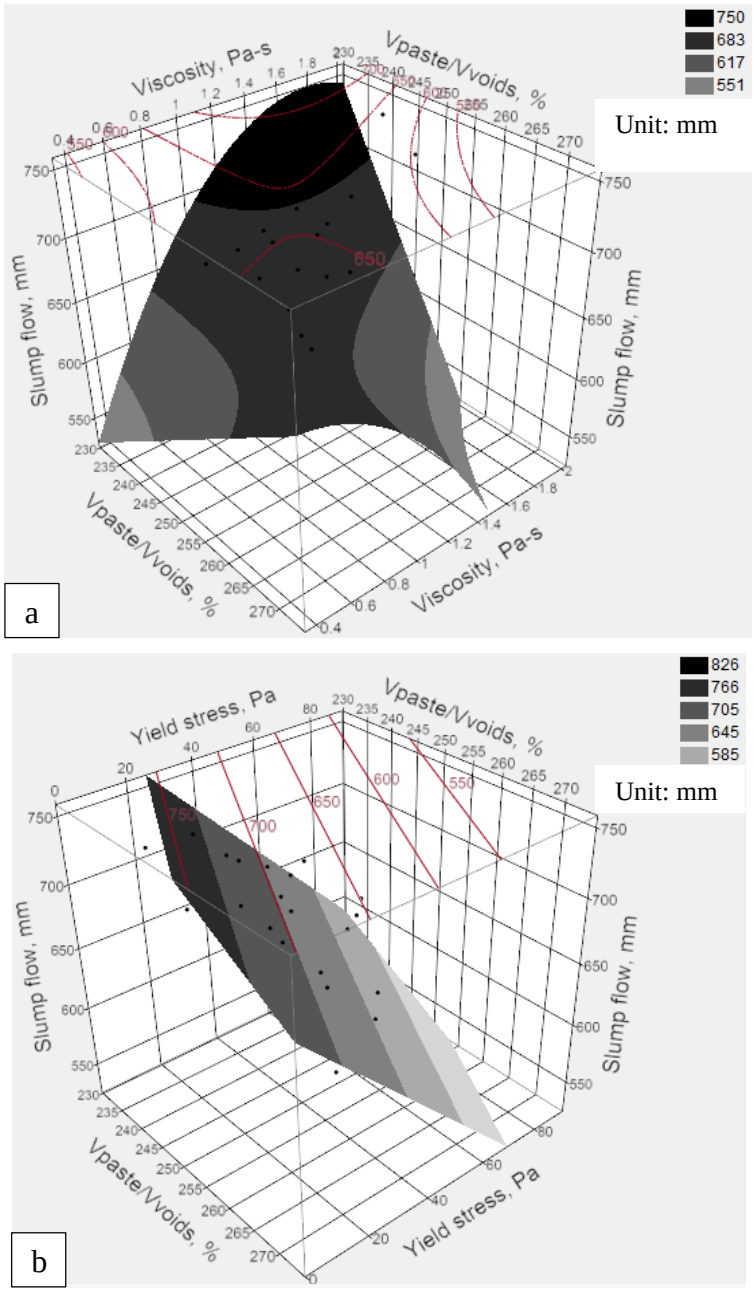


**Figure 5. Response surface plots show the relationship among Vpaste/Vvoids, slump flow, and (a) viscosity; (b) yield stress.**

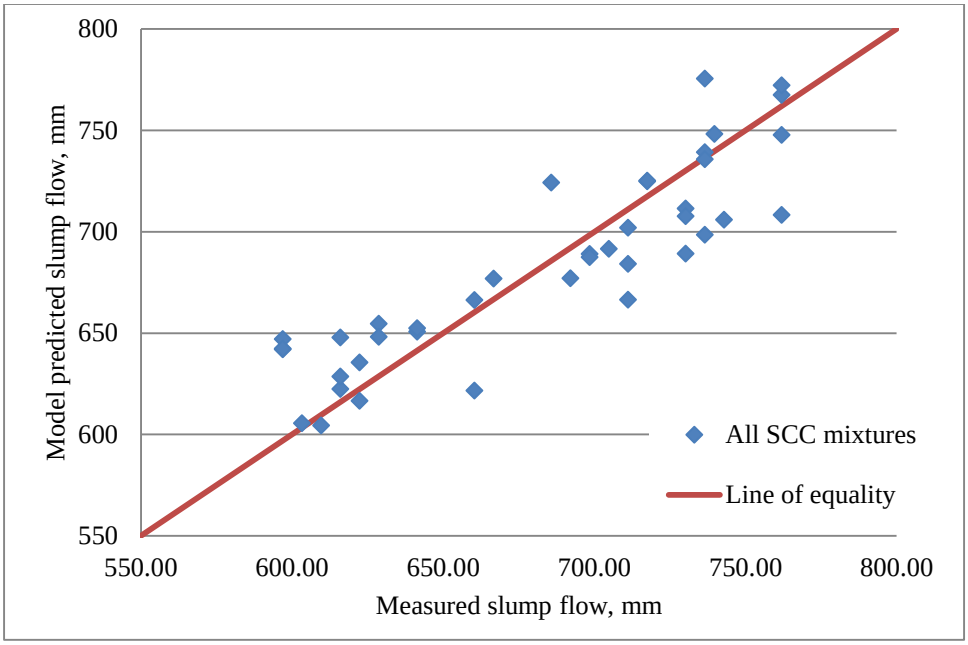


**Figure 6. Measured slump flow versus model predicted slump flow.**

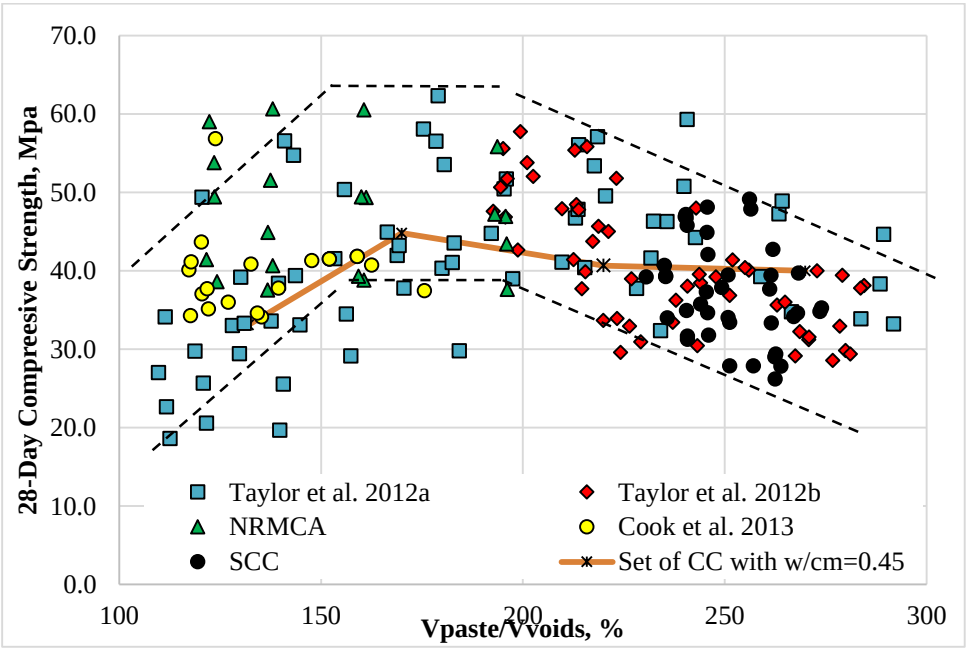


**Figure 7. Correlation between Vpaste/Vvoids and compressive strength at 28 days based on data retrieved from literature and present study (Cook et al. 2013; NRMCA; Taylor et al. 2012a & 2012b).**

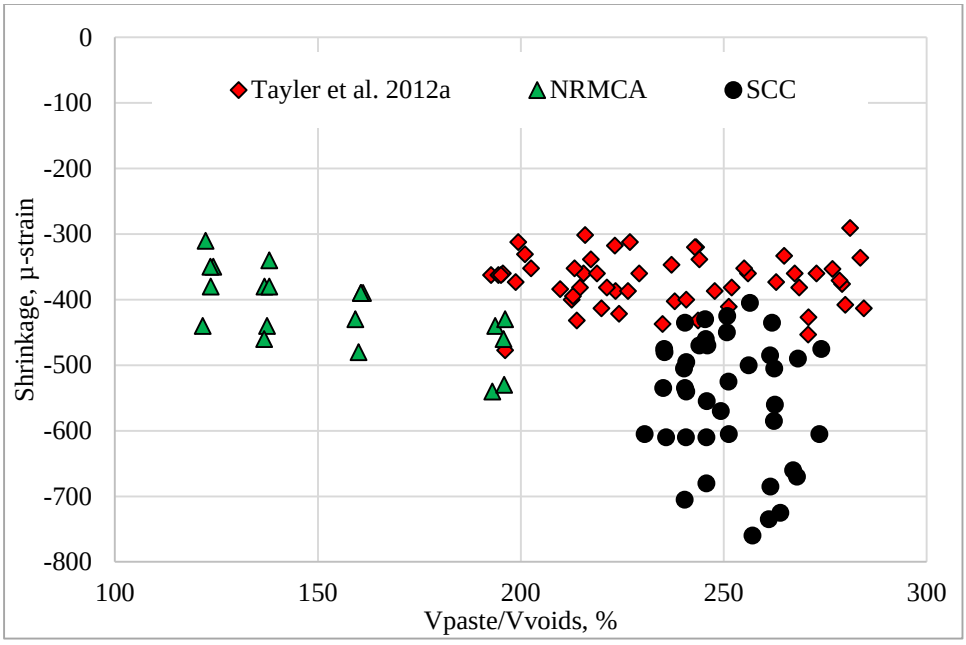


**Figure 8. Overview of the effect of Vpaste/Vvoids on free shrinkage at 56 days for CC mixtures (using data reported by Taylor et al. 2012a and NRMCA) and SCC mixtures in this study.**

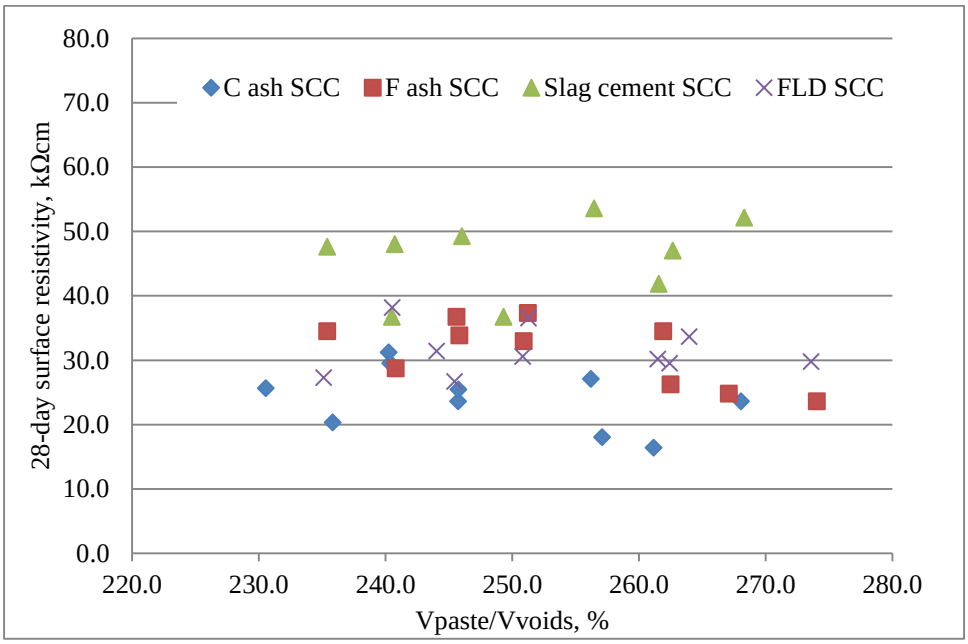


**Figure 9. The effect of Vpaste/Vvoids on surface resistivity with varied SCMs types of SCC mixtures at 28 days.**

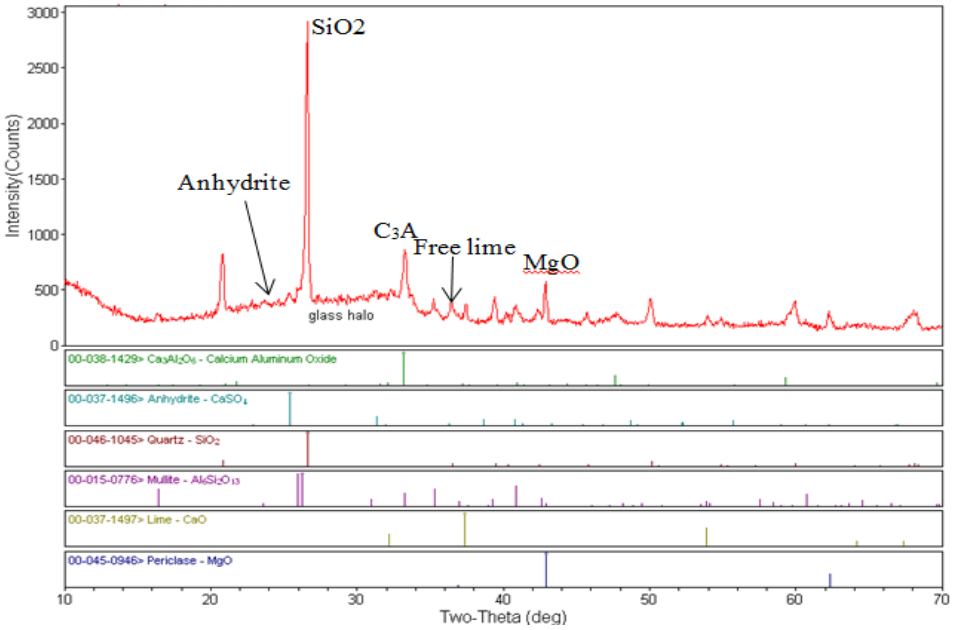


**Figure 10. X-ray diffractograms of class C fly ash.**

# CHAPTER 5. IMAGE ANALYSIS APPLICATIONS ON ASSESSING STATIC STABILITY AND FLOWABILITY OF SELF-CONSOLIDATING CONCRETE

A paper submitted to Journal of Cement and Concrete Composites

*Xuhao Wang[1], Kejin Wang[2], Jianguo Han[3], Peter Taylor[4]*

## ABSTRACT

A digital image processing (DIP) method associated with a MATLAB algorithm is used to evaluate cross sectional images of self-consolidating concrete (SCC). Parameters, such as inter-particle spacing between coarse aggregate particles and average mortar to aggregate ratio defined as average mortar thickness index (MTI), were derived from DIP method and applied to evaluate the static stability and develop statistical models to predict flowability of SCC mixtures. The proposed DIP method and MATLAB algorithm can be successfully used to derive inter-particle spacing and MTI and quantitatively evaluate the static stability on hardened SCC samples. These parameters can be applied to overcome the limitations and challenges of existing theoretical frames and construct statistical models associated with rheological parameters to predict flowability of SCC mixtures. The outcome of this study can

[1] PhD candidate, Department of Civil, Construction and Environmental Engineering, Iowa State University, 136 Town Engineering, Ames, Iowa 50011, Tel: 515-294-2252, Email: wangxh@iastate.edu

[2] Professor, Department of Civil, Construction and Environmental Engineering, Iowa State University, 492 Town Engineering, Ames, Iowa 50011, Tel: 515-294-2152, Email: kejinw@iastate.edu

[3]Lab Director, Institute of Building Materials, Department of Civil Engineering, Tsinghua University, Beijing 100084, China, Tel: 86-010-62797764, Email: hanjg@tsinghua.edu.cn

[4]Associate Director, National Concrete Pavement Technology Center, Iowa State University, Ames, Iowa 50011, Tel: 515-294-9333, Email: ptaylor@iastate.edu

be of practical value for providing an efficient and useful tool in designing mixture proportions of SCC.

**Keywords:** Self-consolidating concrete; image analysis; rheology; statistical model and analysis

## INTRODUCTION

Aggregate as a primary component occupies up to 80% of concrete volume. It can thus exert a large influence on concrete performance (Ozen and Guler, 2014). Aggregate characteristics, such as size, distribution, and shape, are key parameters of mixture design that affect workability of concrete mixtures (Mindess et al. 2003). A well-proportioned self-consolidating concrete (SCC) mixture can be achieved by controlling the aggregate system, paste quality, and paste quantity. For a given paste quality, the lower the paste quantity, the more economical the concrete is. To achieve a minimal paste quantity for a given concrete performance, a well-graded aggregate system is demanded because the dense packing of aggregate particles results in less voids for paste to fill in (Atkins, 2003). Thus, additional paste in a designed concrete mixture can function as a lubricant layer to coat the surfaces of aggregate particles and make the mixture have desirable workability. The thickness of this paste layer is referred as excess paste thickness. Achieving the designed aggregate distribution and proper excessive paste thickness is critical to control certain engineering properties and structure performance of concrete (Ozen and Guler, 2014).

In this study, digital image process and analysis (DIP) method is used to evaluate the static stability and develop statistical models to predict flowability of hardened SCC mixtures

designed for cast-in-place applications. Inter-particle spacing between coarse aggregates and average mortar to coarse aggregate ratio defined as average mortar thickness index (MTI) hereafter can be estimated using proposed algorithm in DIP method (as illustrated in Figure 2). MTI is then used to build statistical models associated with mortar rheology parameters to predict flowability of SCC mixtures. The following flow chart illustrates the main structure of this research (Figure 1).

## BACKGROUND

### Excess paste theory and Paste-to-voids volume ratio concept

Previous researchers have investigated the effects of aggregate distribution and paste quantity on the properties of conventional concrete (CC) and SCC mixtures using: (1) excess paste/mortar theory (Hu and Wang 2007; Bui et al. 2002); (2) paste-to-aggregate void volume ratio concept (Wang et al. 2014; Yurdakul et al. 2013; Koehler and Fowler 2007).

The "excess paste theory" was originally proposed by Kennedy (1940). The key of this theory was known as two-phase theory in which a paste phase is used to fill up the voids between the aggregate phase. A desired workability can be achieved by the use of sufficient paste volume to fill the voids so as to control frictions between aggregate particles. The paste layer around aggregate particles needs to be thick enough to achieve a good workability and thin enough to prevent aggregate from segregating (Kosmatka et al. 2008; Koehler and Fowler, 2007; Kennedy, 1940). Hu and Wang (2007) extended this theory to "excess mortar theory", in which paste and fine aggregate were considered as a whole system to provide segregation resistance and lubrication effect.

The "excess paste theory" was used to design SCC mixture proportions by Bui et al. (2002). The average spacing between aggregate particle surfaces (particles are assumed to be spherical), $D_{ss}$, and the average aggregate diameter, $D_{av}$, were estimated through Equations 1 and 2. These two parameters combined with paste rheology models were used to design SCC mixture proportions and predict workability. Figure 2 shows the schematic relationship among aggregate spacing, average aggregate diameter, and aggregate system used in designing SCC mixture proportions and MTI and inter-particle spacing defined in current study (Bui et al. 2002).

$$D_{ss} = D_{av}\left(\sqrt[3]{1 + \frac{V_p - V_{void}}{V_c - V_p}} - 1\right) \quad \text{Eq. (1)}$$

where $V_p$ = paste volume; $V_{void}$ = volume of voids in densely compacted aggregate determined in accordance with ASTM C29; $V_c$ = total concrete volume; and $D_{av}$ = the average aggregate diameter, which is given by

$$D_{av} = \frac{\sum d_i m_i}{\sum m_i} \quad \text{Eq. (2)}$$

where $d_i$ = average size of aggregate fraction i; and $m_i$ = percentage of aggregate mass retained between upper and lower sieve sizes in fraction i.

An alternative concept, based on the paste-to-voids volume ratio (Vpaste/Vvoids), was applied to pavement mixtures by Yurdakul et al. (2013) and SCC mixtures by Wang et al. (2014) in accordance with Koehler and Fowler's (2007) idea of relating performance of a mixture to paste volume for a given aggregate system. The concept aims at providing a quantitative method to consider the interaction between aggregate system and paste in a mixture whilst still meeting project requirements. It is believed to be more practical than

parameters of "cementitious content" or "paste content" due to the differences between aggregate systems (Yurdakul, 2013).

It can be derived by calculating the paste volume of concrete mixtures and dividing that value by the volume of voids in the combined aggregate system determined in accordance with ASTM C29. The paste volume comprises the volume of water, the cementitious materials, and measured air in the system. If all the voids between the aggregates are filled with paste with no excess, the ratio is 100%.

**Digital image processing**

Although calculations have been developed to assess excessive paste thickness, the limitations of the calculations include:

- For excess paste theory, aggregate particles are assumed to be spherical that is never the case.
- For excess paste theory, aggregate particles are considered to be packed in a cubic lattice.
- For both theories, the segregation phenomenon of CC and SCC mixture when experiencing excess vibration or poor paste quality may result in different performance between the actual and designed mixture. The degree of segregation can be an important criterion that can dramatically affect aggregate distribution.

To overcome some of these limitations, DIP method may be suitable. DIP method has been popularly applied in characterizing portland cement concrete and asphalt concrete mixtures. It can offer powerful tools to distinguish among different features on a cross section of a hardened sample and to quantify a number of geometric and distribution variables that affect the properties of concrete (Ozen, 2007). The following advantages have been proposed according to Das (2006):

- It is a rapid method that can be applied in real-time for quality control in aggregate plants;
- A large number of aggregates can be evaluated at one time and the statistical reliability is enhanced;
- It is relatively free from subjectivity associated with human errors;
- It is easy to characterize the aggregate features in a concrete sample which may be difficult to measure and analyze by physical means.

In general, the DIP method comprises several steps: image acquisition, pre-processing, segmentation, representation and description, and recognition and interpretation (Ozen 2007). The acquisition of images can be achieved by using an analog or digital camera.

After converting the image scene into a digitized form and sending to computer for recording, pre-processing is to improve the image so that further processing applications can be implemented, such as enhancement of the specific image features, noise removal, and elimination of the features that are not the area of interest (Gonzalez and Woods, 2001).

In a planar image, a segmentation operation can produce a binary image in which the object pixels are represented through a selected "thresholding" procedure. Pixels sharing similar brightness levels or color are clustered (Gonzalez and Woods, 2001). The discontinuities of the boundaries between parted regions can be recognized (Ozen 2007). This is a critical procedure for DIP because various factors may degrade the success of thresholding, such as poor contrast, non-uniform illumination, inherent noise from electronics, and noise from background. Literature has proposed three ways to tackle the challenge of selecting an optimum threshold to extract the object characteristics from the digital image: histogram shape, pixel clustering and entropy analysis (Sezgin and Sankur, 2004). Ozen and Guler (2014) pointed out the limitations of each way and proposed an algorithm for optimizing the threshold value to increase the accuracy of image analysis.

A set of row pixel data comprising the boundary information of the selected area of interest is developed for representation and description phase. “External representation” focuses on shape characteristics, such as corners and inflections, while “internal representation” focuses on color and texture. Next step is the description of the data based on the chosen representation to highlight the objects of interest (Ozen, 2007; Gonzalez and Woods, 2001).

“Recognition” is the following step to assign a label to an object depending on the information provided by it descriptors. “Interpretation” is then used as a process to assign meaning to an ensemble of the recognized objects (Gonzalez and Woods, 2001).

DIP method has been widely used for the following applications:

- Development of a method of selecting an optimum threshold value and analyzing aggregate size distribution of concrete sections (Ozen and Guler, 2014);
- Analysis on crack length and fracture properties - using Digital Image Correlation technique to well match the crack mouth opening displacement and vertical load-point displacement measured experimentally. (Yao et al. 2011; Shah and Kishen, 2011);
- Evaluation of concrete brittleness using fractured aggregate area ratio method – applying digital image analysis to capture the fractured aggregate particles and fracture surface contour (Han and Yan, 2011);
- Measurement of particle tracking and pore size distribution (Yang et al. 2009; Aydilek et al. 2007; Guler et al. 1999);
- Investigation of the relationship between aggregate shape parameters and concrete strength (Ozen, 2007);
- Quantitative determination of the static segregation resistance of SCC mixtures (Shen et al. 2007);
- Determination of aggregate shape properties using X-ray tomographic methods and the effect of shape on concrete rheology (Erdogan, 2005);

- Determination of parameters of the air-void system in hardened concrete (ASTM C457 1998).

**MIX PROPORTION AND MATERIALS**

Forty SCC mixtures were made with limestone and river gravel coarse aggregate. Each coarse aggregate was used in three different nominal maximum sizes (NMSA), 19.0 mm, 12.5 mm, and 9.5 mm. The aggregate gradations and the physical properties of the aggregates are reported in a separate paper (Wang et al. 2014).

Cementitious blends were used containing 25% Class C fly ash, 25% Class fly ash, 30% slag cement, or 15% limestone dust and 20% Class F fly ash. The chemical composition of each cementitious material was reported in a separate paper (Wang et al. 2014).

The chemical admixtures, Air-Entraining Agent (AEA), polycarboxylate based High Range Water Reducer (HRWR), and Viscosity-Modifying Admixture (VMA), were used to achieve the following targeted parameters for the SCC mixtures designed for bridge construction applications:

- Low slump flow range between 550 and 650 mm or high flow range between 650 and 750 mm
- Visual stability index, (VSI)≤1
- J-ring ≤ 75 mm

The mix proportions of all the SCC mixtures are shown in Table 1. The average spacing between aggregate particle surfaces, $D_{ss}$, and the average aggregate diameter, $D_{av}$, calculated from Equations 1 and 2 based upon excess paste theory and estimated Vpaste/Vvoids are listed in Table 1 as well.

## TEST PROCEDURES

### Workability

ASTM C1611 and C1621 were used to determine the slump flow, segregation resistance, and blocking assessment for SCC mixtures. The flow time for SCC mixture reaching diameter of 500 mm, $t_{50}$, and flow time until concrete stopped flowing, $t_{final}$, during the slump flow test were recorded.

The difference between slump flow soon after mixing and 30 minutes after mixing was an indication of the workability retention.

### Air content

Air contents were obtained in accordance with ASTM C231.

### Mortar rheology

The Bingham parameters, yield stress to initiate flow, and viscosity were determined using a Brookfield rheometer. Mortar samples were prepared from the sieved concrete mixtures using a 4.75 mm size sieve (#4 sieve). It was then placed in a 50 mm diameter by 100 mm tall cylindrical vessel and sheared with a 15 by 30 mm vane spindle. The loading history was employed according to Lomboy et al. (2013):

- Pre-shear from 0 to 0.2 $s^{-1}$ in first 180 s
- Sustained pre-shear at 0.2 $s^{-1}$ for 60 s
- 60 s of increasing spindle speed from 0.2 to 100 $s^{-1}$
- 60 s of decreasing spindle speed to 0.

The downward curve can be used to capture the yield stress, $\tau$, and viscosity, $\eta$, of the sieved mortar mixtures. The intersection with the y-axis and the slope of the linear fit Bingham model between 20 and 80 1/s shear rate of the downward curve represent the yield stress and viscosity, respectively.

## IMAGE ANALYSIS

One 100 × 200 mm concrete cylinder was prepared for each mixture and cured for 28 days. Each concrete cylinder was then cut into four equal pieces using a diamond saw. This process produced four cross sectional surfaces with no overlap as depicted in Figure 3. The thickness of the cut disks was greater than 19 mm which is the largest NMSA of coarse aggregate used in this study. The results derived by DIP method for each mixture were averaged from the four cross sectional surfaces.

The flow chart of image pre-and post-processing procedures is shown in Figure 4. Pre-processing stage comprised image acquisition, format conversion, thresholding, and image binarization. A binary image was derived from this stage and proceeds to post-processing treatment. Post-processing procedures were used to quantitatively extract the information about the region of interest.

### Stage I – Pre-processing procedures

A single-lens reflex camera was used to capture the four cross sectional surfaces for each mixture as shown in Figure 5(a). After cutting, the exposed aggregate particles on the four cross sectional surfaces were manually marked using a permanent and black marker. Thus, the contrast was enhanced for further image analysis after this treatment process as shown in Figure 5(b). In order to calibrate the distance measurements and keep the image sizes moderate for processing, the pixel and resolution were set to be 5184×3456 and 150 dpi, respectively. Adobe Photoshop (2014) was then employed to separate the aggregate particles that were in contact so that the boundaries can be identified accurately from the image.

Three algorithms were developed in MATLAB® (2013) for the following pre-processing steps to derive a binary image as shown in Figure 5(c) for post-processing steps:

- Converted image format from a true color or Red-Green-Blue (RGB) to a grey scale image in which 0 stands for white and 255 stands for black.
- Applied Otsu's (1979) method which is a simple but effective tool to separate aggregate particles from background by choosing the threshold to minimize the intra-class variance of the thresholded black and white pixels. This image thresholding process is also known as segmentation for object regions.
- Applied an algorithm by Ozen and Guler (2014) to screen out the particles whose lengths of the diameter of a fictitious circle having the same area as the particles, are smaller than 4.76 mm (#4 mesh sieve), as illustrated in Figure 6. The diameter of the fictitious circle can be calculated in Equation 3:

$$D = \sqrt{\frac{4A}{\pi}} \qquad \text{Eq. (3)}$$

where, D=diameter of an equivalent-area circle; A=area of aggregate particles.

**Stage II – Post-processing procedures**

The centroids of each aggregate particle were found through algorithm developed in MATLAB® for each image. Delaunay Triangulation Algorithm, a surface triangulation scheme, was applied to analyze the spatial distributions of the particles. According to Shewchuk (1996), "it is a triangulation of the point set with the property that no point in the point set falls in the interior of the circumcircle (circle that passes through all three vertices) of any triangle in the triangulation".

Based on Delaunay Triangulation Algorithm, another algorithm was developed to calculate: (1) the area ratio of mortar to aggregate within each triangle (as shown in Figure 2); (2) the inter-particle spacing, that is the length of the edge between the centroids of the particles (as shown in Figure 2). The histograms of mortar to aggregate ratios and the inter-particle spacing within each triangle were plotted in Figure 5(e) and (f). Therefore, the

averaged mortar to coarse aggregate area ratio or MTI and inter-particle spacing between coarse aggregate were derived for each mixture.

## RESULTS AND DISCUSSION

The measured fresh properties and average inter-particle spacing and MTI obtained from DIP method of SCC mixtures are summarized in Table 2. The results derived from DIP method can be used to assess static stability in accordance with particle distribution in the hardened cross sections and establish rheological models.

### Workability

The slump flow of all the mixtures fell into either low flow range between 550 and 650 mm or high flow range between 650 and 750 mm ranges. The $t_{50}$ times were around 2s and the $t_{final}$ times were ranged from 5.5 to 10.0s. Low viscosity was indicated by the shorter time of $t_{50}$ and $t_{final}$.

In terms of passing ability, three mixtures made with 19 mm coarse aggregate and targeted low flow range exceeded an acceptance limit set by Koehler and Fowler (2007), in which the difference between the height of concrete inside and outside the J-ring should be less than 13 mm. However, this limit may be acceptable for some applications requiring lower passing ability, such as bridge foundations.

All the mixtures were identified as “no visible blocking” or “minimal to noticeable blocking” categories in accordance with ASTM C1621 for blocking assessment.

**Particle distribution analysis**

One of the most important applications of DIP results is to assess the static stability in a hardened SCC mixture. Two ways to estimate the static stability based on particle distribution analysis from DIP method are introduced as follows.

Similar to Shen et al. (2007) proposed DIP method to determine the static segregation resistance of SCC mixtures by examination of the hardened concrete, a comparison of the mortar/aggregate volume ratio in different layers of cut concrete cylinders were applied to the mixtures in this study associated with criteria of hardened visual stability index (HVSI) as shown in Table 3 (Illinois Test Procedure SCC-5, 2004).

A cross section of the typical mixture, H-c(LS)-F, is shown in Figure 7. After pre-processing treatment, the cross section was cut into four layers with equal dimensions. MATLAB algorithm was used to determine the mortar/aggregate volume ratio for each layer that is the white/black area ratio in Figure 7. The advantages of this method are: 1) provide a quantitative manner to extrapolate the static segregation potential based on particle distribution; 2) more accurate than the VSI evaluated right after mixing because the segregation may occur during the casting process.

The comparison of two cross sections from two typical mixtures, H-c(LS)-F and H-a(G)-F, are shown in Figure 8. This plot shows the measured mortar/aggregate volume ratios of both mixtures from DIP analysis. H-a(G)-F mixture seems to have a higher segregation potential, while H-c(LS)-F mixture is relatively stable. It is because that the ratio in the first layer is much higher than that in the other layers and the variance between designed and measured ratios is large in the first layer as well. Therefore, combined with the criteria proposed in Table 3, the HVSI can be assessed and listed in Table 2.

Histogram analysis of mortar to aggregate area ratio in Delaunay triangles (Figure 5(e)) provides another quantitative way to estimate static stability of SCC mixtures:

1. Set the designed mortar/aggregate volume ratio as upper limits for each mixture;
2. Set the designed mortar/aggregate volume ratio subtract the standard deviation of all ratios as lower limits for each mixture;
3. Sum up the probability density within the range (between the lower and upper limits) for each mixture.

The analyzed cross section with higher probability density within the range is expected to be more uniformly distributed. The probability density of each mixture within the range is presented in Table 2.

For each mixture, the probability density is averaged from the four cross sections analyzed through DIP method. A plot of HVSI versus probability density of each mixture is shown in Figure 9. The probability density seems to be inversely correlated to HVSI, i.e., higher density yields a lower HVSI rating that indicates a lower segregation potential in the mixture. Four typical cross sections are shown in Figure 9 with an increased probability density and decreased HVSI. The probability density of 60% appears to be a reasonable threshold for indicating a uniformly distributed SCC mixture.

**Rheological models**

Research has been conducted to estimate slump flow or rheological parameters of concrete by considering concrete as a suspension in which solids are dispersed into a fluid phase (Erdem et al. 2009). This study is trying to establish a relationship among concrete slump flow, MTI, mortar yield stress and viscosity so that it can serve as a reference for future mix proportioning of SCC.

A statistical analysis software (JMP 2005) was used to generate quadratic response surface models for the slump flow of SCC mixtures as a function of MTI, yield stress, and viscosity, as shown in Figures 10 (a) and (b). The contour lines developed from the response surfaces are shown on the top surface in 2-Dimension. The response surfaces are divided into visualized ranges using the discrete gradients. The legends in Figures 10 (a) and (b) indicate the slump flow ranges for each gradient. These figures show the trend on how slump flow changes with varied MTI and rheological parameters and provide a manner to quantitatively predict the workability of SCC mixtures.

Equation (4) gives the mathematical expression of the prediction model on slump flow which is valid for SCC mixtures tested in this study. The regression coefficient ($R^2$ value) of 80% for prediction equation indicated a good regression model.

$$SF = 657.21 + 36.44 \times MTI - 1.56 \times \tau - 114.07 \times (MTI - 1.89) \times (\eta - 0.99) - 93.74 \times (\eta - 0.99)^2 + 0.04 \times (\tau - 33.41)^2 \quad \text{Eq. (4)}$$

where, SF = slump flow in mm; $\tau$ = yield stress; $\eta$= viscosity. The t test indicated that all the terms shown in the prediction equation are statistically significant. Simplify the Eq. (4), a linear relationship can be derived between slump flow and MTI in Eq. (5). For a given yield stress, viscosity tends to significantly affect slump flow: when the mortar viscosity is less than 1.30 yielding a positive coefficient of MTI, higher MTI may result in a higher slump flow; when the viscosity is greater than 1.30, lower slump flow is expected with an increased MTI.

$$SF = 397 + 0.04\tau \times (\tau - 106) - 94\eta \times (\eta - 4.27) + 149 \times (1 - 0.77\eta) \times MTI \quad \text{Eq. (5)}$$

Figure 11 shows the relationship between measured and model predicted slump flow. The data closely scattered around the line of equality confirmed that the model can accurately predict slump flow of SCC mixtures in this study.

**Relationship between results from DIP method and existing theoretical frames**

The MTI derived from DIP method was correlated to existing theoretical frames: (a) paste-to-voids volume ratio concept and (b) excess paste theory. Figures 12 (a) and (b) give the relationship between MTI and Vpaste/Vvoids and $D_{ss}$, respectively.

The gradation of gravel and limestone aggregates with same NMAS were similar. Limestone particles of higher angularity tend to increase the packing density, thus, resulting in less void content in the combined aggregate system (Quiroga and Fowler, 2003). The similar relationship is found between MTI and $D_{ss}$ for SCC mixtures with different aggregate as shown in Figure 12 (b). At a given binder content, size and sand-to-aggregate ratio system, less mortar is needed to fill in the denser limestone particle system, resulting in a lower mortar to aggregate ratio, i.e., MTI, and smaller aggregate spacing, i.e., $D_{ss}$. Also, an increased effect on packing density with decreased size of aggregate particles is observed on limestone and gravel mixtures. This confirms the findings from Compressible Packing Model proposed by De Larrard (1999).

A linear relationship is established for average inter-particle spacing derived from DIP method and parameter in excess paste theory as plotted in Figure 13. This correlation illustrates that the average aggregate spacing obtained from excess paste theory can be used to predict the actual average inter-particle spacing of coarse aggregate estimated from hardened concrete mixtures, despite the coarse aggregate sizes and types. In addition, the

increased effect on packing density with decreased size of limestone and gravel aggregate particles can be observed as well. The prediction equation is given in Eq. (6) as follows:

$$\text{Actual average coarse aggregate spacing} = 19.4 \times D_{ss} + 5.0 \quad \text{Eq. (6)}$$

The relationship associated with the rheological parameters can be used to predict the workability and develop mixture design of SCC mixtures.

## CONCLUSIONS

The proposed DIP method and MATLAB algorithm can be successfully used to derive MTI and average inter-particle spacing between coarse aggregate on hardened concrete samples and quantitatively assess the static stability of a SCC mixture. They provide efficient and useful tools in designing mixture proportions of SCC. The following outcomes can be drawn based on the analysis of this research:

- Layered cross sectional and histogram analysis of mortar to aggregate area ratio provide quantitative ways to estimate static stability of SCC mixtures. The probability density of 60% from histogram analysis appears to be a reasonable threshold for indicating a uniformly distributed SCC mixture.
- The MTI can be used to establish a statistical response surface model to predict the flowability of SCC mixtures associated with rheological parameters in this research. For a given mortar yield stress, a critical mortar viscosity of 1.30 tends to significantly affect the trend of slump flow changing with MTI.
- The investigated relationship between MTI from DIP method and $D_{ss}$ and Vpaste/Vvoids from existing theoretical frames is well correlated. Therefore, the parameters derived from DIP method should be used to evaluate the performance of SCC mixtures because they have potentials to overcome the limitations of “excess paste/mortar theory” and paste-to-voids volume ratio concept.
- A prediction equation is developed for estimating the actual average inter-particle spacing of coarse aggregate in a mixture from the average aggregate spacing calculated from “excess paste theory”.

**ACKNOWLEDGEMENTS**

The authors acknowledge the research sponsorship and the collaboration among Iowa State University (ISU), the University of Nebraska – Lincoln (UNL), and Northwestern University (NU). The authors would like to give special thanks to Dr. George Morcous from UNL for his guidance, suggestions, and contributions to this sponsored research project and the ideas of this paper. The opinions, findings, and conclusions presented in this paper are those of the authors and do not reflect those of the research sponsors.

**REFERENCES**

Adobe Photoshop, Adobe Systems Incorporated, 2014.

ASTM C29. "Standard Test Method for Bulk Density ("Unit Weight") and Voids in Aggregate," American Society for Testing and Materials, Pennsylvania, 1999.

ASTM C457. "Standard Test Method for Microscopical Determination of Parameters of the Air Void System in Hardened Concrete," American Society for Testing and Materials, Pennsylvania, 1998.

ASTM C1611. "Standard Test Method for Slump Flow of Self-Consolidating Concrete," American Society for Testing and Materials, Pennsylvania, 2005.

ASTM C1621. "Standard Test Method for Passing Ability of Self-Consolidating Concrete by J-Ring," American Society for Testing and Materials, Pennsylvania, 2009.

Atkins, H., "Highway Materials, Soils, and Concretes," fourth edition, Upper Saddle River: Prentice Hall, Pearson Education; 2003 (NJ 07458. USA).

Aydilek, A.; D'Hondt, D.; Holtz, R., "Comparative Evaluation of Geotextile Pore Sizes Using Bubble Point Test and Image Analysis," Geotechnical Test Journal, 30 (3):173–81, 2007.

Bui, V.; Akkaya, Y.; and Shah, S., "Rheological Model for Self-Consolidating Concrete," ACI Material Journal, V. 99, No. 6, 2002.

Das, A., "A Revisit to Aggregate Shape Parameters", Workshop on Aggregates flakiness and elongation indices – *(WSOA)*, New Delhi, 2006.

De Larrard, F., "Concrete Mixture Proportioning: A Scientific Approach," London, 1999.

Erdem, T.; Khayat, K.; and Yahia, A., "Correlating Rheology of Self-Consolidating Concrete to Corresponding Concrete-Equivalent Mortar," ACI Materials Journal, V. 106, No. 2, pp. 154-160, 2009.

Erdogan, S., "Determination of Aggregate Shape Properties Using X-ray Tomographic Methods and the Effect of Shape on Concrete Rheology," PhD dissertation, the University of Texas at Austin, 2005.

Gonzalez, R.; Woods R., "Digital Image Processing", Prentice Hall, USA, 2001.

Guler, M.; Edil, T.; Bosscher, P., "Measurement of Particle Movement in Granular Soils Using Image Analysis," Journal of Computational Civil Engineering, 13(2):116–22, 1999.

Han, J.; Yan, P., "New Concrete Brittleness Evaluating Method—Fractured Aggregate Area Ratio Method," Concrete, Number 2, 2011.

Hu, J., and Wang, K., "Effects of Size and Uncompacted Voids of Aggregate on Mortar Flow Ability," Journal of Advanced Concrete Technology, 5, pp. 75-85, 2007.

JMP 8.0.0. Statistical Discovery. SAS Institute Inc., 2005.

Kennedy, C., "The Design of Concrete Mixes," Journal of the American Concrete Institute, 36, pp. 373-400, 1940.

Koehler, E., and Fowler, D., "Aggregates in Self-Consolidating Concrete," International Center for Aggregates Research (ICAR), Austin, TX, 2007.

Kosmatka, S.; Kerkhoff, B.; and Panarese, W., "Design and Control of Concrete Mixtures," 14th ed., Portland Cement Association, Skokie, IL, USA, 2008.

MATLAB, The MathWorks, Inc., 2013.

Mindess, S.; Young, J.; and Darwin, D., "Concrete," second edition, Upper Saddle River: Prentice Hall, Pearson Education, Inc.; 2003 (NJ 07458. USA).

Ozen, M.; Guler, M., "Assessment of Optimum Threshold and Particle Shape Parameter for the Image Analysis of Aggregate Size Distribution of Concrete Sections," Optics and Lasers in Engineering, 53, pp. 122-132, 2014.

Ozen, M., "Investigation of Relationship between Aggregate Shape Parameters and Concrete Strength Using Imaging Techniques," Master thesis, Middle East Technical University, Turkey, 2007.

Otsu, N., "A Threshold Selection Method from Gray-Level Histograms," IEEE Transactions on Systems, Man, and Cybernetics, 9(1): 62-66, 1979.

Quiroga, P.; Fowler, D., "The Effects of Aggregates Characteristics on The Performance of Portland and Cement Concrete," Project report ICAR 104-1F, the University of Texas at Austin, 2003.

Sezgin, M.; Sankur, B., "Survey Over Image Thresholding Techniques and Quantitative Performance Evaluation," Journal of Electron Imaging, 13(1):146–65, 2004.

Shah, S.; Kishen, J., "Fracture Properties of Concrete-Concrete Interfaces Using Digital Image Correlation," Experimental Mechanics, 51(3), 303–13, 2011.

Shen, L.; Struble, L.; Lange, D., "New Method for Measuring Static Segregation of Self-Consolidating Concrete," Journal of ASTM International, Volume 35, Issue 3, 2007.

Shewchuk, J., "Triangle: Engineering A 2D Quality Mesh Generator and Delaunay Triangulator," First Workshop on Applied Computational Geometry, 124-133, 1996.

Standard Test Method for Static Segregation of Hydraulic-Cement Self-Consolidating Concrete Using the Column Technique, Illinois Test Procedure *SCC-5*, July 1, 2004.

Wang, X.; Taylor, P.; Wang, K.; and Morcous, G., "Using Paste-to-Voids Ratio Evaluating the Performance of Self-Consolidating Concrete Mixtures," Paper submitted to Journal of Construction and Building Materials, 2014.

Yang, Z.; Peng, X.; Lee, D.; Chen, M., "An Image-Based Method for Obtaining Pore-Size Distribution of Porous Media," Environmental Science Technology, 43 (9):3248–53, 2009.

Yao, X.; Yao, M.; Xu, B., "Automated Measurements of Road Cracks Using Line-Scan Imaging", Journal of Test Evaluation, 39(4):1–9, 2011.

**LIST OF TABLES**

**LIST OF FIGURES**

**Table 1(a) – Mix proportions for limestone mixtures**

| ID | C I,II | SCM | Filler | CA | FA | Water | HRWRA | VMA | AEA | Paste Volume | Vpaste/Vvoids | Designed mortar/agg | Dss |
|---|---|---|---|---|---|---|---|---|---|---|---|---|---|
| | kg/m3 | kg/m3 | kg/m3 | kg/m3 | kg/m3 | kg/m3 | ml/100kg SCMs | ml/100kg | ml/100kg | % | % | | mm |
| L-a(LS)-C | 315 | 105 | 0 | 915 | 749 | 166 | 652.0 | 0 | 97.8 | 36.5 | 230.5 | 1.9 | 0.408 |
| L-a(LS)-F | 315 | 105 | 0 | 915 | 749 | 166 | 489.0 | 0 | 97.8 | 37.0 | 235.4 | 1.9 | 0.427 |
| L-a(LS)-S | 309 | 132 | 0 | 915 | 749 | 166 | 652.0 | 0 | 97.8 | 37.0 | 235.4 | 1.9 | 0.427 |
| L-a(LS)-FLD | 271 | 83 | 62 | 915 | 749 | 166 | 586.8 | 0 | 97.8 | 37.0 | 235.1 | 1.9 | 0.426 |
| H-a(LS)-C | 337 | 112 | 0 | 901 | 737 | 166 | 521.6 | 0 | 52.2 | 37.5 | 240.2 | 1.9 | 0.446 |
| H-a(LS)-F | 337 | 112 | 0 | 901 | 737 | 166 | 521.6 | 130 | 52.2 | 38.0 | 245.6 | 1.9 | 0.467 |
| H-a(LS)-S | 320 | 137 | 0 | 908 | 743 | 166 | 521.6 | 130 | 52.2 | 37.5 | 240.5 | 1.9 | 0.447 |
| H-a(LS)-FLD | 290 | 89 | 63 | 901 | 737 | 166 | 782.4 | 0 | 97.8 | 37.8 | 244.0 | 1.9 | 0.461 |
| L-b(LS)-C | 317 | 106 | 0 | 867 | 769 | 175 | 521.6 | 0 | 65.2 | 37.5 | 245.7 | 2.1 | 0.297 |
| L-b(LS)-F | 317 | 106 | 0 | 867 | 769 | 175 | 391.2 | 130 | 97.8 | 38.0 | 250.9 | 2.1 | 0.310 |
| L-b(LS)-S | 311 | 129 | 0 | 874 | 775 | 175 | 521.6 | 0 | 97.8 | 37.8 | 249.3 | 2.1 | 0.306 |
| L-b(LS)-FLD | 273 | 84 | 63 | 867 | 769 | 175 | 391.2 | 0 | 97.8 | 38.0 | 250.8 | 2.1 | 0.310 |
| H-b(LS)-C | 339 | 113 | 0 | 854 | 757 | 175 | 586.8 | 196 | 52.2 | 38.5 | 256.2 | 2.1 | 0.323 |
| H-b(LS)-F | 339 | 113 | 0 | 854 | 757 | 175 | 521.6 | 196 | 65.2 | 39.0 | 261.9 | 2.1 | 0.337 |
| H-b(LS)-S | 322 | 138 | 0 | 860 | 763 | 175 | 619.4 | 196 | 65.2 | 38.5 | 256.5 | 2.1 | 0.323 |
| H-b(LS)-FLD | 291 | 90 | 67 | 854 | 757 | 175 | 456.4 | 196 | 65.2 | 39.0 | 261.5 | 2.1 | 0.336 |
| H-c(LS)-C | 348 | 116 | 0 | 791 | 791 | 181 | 717.2 | 0 | 81.5 | 39.5 | 240.4 | 2.4 | 0.226 |
| H-c(LS)-F | 348 | 116 | 0 | 791 | 791 | 181 | 684.6 | 196 | 97.8 | 40.0 | 245.8 | 2.4 | 0.237 |
| H-c(LS)-S | 331 | 142 | 0 | 798 | 798 | 181 | 782.4 | 0 | 97.8 | 39.5 | 240.7 | 2.4 | 0.226 |
| H-c(LS)-FLD | 299 | 92 | 69 | 791 | 791 | 181 | 717.2 | 0 | 97.8 | 40.0 | 245.5 | 2.4 | 0.236 |

**Table 1(b) – Mix proportions for gravel mixtures**

| ID | C I,II | SCM | Filler | CA | FA | Water | HRWRA | VMA | AEA | Paste Volume | Vpaste/Vvoids | Designed mortar/agg. volume | Dss |
|---|---|---|---|---|---|---|---|---|---|---|---|---|---|
| | kg/m3 | kg/m3 | kg/m3 | kg/m3 | kg/m3 | kg/m3 | ml/100kg SCMs | ml/100kg SCMs | ml/100kg SCMs | % | % | | mm |
| L-a(G)-C | 315 | 105 | 0 | 911 | 746 | 166 | 456.4 | 0 | 97.8 | 36.5 | 235.8 | 1.9 | 0.396 |
| L-a(G)-F | 315 | 105 | 0 | 911 | 746 | 166 | 391.2 | 0 | 97.8 | 37.0 | 240.8 | 1.9 | 0.413 |
| L-a(G)-S | 309 | 132 | 0 | 911 | 746 | 166 | 521.6 | 0 | 97.8 | 37.0 | 240.8 | 1.9 | 0.413 |
| L-a(G)-FLD | 271 | 83 | 62 | 911 | 746 | 166 | 391.2 | 0 | 97.8 | 37.0 | 240.5 | 1.9 | 0.412 |
| H-a(G)-C | 337 | 112 | 0 | 897 | 734 | 166 | 652.0 | 196 | 97.8 | 37.5 | 245.8 | 1.9 | 0.431 |
| H-a(G)-F | 337 | 112 | 0 | 897 | 734 | 166 | 652.0 | 196 | 97.8 | 38.0 | 251.2 | 1.9 | 0.451 |
| H-a(G)-S | 320 | 137 | 0 | 904 | 740 | 166 | 652.0 | 196 | 97.8 | 37.5 | 246.0 | 1.9 | 0.432 |
| H-a(G)-FLD | 290 | 89 | 67 | 897 | 734 | 166 | 847.6 | 196 | 97.8 | 38.0 | 251.3 | 1.9 | 0.451 |
| L-b(G)-C | 317 | 106 | 0 | 864 | 766 | 175 | 456.4 | 0 | 97.8 | 37.5 | 257.1 | 2.1 | 0.340 |
| L-b(G)-F | 317 | 106 | 0 | 864 | 766 | 175 | 293.4 | 0 | 97.8 | 38.0 | 262.5 | 2.1 | 0.354 |
| L-b(G)-S | 311 | 133 | 0 | 864 | 766 | 175 | 391.2 | 0 | 97.8 | 38.0 | 262.7 | 2.1 | 0.354 |
| L-b(G)-FLD | 273 | 84 | 63 | 864 | 766 | 175 | 391.2 | 0 | 97.8 | 38.0 | 262.4 | 2.1 | 0.354 |
| H-b(G)-C | 339 | 113 | 0 | 850 | 754 | 175 | 717.2 | 196 | 97.8 | 38.5 | 268.1 | 2.1 | 0.368 |
| H-b(G)-F | 339 | 113 | 0 | 850 | 754 | 175 | 652.0 | 391 | 97.8 | 39.0 | 274.1 | 2.1 | 0.383 |
| H-b(G)-S | 322 | 138 | 0 | 857 | 760 | 175 | 782.4 | 326 | 97.8 | 38.5 | 268.3 | 2.1 | 0.368 |
| H-b(G)-FLD | 291 | 90 | 67 | 850 | 754 | 175 | 652.0 | 196 | 97.8 | 39.0 | 273.6 | 2.1 | 0.381 |
| H-c(G)-C | 348 | 116 | 0 | 788 | 788 | 181 | 652.0 | 0 | 97.8 | 39.5 | 261.2 | 2.3 | 0.272 |
| H-c(G)-F | 348 | 116 | 0 | 788 | 788 | 181 | 586.8 | 0 | 97.8 | 40.0 | 267.1 | 2.3 | 0.283 |
| H-c(G)-S | 331 | 142 | 0 | 795 | 795 | 181 | 782.4 | 228 | 97.8 | 39.5 | 261.6 | 2.3 | 0.272 |
| H-c(G)-FLD | 291 | 92 | 69 | 788 | 788 | 181 | 619.4 | 0 | 97.8 | 39.7 | 264.0 | 2.3 | 0.277 |

Note: C = Class C fly ash; F = Class F fly ash; S = slag cement; FLD = F fly ash and limestone dust; a = 19.0 mm NMSA; b = 12.5 mm NMSA; c = 9.5 mm NMSA; H = high slump flow range (i.e., 650 - 750 mm); L = low slump flow range (i.e., 550 – 650 mm); C I,II = Type I/II portland cement; LD = limestone dust; CA = coarse aggregate; FA = fine aggregate; LS = crushed limestone; G = river gravel; SCMs = supplementary cementitious materials.

**Table 2(a) – Fresh properties and DIP results of limestone SCC mixtures**

| ID | Slump/Slump Flow after mixing | | | | J-ring test | | Total air | Unit Weight | Slump flow after 30 mins of mixing | Yield stress | Viscosity | HVSI | Probability density | Ave. inter-particle distance | Ave. mortar thickness index (MTI) |
|---|---|---|---|---|---|---|---|---|---|---|---|---|---|---|---|
| | T50(s) | Tfinal (s) | D (mm) | VSI | ΔD (mm) | ΔH (mm) | % | kg/m3 | D (mm) | Pa | Pa-s | | % | mm | |
| L-a(LS)-C | 1.9 | 7.9 | 610 | 0.0 | 32 | 13 | 6.2 | 2297 | 514 | 78.7 | 1.07 | 0.0 | 81 | 13.28 | 1.06 |
| L-a(LS)-F | 1.2 | 6.8 | 660 | 0.0 | 51 | 11 | 6.0 | 2262 | 559 | 62.0 | 0.93 | 0.0 | 80 | 14.78 | 1.19 |
| L-a(LS)-S | 1.7 | 6.5 | 641 | 0.0 | 38 | 14 | 8.0 | 2223 | 552 | 53.5 | 1.17 | 0.0 | 74 | 13.82 | 1.13 |
| L-a(LS)-FLD | 1.9 | 7.9 | 597 | 0.0 | 25 | 13 | 5.5 | 2291 | 527 | 49.9 | 0.83 | 0.0 | 71 | 12.89 | 1.25 |
| H-a(LS)-C | <2 | 6.8 | 705 | 0.5 | 16 | 14 | 5.2 | 2310 | 692 | 37.9 | 1.73 | 1.0 | 64 | 15.31 | 1.32 |
| H-a(LS)-F | <2 | 7.8 | 730 | 1.0 | 25 | 11 | 3.5 | 2342 | 718 | 26.8 | 0.87 | 1.0 | 58 | 13.75 | 1.39 |
| H-a(LS)-S | 2.0 | 6.2 | 740 | 0.5 | 3 | 10 | 6.5 | 2262 | 702 | 10.7 | 1.95 | 0.5 | 62 | 14.07 | 1.45 |
| H-a(LS)-FLD | 1.3 | 7.0 | 699 | 0.5 | 44 | 11 | 6.0 | 2278 | 629 | 53.1 | 1.08 | 1.0 | 60 | 13.44 | 1.47 |
| L-b(LS)-C | <2 | 6.8 | 616 | 0.0 | 22 | 8 | 4.0 | 2339 | 533 | 45.4 | 0.97 | 0.0 | 76 | 10.87 | 1.18 |
| L-b(LS)-F | <2 | 7.1 | 616 | 0.0 | 25 | 6 | 5.0 | 2287 | 578 | 51.6 | 1.07 | 0.0 | 80 | 10.47 | 1.35 |
| L-b(LS)-S | <2 | 6.8 | 597 | 0.0 | 25 | 17 | 6.8 | 2255 | 546 | 47.1 | 1.39 | 0.0 | 78 | 11.96 | 1.48 |
| L-b(LS)-FLD | <2 | 8.3 | 629 | 0.0 | 6 | 6 | 5.0 | 2268 | 572 | 40.7 | 0.89 | 0.0 | 77 | 11.89 | 1.49 |
| H-b(LS)-C | 2.0 | 9.8 | 711 | 0.5 | 29 | 13 | 3.0 | 2342 | 622 | 29.3 | 0.71 | 0.0 | 68 | 10.89 | 1.78 |
| H-b(LS)-F | <2 | 6.9 | 711 | 0.5 | 13 | 16 | 6.5 | 2326 | 648 | 39.5 | 1.03 | 1.0 | 59 | 10.20 | 1.87 |
| H-b(LS)-S | <2 | 6.7 | 730 | 0.5 | 19 | 8 | 7.5 | 2281 | 648 | 14.8 | 1.08 | 0.5 | 61 | 10.93 | 1.56 |
| H-b(LS)-FLD | <2 | 6.5 | 667 | 0.0 | 19 | 11 | 4.5 | 2310 | 610 | 30.9 | 0.82 | 0.0 | 71 | 11.89 | 1.99 |
| H-c(LS)-C | <2 | 6.8 | 737 | 0.0 | 25 | 6 | 5.0 | 2291 | 679 | 24.6 | 1.00 | 0.0 | 78 | 9.28 | 1.92 |
| H-c(LS)-F | <2 | 7.6 | 699 | 0.0 | 19 | 8 | 6.5 | 2291 | 629 | 27.6 | 0.88 | 0.0 | 72 | 9.16 | 2.28 |
| H-c(LS)-S | 2.7 | 6.5 | 686 | 0.0 | 13 | 6 | 7.0 | 2249 | 635 | 20.3 | 1.73 | 0.0 | 66 | 9.77 | 2.13 |
| H-c(LS)-FLD | 1.7 | 8.9 | 692 | 0.0 | 19 | 13 | 6.5 | 2239 | 641 | 33.3 | 1.09 | 0.0 | 72 | 9.16 | 2.38 |

**Table 2(b) – Fresh properties and DIP results of gravel SCC mixtures**

| ID | Slump/Slump Flow after mixing | | | | J-ring test | | Total air | Unit Weight | Slump flow after 30 mins of mixing | Yield stress | Viscosity | HVSI | Probability density | Ave. inter-particle distance | Ave. mortar thickness index (MTI) |
|---|---|---|---|---|---|---|---|---|---|---|---|---|---|---|---|
| | T50 (s) | Tfinal (s) | D (mm) | VSI | ΔD (mm) | ΔH (mm) | % | kg/m3 | D (mm) | Pa | Pa-s | | % | mm | |
| L-a(G)-C | 1.6 | 6.4 | 616 | 0.0 | 13 | 14 | 8.0 | 2236 | 527 | 87.6 | 1.89 | 0.0 | 64 | 12.10 | 1.27 |
| L-a(G)-F | 1.2 | 6.8 | 622 | 0.0 | 32 | 14 | 7.4 | 2287 | 559 | 50.7 | 0.79 | 0.0 | 74 | 13.27 | 1.23 |
| L-a(G)-S | 1.9 | 6.5 | 660 | 0.0 | 32 | 17 | 7.8 | 2178 | 578 | 45.2 | 1.42 | 0.0 | 76 | 12.80 | 1.70 |
| L-a(G)-FLD | 1.4 | 7.7 | 597 | 0.0 | 19 | 13 | 6.6 | 2265 | 527 | 43.5 | 0.64 | 0.0 | 77 | 13.14 | 1.30 |
| H-a(G)-C | 1.3 | 7.3 | 711 | 1.0 | 51 | 6 | 5.7 | 2265 | 654 | 38.6 | 1.23 | 1.5 | 66 | 13.36 | 1.49 |
| H-a(G)-F | 1.2 | 7.8 | 762 | 1.0 | 25 | 3 | 5.5 | 2300 | 705 | 18.6 | 0.82 | 1.5 | 52 | 11.68 | 2.25 |
| H-a(G)-S | 2.3 | 8.7 | 718 | 0.5 | 25 | 6 | 5.7 | 2166 | 670 | 13.5 | 1.98 | 1.0 | 58 | 12.56 | 1.84 |
| H-a(G)-FLD | 1.6 | 7.3 | 718 | 1.0 | 32 | 6 | 4.6 | 2287 | 641 | 12.8 | 0.57 | 1.0 | 52 | 13.84 | 2.01 |
| L-b(G)-C | 1.0 | 6.0 | 622 | 0.0 | 13 | 6 | 5.6 | 2252 | 546 | 55.2 | 0.77 | 0.0 | 79 | 10.17 | 1.36 |
| L-b(G)-F | 1.4 | 5.5 | 629 | 0.0 | 6 | 6 | 6.0 | 2281 | 578 | 44.5 | 0.62 | 0.0 | 78 | 12.00 | 1.58 |
| L-b(G)-S | 1.8 | 10.0 | 603 | 0.0 | 6 | 13 | 6.5 | 2185 | 546 | 31.1 | 1.15 | 0.0 | 75 | 11.23 | 1.85 |
| L-b(G)-FLD | 1.0 | 5.9 | 641 | 0.0 | 6 | 6 | 5.6 | 2265 | 572 | 25.9 | 0.59 | 0.0 | 81 | 10.86 | 1.68 |
| H-b(G)-C | 1.5 | 7.9 | 730 | 0.5 | 13 | 8 | 6.0 | 2265 | 622 | 26.0 | 0.52 | 1.0 | 65 | 11.32 | 2.58 |
| H-b(G)-F | 1.1 | 7.4 | 737 | 2.0 | 6 | 6 | 6.0 | 2284 | 660 | 8.4 | 0.40 | 2.0 | 52 | 12.16 | 3.04 |
| H-b(G)-S | 2.3 | 9.7 | 762 | 2.0 | 6 | 6 | 7.8 | 2182 | 679 | 1.4 | 0.68 | 2.0 | 51 | 12.85 | 2.65 |
| H-b(G)-FLD | 0.9 | 6.2 | 762 | 1.5 | 13 | 5 | 7.6 | 2233 | 686 | 15.8 | 0.46 | 2.0 | 49 | 13.82 | 2.78 |
| H-c(G)-C | 1.4 | 7.2 | 743 | 0.0 | 6 | 6 | 6.6 | 2259 | 679 | 18.9 | 0.88 | 0.5 | 74 | 10.22 | 3.25 |
| H-c(G)-F | 1.3 | 9.5 | 737 | 0.0 | 6 | 6 | 6.0 | 2255 | 648 | 9.8 | 0.74 | 0.0 | 76 | 10.58 | 3.48 |
| H-c(G)-S | 1.8 | 7.6 | 762 | 2.0 | 6 | 6 | 5.4 | 2220 | 692 | 0.0 | 0.53 | 2.0 | 58 | 10.39 | 3.35 |
| H-c(G)-FLD | 1.1 | 5.8 | 737 | 0.0 | 19 | 6 | 6.2 | 2233 | 660 | 11.4 | 0.69 | 0.0 | 78 | 11.05 | 3.36 |

Note: D = slump flow diameter; ΔD = slump flow diameter - J-ring flow diameter; ΔH = the difference between the height of concrete inside the ring and outside the ring at four locations around the ring.

**Table 3 – Visual stability index of hardened specimens rating criteria (Illinois Test Procedure SCC-5)**

| Rating | Criteria |
|---|---|
| 0 - stable | No mortar layer at the top of the cut plane and no variance in size and percent area of coarse aggregate distribution from top to bottom. |
| 1 - stable | No mortar layer at the top of the cut plane but slight variance in size and percent area of coarse aggregate distribution from top to bottom. |
| 2- unstable | Slight mortar layer, less than 25 mm (1 in.) tall, at the top of the cut plane and distinct variance in size and percent area of coarse aggregate distribution from top to bottom |
| 3- unstable | Clearly segregated as evidenced by a mortar layer greater than 25 mm (1 in.) tall and/or considerable variance in size and percent area of coarse aggregate distribution from top to bottom |

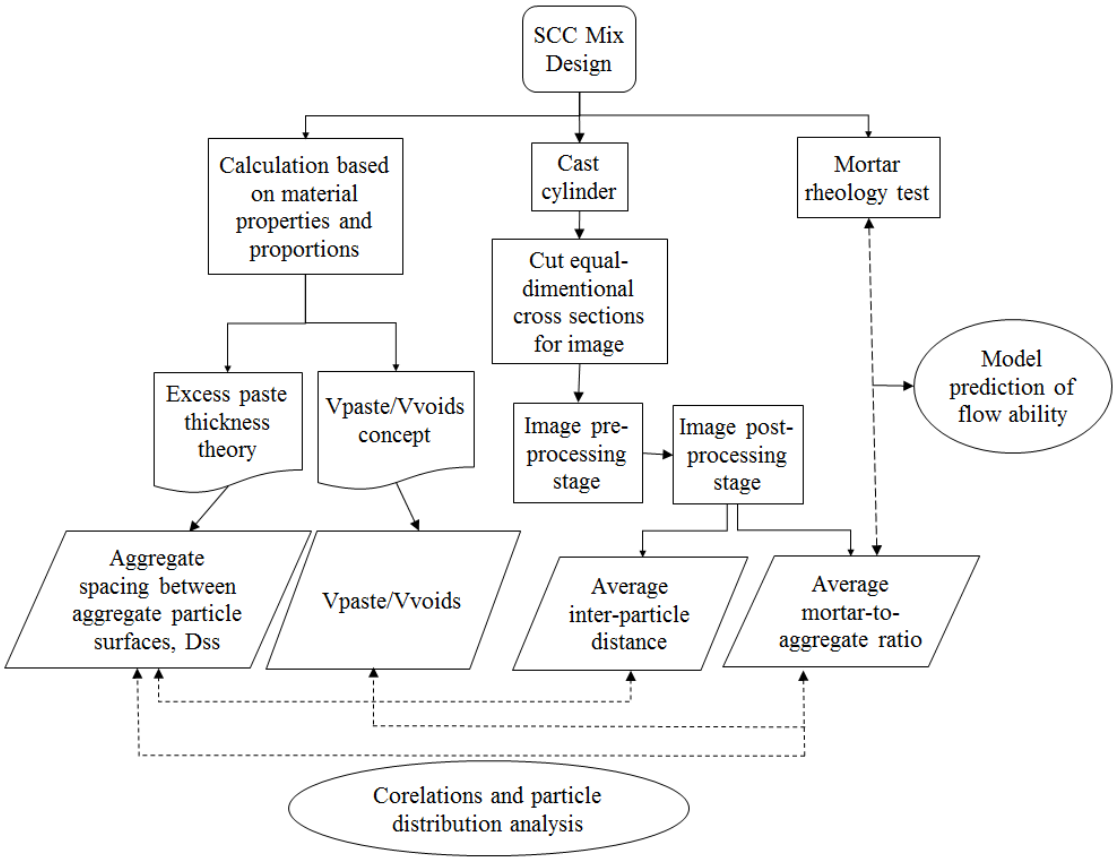


**Figure 1: Research plan flow chart.**

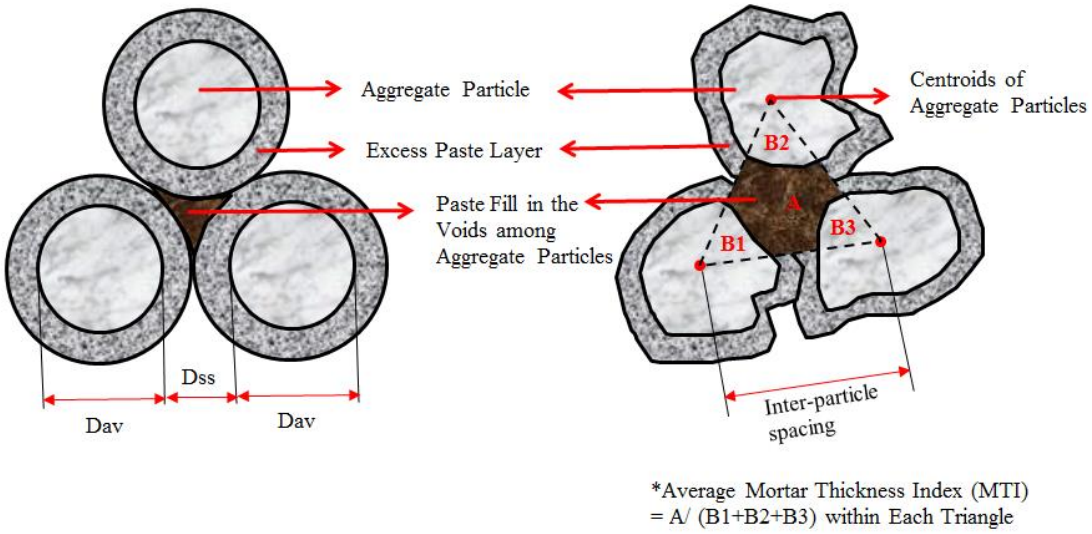


**Figure 2 – Aggregate system, aggregate spacing $D_{ss}$, and average aggregate diameter $D_{av}$ used in excess paste theory (left); MTI and inter-particle spacing defined in this study (right).**

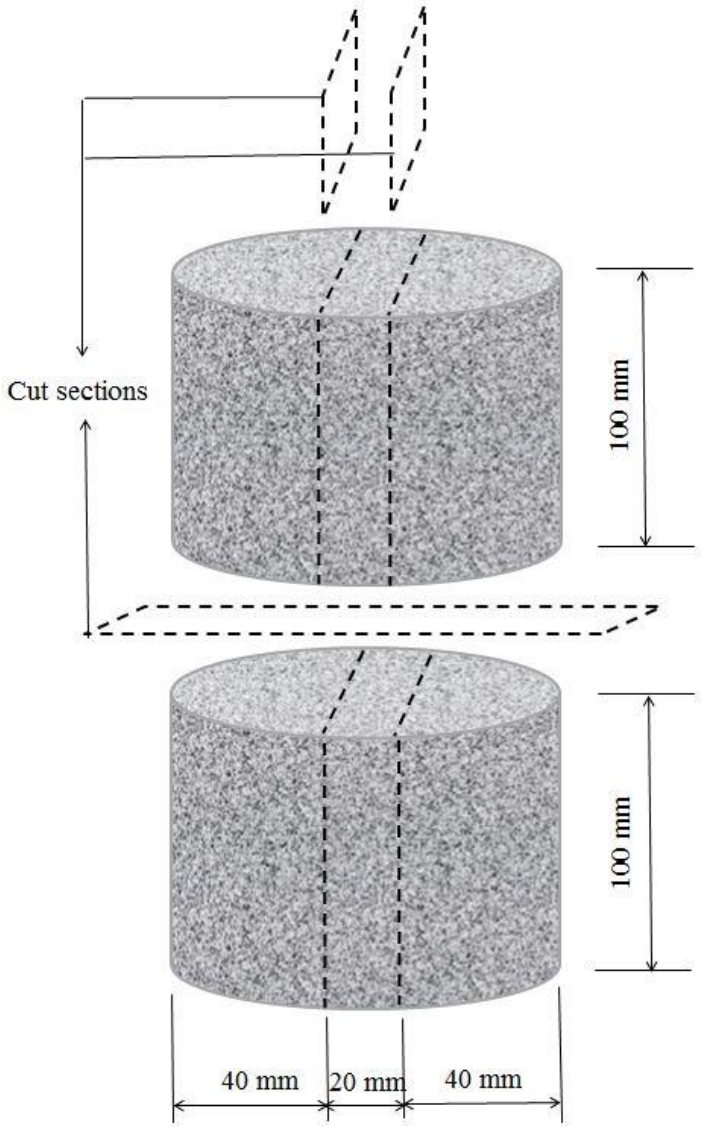


**Figure 3 – Concrete sample showing cut section locations.**

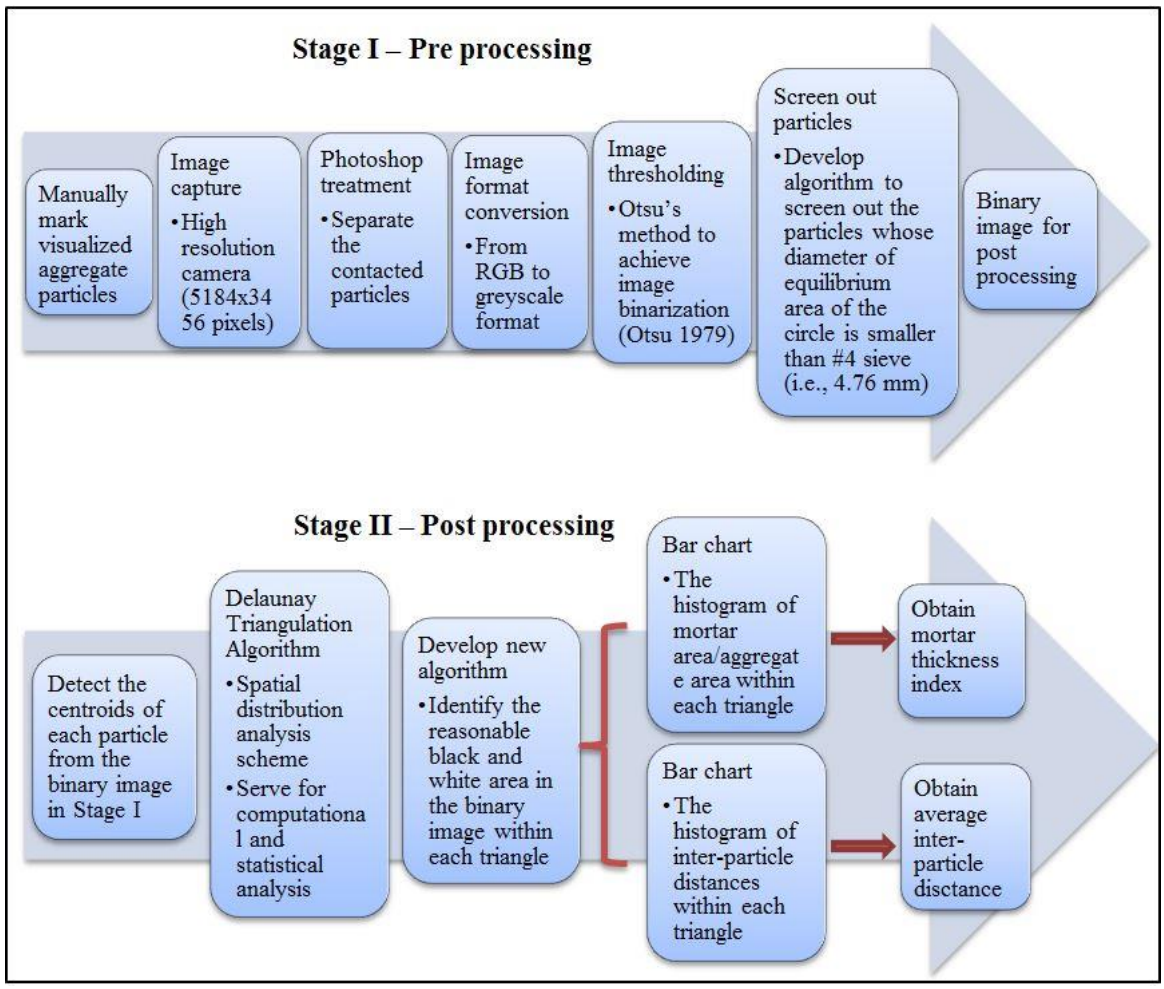


**Figure 4 – Flow chart of image pre and post processing used in this study.**

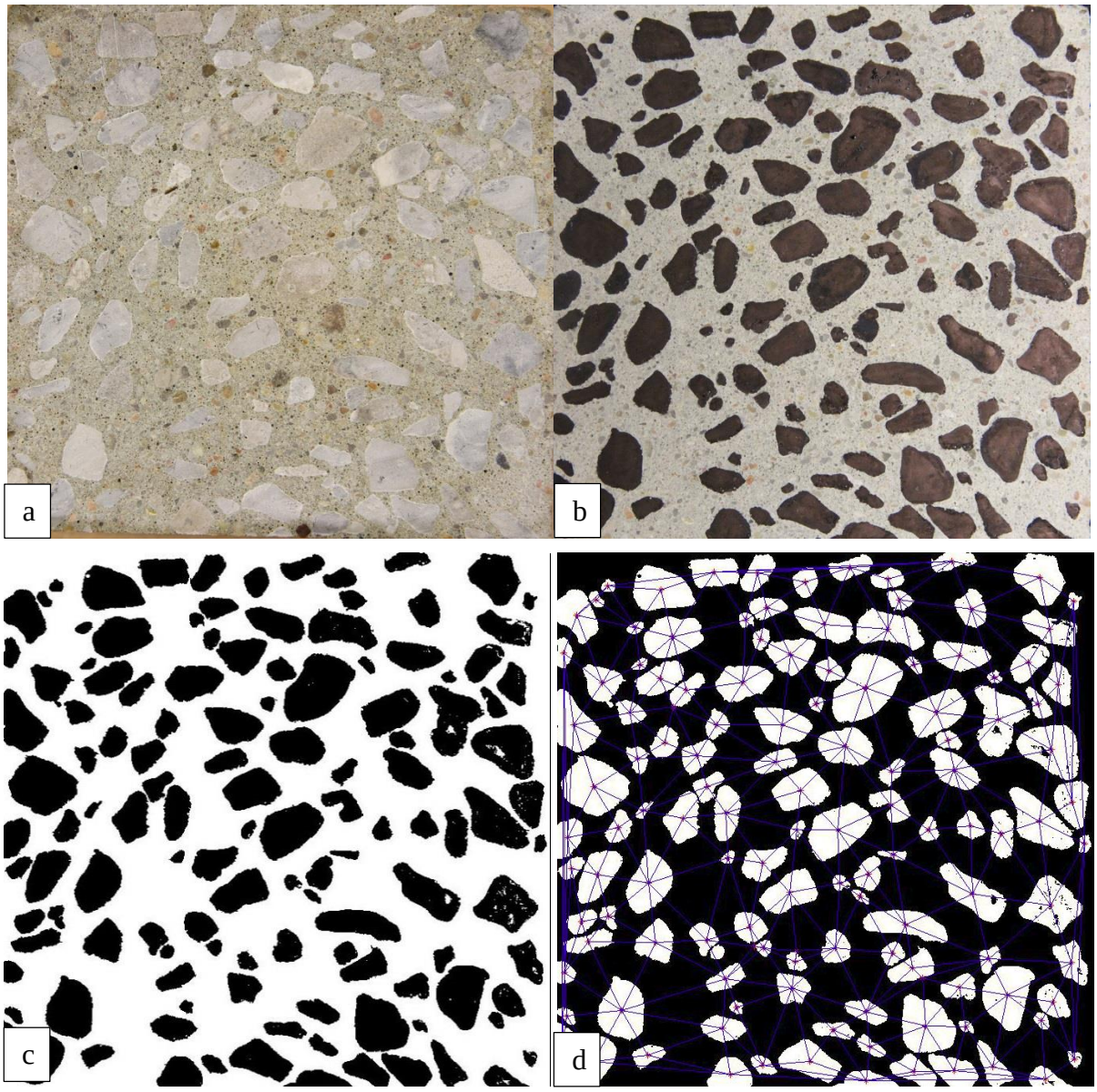

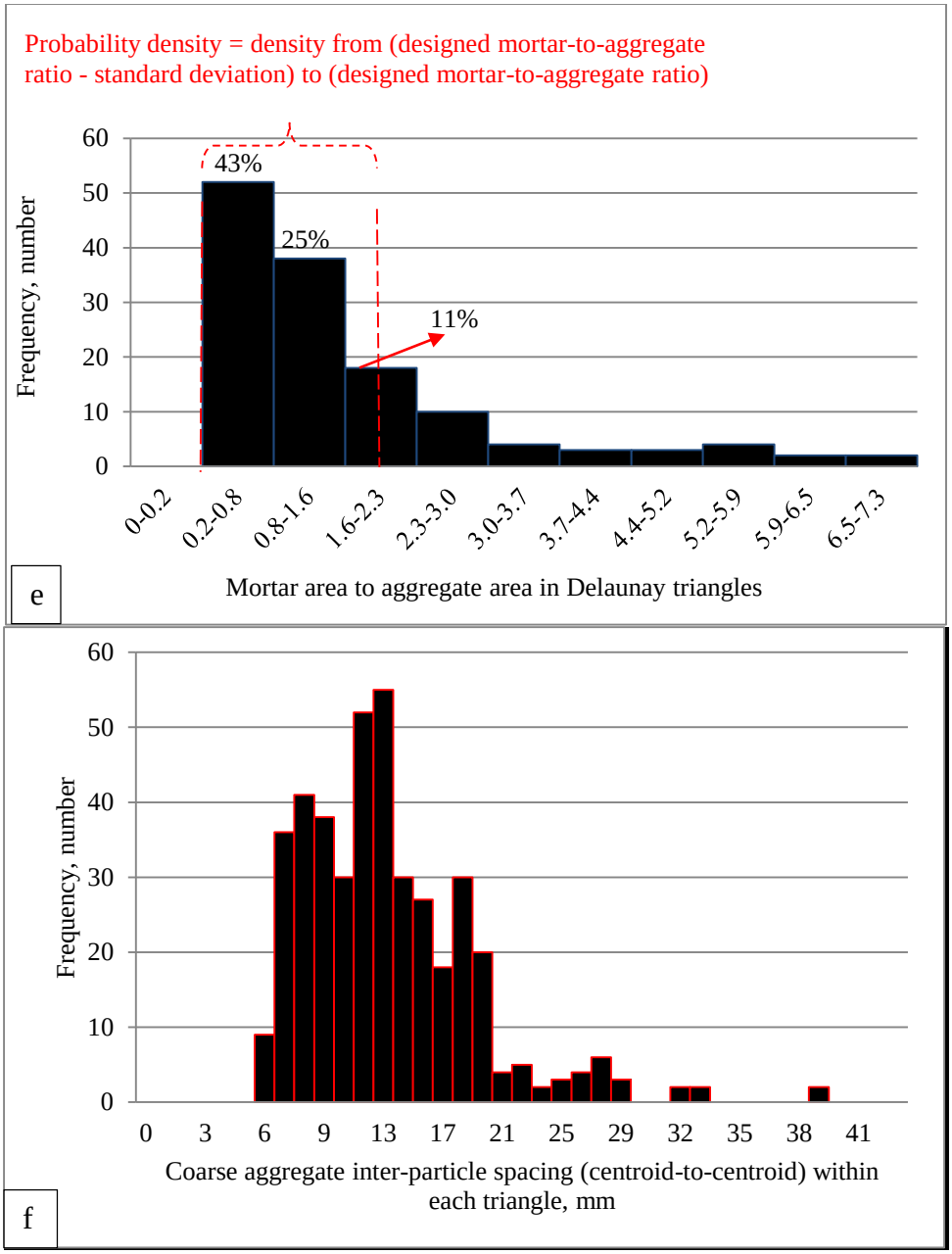


**Figure 5 – Major steps involved in DIP: (a) original image; (b) image with marked aggregate particles; (c) binary image used for post-processing steps; (d) binary image with marked centroids of particles and Delaunay triangles; (e) histogram of mortar to aggregate area in Delaunay triangles; (f) histogram of inter-particle spacing within triangles.**

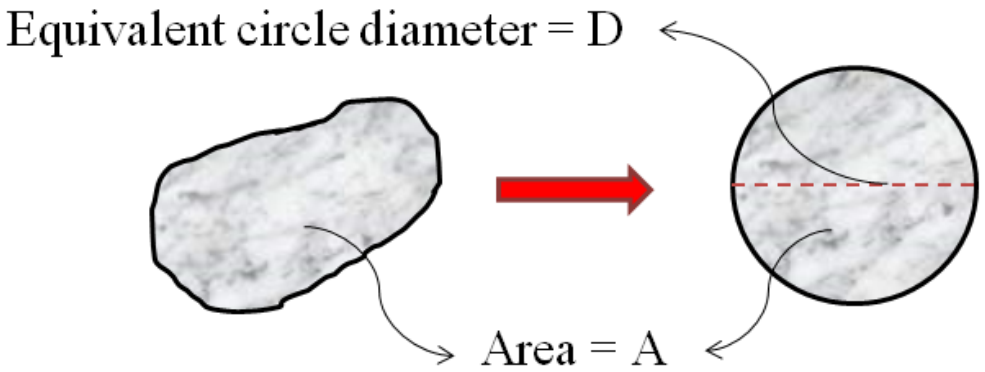


**Figure 6 – Equivalent circle diameter of aggregate particle.**

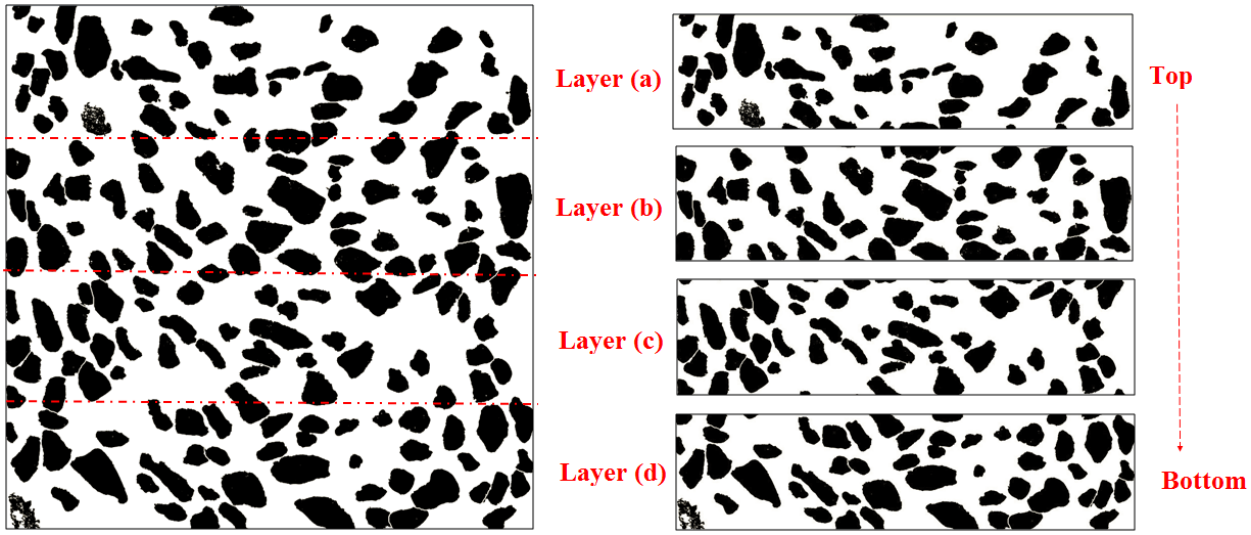


**Figure 7 - Four layers cut from the cross section of mixture H-c(LS)-F.**

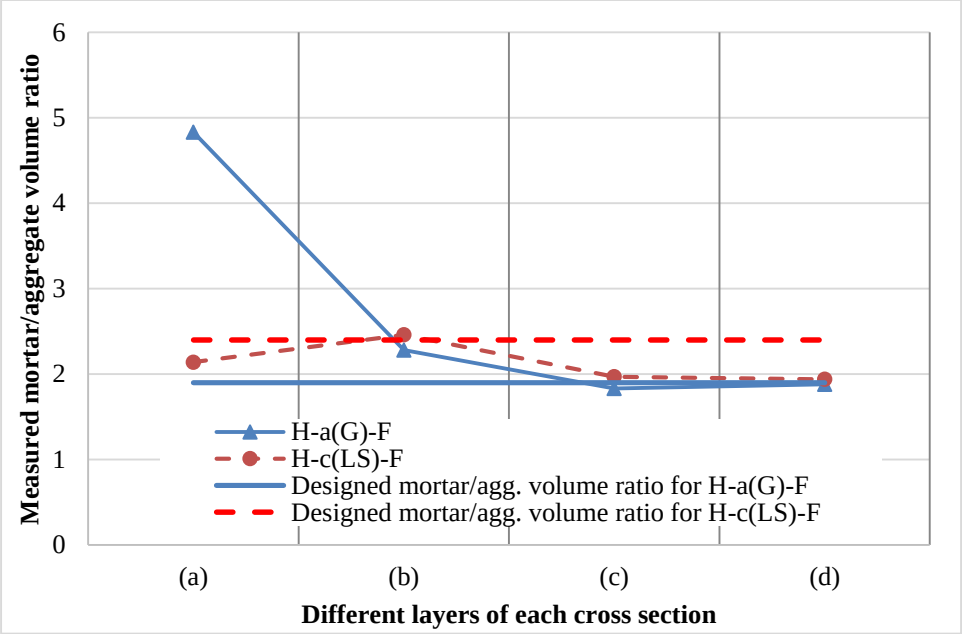


**Figure 8 – Mortar/aggregate volume ratio comparison of two typical cross section layers.**

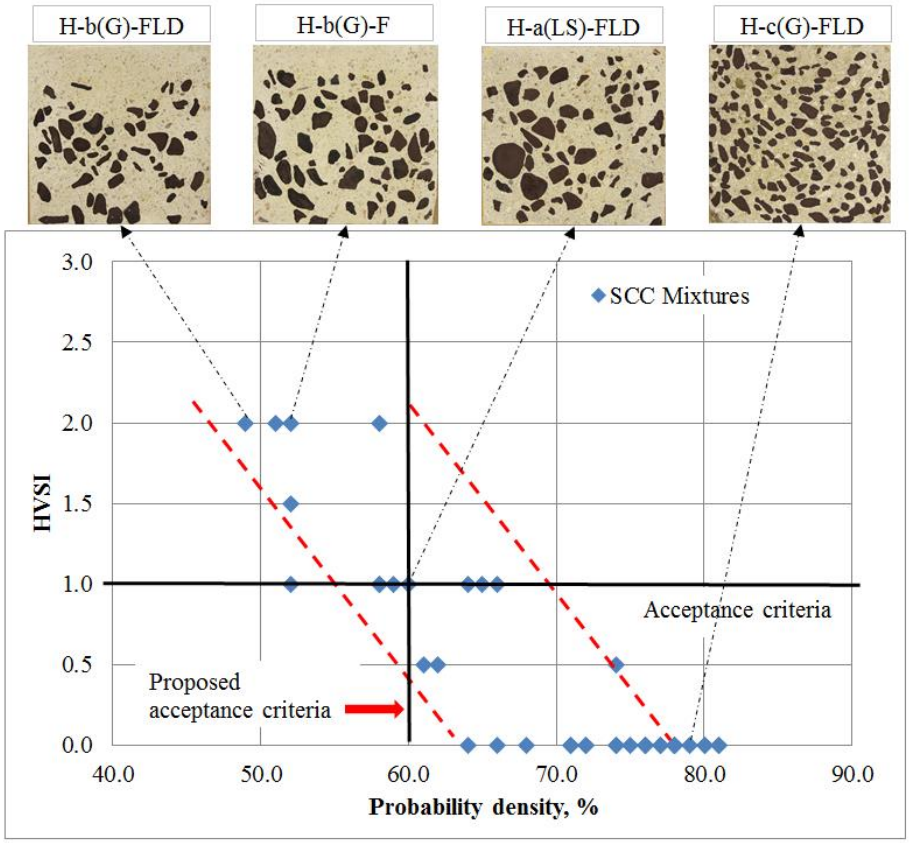


**Figure 9 – Probability density vs. HVSI**

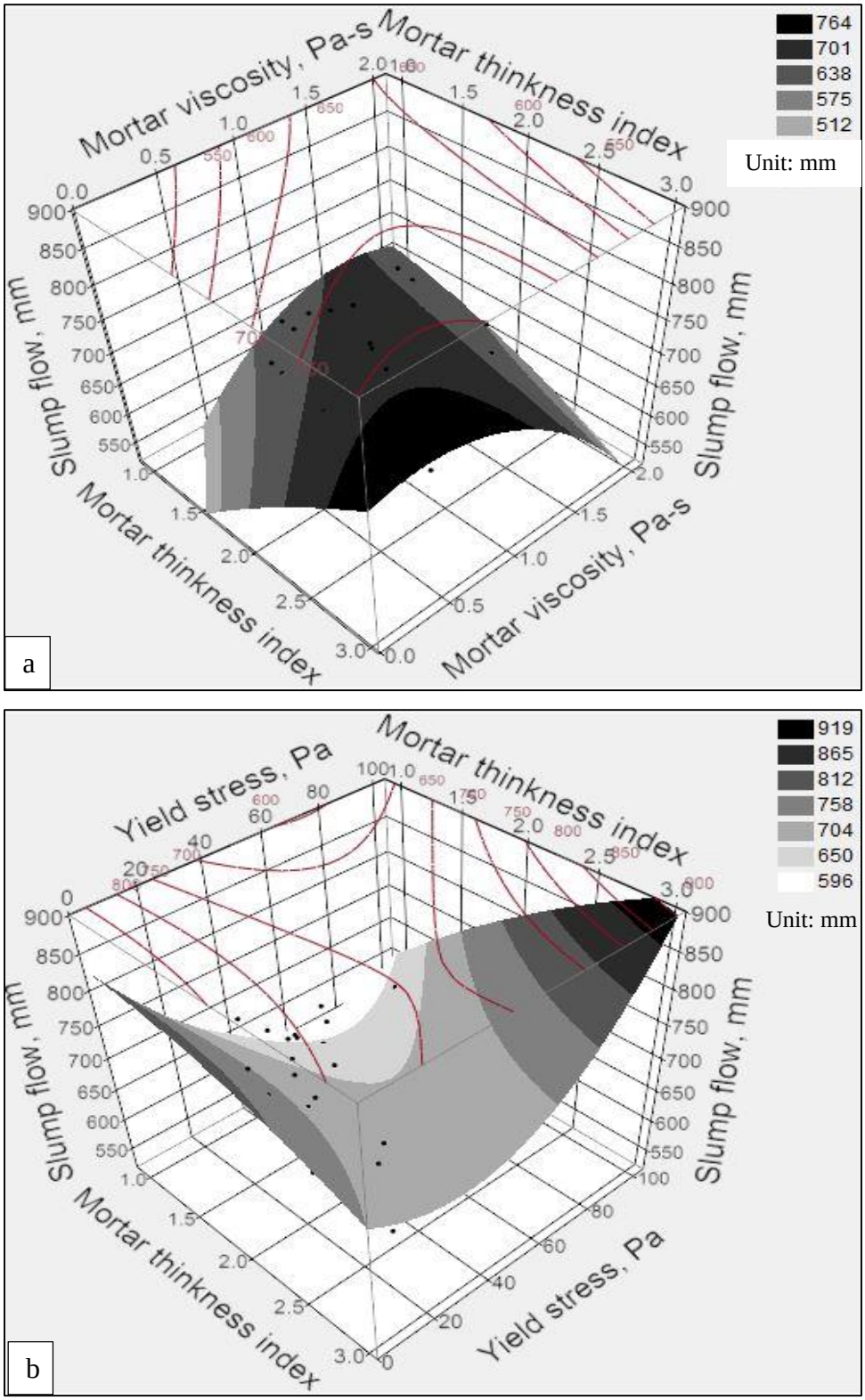


**Figure 10 – Response surface plots show the relationship among MTI, slump flow, and (a) mortar viscosity; (b) yield stress.**

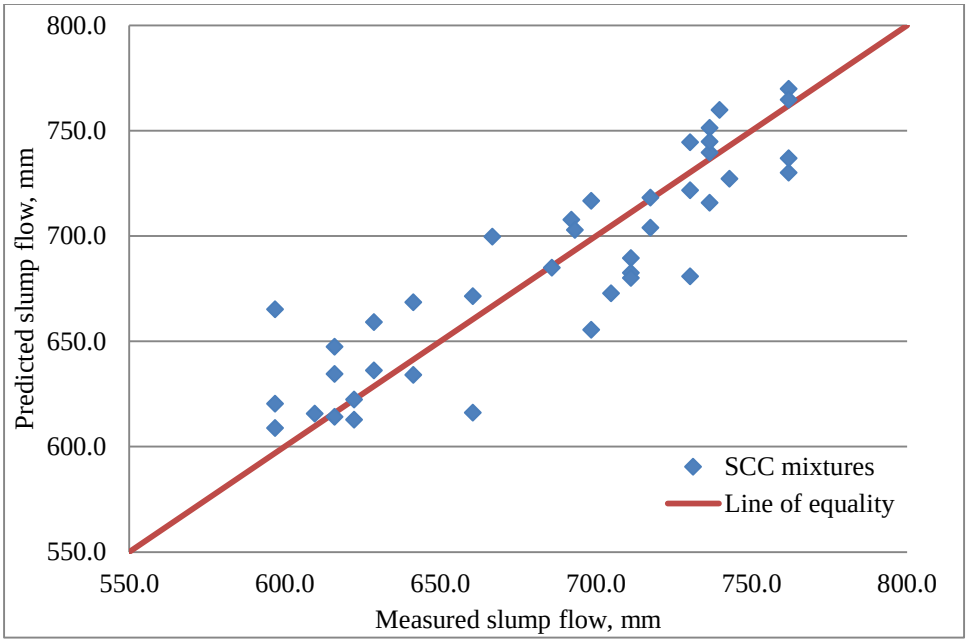


**Figure 11 – Model predicted and measured slump flow.**

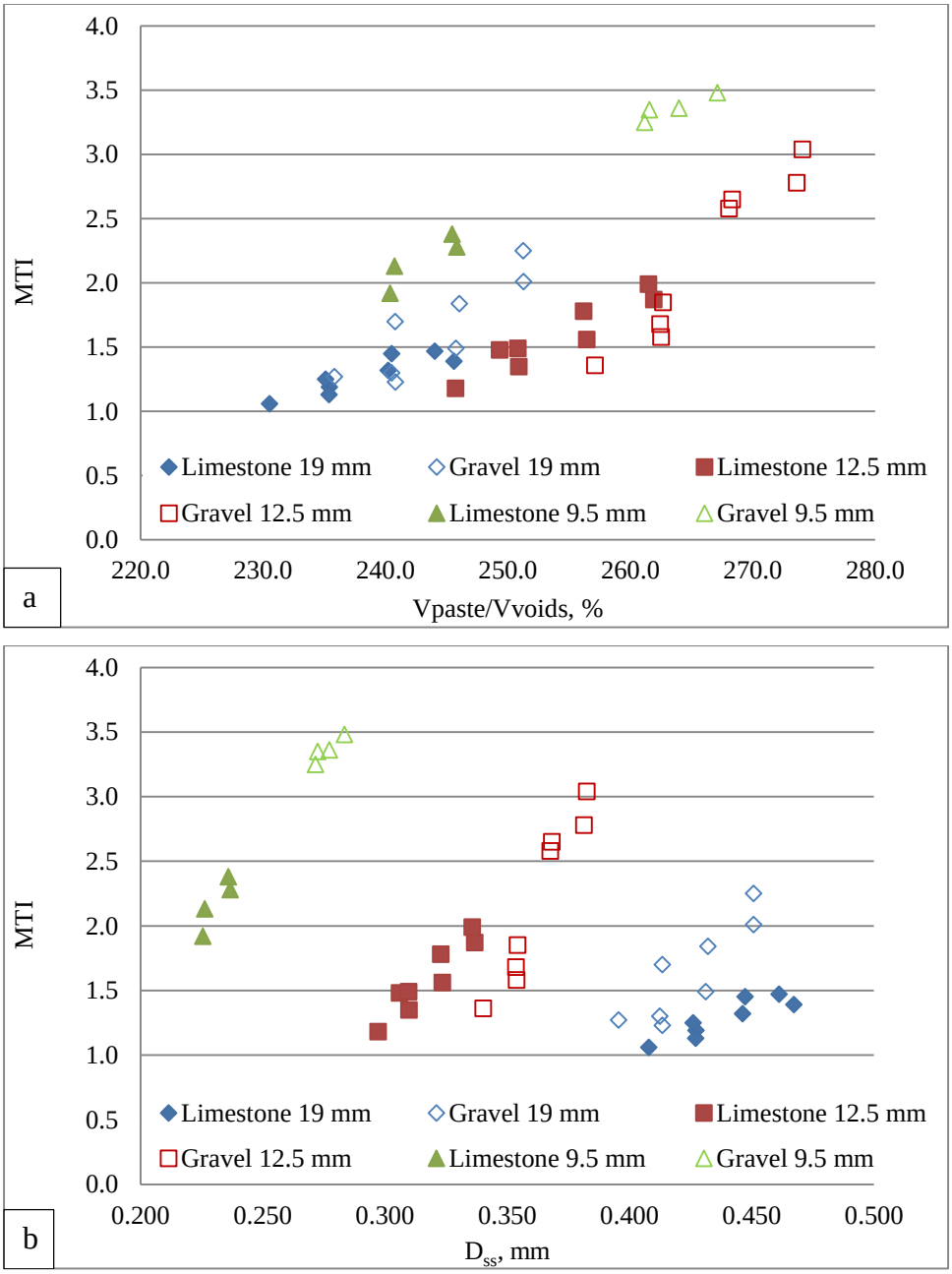


**Figure 12 – MTI vs. (a) Vpaste/Vvoids; (b) $D_{ss}$ on SCC mixtures with different sizes and types of coarse aggregate.**

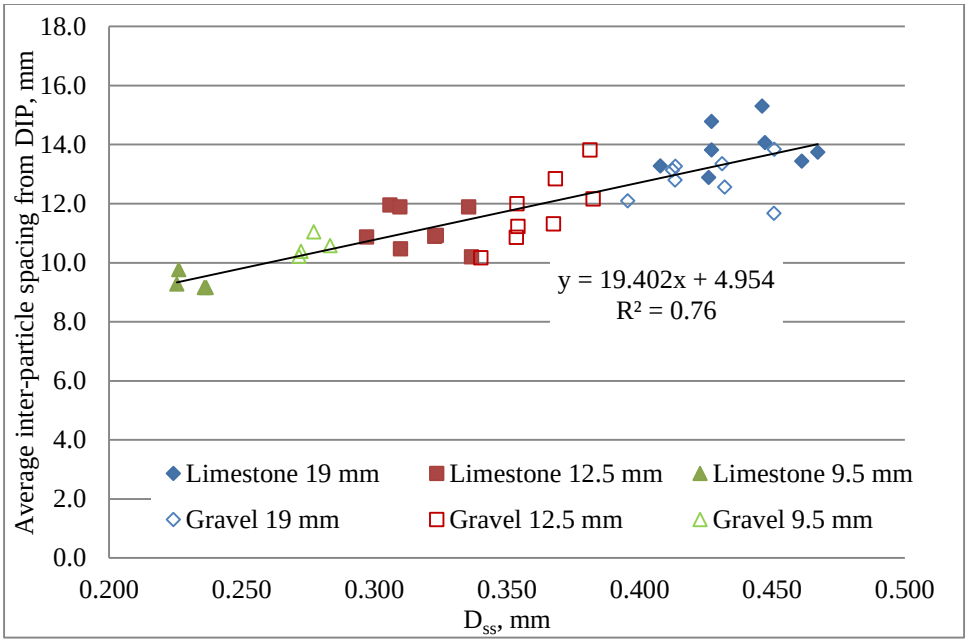


**Figure 13 – Average inter-particle spacing from DIP method vs. $D_{ss}$.**

# CHAPTER 6. USING ULTRASONIC WAVE PROPAGATION MONITORING STIFFENING PROCESS OF SELF-CONSOLIDATING CONCRETE

A paper submitted to ACI Materials Journal

*Xuhao Wang[1], Peter Taylor[2], Kejin Wang[3], Malcolm Lim[4]*

## ABSTRACT

Concrete setting behavior and strength development strongly influence scheduling of construction operations, such as surfacing, trowelling, jointing, saw-cutting and formwork removal. The aim of this study is to investigate technologies available to monitor changing properties of a fresh mixture, particularly for use with self-consolidating concrete (SCC). This study is to use longitudinal (P-wave) ultrasonic wave propagation to monitor the setting and stiffening behavior of self-consolidating concrete.

A number of techniques were used to monitor setting time, stiffening and formwork pressure of SCC mixtures. These included longitudinal (P-wave) ultrasonic wave propagation, penetrometer based setting time, semi-adiabatic calorimetry, and formwork pressure. Tests were conducted on a large matrix of SCC mixes, designed for bridge

[1] Research Assistant, Department of Civil, Construction and Environmental Engineering, Iowa State University, 136 Town Engineering, Ames, Iowa 50011, Tel: 515-294-2252, Email: wangxh@iastate.edu

[2] Associate Director, National Concrete Pavement Technology Center, Iowa State University, Ames, Iowa 50011, Tel: 515-294-9333, Email: ptaylor@iastate.edu

[3] Professor, Department of Civil, Construction and Environmental Engineering, Iowa State University, 492 Town Engineering, Ames, Iowa 50011, Tel: 515-294-2152, Email: kejinw@iastate.edu

[4] General Manager, PROCEQ Technical and Application Services, 4217 Grove Avenue, Gumee, Illinois 60031, Email:Malcolm.lim@proceq.com

construction applications. The mixtures were made with different aggregate types, sizes, and different cementitious materials. The P-wave test and calorimetric measurements can be used to monitor the stiffening and setting of SCC mixtures. The use of $V_p$ reaching the velocity in water and the infelction point on a UPV curve overestimates the initial setting time. The laboratory formwork pressure device can be used as an indicator of initial set of concrete mixtures. However, the device with overhead air pressure may not be able to rigorously simulate the in-situ formwork pressure beyond initial set.

**Keywords:** ultrasonic pulse velocity; p-wave; formwork pressure; calorimetry; setting time; self-consolidating concrete

## INTRODUCTION

Concrete setting behavior and strength development strongly influence scheduling of construction operations, such as surfacing, trowelling, jointing, saw-cutting and formwork removal. Various test methods have been developed to evaluate the stiffening behavior of concrete, such as the penetration resistance test, formwork pressure development, ultrasonic pulse velocity application, and calorimetry measurement (Chung et al. 2010; Khayat 2009; Sandberg and Liberman 2007; Lee et al. 2004; Smith et al. 2002; Chotard et al. 2001; ASTM C403 1999).

In order to provide better quality control and predict construction activities, continuous monitoring on early age concrete behavior using field materials under field environment can result in benefits (Inaudi and Glisic 2006):

1. It helps to improve the knowledge concerning mixture behavior and improve calibration of numerical models.
2. It gives an early indication of malfunction so that precautions can be made in time.

**Penetration resistance test**

In ASTM C 403, penetration resistance is used to measure the setting and hardening behavior of a mixture. The initial and final setting times are defined as the times required for mortar extracted from the concrete to reach 500 [3.5 MPa] and 4000 psi [27.6 MPa], respectively, of resistance to penetration of a cylindrical probe. The test is labor intensive, especially for mixtures with a prolonged set time (Suraneni 2011).

**Calorimetry measurement**

Calorimetry is the measurement of heat lost or gained during a chemical reaction such as cement hydration. The measurements can be used to assess hydration related properties, such as setting, stiffening, and maturity based on the obtained temperature-time curve. The test can also be used to assess the effect of mineral and chemical additives on the hydration kinetics and to check for incompatibility (Wang et al. 2006; Sandberg and Roberts 2005; Lerch 1987; Bensted 1946). It can be performed under isothermal conditions on paste in accordance with ASTM C1679, or under adiabatic or semi-adiabatic conditions on concrete or mortar.

Previous work reported in the literature has explored the use of semi-adiabatic calorimetry to define “thermal” setting times and to correlate them with setting times determined in accordance with ASTM C403 (Taylor et al. 2006). Figure 1 illustrates the method of a selected “fraction” of the main hydration response temperature rise (Sandberg and Liberman 2007). Because there may be variability in the magnitudes and shapes of the thermal profile of different mixtures, this method is suggested as the most efficient way to evaluate thermal setting times for comparison. In the thermal profile obtained from semi-

adiabatic calorimetry, 20% and 50% fraction thermal setting time are somewhat arbitrarily chosen as initial and final setting times, respectively.

**Ultrasonic pulse velocity (P-wave)**

There are two types of ultrasonic pulse velocity methods in use: wave transmission method and wave reflection method. The former method measures the velocity, relative energy and frequency of primary or compressional waves (P-waves) traveling through a material while the latter method monitors the reflection loss of transverse or shear waves (S-waves) at an interface between a steel plate and the cementitious material over time (Voigt et al. 2005). Both of the methods are based on Biot's theory (Biot 1956).

Based on Biot's theory, two compressional waves (fast and slow P-waves) and one shear wave propagate in a fluid saturated porous solid. The fast wave exists in all frequency ranges while the slow wave only exists in a high frequency range (Zhu et al. 2011). Studies have also shown that P-waves are less sensitive to difficulties with the sample-transducer contact than S-waves and allow a more accurate determination of the velocity through concrete due to their high signal-to-noise ratio (Robeyst et al. 2008). Both methods have been used to assess

- Setting behavior (Robeyst et al. 2008; Trinik et al. 2008; Grosse et al. 2006; Voigt et al. 2005; Subramaniam et al. 2005; Reinhardt and Grosse 2004; Ye et al. 2003; Chotard et al. 2001; Ozturk et al. 1999; Whitehurst 1951);
- Strength development (Pinto 2007; Erfurt 2002; Keating et al. 1989b; Byfors 1980; Elvery and Ibrahim 1976);
- Formwork pressure development (Suraneni 2011);
- Chemical shrinkage (Voigt et al. 2005).

S- and P-wave velocities, relative energy as well as the frequency spectrum can indicate the setting and hardening behavior of concrete. Researchers have sought to correlate UPV data with the penetration resistance method using features of the ultrasonic velocity curves over time. These features include the point where P-wave velocity ($V_p$) starts to increase, the inflection point, or when $V_p$ reaches the velocity of sound in water, i.e., 4700 ft/s [1430 m/s] (Zhu et al. 2011).

**Formwork pressure development**

The motivation for the industry to adopt SCC technology includes a shortened casting time, reduced noise and labor, and production of aesthetic surfaces with high quality. However, the fluid nature of SCC often leads to a high lateral pressure to the concrete formwork. For an element type, formwork pressure development is significantly influenced by casting rate and method, ambient environmental condition, rheological behavior, setting time, and binder type and content of the concrete (Khayat 2009; Gregori et al. 2008) .

The ACI guide to formwork (ACI 2004) recommends that the time to formwork removal should be based on maturity, rebound numbers, penetration resistance, or pullout tests to correlate the field concrete strength to elapsed time on removal of the formwork. There is limited data reported on the relationship between formwork pressure decay and form removals.

Each method discussed above has its own features and limitations and their application in assessing different properties of early age concrete is summarized in Table 1.

## RESEARCH SIGNIFICANCE

In order to provide a better quality control and predict construction activities for in-situ SCC mixtures, more reliable and accurate techniques need to be investigated to evaluate the stiffening and setting behavior of concrete. In this study, ultrasonic wave propagation and calorimetric measurement techniques provide solutions for in-situ and continuous monitoring of the stiffening and setting behaviors of SCC mixtures. Ultrasonic wave propagation also serves a strong support of predicting saw-cutting windows of concrete pavements using these techniques in the forthcoming study.

## EXPERIMENTAL INVESTIGATION

Two sets of concrete mixes were studied including six conventional concrete (CC) and 24 SCC mixtures.

### Materials and mix proportions

All six CC mixtures contained 25% Class F fly ash. Three were made with limestone coarse aggregate and the other three were made with gravel of differing sizes.

24 SCC mixes, designed for bridge construction applications, were developed all with the following targeted parameters:

- 22 to 30 in. [558.8 mm to 762.0] slump flow
- Visual stability index, (VSI)≤1
- J-ring ≤ 3 in. [76.2 mm]

The SCC mixes were made with limestone and river gravel coarse aggregates. Each coarse aggregate was used in three different nominal maximum sizes, 3/4” [19.0 mm], 1/2” [12.5 mm], and 3/8” [9.5 mm]. The physical properties of the aggregates are shown in Table 2 and the aggregate gradations are given in Figure 2.

Cementitious blends included, 25% Class C, 25% Class F fly ashes, 30% slag cement, or 15% limestone dust with 15% replacement for cement, were used. Table 3 gives the physical and chemical properties of cementitious materials.

The chemical admixtures used were Air-Entraining Agent (AEA), polycarboxylate based High Range Water Reducer (HRWR), and Viscosity-Modifying Admixture (VMA).

The mix proportions and fresh concrete properties of the mixtures are shown in Table 4.

## ANALYTICAL PROCEDURE

### Penetration resistance

Setting times of all mixes were determined in accordance with ASTM C 403.

### Semi-adiabatic calorimetry

A commercial semi-adiabatic calorimeter was used to monitor temperature changes of concrete samples (Figure 3) (Sandberg and Liberman 2007). Four cylinders were tested from each mixture for 24 hours after mixing.

### Ultrasonic pulse velocity

A commercial UPV device was used that comprised

- An integrated waveform display for system setup
- Two ultrasonic longitudinal wave transducers with a frequency of 54 kHz
- A plexiglass rod with a known velocity for calibration

Data was collected using a laptop computer. The monitoring system is shown in Figure 4.

Concrete specimens were cast in 4 [101.6 mm] by 8 in. [203.2 mm] cylinders after mixing. The sample was placed in a steel frame so that both transducers were centered. The bottom transducer was in contact with the bottom of the mold, while a plexiglass sheet sized to fit inside the form was placed between the top concrete surface and the top transducer. A

commercial gel couplant was applied between the transducers and the mold/plexiglass to reduce attenuation of the wave at the interfaces.

The UPV test was started two hours after mixing so that the SCC mixes could hold the weight of the top transducer. The velocity of the P-wave through the concrete was recorded every minute for up to 1000 minutes in a constant lab environment (73±3 ˚F [22±2 ˚C] and 50±5% relative humidity). The Vp was calculated as follows:

$$\mathrm{Vp} = \mathrm{L}/t_p \qquad \text{Eq. (1)}$$

where L is the length of the longitudinal wave path through the specimen (8 in. [203.2 mm] in this study) and $t_p$ is the travel time of the ultrasonic pulse through L.

**Formwork pressure measurements**

The lateral pressure of both CC and SCC mixes was measured using the test setup shown in Figure 5 (Lomboy et al. 2013). The pressure measurement device comprised a 3 ft [0.9 m] long by 8 in. [203.2 mm] diameter water pipe with removable steel end caps. Three flush diaphragm pressure sensors were installed through the side of the pipe 12 in. [304.8 mm] apart in order to measure the pressure distribution over the height of the column. An air pressure gauge and an air valve were installed at the top cap to simulate high concrete pressures by increasing the air pressure at the top portion of the concrete column.

Approximately 40 minutes after mixing, concrete was poured in the pipe at a rate of 6 in./min [152.4 mm/min] to simulate reasonable field concrete practice. The CC mixes were consolidated with an internal vibrator in 12 in. [304.8 mm] lifts. No mechanical consolidation was used for SCC mixes. When the concrete was filled up to 12 in. [304.8 mm] above the top sensor, air was pumped into the pipe at the same rate up to 30 psi [0.2 MPa] to simulate 30

feet [9.1 m] of concrete head. The pressure at each sensor was recorded every one minute until the lateral pressure reached a constant value.

## RESULTS AND DISCUSSION

### Set Time

A typical UPV test result from literature is shown in Figure 6(a). The UPV evolution curve can be divided into three steps (Lee et al. 2004; Smith et al. 2002; Chotard et al. 2001):

- Step 1: ultrasonic wave propagation through the liquid-like viscous suspension.
- Step 2: the quantity of hydration product change. More and more cement particles continue to become connected due to newly formed hydration products filling in the pores such that $V_p$ keeps increasing.
- Step 3: the $V_p$ levels off. The formation of hydration products slows down such that UPV approaches an asymptotic value in the solid structure.

The notations, $t_A$, $t_B$, and $t_C$, represent when $V_p$ starts to increase, reaches the velocity in water (4700 ft/s [1430 m/s]), and increases to the inflection point, C, of a UPV curve, respectively.

$t_A$ and $t_B$ can be determined by observation from plot. $t_C$ can be derived by using a bi-logistic function due to its ability to describe quantities that grow exponentially at the outset after which the growth is gradually decelerated, producing two S-shaped curves (Grosse et al. 2006). The point of inflection, $t_C$, derived by curve fitting using programing algorithm (with 95% confidence bounds) and the bi-logistic function is shown in Equation (2).

$$V(t) = \frac{k_1}{1+e^{(t-t_1)/dt1}} + \frac{k_2}{1+e^{(t-t_2)/dt2}} + c \qquad \text{Eq. (2)}$$

where $k_1$, $k_2$, $dt_1$, and $dt_2$ are fitting parameters. $t_1$ or $t_2$ is the time where the inflection point is located at depending on the value.

Typical evolution of UPV measured in current study as shown in Figure 6(b) is similar to that of literature, except that there is no curved transition between step 1 and 2. The makes the identification of initial set easier because there is a marked change in UPV. The use of a bi-logistic approach, however, may be invalid in such case.

Correlations between different methods of assessing setting time are presented in Figure 7.

Care must be taken when attempting to correlate these measurements because they are measuring fundamentally different things. UPV data is a function of the dynamic modulus of the system and is governed by the interaction between hydration products as they grow – it is a physical phenomenon. Temperature based data are reflecting the reaction rates of reagents in the system, i.e., chemical phenomena. These reactions may be producing the products leading to physical changes, but the physical changes may only occur some time after the chemical reaction starts because if they are spaced far apart (e.g. high w/c ratio), time is required for reaction products to span the space between them.

Regardless of mix composition, the initial setting times determined using ASTM C403 agree well when $V_p$ starts to increase (Figure 7a).

Set times determined using inflection points of the UPV curve seem to be poorly correlated with the penetrometer data as shown in Figure 7b. This is likely because the determination of inflection points is subjective to UPV curve duration, shape, and curve fitting algorithm. In addition, while change in slope of a velocity plot may be explained by hydration phenomena, this has little to do with observable physical changes in the mixture.

Figure 7c represents the time when $V_p$ reaches the velocity in water, i.e., approximately 4700 ft/s [1430 m/s]. This approach seems to overestimate setting times when compared to the penetrometer data.

Correlation between set times reported by the calorimetry fraction method and penetrometer data is shown in Figure 7d. Although the correlation is not as good as $V_p$ acceleration, the approach appears to be able to predict setting times reasonably well.

In general, the initial setting times of SCC mixes were longer than those obtained in CC mixes. The primary reason for this is likely the extensive use of polycarboxylate-based HRWR which may have a retarding effect. The side chains of polycarboxylate-based polymers are active at longer distances far from the cement grain and not incorporated into hydration products early. They may also remain in aqueous solution and adsorb onto cement particles gradually over time to delay the hydration reaction such that the hardening process is delayed (Koehler and Fowler 2007).

Class C fly ash mixes may retard the alite hydration, therefore, delay the setting times. It is because they may contain reactive aluminate that will consume soluble calcium sulfate causing potential sulfate deficiency in the system (Sandberg and Roberts 2005). It has been proposed that the reaction of $C_3A$ from the class C fly ash and cement with sulphate from both sources generates large amounts of ettringite, which precipitates on $C_3A$ and tricalcium silicate ($C_3S$) and slows the hydration of both (Mehta and Monteiro 2006). This explains the delay observed in the time to reach the maximum heat evolution in class C fly ash mixes. This is supported by the chemical composition of the materials. The elemental analyses of both class C and F fly ashes (Table 2) show that alumina contents of the fly ashes are similar. However, Figure 8 shows the X-ray diffraction (XRD) data for both fly ashes and the

diffractograms indicate that tricalcium aluminate ($C_3A$), sulfur bearing minerals (anhydrite) and calcium oxide are present in the class C fly ash.

**Formwork pressure**

The average formwork pressures are presented as lateral pressure at 1.5 feet [0.5 m] from the bottom of the form in Figure 9. The initial pressures for SCC and CC mixes are similar, which are equal to their full hydrostatic pressures. Although it is commonly assumed that CC mixes will exert less pressure, the internal vibrator during casting fluidizes the mixture to develop a full hydrostatic pressure. After placement, the pressures start to decrease at different rates depending on mix type.

For all mixes in this study, it was observed that the lateral pressure exhibited a jump some time after placing. A similar phenomenon has been reported by Khayat (2009). It is most likely due to autogenous shrinkage of the concrete at about the time of initial set causing a reduction of volume that results in the mixture pulling away from the walls of the form. This then allows the pressurized air to reach the pressure sensor directly and so increase the reported form pressure.

However, this is not the case in construction of tall elements. Khayat (2012) reported a field demonstration project of a 14.4 feet [4.4 m] tall wall filled with SCC and the same diaphragm sensors were installed at different heights. The lateral pressure at 1.6 feet [0.5 m] from the bottom of wall is presented in Figure 10 showing the reduction of lateral pressure with time without the jump in pressure at setting time.

Based on this, formwork pressure may not be worth tracking after the jump when using the air pressure approach. In this study, the time interval between placement and the pressure jump was recorded and appears to be well correlated to the start of a rise in $V_p$ with $R^2$ value

of 73% as shown in Figure 11. This confirms that the pressure jump is occurring around the time of initial set. The relationship between early-age shrinkage and setting behavior of SCC mixes should be further studied to better simulate the field formwork construction in the laboratory environment.

## CONCLUSIONS

The following conclusions are derived from the present study:

- P-wave propagation method can be used to monitor setting of CC and SCC mixes.
- The calorimetry test also provides a potential means of assessing initial setting times without the need to remove coarse aggregate. One limit to this is that it is not conducted at the same temperature of the mixture. Therefore, variation in weather will not be accounted for.
- The use of $V_p$ reaching the velocity in water and the inflection point on a UPV curve overestimates the initial setting time.
- The laboratory formwork pressure device can be used as an indicator of initial set of concrete mixture. However, the device with overhead air pressure may not be able to rigorously simulate the in-situ formwork pressure beyond initial set.

## ACKNOWLEDGMENTS

The authors acknowledge the research sponsorship and the collaboration between Iowa State University (ISU) and the University of Nebraska – Lincoln (UNL).

## REFERENCES

ACI Committee 347. Guide to Formwork for Concrete (ACI 347-04), American Concrete Institute, Farmington Hills, MI., 2004.

ASTM C403. “Standard Test Method for Time of Setting of Concrete Mixtures by Penetration Resistance,” American Society for Testing and Materials, Pennsylvania, 1999.

Bensted, J., "Some Applications of Conduction Calorimetry to Cement Hydration. Adv. Cement Res., Vol. 1, No. 1, pp 35-44, 1946.

Biot, M., "Theory of Propagation on Elastic Waves in A Fluid-Saturated Porous Solid. I. Low-Frequency Range," The Journal of the Acoustical Society of America, 28 (2), pp. 168-178, 1956.

Biot, M., "Theory of Propagation on Elastic Waves in A Fluid-Saturated Porous Solid. II. Higher-Frequency Range," The Journal of the Acoustical Society of America, 28 (2), pp. 179-191, 1956.

Byfors, J., "Plain Concrete at Early Ages," CBI-Report 3:80, Swedish Cement and Concrete Research Institute, Stockholm, 1980.

Chotard, T.; Gimet-Breart, N.; Smith, A.; Fargeot, D.; Bonnet, J.; and Gault, C., "Application of Ultrasonic Testing to Describe The Hydration of calcium aluminate cement At The Early Age," Cement and Concrete Research, 31 (3), pp. 405–412, 2001.

Chung, C-W.; Mroczek, M.; Park, I.; and Struble, L., "On the Evaluation of Setting Time of Cement Paste Based on ASTM C403 Penetration Resistance Test," Journal of Testing and Evaluation, Vol. 38, No.5, pp. 61-68, 2010.

Elvery, R., and Ibrahim, L., "Ultrasonic Assessment of concrete strength at Early Ages," Magazine of Concrete Research, vol. 28, no. 97, pp. 181–190, 1976.

Erfurt, W., "Erfassung von Gef¨ugever¨anderungen in Beton durch Anwendung zerst¨orungsfreier Pr¨ufverfahren zur Einsch¨atzung der Dauerhaftigkeit (Determination of microstructural changes in concrete with nondestructive test methods to evaluate the concrete durability)," PhD thesis, Bauhaus–University Weimar, Weimar, Germany, (in German), 2002.

Gregori, A.; Ferron, R.; Sun, Z.; and Shah, S., "Experimental simulation of Self-Consolidating Concrete Formwork Pressure," ACI Materials Journal, 105(1), pp. 97-104, 2008.

Grosse, C.; Reinhardt, H.; Krüger, M.; and Beutel, R., "Ultrasonic Through-Transmission Techniques for Quality Control of Concrete During Setting and Hardening, in: H.W. Reinhardt (Ed.)," Advanced Testing of Fresh Cementitious Materials, Stuttgart, pp. 83–93, 2006.

Inaudi, D., and Glisic, B., "Continuous Monitoring of Concrete Bridges During Construction and Service as A Tool for Data-Driven Bridge Health Monitoring," IABMAS'06 The Third Int'l Conference on Bridge Maintenance, Safety and Management, Porto, Portugal, July16-19, 2006.

Keating, J.; Hannant, D.; and Hibbert, A., "Correlation between Cube Strength, Ultrasonic Pulse Velocity and Volume Change for Oil Well Cement Slurries," Cement and Concrete Research, vol. 19, no. 5, pp. 715–726, 1989b.

Khayat, K., "Evaluation of Thixotropy of SCC and Influence on Concrete Performance," 54th Congresso Brasilleiro do Concr eto Maceio, IBRACON, 2012.

Khayat, K., "Self-consolidating Concrete Formwork Pressure," Final report, University of Sherbrooke, 2009.

Koehler, E., and Fowler, D., "Aggregate in Self-Consolidating Concrete," Final report, International Center for Aggregate Research (ICAR) Project 108, The University of Texas at Austin, 2007.

Lee, H.; Lee, K.; Kim, Y.; and Bae D., "Ultrasonic in-situ monitoring of Setting Process of High-Performance Concrete," Cement and Concrete Research, 34, pp. 631-640, 2004.

Lerch, W., "The influence of gypsum on the hydration and properties of Portland Cement Pastes," Proceedings, Vol. 46, of the American Society for Testing Materials, 1987.

Lomboy, G.R.; Wang, X.; and Wang. K., "Rheological Behavior and Formwork Pressure of SCC, SFSCC, and NC Mixtures," Proceedings of 5th North American Conference on the Design and Use of Self-Consolidating Concrete, Chicago, 2013.

Mehta, P., and Monteiro, P., "Concrete Microstructure, Properties, and Materials," New York: the McGrawHill Companies, Inc., 2006.

Ozturk, T.; Rapport, J.; Popovics, J.; and Shah, S., "Monitoring The Setting and Hardening of Cement-Based Materials with Ultrasound," Concrete Science and Engineering, Vol. 1, No.2, pp. 83-91, 1999.

Pinto, C., "Effect of Silica Fume and Superplasticizer Addition on setting behavior of High-Strength Mixtures," Journal of the Transportation Research Board, Vol.1574, pp. 56-65, 2007.

Reinhardt, H., and Grosse, C., "Continuous monitoring of setting and hardening of Mortar and Concrete," Construction and Building Materials, 18 (3), pp. 145–154, 2004.

Robeyst, N.; Gruyaert, E.; Grosse, C.; and Belie, N., "Monitoring the setting of Concrete Containing Blast-Furnace Slag by Measuring the Ultrasonic P-Wave Velocity," Cement and Concrete Research, 38, pp. 1169-1176, 2008.

Sandberg, J., and Liberman, S., "Monitoring and Evaluation of cement hydration by Semi-Adiabatic Field Calormetry, Journal of American Concrete Institute, Volume 241, pp. 13-24, 2007.

Sandberg, P., and Roberts, L., "Cement-Admixture Interactions Related to Aluminate Control," J. of ASTM Int., Vol. 2, No. 6, 2005.

Smith, A.; Chotard, T.; Gimet-Breart, N.; and Fargeot, D., "Correlation between Hydration Mechanism and Ultrasonic Measurements in An Aluminous Cement: Effect of Setting Time and Temperature on The Early Hydration, J. Eur. Ceram. Soc., 22, pp. 1947-1958, 2002.

Subramaniam, K.; Lee, J.; and Christensen, B., "Monitoring The Setting Behavior of Cementitious Materials Using One-Sided Ultrasonic Measurements," Cement and Concrete Research, Vol. 35, pp. 850-857, 2005.

Suraneni, P., "Ultrasonic Wave Reflection Measurements on Self-Compacting Pastes And Concretes," Master thesis in University of Illinois at Urbana-Champaign, 2011.

Taylor, P.; Johansen, V.; Graf, L.; Kozikowski, R.; Zemajtis, J.; and Ferraris, C., "Identifying Incompatible Combinations of Concrete Materials: Volume I-Final Report," FHWA-HRT-06-079 report, August, 2006.

Trinik, G.; Turk, G.; Kavcic, F.; and Bosiljkov, V., "Possibility of Using the Ultrasonic Wave Transmission Method to Estimate Initial Setting Time of Cement Paste," Cement and Concrete Research, 38, pp. 1336-1342, 2008.

Voigt, T.; Grosse, C.; Sun, Z.; Shah, S.; and Reinhardt, H., "Comparison of Ultrasonic Wave Transmission and Reflection Measurements with P- and S-Waves on Early Age Mortar and Concrete," Materials and Structures 38, pp. 729-738, 2005.

Wang, H.; Qi, C.; Farzam, H.; and Turici, J., "Interactions of Materials Used in Concrete," Concrete International, Vol. 28, no. 4, pp. 47-52, 2006.

Whitehurst, E., "Use of The Soniscope for Measuring Setting Time of Concrete," ASTM Proceedings, vol. 51, pp. 1166–1183, 1951.

Winden van der, N., and Brant, A., "Ultrasonic Testing for Fresh Mixes," Concrete, vol. 11, no. 12, pp. 25–28, 1977.

Ye, G.; Van Breugel, K.; and Fraaij, A., "Experimental Study and Numerical Simulation on The Formation of Microstructure in Cementitious Materials at Early Age," Cement and Concrete Research, 33 (2), pp. 233–239, 2003.

Zhu, J.; Kee, S.; Han, D.; and Tsai, Y., "Effects of Air Voids on Ultrasonic Wave Propagation in Early Age Cement Pastes," Cement and Concrete Research. 41, pp. 872-881, 2011.

**LIST OF TABLES**



**LIST OF FIGURES**

Figure 10. Formwork pressure decay of 14.4 feet [4.4 m] wall structure at the casting rate of 32.8 feet/hour [10 m/hr] (Gregori et al. 2004).

Figure 11. Correlations between elapsed time from concrete being placed to pressure jump and elapsed time of $V_p$ start to increase.

**Table 1. The relationship between test methods and the properties that they measure**

| Test method | Early age concrete performance | | | | limitations |
|---|---|---|---|---|---|
| | Stiffening | Setting | Hardening | Strength | |
| Penetration resistance [1] | Not useful | Standard test to measure setting times | Up to final set | Penetration resistance of sieved mortar mixture, but not useful to predict concrete strength | The definitions of initial and final setting based on penetration resistance seem to be arbitrary. It is a time consuming method with large error of single operator and multi-laboratory. |
| Calorimetry [9-13] | Not useful | Potential to predict setting time based on temperature rise | Not useful | Maturity is used very often by field engineers to predict early age strength of concrete. | Need more guidelines to interpolate hydration temperature with concrete performance. |
| Wave propagation method [15-34] | Not useful | Features on UPV development have a potential to predict initial setting time. | Not useful | Can be used to predict elastic modulus and Poisson's ratio associated with Rayleigh wave | Contradictory conclusions may be drawn from previous researchers. |
| Formwork pressure [2, 35] | Highly related to thixotropy of a mixture before setting | Autogenous shrinkage caused volume change occurs around initial setting time. | Not useful | Not useful | Laboratory test apparatus may not be able to rigorously simulate the in-situ formwork pressure beyond initial set. |

**Table 2. The physical properties of aggregates**

| Aggregates used in the research | | Type | Nominal Maximum Size, in. (mm) | Absorption, % | Fineness Modulus | Specific Gravity |
|---|---|---|---|---|---|---|
| Coarse Aggregate | a(LS) | Limestone | 3/4 (19.0) | 1.3 | - | 2.66 |
| | b(LS) | Limestone | 1/2 (12.5) | 1.3 | - | 2.66 |
| | c(LS) | Limestone | 3/8 (9.5) | 1.3 | - | 2.66 |
| | a(G) | gravel | 3/4 (19.0) | 1.1 | - | 2.74 |
| | b(G) | gravel | 1/2 (12.5) | 1.4 | - | 2.68 |
| | c(G) | gravel | 3/8 (9.5) | 1.4 | - | 2.69 |
| Fine Aggregate | | River sand | - | 0.5 | 2.62 | 2.68 |

Note: "-" indicates that the data are not available.

**Table 3. Chemical compositions of cementitious materials**

| Chemical Composition, % | Type I/II Cement | Class F fly ash | Class C fly ash | Slag cement |
|---|---|---|---|---|
| $SiO_2$ | 20.10 | 50.87 | 42.46 | 37.00 |
| $Al_2O_3$ | 4.44 | 20.17 | 19.46 | 9.00 |
| $Fe_2O_3$ | 3.09 | 5.27 | 5.51 | 0.68 |
| $SO_3$ | 3.18 | 0.61 | 1.20 | - |
| CaO | 62.94 | 15.78 | 21.54 | 36.86 |
| MgO | 2.88 | 3.19 | 4.67 | 10.40 |
| $Na_2O$ | 0.10 | 0.69 | 1.42 | 0.30 |
| $K_2O$ | 0.61 | 1.09 | 0.68 | 0.38 |
| $P_2O_5$ | 0.06 | 0.44 | 0.84 | 0.01 |
| $TiO_2$ | 0.24 | 1.29 | 1.48 | 0.44 |
| SrO | 0.09 | 0.35 | 0.32 | 0.04 |
| BaO | - | 0.35 | 0.67 | - |
| LOI | 2.22 | 0.07 | 0.19 | - |
| Total | 99.95 | 100.17 | 100.44 | 95.11 |

Note: "-" indicates that the data are not available.

**Table 4. Mix proportions and fresh concrete properties**

| Mixture Identification | Mixture Design | | | | | | | | | Fresh SCC Properties | | | | | | |
|---|---|---|---|---|---|---|---|---|---|---|---|---|---|---|---|---|
| ID | C I,II | SCM | LD | CA | FA | Water | HRWR | VMA | AEA | Slump Flow | | | | J-Ring | Air content | Unit Weight |
| | lb/cy | lb/cy | lb/cy | lb/cy | lb/cy | lb/cy | oz/cwt | oz/cwt | oz/cwt | $T_{50}$ (s) | $T_{final}$ (s) | D (in.) | VSI | ΔD (in.) | % | lb/cf |
| CC -a(LS) | 497 | 166 | 0 | 1674 | 1177 | 285 | 0.0 | 0 | 0.6 | - | - | - | - | - | 5.0 | 145.0 |
| CC -b(LS) | 591 | 197 | 0 | 1485 | 1173 | 315 | 0.0 | 0 | 0.8 | - | - | - | - | - | 4.5 | 146.8 |
| CC -c(LS) | 572 | 191 | 0 | 1350 | 1356 | 305 | 0.0 | 0 | 1.5 | - | - | - | - | - | 5.5 | 141.5 |
| CC -a(G) | 459 | 153 | 0 | 1674 | 1277 | 260 | 0.0 | 0 | 1.5 | - | - | - | - | - | 5.3 | 146.2 |
| CC -b(G) | 516 | 172 | 0 | 1485 | 1358 | 275 | 0.0 | 0 | 1.5 | - | - | - | - | - | 6.5 | 141.8 |
| CC -c(G) | 534 | 178 | 0 | 1350 | 1455 | 285 | 0.0 | 0 | 1.5 | - | - | - | - | - | 7.8 | 139.2 |
| SCC-a(LS)-C | 568 | 189 | 0 | 1518 | 1242 | 280 | 8.0 | 0 | 0.8 | <2 | 6.8 | 27.8 | 0.0 | 0.63 | 5.2 | 144.2 |
| SCC-a(LS)-F | 568 | 189 | 0 | 1518 | 1242 | 280 | 8.0 | 2 | 0.8 | <2 | 7.8 | 28.8 | 1.0 | 1.00 | 3.5 | 146.2 |
| SCC-a(LS)-S | 539 | 231 | 0 | 1530 | 1252 | 280 | 8.0 | 2 | 0.8 | 2.0 | 6.2 | 29.1 | 0.5 | 0.13 | 6.5 | 141.2 |
| SCC-a(LS)-FLD | 488 | 150 | 106 | 1518 | 1242 | 280 | 12.0 | 0 | 1.5 | 1.3 | 7.0 | 27.5 | 0.5 | 1.75 | 6.0 | 142.2 |
| SCC-b(LS)-C | 535 | 178 | 0 | 1462 | 1297 | 295 | 8.0 | 0 | 1.0 | <2 | 6.8 | 23.6 | 0.0 | 0.88 | 4.0 | 146.0 |
| SCC-b(LS)-F | 535 | 178 | 0 | 1462 | 1297 | 295 | 6.0 | 2 | 1.5 | <2 | 7.1 | 24.3 | 0.0 | 1.00 | 5.0 | 142.8 |
| SCC-b(LS)-S | 525 | 217 | 0 | 1474 | 1307 | 295 | 8.0 | 0 | 1.5 | <2 | 6.8 | 23.5 | 0.0 | 1.00 | 6.8 | 140.8 |
| SCC-b(LS)-FLD | 460 | 141 | 106 | 1462 | 1297 | 295 | 6.0 | 0 | 1.5 | <2 | 8.3 | 24.8 | 0.0 | 0.25 | 5.0 | 141.6 |
| SCC-c(LS)-C | 587 | 196 | 0 | 1334 | 1334 | 305 | 11.0 | 0 | 1.3 | <2 | 6.8 | 23.6 | 0.0 | 1.00 | 5.0 | 143.0 |
| SCC-c(LS)-F | 587 | 196 | 0 | 1334 | 1334 | 305 | 10.5 | 3 | 1.5 | <2 | 7.6 | 27.5 | 0.0 | 0.75 | 6.5 | 143.0 |
| SCC-c(LS)-S | 558 | 239 | 0 | 1345 | 1345 | 305 | 12.0 | 0 | 1.5 | 2.7 | 9.5 | 27.0 | 0.0 | 0.50 | 7.0 | 140.4 |
| SCC-c(LS)-FLD | 504 | 155 | 116 | 1334 | 1334 | 305 | 11.0 | 0 | 1.5 | 1.7 | 8.9 | 27.3 | 0.0 | 0.75 | 6.5 | 139.8 |
| SCC-a(G)-C | 568 | 189 | 0 | 1512 | 1237 | 280 | 10.0 | 3 | 1.5 | 1.3 | 7.3 | 28.0 | 1.0 | 2.00 | 5.7 | 141.4 |
| SCC-a(G)-F | 568 | 189 | 0 | 1512 | 1237 | 280 | 10.0 | 3 | 1.5 | 1.2 | 7.8 | 30.0 | 1.0 | 1.00 | 5.5 | 143.6 |
| SCC-a(G)-S | 539 | 231 | 0 | 1524 | 1247 | 280 | 10.0 | 3 | 1.5 | 2.3 | 8.7 | 28.3 | 0.0 | 1.00 | 5.7 | 135.2 |
| SCC-a(G)-FLD | 488 | 150 | 113 | 1512 | 1237 | 280 | 13.0 | 3 | 1.5 | 1.6 | 7.3 | 28.3 | 1.0 | 1.25 | 4.6 | 142.8 |
| SCC-b(G)-C | 535 | 178 | 0 | 1456 | 1291 | 295 | 7.0 | 0 | 1.5 | 1.0 | 6.0 | 24.5 | 0.0 | 0.50 | 5.6 | 140.6 |
| SCC-b(G)-F | 535 | 178 | 0 | 1456 | 1291 | 295 | 4.5 | 0 | 1.5 | 1.4 | 5.5 | 24.8 | 0.0 | 0.25 | 6.0 | 142.4 |
| SCC-b(G)-S | 525 | 225 | 0 | 1456 | 1291 | 295 | 6.0 | 0 | 1.5 | 1.8 | 10.0 | 23.8 | 0.0 | 0.25 | 6.5 | 136.4 |
| SCC-b(G)-FLD | 460 | 141 | 106 | 1456 | 1291 | 295 | 6.0 | 0 | 1.5 | 1.0 | 5.9 | 25.3 | 0.0 | 0.25 | 5.6 | 141.4 |
| SCC-c(G)-C | 587 | 196 | 0 | 1329 | 1329 | 305 | 10.0 | 0 | 1.5 | 1.4 | 7.2 | 29.3 | 0.0 | 0.25 | 6.6 | 141 |
| SCC-c(G)-F | 558 | 239 | 0 | 1340 | 1340 | 305 | 12.0 | 4 | 1.5 | 1.8 | 7.6 | 30.0 | 2.0 | 0.25 | 5.4 | 138.6 |
| SCC-c(G)-S | 587 | 196 | 0 | 1329 | 1329 | 305 | 9.0 | 0 | 1.5 | 1.3 | 9.5 | 29.0 | 0.0 | 0.25 | 6.0 | 140.8 |
| SCC-c(G)-FLD | 491 | 155 | 116 | 1329 | 1329 | 305 | 9.5 | 0 | 1.5 | 1.1 | 5.8 | 29.0 | 0.0 | 0.75 | 6.2 | 139.4 |

Note: C = Class C fly ash; F = Class F fly ash; S = slag cement; FLD = F fly ash and limestone dust; a = 3/4" NMSA; b = 1/2" NMSA; c = 3/8"NMSA; C I,II = Type I/II portland cement; LD = limestone dust; CA = coarse aggregate; FA = fine aggregate; LS = crushed limestone; G = river gravel; T50 = flow time for SCC reaching diameter of 20 in.; Tfinal = flow time until flow stopping; D = slump flow diameter; ΔD = slump flow diameter - J-ring flow diameter; "-" indicates the data are not available. 1lb = 0.45 kg; 1 cy = 0.76 m3; cwt = 100 lb of cementitious materials; 1 oz = 29.6 ml; 1 in. = 25.4 mm.

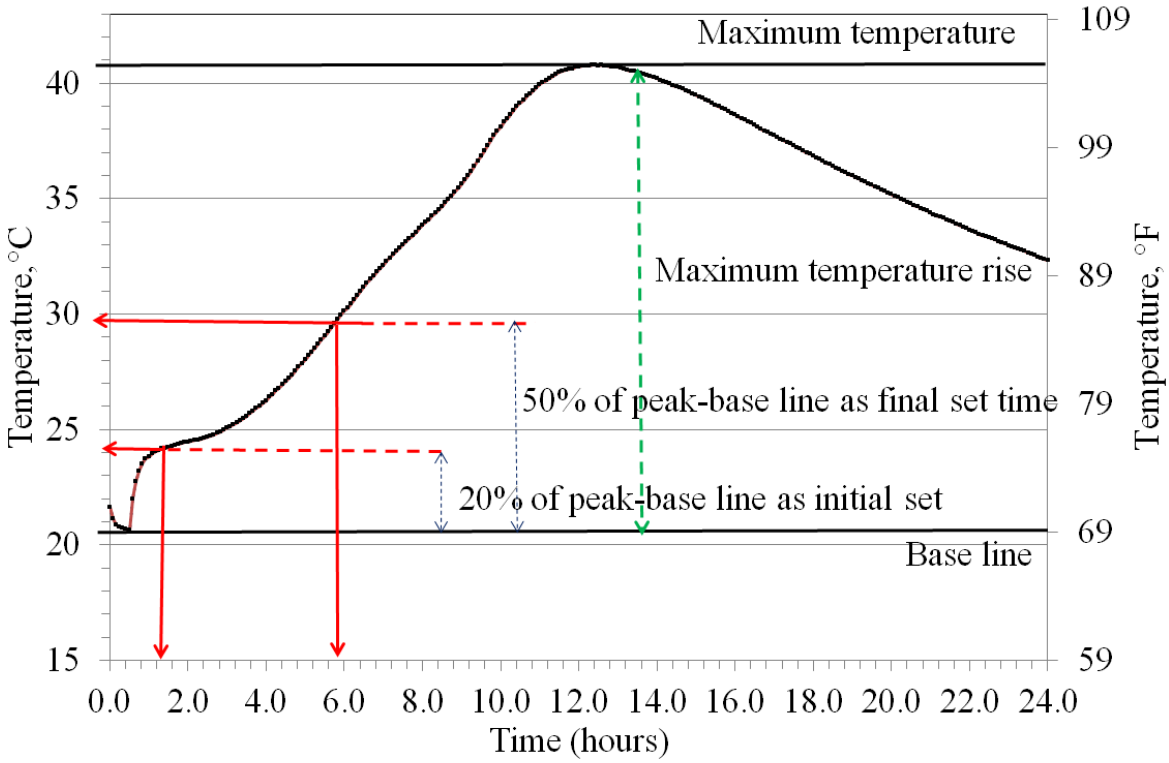


**Figure 1. Calculation of setting times determined by "fraction" method of a typical thermal profile.**

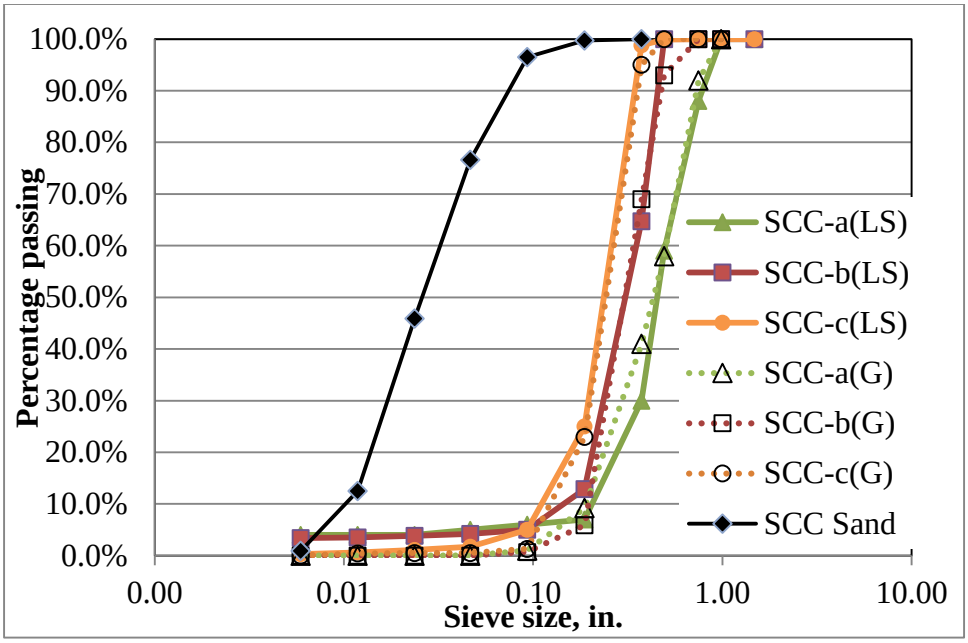


**Figure 2. Aggregate gradations.**

**Figure 3. Calorimetry test equipment for heat of hydration of concrete.**

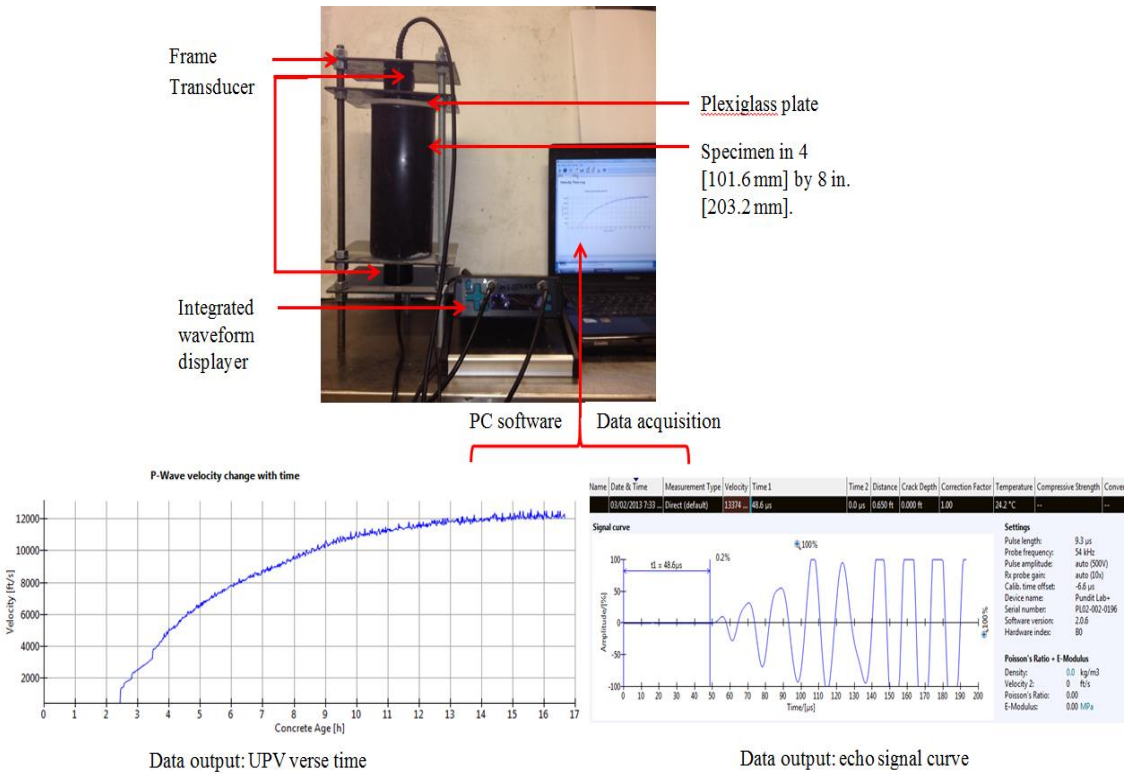


**Figure 4. Test setup and data acquisition system of UPV measurement.**

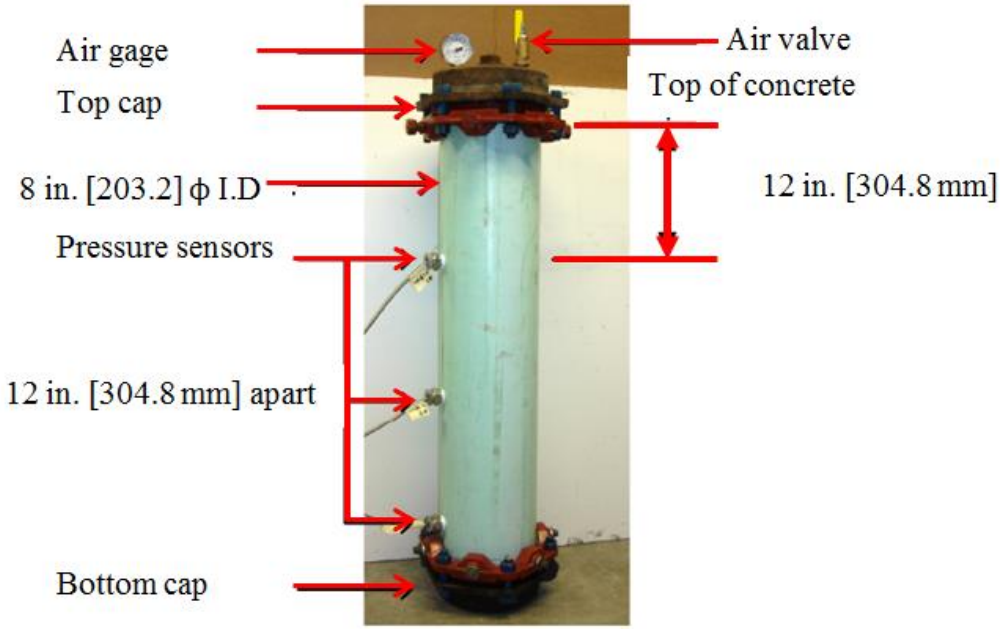


**Figure 5. Form pressure device setup (Lomboy et al. 2013).**

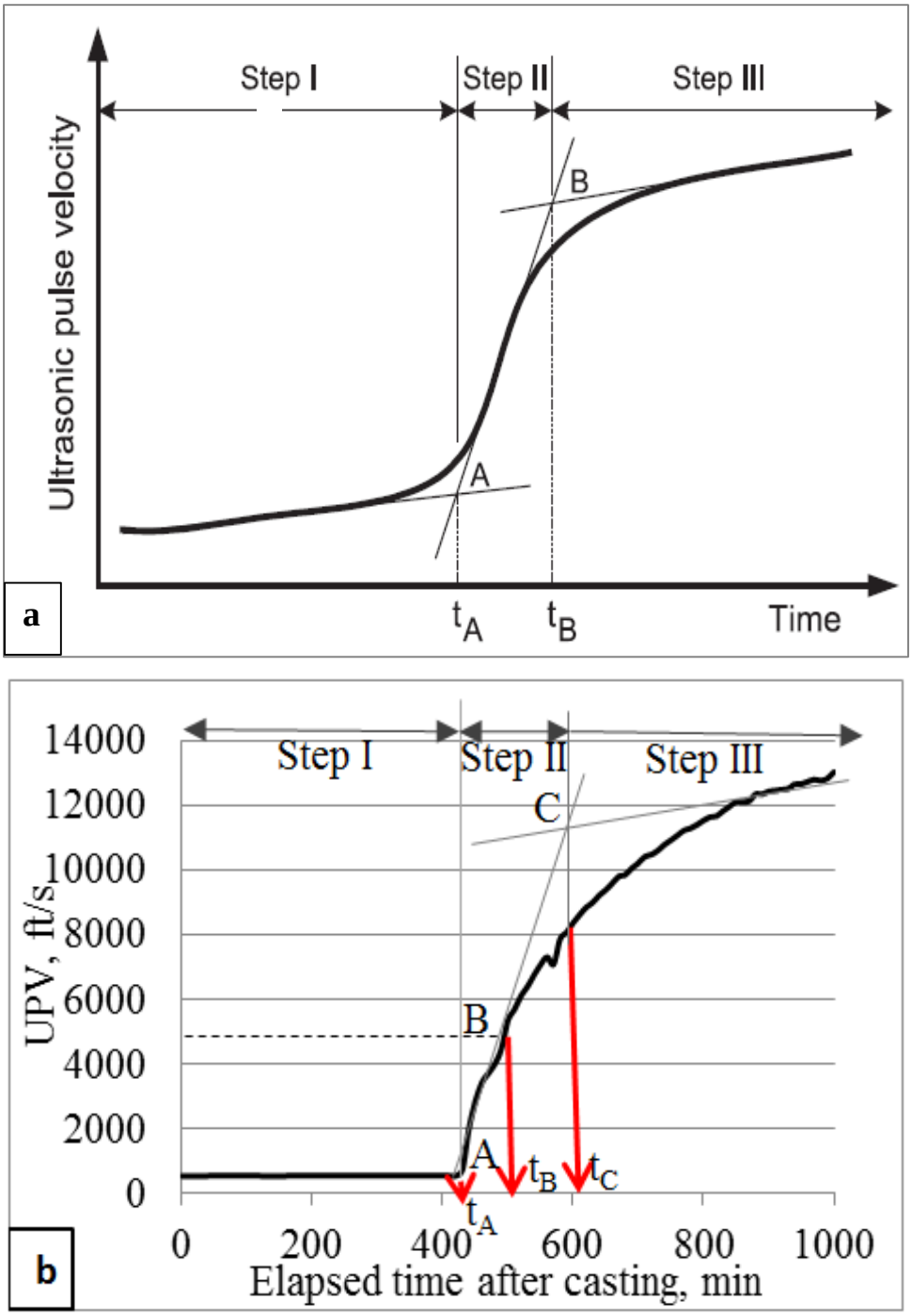


**Figure 6. Schematic representation of typical evolution of UPV from (a) Lee et al. (2004) ; (b) current study.**[*1 ft = 0.3 m.]

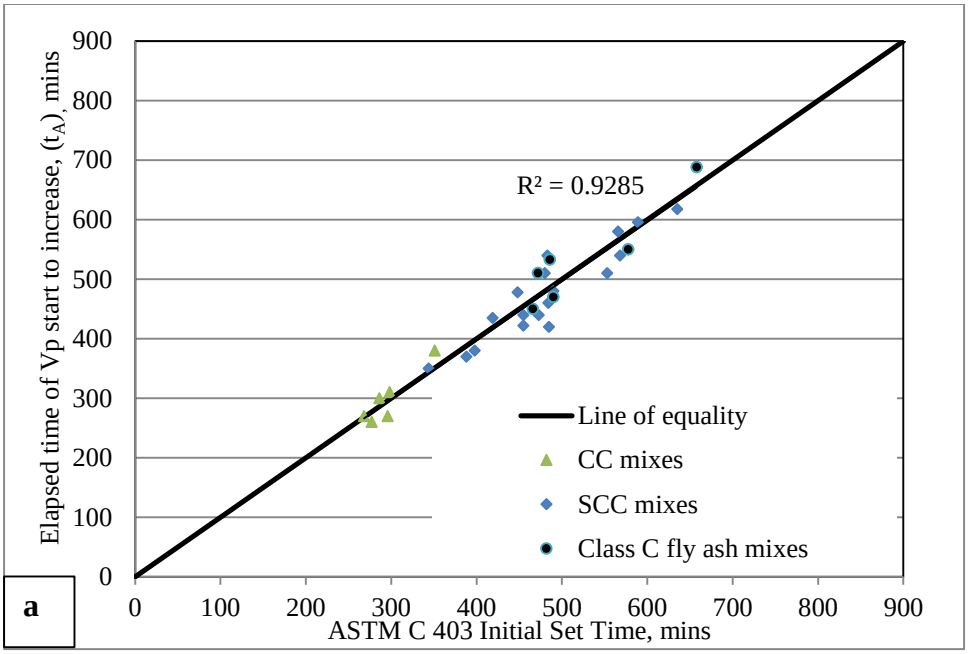


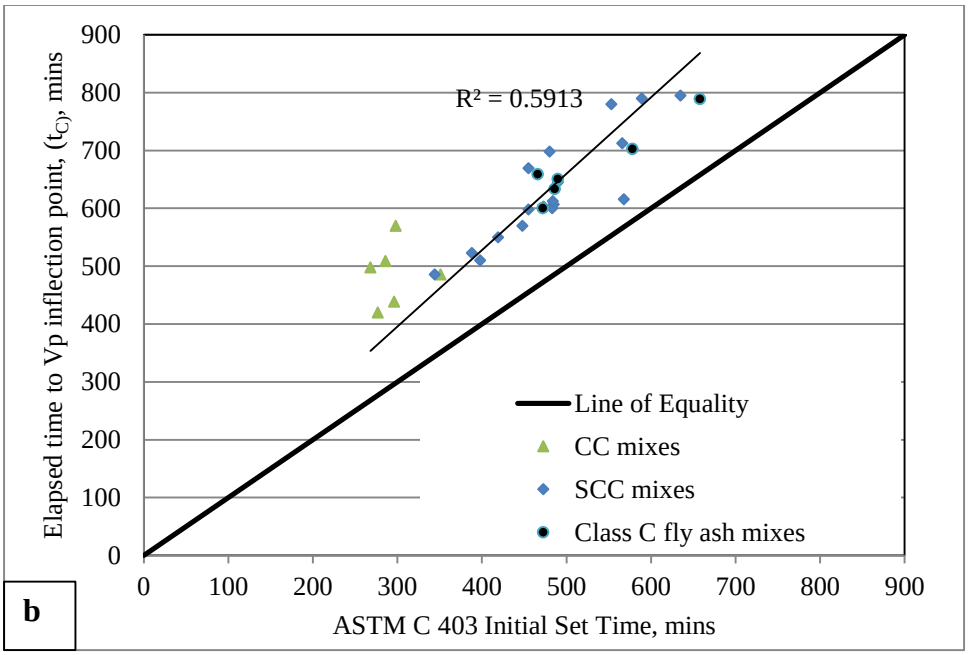

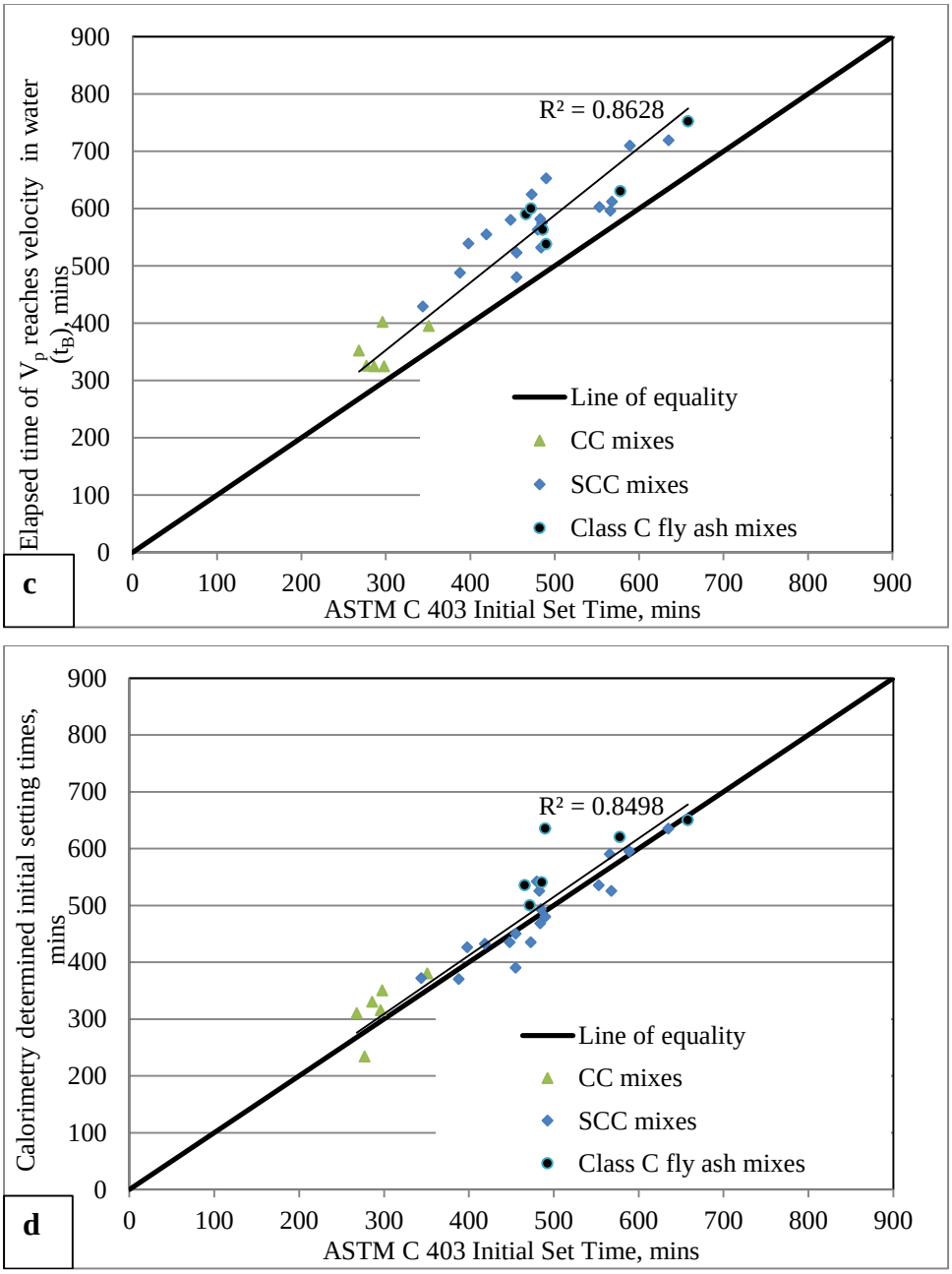


**Figure 7. Correlations of initial setting time measurements determined by different features and methods: ASTM C403 initial setting time vs. (a) elapsed time of $V_p$ start to increase, $t_A$; (b) elapsed time to $V_p$ inflection points, $t_C$; (c) elapsed time of $V_p$ reaches velocity in water, $t_B$; (d) Calorimetry determined initial setting times.**

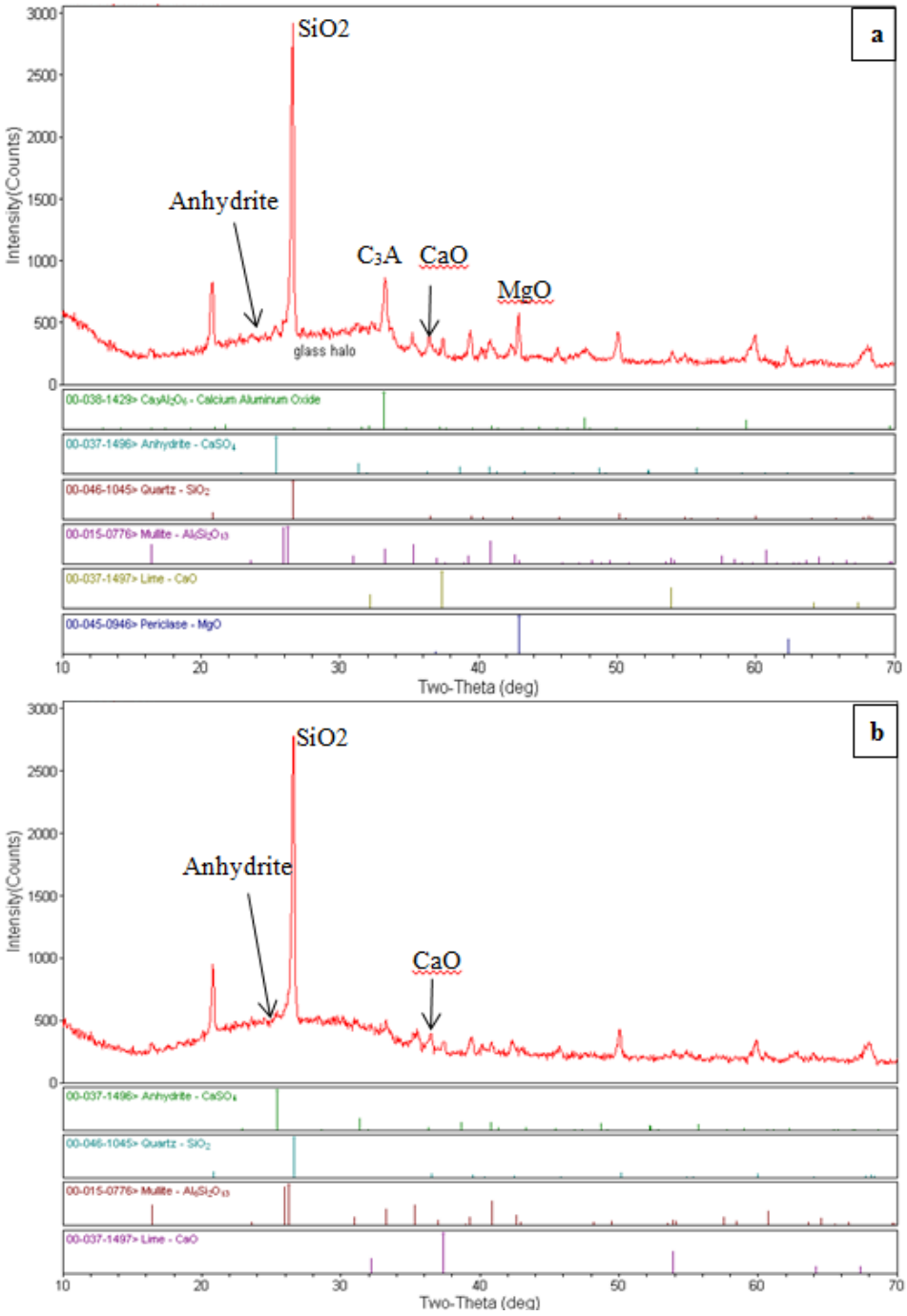


**Figure 8. X-ray diffractograms of (a) class C fly ash; (b) class F fly ash.**

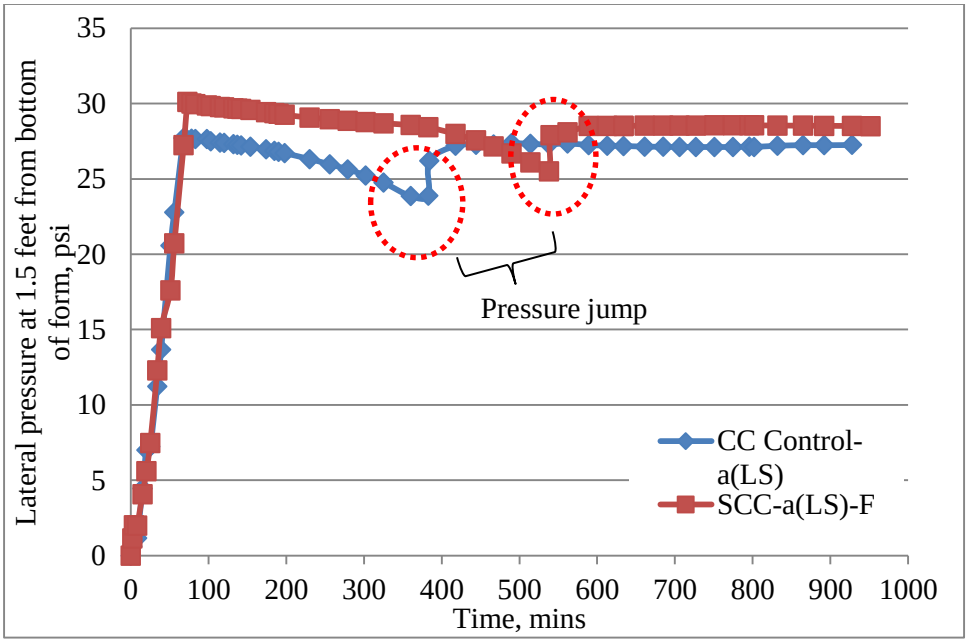


**Figure 9. Formwork pressure development of selected mixes.**[*1 ft = 0.3 m.]

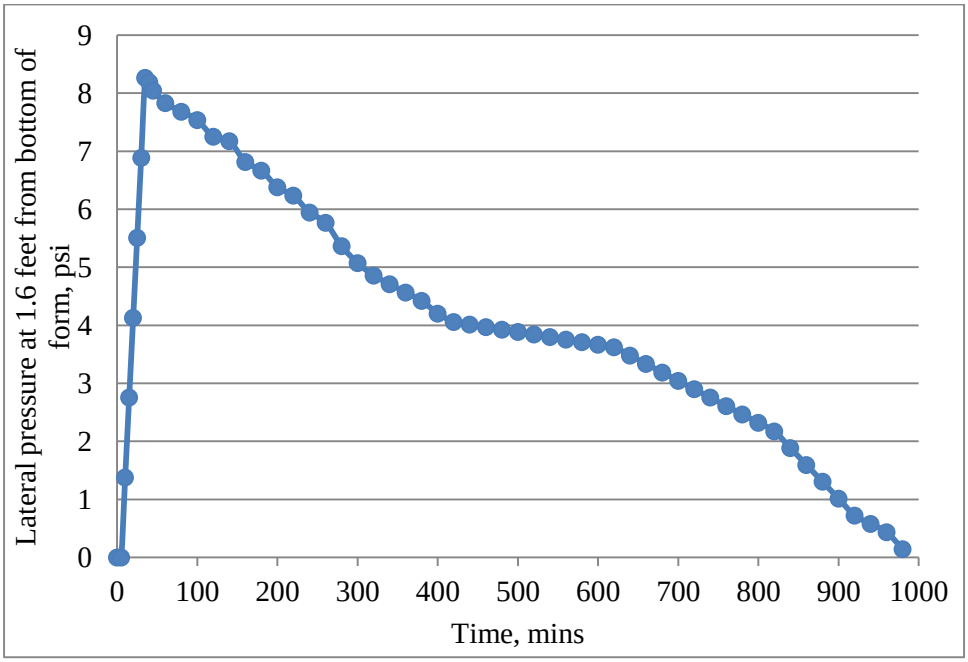


**Figure 10. Formwork pressure decay of 14.4 feet [4.4 m] wall structure at the casting rate of 32.8 feet/hour [10 m/hr] (Gregori et al. 2004).**

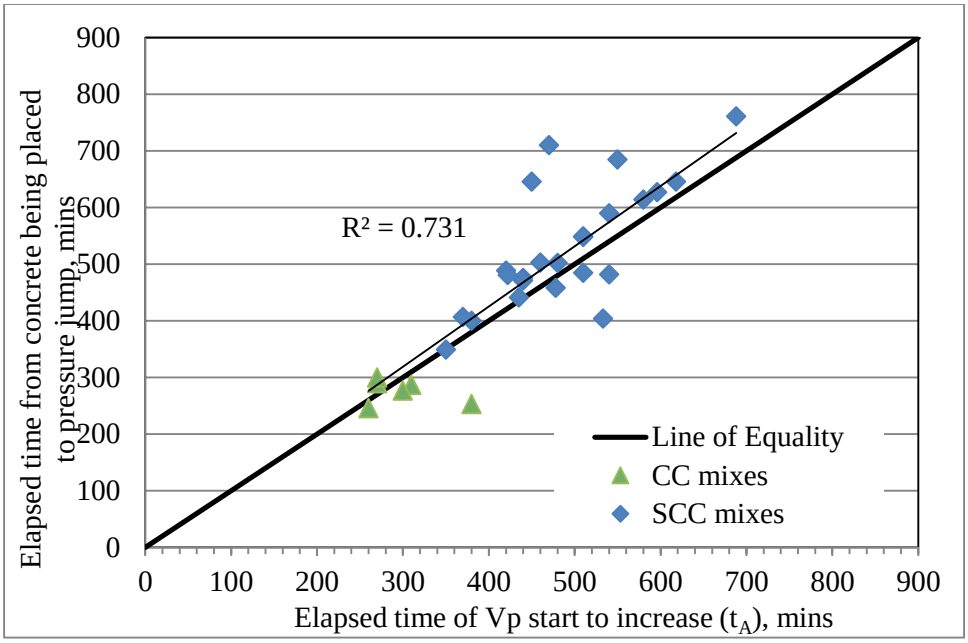


**Figure 11. Correlations between elapsed time from concrete being placed to pressure jump and elapsed time of $V_p$ start to increase.**

# CHAPTER 7. GENERAL CONCLUSIONS

This study provides practical applications on how to use particle packing theory, paste-to-voids volume ratio concept, statistical analysis and modeling, digital image processing method and programing algorithm, and non-destructive analysis to design mix proportioning and measure and control the performance of cast-in-place SCC mixtures for bridge structures. The modified Brouwers' mix design algorithm using particle packing concept can be appropriately applied to produce SCC mix proportions for CIP applications, especially with the distribution modulus between 0.23 and 0.29. Relatively economical SCC mixtures can be developed with this modified algorithm that meets the proposed criteria and thresholds of CIP applications in fresh and hardened states. The proposed DIP method and MATLAB algorithm can be successfully used to derive MTI and average inter-particle spacing between coarse aggregate on hardened concrete samples and quantitatively assess the static stability of a SCC mixture. They provide efficient and useful tools in designing mixture proportions of SCC. In addition, the concept of paste-to-voids volume ratio is appropriate to assess the performance of SCC mixtures and the P-wave test and calorimetric measurements can be efficiently used to monitor the stiffening and setting of SCC mixtures.

The main conclusions of this study are as follows:

1. The modified Brouwers mix design algorithm using particle packing concept can be appropriately applied to produce SCC mix proportions and yield a relatively economical mixture. The distribution modulus generally ranges from 0.23 to 0.29.
2. Almost all mixes designed using the modified Brouwers method exhibit good performance on workability, surface resistivity, strength, air structure, and shrinkage based on the criteria obtained from literature. Relationships were found

between slump and Bingham parameters, yield stress of mortar and yield torque of corresponding concrete, and fresh air content and hardened air content.

3. The Vpaste/Vvoids concept can be used in SCC mixtures to assess workability, strength, permeability, and drying shrinkage. Statistical analysis, such as response surface models and HSD tests, provides a systematic and quantitative means to predict and assess performance of SCC mixtures. It is also an efficient tool to identify the significance of influence factors on concrete performance.
4. Layered cross sectional and histogram analysis of mortar to aggregate area ratio from DIP method provide quantitative ways to estimate static stability of SCC mixtures. The probability density of 60% from histogram analysis appears to be a reasonable threshold for indicating a uniformly distributed SCC mixture. The MTI can be used to establish a statistical response surface model to predict the flowability of SCC mixtures associated with rheological parameters in this research. For a given mortar yield stress, a critical mortar viscosity of 1.30 tends to significantly affect the trend of slump flow changing with MTI.
5. The investigated relationship between MTI from DIP method and $D_{ss}$ and Vpaste/Vvoids from existing theoretical frames is well correlated. Therefore, the parameters derived from DIP method should be used to evaluate the performance of SCC mixtures because they have potentials to overcome the limitations of "excess paste/mortar theory" and paste-to-voids volume ratio concept.
6. For different performance measurement approaches, P-wave propagation method can be used to monitor setting of CC and SCC mixes. The calorimetry test also provides a potential means of assessing initial setting times without the need to remove coarse aggregate. One limit to this is that it is not conducted at the same temperature of the mixture. Therefore, variation in weather will not be accounted for. The laboratory formwork pressure device can be used as an indicator of initial set of concrete mixture. However, the device with overhead air pressure may not be able to rigorously simulate the in-situ formwork pressure beyond initial set.

# CHAPTER 8. RECOMMENDATIONS FOR FUTURE RESEARCH

This work aims at comprehensively understanding the relationship among the aggregate system, paste quality, and paste quantity to produce SCC mixtures with improved particle packing system and reduced paste quantity while remaining concrete quality and performance. Efforts have been made to investigate the different performance between SCC and CC mixtures in fresh and hardened concrete properties for years. However, SCC mixtures applications in cast-in-place transportation structures should be more focused in next several decades to improve the sustainability and applicability of concrete.

A popular theory, particle packing, has a large potential to produce economical concrete mixtures without scarifying concrete performance. Following the proposed particle packing based design method, diverse types and sources of materials should be used to assess the economic feasibility and variability of this method in order to further improve the applicability. More distribution moduli should be verified to build up a database for different materials and practical applications.

More non-destructive analysis tools should be evaluated in the field and laboratory environment so that these techniques are more reliable and can provide quality control/assurance more efficiently. DIP method can be a very useful technique to evaluate the hardened mixture. Inter-discipline may be helpful on the efficiency of evaluating concrete mixtures and develop new techniques, such as programing algorithm in DIP method.

Field demonstrations of designed SCC mixtures are extremely important to further improve the design method and consult the performance issues. Therefore, how to apply a

good SCC mixture designed and evaluated in the laboratory to be successfully survived in transportation and building structures in the field is a focus on future research as well.

# APPENDIX A. PAPERS AND REPORT ABSTRACTS FROM ADDITIONAL RESEARCH

# RHEOLOGICAL BEHAVIOR AND FORMWORK PRESSURE OF NC, SCC AND SFSCC MIXTURES

A paper accepted to be published in Journal of Cement and Concrete Composites SI: SCC2013

*Gilson R. Lomboy[1], Xuhao Wang[2] and Kejin Wang[3]*

## ABSTRACT

This paper presents the rheological properties of normal concrete (NC), self-consolidating concrete (SCC) and semi-flowable self-consolidating concrete (SFSCC) and their relation to formwork pressure decline. The rheological study was conducted on concrete and mortar. IBB and Brookfield rheometers were used to determined rheological properties at 15 to 90 minutes after mixing. The loading histories of concrete were with pre-shear, while with or without pre-shear for mortar. Formwork pressures were measured using a 200mm (8inch) diameter form. Other concrete properties measured were setting time, hydration temperature and compressive strength development. The Bingham model was insufficient to describe the rheological behavior of SCC, evident by the negative yield stress and torque. The initial viscosity and yield stress of SFSCC was higher compared to NC and the

[1] Postdoctoral Fellow, Department of Civil and Environmental Engineering, Northwestern University2145Sheridan Road, Tech A236, Evanston, IL 60208, gilson.lomboy@northwestern.edu

[2] Research Assistant, Department of Civil, Construction and Environmental Engineering, Iowa State University, 136 Town Engineering, Ames, Iowa 50011, wangxh@iastate.edu

[3] Professor, Department of Civil, Construction and Environmental Engineering, Iowa State University, 492 Town Engineering, Ames, Iowa 50011, kejinw@iastate.edu

comparative thixotropy of mortar mixtures varied depending on the loading history. In concrete mixtures, yield torque increased with time while flow curve slope and concrete thixotropy did not. All the initial formwork pressures were the same for the three types of concrete. SCC had the fastest decrease in formwork pressure, followed by SFSCC, then by NC. This correlates with the rate of thixotropy increase of mortar.

**Keywords**: Rheology, Formwork Pressure, SCC, SFSCC

# EFFECT OF INTERPARTICLE ACTION ON SHEAR THICKENING OF CEMENTITIOUS SUSPENSIONS

A paper submitted to Journal of Cement and Concerte Composites

*Gang Lu*[1], *Xuhao Wang*[2], *Kejin Wang*[3]

## ABSTRACT

Nowadays, it is widely accepted the shear thickening effects in concrete rheology are principally due to interactions within the colloidal phase. However, in highly flowable cement-based composites, such as Self-Consolidating Concrete, due to low yield stress of fluid matrix material, aggregate particles flow at high speeds in concrete and collisions happen. At the macroscopic level, particle cluster also presents at high flow rate. Thus, aggregate particle flow and collision can be another source for shear thickening, in addition to the shear thickening effect from the colloidal phase. To support this view, a particle-fluid model developed previously for predicting the relationship between the shear stress and shear strain rate of cementitious suspensions was utilized to explain the cause of shear thickening in cementitious composites at the macroscopic level. Factors that affect shear thickening potential in flowing cementitious suspensions were studied. The model was capable to explain the mechanism of shear thickening in cementitious

[1] Senior Engineer at KT Engineering, Inc., Frederick, MD, USA

[2] Research Assistant, Department of Civil, Construction and Environmental Engineering, Iowa State University, 136 Town Engineering, Ames, Iowa 50011, wangxh@iastate.edu

[3] Professor, Department of Civil, Construction and Environmental Engineering, Iowa State University, 492 Town Engineering, Ames, Iowa 50011, kejinw@iastate.edu

suspensions. Experimental work was completed to support this view as well as the theoretical approach.

**Keywords**: Mortar; Rheology; Interparticle forces; Shear stress; Thickening.

# COMPARISON OF SETTING TIME MEASURED USING ULTRASONIC WAVE PROPAGATION WITH SAW-CUTTING TIMES ON PAVEMENTS IN IOWA

**Technical Report**
**January 2014**

**Principal Investigator**
Peter Taylor, Associate Director
National Concrete Pavement Technology Center, Iowa State University

**Research Assistant**
Xuhao Wang

**Authors**
Peter Taylor and Xuhao Wang

Sponsored by
FHWA Pooled Fund Study TPF-5(205): Colorado, Iowa (lead state), Kansas,

Michigan, Missouri, New York, Oklahoma, Texas, Wisconsin

Preparation of this report was financed in part

through funds provided by the Iowa Department of Transportation

through its Research Management Agreement with the

Institute for Transportation

(InTrans Project 10-374)

A report from

**National Concrete Pavement Technology Center**

**Iowa State University**

2711 South Loop Drive, Suite 4700

Ames, IA 50010-8664

Phone: 515-294-8103

Fax: 515-294-0467

www.cptechcenter.org

## EXECUTIVE SUMMARY

Concrete setting behavior strongly influences scheduling of construction operations, such as surfacing, trowelling, jointing, and saw-cutting. To conduct pavement finishing and sawing activities effectively, it is useful for contractors to know when a concrete mixture is going to reach initial set, or when the sawing window will open. Monitoring the set time of a fresh mixture also provides a tool to assess the uniformity between material and concrete batches.

The aim of this project was to confirm that initial set could be measured using an ultrasonic pulse velocity (UPV) approach, and to assess whether there was a relationship between initial set and sawing time for pavement concrete in the field.

Eight construction sites were visited in Iowa over a single summer/fall period. At each site, initial set was determined using a p-wave propagation technique with a commercial device. It was also determined on mortar samples in accordance with ASTM C 403. Calorimetric data were collected using a commercial semi-adiabatic device on some of the sites.

The data collected to date revealed the following:

- UPV approaches appear to be able to report initial set times
- It seems that early entry sawing time can be predicted for the range of mixtures tested here